UNIVERSITAT DE BARCELONA

Identification and functional characterization of P1N-PISPO, a new gene product present in sweet potato potyviruses

Ares Mingot Martí

Aquesta tesi doctoral està subjecta a la llicència ***Reconeixement 3.0. Espanya de Creative Commons***.

Esta tesis doctoral está sujeta a la licencia ***Reconocimiento 3.0. España de Creative Commons***.

This doctoral thesis is licensed under the ***Creative Commons Attribution 3.0. Spain License***.

UNIVERSITAT DE BARCELONA

FACULTAT DE FARMACIA

DEPARTAMENT DE BIOQUÍMICA i BIOLOGIA MOLECULAR

IDENTIFICATION AND FUNCTIONAL CHARACTERIZATION OF P1N-PISPO, A NEW GENE PRODUCT PRESENT IN SWEET POTATO POTYVIRUSES

ARES MINGOT MARTÍ

2016

UNIVERSITAT DE BARCELONA

FACULTAT DE FARMÀCIA

DEPARTAMENT DE BIOQUÍMICA i BIOLOGIA MOLECULAR

PROGRAMA DE DOCTORAT DE BIOTECNOLOGIA

IDENTIFICATION AND FUNCTIONAL CHARACTERIZATION OF P1N-PISPO, A NEW GENE PRODUCT PRESENT IN SWEET POTATO POTYVIRUSES

Memòria presentada per Ares Mingot Martí per optar al títol de doctor per la Universitat de Barcelona

Director	Doctorand	Tutor
Dr. Juan José López-Moya	Ares Mingot Martí	Dr. Albert Ferrer Prats

ARES MINGOT MARTÍ
2016

Aquest treball s'ha realitzat al Laboratori de Virologia de Plantes dins del Programa d'investigació de Respostes a l'estrès, en el Centre de Recerca en Agrigenòmica, Barcelona, sota la direcció del Dr. Juan José López-Moya. A més a més part del treball s'ha dut a terme gràcies a una estada breu en el Laboratori de "RNA silencing and disease resistance" de Sir David Baulcombe en el Departament de "Plant sciences", University of Cambridge, Anglaterra.

Al meu germà,
allà on siguis

ACKNOWLEDGEMENTS

Doncs fins aquí he arribat, la última part d'aquesta tesi però la més emotiva (i segurament la més llegida ☺). Com deia un filòsof xinès, "La gratitud és la memòria del nostre cor". Espero que la meva no em falli i pugui deixar reflectit l'agraïment a tots aquells que heu contribuït a que aquest moment sigui realitat.

En primer lugar, y como no podía ser de otra manera, muchas gracias Juanjo por darme la oportunidad de realizar esta tesis. Muchísimas gracias por enseñarme tanto, por guiarme y por estar siempre dispuesto a escucharme y ayudarme (son incontables las veces que he entrado en el despacho…). He aprendido y disfrutado muchísimo, ha sido un placer tenerte como director.

En segundo lugar, quiero tener una mención especial para Adrián. Mil gracias por acogerme en Cambridge, por cuidarme desde el primer momento (tanto tú como Imma) y por transmitirme tu pasión por la ciencia. Y como no, por todos los momentos de risas y los Me piro vampiros compartidos en Cambridge. Gracias también a nuestros colaboradores de Madrid y Cambridge. A Juan Antonio por sus consejos y el tiempo invertido en PISPO, a Bernardo por todos esos experimentos de radio y a David por resolver siempre con entusiasmo todas nuestros pedidos bioinformáticos. Eso sí David, quedan pendientes una sevillanas para celebrar mi tesis, jejeje. Regarding my stage in Cambridge, I would like to acknowledge the kindness of Sir David, thank you for hosting me and for your time. Many thanks to all the people of the lab, and specially to Claire, thanks for helping me with English and being so kind! I evidentment a l'Àlex, gràcies petit per totes les tardes al lab cantant música catalana, em vas fer sentir com a casa. Fora del lab vaig conèixer a moltíssima gent que va fer que la meva estada fos genial però tres persones es mereixen unes línies per a ells sols. Pau i Sílvia, gràcies per tots els moments compartits (Carnaval de Notting Hill, Road Trip, barbacoes, festes i més festes i sobretot les classes de Swing, ehh Pau i David!!), per tot el suport i per seguir sent uns grans amics. M'encanta que ens seguim veient! I per últim, mil gràcies Nat! Gairebé no havíem coincidit al CRAG, però a Cambridge em vas demostrar que ets una gran amiga! Gràcies per acollir-me, tinc moltes ganes de veure't!

I ara si, ha arribat el moment dels meus companys del CRAG. Evidentment la primera posició l'ocupa la gent del meu lab, el VirLab, que com tothom sap és el millor lab del CRAG ☺. Quan vaig arribar, em vaig trobar a les meves "abueletes" preferides, la Lluïsa i la Maria. Lluïsa mil gracies per ser tan pacient, tan bona professora i tan bona persona (Saps que t'estimo i t'admiro moltíssim!). María, tranqui, tu línea no va a ser menos, jejeje. Me encantó compartir contigo mi primer año (menos las tardes de M-Clan, claro), eres una luchadora nata y sobretodo una amiga de tus amigos (Estoy muy orgullosa de tenerte como amiga!). Se echa mogollón de menos el Hasta Luego florecillas! Després em vaig quedar soleta, però de seguida van anar arribant la Bia, la Maria, la Marisa, el Bader (Gracias por aguantar a tanta mujer junta!) i per últim la Mariona (Gràcies per la teva disposició i la teva amabilitat, ets un encant!). Gracias Bia

por tu templanza, por aportar siempre un toque de buen humor al lab y por estar a mi lado en los momentos mas estresantes. Marieta, la meva creueta ☺, gracies per recordar-me tan el caràcter lleidatà i per ser una tia amb tanta empenta! I por último, mil gracias Marisa. Eres un amor y siempre estás ahí cuando se te necesita. Como mindundi sénior del lab estoy muy orgullosa de dejarte el relieve, vas a triunfar (Eso sí, vuela florecilla vuela!).

Como no, a mis labos de acogida. ¡No se que habría hecho sin vosotros! Al otro virusitus team, a Montse por todos los consejos y las charlas infinitas (¿Recuerdas el día que llevaba 2 horas en tu despacho, mientras medio CRAG me buscaba?). A Laura, Celia y Jan por todos los meetings y experimentos compartidos. Y como no a mi querida abuelita Ana, ha sido un placer conocerte, tenerte a mi lado y compartir momentos craft contigo. Mil gracias por cuidarme cuando estaba sola y perdida en el mundo de los boniatos. ¡Te deseo lo mejor en las américas y espero verte prontito! A nuestros vecinos, Belén y Aaron. A ti Aarón por estar siempre dispuesto a escucharme y aconsejarme, fuiste un gran apoyo (Y no olvido las barricadas, tu ya me entiendes). Al Pink Lab, a Blanca y a María por dejarme ser como una más del labo. Cris, reineta, m'has demostrat que ets una lluitadora i que sempre podré comptar amb tu. Ets molt gran i vals molt! En breu, celebrarem que ja som doctores (amb un cafè de "marujas" i amb uns bailoteos dels que tu i jo sabem). Pat i Mire gràcies per tots els cafès i pitis, han estat unes teràpies estupendes. Pat, gràcies per estar sempre disposada a ajudar-me i per ensenyar-nos que val la pena ser científic. Mire, gràcies pel teu positivisme i per sempre tenir una paraula reconfortant quan la necessito. Sé que no cal dir-ho, però estic segura que no perdrem el contacte. I a la resta dels integrants del Pink Lab, gràcies per ser tants bons companys: a la Rossany (¡Ánimos, ya no queda nada!), a la Raquel (Ets una currante!), al Marcel (La teva alegria s'encomana, no pas tant els teus acudits!), al Marcelo (Gracias por tratarnos tan bien, siempre serás un señor!), a la Lidi y a la Soni (Gracias por tus "northern" consejos). Y por último pero no menos importante a todos los integrantes del 1.02, los Sorayos y los Peps. A Soraya y a Paula por tratarme siempre con tanto cariño y permitirme hacer en vuestro lab tantas PCRs. A Luís por hacerme reír tanto y por todos los momentazos compartidos (véase primera cena de Navidad o aguas termales en el medio de la nada). A Minki por ser parte de las "abuelitas" y por cuidarme siempre como una mami. Y como no, a mis queridas Andreita y Cris. Empezamos juntas y casi acabaremos juntas. Habéis sido mis dos pilares y eso no tiene precio. Andrea, gracias por estar siempre ahí y por ser capaz de decirme las cosas tal y como son. Y como no por todo el vocabulario ecuatoriano que he aprendido como por ejemplo: Se me vira el hígado! Cris, gràcies per ser tan generosa i una de les persones més bones que conec. Sempre podré comptar amb tu!

Y seguimos con la primera planta. A mis ex-vecinos, Crina, Freddy, Montse, Marina,... Crina, ha sido un placer compartir todo este tiempo contigo, por fin hemos llegado al final (Nos queda un viaje pendiente con Pablo, para celebrar que los FPIs del 2011 ya

somos doctores!). Freddy, eres genial y vas a llegar muy lejos (Te quiero muchoooo!!!). Als Montes; a la Guio, a la Judith i a l'Arnau. Sou un equip de catalans collonut!! A los Palomos, los tres mosqueteros: Pablo, Jorge y Luís. Pablo, siempre me has demostrado que puedo contar contigo, eres un amigo de los de verdad. ¡Te deseo todo lo mejor en esta nueva etapa! Jorgito, aunque hables tan rápido, me encanta tu forma de ser y tu estilo "vegano-hipster" (como ves, te quiero demasiado para eliminarte de los agradecimientos). A ti Luís, llegaste de los últimos pero ya te has convertido en el político del CRAG. ¡Como voy a echar de menos chincharte y hacerte subir por las paredes! Y por último a Agnese, a Moni (Recupera't aviat reina, tu pots amb això i més) y a Helena, gracias por haberme hecho reír tanto en los descansos.

I ara a per la resta del CRAG. Al Joanet, tot i que fa molt temps que vas marxar sempre somric quan penso en tu. A la Martona, qui ens hagués dit que jo acabaria al CRAG i tu a l'altra punta del món. M'has demostrat que un pot fer allò que es proposa. Crec que serà impossible venir a Nova Zelanda abans de que acabis, però tingués segur que celebrarem el nostre títol "por todo lo alto". Et trobo molt a faltar, reina! A la Clareta i al Jordi, els tècnics més trempats que he conegut mai. Clara, vull que sàpigues que alguns dels moments més divertits de la meva tesis han passat al teu costat (Com per exemple muntar el "CRAG hermano shore" per la tesi de la Maria o bé sortir un ratet i acabar en "hoy me desmeleno y me saco las bragas", jajajajaja no puc parar de riure...). A la Laurix, unos de los últimos gran fichajes del CRAG. Me encanta que seas tan echada para adelante, que siempre le saques hierro a los problemas, y como no que estés dispuesta a compartir mediodías de vermut con una servidora. I també al Lucio, a la Rosa, a la Mariana, al Julio, al Nico, al Pep, a la Rossana, a la M José... En definitiva, a tota la gent que fa que el CRAG sigui un lloc on es treballa molt a gust! No voldria deixar d'agrair a la gent dels serveis del CRAG (Ángel, Mercè, Alejandro, Pilar, Mercè,...), aquells que fan que la nostra feina sigui molt més fàcil. Però en especial a la Pilar; per tenir una paciència il·limitada amb tots nosaltres, per la teva disposició a trobar solucions a tots els nostres problemes, i sobretot per sempre fer-ho sense perdre el bon humor. I encara que no estigui físicament al CRAG, a la Marta per tot el que em va ensenyar sobre "real-time" i perquè tot i ser la dona del "jefe", les millors quedades d'abueles han estat amb tu present.

També m'agradaria dedicar aquestes línies a la gent relacionada amb la ciència que va contribuir d'alguna manera a que comences el doctorat. Al Jesús Avilla, gràcies per formar-me i per animar-me a començar aquesta etapa. Al rafa, gracias por confiar en mi y por aconsejarme sobre mi futuro. Me encanta compartir una publicación contigo y seguir viéndonos de vez en cuando. A l'Albert, gràcies per donar-me l'oportunitat de fer les pràctiques de màster amb el teu equip. I per últim gràcies a la Paola i al David, per ensenyar-me des de zero les bases de la biologia molecular.

A continuació als amics de sempre. Tot i que cada costa més veure'ns, em sento feliç quan ho fem i veig que res no canvia. Tenir amics com vosaltres em fa sentir molt

afortunada! A tot el grup de suquetins, Suchs és guai i en gran part es deu a vosaltres. A la Laura, per ser tan valenta. A la Carmen, per ser tan oberta i disposada a fer tot allò que se li proposa. A la M José, per ensenyar-nos que la discreció és una virtut. A la M Rosa, per recolzar les decisions dels altres. A la Janet, per aportar el toc de gràcia en les trobades. A l'Àngel, per ser un tio tan divertit. A la Marta per no oblidar mai les dates importants i estar sempre present en els moments claus. A la Isa, per estimar-me tant i recolzar-me sempre que ho he necessitat. I a la Mariona, per tot, per compartir la vida amb mi. Als agronomets; els que vàreu aparèixer en una de les etapes més divertides i emocionants de la meva vida. Com ja sabeu: ¿Quienes son los mejores? Los agricultores.... Al Panton, pel seu carisma i per haver estat el millor company de fruti. Al David, per aportar sempre un toc d'estil al grup. Al Toni, per saber seguir endavant. Al Sala, per haver-me explicat milers de cops els exercicis d'hidràulica i regs. A l'Enric, perquè quan no hi ets et trobem a faltar. A l'Oriol, per aguantar-me i per ser tan gracioset també. A l'Edu, per ser el millor amic que puc tenir. A la Carmen, per no tenir filtre i per totes les hores que hem passat al pedrís. A la Laura, per escoltar-me i perquè hem estat capaces de seguir veient-nos a Barcelona. A l'Ester, per ensenyar-nos que la constància fa que arribis molt lluny. A Iraia, por todos esos jueves irrepetibles y por tus no se médicos. A l'Alexandra, per ser capaç de fer-me riure i divertir-me en els bons i sobretot en els mals moments. I a la Irene, per ensenyar-me que els amics són per sempre. I també a la Sara, perquè els moments a agrònoms juntes són inoblidables (Recordes el Dime el seno de? 696...). A la Marta i al David, per poder compartir una gran amistat i per molts més viatges junts. A Kina y a Elia por que la época del piso en Córsega será muy difícil de olvidar (Toca quedada en Barcelona ya, wey!) . Al José, a la Bettsy, al Rafel i a la Clara, perquè ja formeu part de la meva família a Barcelona. Y por último a ti Ana, por haber sido una de mis mejores amigas y porque sé que seguirás siéndolo.

A la família Fons-Duocastella, per acollir-me i fer-me sentir com a casa. A la Clara i al Marc, per ser uns cunyats tan estupendus. I a l'Aram i l'Irati, per ser l'alegria de la família. I ja per últim, a les persones més importants de la meva vida, aquelles que han fet que sigui qui sóc. Em plena d'orgull, tenir els pares que tinc. Pares, gràcies per ser les persones més fortes i integres que conec, i sobretot gracies per haver-me inculcat els vostres valors i pel suport de tots aquests anys. Sense vosaltres no hauria arribat fins aquí. Lluís, milions de gràcies per cuidar-me, per fer-me costat en els bons i en els mals moments, per fer-me feliç i per estar disposat a compartir la vida amb mi. T'estimo moltíssim!

I ARA SI QUE SI, ACABO DEDICANT LA MEVA TESIS AL JAUMET, SÉ QUE ALLÀ ON SIGUIS ESTARÀS MOLT ORGULLÓS DE MI!!

SUMMARY

SUMMARY

Sweet potato feathery mottle virus (SPFMV) (*Potyvirus* genus, *Potyviridae* family) causes important yield losses in sweet potato crops, in particular in co-infections with the unrelated crinivirus *Sweet potato chlorotic stunt virus* (SPCSV). This thesis addresses the characterization of some novel aspects in the infectious cycle of SPFMV, such as the expression, production and function of a new gene product named P1N-PISPO. A better understanding of SPFMV genome organization and the functions of their gene products might be relevant to improve the control strategies against this virus and the associated diseases in sweet potato crops.

The positive-sense RNA genome of SPFMV contains a large ORF, translatable as a polyprotein yielding a set of functional mature gene products (P1, HCPro, P3, 6K1, CI, 6K2, VPg-NIa, NIb and CP), and a short ORF named PIPO in the -1 frame, embedded within the P3 region. In addition to this organization, common to all the members of the *Potyvirus* genus, another ORF named PISPO was predicted in the genome. PISPO is in the -1 frame within the P1 region of SPFMV and other related potyviruses, starting at a conserved $G_{1\text{-}2}A_{6\text{-}7}$ motif, similar to the motif found upstream of PIPO. The expression of PISPO during SPFMV viral infection could result in the production of a putative new gene product P1N-PISPO.

In the present work, the presence of the PISPO frame has been investigated in a Spanish isolate of SPFMV infecting *Ipomoea batata* plants. The genome sequence of this isolate has been assembled from NGS data, showing that the expected trans-framed PISPO sequences is present, preceded by a G_2A_6 motif. A specific analysis of the NGS data has revealed a significant proportion of transcripts with an extra A in the motif at the beginning of PISPO, as well as a lower proportion of transcripts with an extra in the corresponding conserved motif preceding the PIPO region. These results have demonstrated that a polymerase slippage mechanism could generate transcripts containing extra A residues (G_2A_7) to allow the translation of P1N-PISPO and P3N-PIPO gene products. Analysis of the viral gene products present in SPFMV infected plant tissues has been performed using LC-MS/MS after separation in SDS- PAGE, focusing in products

> 50KDa. Peptides corresponding to the P1 protein have been detected from both the N-terminal portion (11 different peptides, 39% coverage), before the frameshifting signal and therefore common for P1 and P1N-PISPO, and in the C- terminal part (2 peptides exclusive for P1, 10% coverage). Interestingly, four peptides exclusive of PISPO, in its unique ORF (21.3% coverage), have been also found. These results have confirmed that both products P1 and P1N-PISPO are expressed and coexisted during SPFMV infection. Furthermore, transient expression of SPFMV gene products coagroinfiltrated with a reporter gene in *Nicotiana benthamiana* have revealed that P1N-PISPO acts as an RNA silencing suppressor, a role normally associated with HCPro in other potyviruses. Moreover, mutation of WG/GW motifs present in P1N-PISPO

abolished its silencing suppression activity, suggesting that the function might require interaction with Argonaute components of the silencing machinery, as was shown for other viral suppressors.

Altogether, the results of this thesis have confirmed the expression of P1N-PISPO during SPFMV infection and they have revealed a polymerase slippage mechanism as the responsible of P1N-PISPO production. Our results also have demonstrated the role of P1N-PISPO as a RNA silencing suppressor.

RESUM

El virus *Sweet potato feathery mottle virus* (SPFMV) (Gènere *Potyvirus*, Família *Potyviridae*) és el causant de pèrdues importants en el rendiment de cultius de moniato, en particular quan es troba en co-infecció amb el crinivirus no relacionat *Sweet potato chlorotic stunt virus* (SPCSV). Aquesta tesis aborda la caracterització d'alguns aspectes innovadors del cicle infectiu SPFMV, tals com l'expressió, la producció i la funció d'un nou producte gènic anomenat P1N-PISPO. Avanços en el coneixement de l'organització genòmica i les funcions dels productes gènics de SPFMV poden ser rellevants per tal de millorar les estratègies de control contra aquest virus i les seves malalties associades en cultius de moniato.

SPFMV presenta un genoma de cadena senzilla i positiva de RNA que conté una pauta de lectura oberta (ORF) llarga, traduïda com una poliproteïna que dóna lloc a un conjunt de productes gènics madurs i funcionals (P1, HCPro, P3, 6K1, CI, 6K2, VPg-NIa, NIb and CP), i una ORF molt més curta anomenada PIPO que es troba en el marc de lectura -1 de la regió P3 de la poliproteïna. A més a més de presentar aquesta organització, comú en tots els membres del gènere, en el seu genoma s'ha observat una ORF addicional anomenada PISPO. PISPO es troba en el marc de lectura -1 dins de la regió gènica de la P1 en SPFMV i els potyvirus més propers, començant en el motiu conservat $G_{1\text{-}2}A_{6\text{-}7}$ i similar al motiu d'inici de PIPO. La expressió de PISPO durant la infecció del virus donaria lloc a la producció del hipotètic producte gènic P1N-PISPO.

En aquest treball, la presència de la pauta de lectura PISPO ha estat investigada en un aïllat Espanyol de SPFMV que infectava plantes d'*Ipomoea batata*. La seqüència genòmica d'aquest aïllat ha esta assemblada a partir de dades obtingudes mitjançant NGS, mostrant que la seqüencia de PISPO és present i precedida per un motiu G_2A_6. Un anàlisis específic de les dades obtingudes per seqüenciació massiva, ha permès identificar una proporció significativa de transcrits que contenen una A extra en el motiu al començament de PISPO, així com una proporció menor de transcrits amb aquesta A extra en el corresponent motiu conservat de PIPO. Aquests resultats han demostrat que un mecanisme d'edició de la polimerasa podria generar transcrits amb residus A extra (G_2A_7), els quals permetrien la traducció dels productes gènics P1N-PISPO i P3N-PIPO. L'anàlisi del productes gènics virals presents en teixits de plantes infectades amb SPFMV s'ha dut a terme mitjançant un experiment de LC-MS/MS focalitzat en els productes més grans a 50 kDa. Pèptids corresponents a la part N-terminal de la proteïna P1 (abans del motiu d'edició) han estat detectats (11 pèptids diferents, 39% de cobertura), podent correspondre tant a P1 com a P1N-PISPO. No obstant, també s'han identificat 2 pèptids exclusius de la part C-terminal de la P1 (10% de cobertura) així com 4 pèptids exclusius de la pauta de lectura de PISPO (21,3% de cobertura). Aquests resultats han confirmat que tant P1 com P1N-PISPO són expressats i co-existeixen durant la infecció de SPFMV.

A més a més, l'expressió transitòria de productes gènics de SPFMV coagroinfiltrats amb un gen reporter en *Nicotiana benthamiana* ha revelat que P1N-PISPO actua com a supressor de silenciament d'ARN, un rol associat normalment a HCPro en altres potyvirus. Per últim, la mutació de motius WG/GW presents en P1N-PISPO aboleix la seva activitat com a supressor, suggerint que la funció pot està lligada a la interacció amb les proteïnes Argonauta de la maquinària de silenciament, tal i com passa en altres supressors virals.

El conjunt de resultats d'aquesta tesis han permès confirmar la expressió de P1N-PISPO durant la infecció de SPFMV i han revelat que un mecanisme d'edició de la polimerasa és el responsable de la seva producció. Per últim el rol de P1N-PISPO com a supressor del silenciament gènic ha estat demostrat.

RESUMEN

El virus *Sweet potato feathery mottle virus* (SPFMV) (Género *Potyvirus*, Familia *Potyviridae*) causa graves daños en los cultivos de boniato, especialmente cuando se encuentra en co-infección con el crinivirus no relacionado *Sweet potato chlorotic stunt virus* (SPCSV). Esta tesis aborda la caracterización de algunos aspectos novedosos del ciclo infectivo de SPFMV, tales como son su expresión, producción y función de un nuevo producto génico denominado P1N-PISPO. Avanzar en el conocimiento de la organización genómica y las funciones de los productos génicos de SPFMV puede ser relevante para mejorar las estrategias de control contra este virus y sus enfermedades asociadas en los cultivos de boniato.

SPFMV es un virus de ARN de cadena sencilla y positiva que contiene una pauta de lectura abierta (ORF), traducible en una poliproteína que da lugar a un conjunto de productos génicos maduros y funcionales (P1, HCPro, P3, 6K1, CI, 6K2, VPg-NIa, NIb and CP), y una ORF mucho más corta llamada PIPO que se encuentra en el marco de lectura -1 de la región P3 de la poliproteína. Además de presentar esta organización, común a todos los miembros del género, en su genoma se ha observado una ORF adicional llamada PISPO. PISPO se encuentra en el marco de lectura -1 en la región génica de la P1 en SPFMV y los potyvirus más cercanos a él, empezando con un motivo $G_{1\text{-}2}A_{6\text{-}7}$ conservado y similar al motivo con que comienza PIPO. La expresión de PISPO durante la infección del virus daría lugar a la producción del hipotético producto génico P1N-PISPO.

En este trabajo, la presencia de la pauta de lectura PISPO ha estado investigada en un aislado español de SPFMV que infectaba plantas de *Ipomoea batata*. La secuencia genómica de este aislado ha sido ensamblada a partir de datos obtenidos mediante NGS, mostrando que la secuencia de PISPO ésta presente y es precedida per un motivo $G_2A_{6.}$ Un análisis específico de les datos de secuenciación, ha permitido identificar una proporción significativa de transcritos con una A extra en el motivo al comienzo de PISPO, así como una proporción menor de transcritos de PIPO con una A extra en el correspondiente motivo conservado de PIPO. Estos resultados han demostrado que un mecanismo de edición de la polimerasa podría generar transcritos con residuos A extra (G_2A_7), permitiendo la traducción de los productos génicos P1N-PISPO y P3N-PIPO. El análisis de los productos génicos virales presentes en tejidos de plantas infectadas con SPFMV se ha realizado mediante LC-MS/MS, focalizado en los productos mayores de 50 kDa. Se han detectado péptidos correspondientes a la parte N-terminal de la proteína P1 (antes del motivo de edición) (11 péptidos diferentes, 39% de cobertura), los cuales pueden corresponder tanto a P1 como a P1N-PISPO. No obstante, también se han identificado 2 péptidos exclusivos de la parte C-terminal de la P1 (10% de cobertura) así cómo 4 péptidos exclusivos de la pauta de lectura PISPO (21,3% de cobertura). Estos resultados han confirmado que tanto P1 cómo P1N-PISPO se expresan y co-existen durante la infección de SPFMV.

Además, la expresión transitoria de productos génicos de SPFMV coagroinfiltrados junto a un gen reportero en *Nicotiana benthamiana* han revelado que P1N-PISPO actúa cómo supresor de silenciamiento de ARN, un rol asociado normalmente a HCPro en otros potyvirus. Por último, la mutación de motivos WG/GW presentes en P1N-PISPO impide que desarrolle su actividad supresora, sugiriendo que la función puede estar relacionada con la interacción con proteínas Argonauta de la maquinaria de silenciamento, así como ocurre en otros supresores.

El conjunto de resultados de esta tesis han permitido confirmar la expresión de P1N-PISPO durante la infección de SPFMV y han revelado que un mecanismo de edición de la polimerasa es el responsable de su producción. Por último se ha demostrado el rol de P1N-PISPO cómo supresor del silenciamento génico.

ABBREVIATIONS

ABBREVIATIONS

- aa: Aminoacid
- ACN: Acetonitrile
- AGO: Argonaute protein
- bp: Base pair
- CI: Cylindrical inclusion
- CP: Coat protein
- d/mpai: Days/Months postagroinfiltration
- DCL: Dicer like protein
- DNA: Deoxyribonucleic acid
- dsRNAs: double-stranded RNAs
- DTT: dithiothreitol
- EA: East African
- GFP: Green fluorescent protein
- HCPro: Helper Component Protease
- ICTV: International Committee on Taxonomy of Viruses
- IgG: Immunoglobulin G
- Kb: Kilo Bases
- KDa: Kilo Daltons
- miRNA: micro RNA
- mRNA: messenger RNA
- MW: Molecular weight
- NCBI: National Center for Biotechnology Information
- NGS: Next generation sequencing
- NIa: Nuclear inclusion type a
- NIb: Nuclear inclusion type b
- nt: Nucleotide
- O: ordinary
- ORF: Open Reading Frame
- P1: Protein P1
- P3: Protein P3
- PCR: Polymerase chain reaction
- PIPO: Pretty Interesting Potyviral ORF
- PISPO: Pretty Interesting Sweet potato Potyviral ORF
- PTGS: Post-transcriptional gene silencing
- qRT-PCR: Real time Reverse transcription-Polymerase chain reaction
- RC: Russet crack

- RDR: RNA-dependent RNA polymerase
- RISC: RNA induced silencing complexes
- RITS: RNA induced transcriptional silencing
- RNA-seq: RNA sequencing
- RNA: Ribonucleid acid
- RNase: Ribonuclease
- RSS: RNA silencing suppressor
- RT: Reverse transcription
- SDS-PAGE: Polyacrylamide gel electrophoresis in presence of SDS
- SPVD: Sweet potato viral disease
- ssRNA: single stranded RNA
- TGS: Transcriptional gene silencing
- UV: ultraviolet
- vasiRNAs: virus-activated small interfering RNAs
- VPg: Viral protein genome-linked
- VRCs: Viral replication complexes
- vsiRNAs: viral small interferent RNAs
- WGE: Wheat germ extract
- SPVD: Sweet potato viral disease
- ssRNA: single stranded RNA
- TGS: Transcriptional gene silencing

VIRUSES MOST CITED (the rest of viruses are listed in table I3)

- SPFMV: *Sweet potato feathery mottle virus*
- SPVG: *Sweet potato virus G*
- SPVC: *Sweet potato virus C*
- SPV2: *Sweet potato virus 2*
- SPMMV: *Sweet potato mild mottle virus*
- SPCSV: *Sweet potato chlorotic stunt virus*
- CVYV: *Cucumber vein yellowing virus*
- PPV: *Plum pox virus*

CONTENTS

CONTENTS

INTRODUCTION

INTRODUCTION

The Potyviridae family

The family *Potyviridae* is the largest taxonomic group of plant-infecting viruses with RNA genomes, and only second after the family *Geminiviridae* (DNA genomes). The *Potyviridae* family currently contains around 180 definite members according to the International Committee on Taxonomy of Viruses (ICTV). In agriculture, several members are considered relevant plant pathogens. They are widespread in cultivated plants and lead to high economical losses (Valli, García, and López-Moya 2015).

Potyviridae family members are positive-strand RNA viruses with a genome structure similar to the viruses found in the *Picornavirale*s order, although they are not formally listed in this order (Le Gall et al. 2008). The *Potyviridae* family is divided into 8 different genera, which groups members according to their genome organization, the sequence similarity and the vector responsible for their natural transmission (Table I1). The most abundant genus is the *Potyvirus* one that contains over 150 members, while the other genera range from 1-2-3 members for *Brambyvirus, Poacevirus* and *Rymovirus* respectively, to 6 members for the rest of genera.

Table I1: Genera of the family *Potyviridae*

Genus[1, 2]	**Type member**	**Vector type**	**Genome**
Brambyvirus	*Blackberry virus Y*	Unknown	Monopartite
Ipomovirus	*Sweet potato mild mottle virus*	Whiteflies	Monopartite
Macluravirus	*Maclura mosaic virus*	Aphids	Monopartite
Potyvirus	*Potato virus Y*	Aphids	Monopartite
Rymovirus	*Ryegrass mosaic virus*	Mites	Monopartite
Tritimovirus	*Wheat streak mosaic virus*	Mites	Monopartite
Poacevirus	*Triticum mosaic virus*	Mites	Monopartite
Bymovirus	*Barley yellow mosaic virus*	Plasmodiophorids	Bipartite

[1] Genera sharing the same genome organization and vector are separated by criteria depending on sequence similarity.

[2] Data from ICTV, release 2014 (http://www.ictvonline.org/virusTaxonomy.asp).

Morphologically, *Potyviridae* virions are flexuous and filamentous particles composed by protein (about 95% of the particle) and RNA (the remaining 5%) (Fig. I1A). The physical arrangement of the components in the particle is considered to derive from a single copy of viral RNA surrounded by about 2000 units of coat protein (CP) disposed

helicoidally, and with the minority presence of other viral gene products (Gabrenaite-Verkhovskaya et al. 2008; Torrance et al. 2006). In the case of *Bymovirus*, the unique genus with a bipartite genome, each RNA segment is separately encapsidated into two different virions with sizes proportional to the segment lengths.

A unique structural trait used for diagnosis and classification into the family is the presence in the infected cells of cytoplasmatic inclusion bodies, known as “pinwheels” due to their peculiar morphology (Fig. I1B).

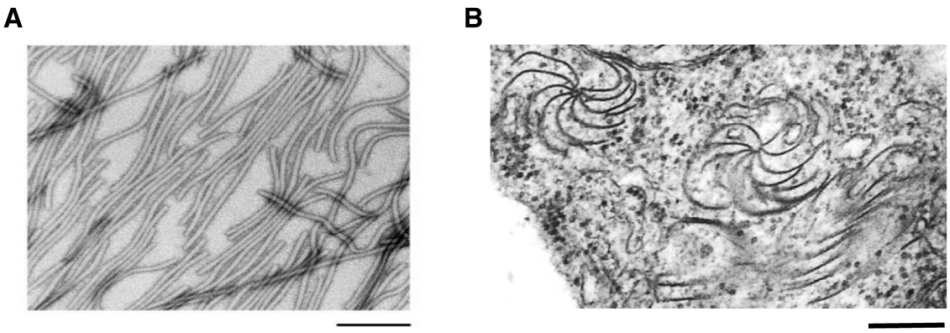

Figure I1: Electron microscopy images of purified virions and structures present in plant cells infected by *Potyviruses*. A) Negative staining of a purified preparation of flexuous virions of *Tobacco etch virus* (TEV) B) Presence of "pinwheel" inclusions in the cytoplasm of a *Nicotiana benthamiana* cell infected by *Plum pox virus* (PPV). Reproduced with permission of D. López-Abella, CIB-CSIC (Madrid, Spain). Bar equals 200 nm.

The genome organization of the monopartite members of the family is based on a unique genomic segment of positive-sense single stranded RNA with a length from 8,2 to 11 Kb. The 5’ end of the genomic RNA is covalently linked to a VPg protein of viral origin, and the 3’ end is polyadenylated. The RNA comprises a large Open Reading Frame (ORF) that encodes for a polyprotein of a significant size (≈350 kDa), flanked by short 5' and 3' untranslated regions. Once translated during the infection process, the polyprotein is cleaved by at least three different endogenous viral proteinases, resulting into a set of mature and multifunctional proteins. At least ten different mature gene products are present in *Potyvirus* members (Fig. I2A), whereas the second gene product denominated HCPro can be either absent or replaced by an extra P1-like proteinase (P1b) in some *Ipomoviruses* (Fig. I2B) (Li et al. 2008; Mbanzibwa et al. 2009; Valli et al. 2006). Interestingly, an extra gene product similar to host pyrophosphatases has been found in some particular viruses (Mbanzibwa et al. 2009). In the case of *Bymoviruses*, the genome is divided into two components encoding for two polyproteins. The first one contains two gene products denominated P2-1 and P2-2 (replacing the common P1 and HCPro), and the other larger genome component encodes products similar to the rest of the common products in the polyprotein, starting at the third P3 protein (Fig. I2C). Another peculiarity found in the *Brambyvirus* type virus is the presence of an AlkB domain within the P1 (Susaimuthu et al. 2008) Finally, a well-conserved second short ORF of around 60 codons, termed PIPO (Pretty

Interesting Potyviral ORF), was predicted to be translated as an overlapping product within the P3 region in all members of the family, yielding a putative product combining the upstream portion of P3 followed by the frameshifted PIPO (P3N-PIPO). This additional gene product was found in plants infected with *Turnip mosaic virus* (TuMV) (Chung et al. 2008).

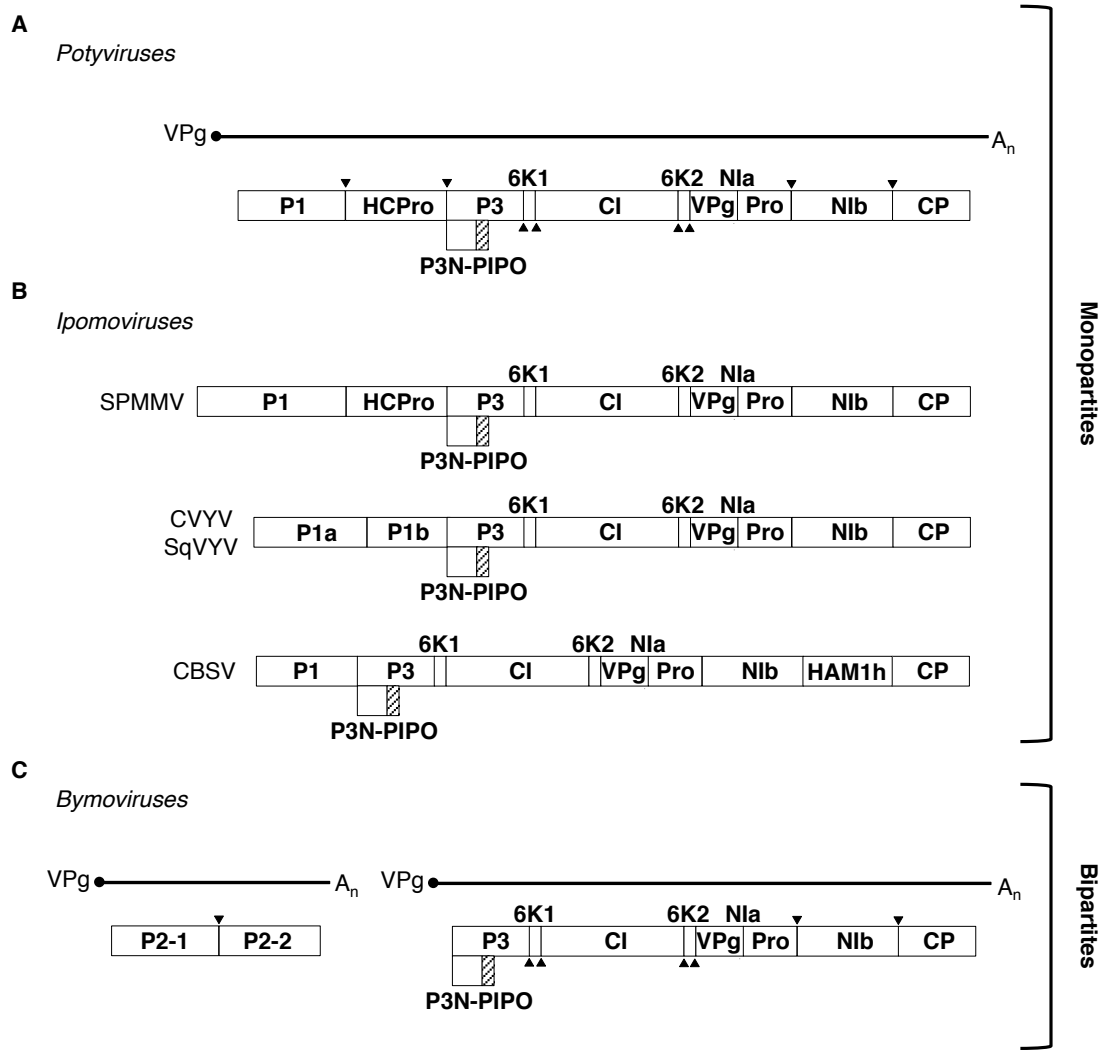

Figure I2: Scheme of *Potyviridae* genomic organizations. Boxes with names represent the different mature gene products. Triangles indicate the catalytic sites in the large polyprotein. A) *Potyviruses* present a single and positive-sense RNA strand translated into a polyprotein with 10 + 1 proteins (in two frames, the large in the 0 frame and the PIPO region in the -1 frame). B) *Ipomoviruses* genomic organization presents peculiarities in the 5' end, where the HCPro is absent or replaced for P1b, and the presence of an additional gene product Maf/HAM1 Pyrophosphatase in CBSV. C) *Bymoviruses* present two single and positive RNA strands translated into two polyproteins. Other minoritary presence of additional gene products or particular domains in certain individual viruses is not depicted (see text for further details).

Focusing in potyviruses, the mature proteins encoded in their genomes develop important functions during the different steps of the infection cycle (Fig. I3) (Ivanov et al. 2014; Riechmann, Laín, and García 1992). If we follow the natural infection process, first the flexuous virions are inoculated in plant cells by aphid vectors, in a process in which both the CP and the HCPro are required (Blanc et al. 1997; Kassanis and Govier 1971; López-Moya, Wang, and Pirone 1999). Following virion uncoating in the cell, potyviral RNA should be translated by the plant machinery. The translated polyprotein is subsequently processed by the 3 viral proteases; P1 and HCPro are able to cleave themselves at their respective C-terminus, and NIa processes the rest of proteins acting both in cis and trans**.** The replication step leads to RNA viral amplification, first synthesizing a negative strand to be used as template for asymmetrical synthesis of abundant positive sense RNA progenies. The synthesis of viral RNAs is carried out by the RNA-dependent-RNA polymerase NIb (Hong and Hunt 1996). NIb synthetizes new RNA strands using VPg as a primer and being helped by the helicase CI that is able to unwind the complementary RNA strands (Laín et al. 1991; Laín, Riechmann, and García 1990; Puustinen and Mäkinen 2004). Once viral RNA is released from viral replication complexes (VRCs), it is exposed to degradation by the RNA silencing pathway. To protect the new RNA, HCPro can suppress the pathway (Kasschau and Carrington 1998). In addition, VPg can act as an auxiliary factor during the suppression of the silencing pathway (Rajamäki and Valkonen 2009). Although the specific mechanism for the cell-to-cell spread of potyviruses is not clear, the involvement of HCPro, P3N-PISPO, CI, VPg and CP in their movement has been reported (Gómez de Cedrón et al. 2006; Rojas et al. 1997; Schaad, Lellis, and Carrington 1997; Wen and Hajimorad 2010). The translation of the new RNA by the plant machinery is enhanced by VPg and P1 (Eskelin et al. 2011; Martínez and Daròs 2014). During the last stages of the infection, the CP is indispensable to encapsidate the RNA in order to form virions (Voloudakis et al. 2004). Moreover, CP is involved in viral transmission by aphids, together with HCPro as mentioned above.

The interest to better understand the infectious cycle of *Potyviruses* has prompted numerous works, and an extensive literature is being published every year. However, there are still many processes not fully understood, and in particular some peculiarities in certain virus members await to be addressed. This is the case of most potyviruses that infect sweet potato plants that will be further described in the next sections.

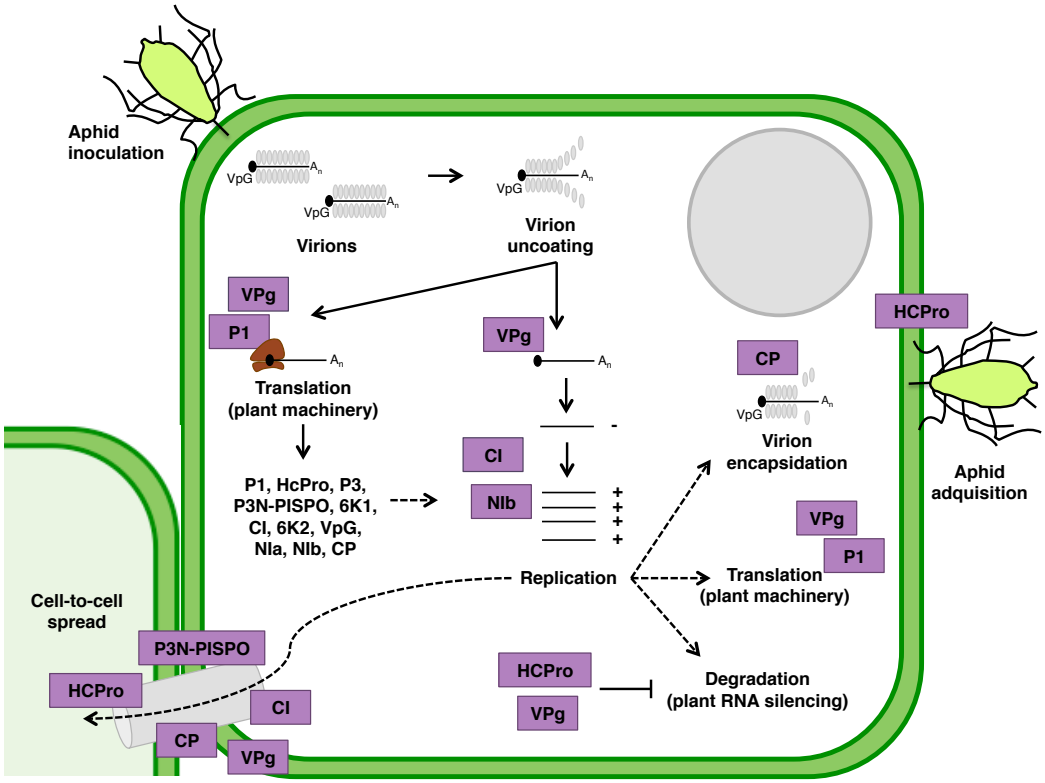

Figure I3: Schematic representation of the involvement of viral proteins during the main steps in the *Potyvirus* infection cycle.

Sweet potato viruses

Sweet potato

Sweet potato (*Ipomoea batatas* (L.) Lam) is one of the oldest domesticated crops. Some data suggest that it might has been originated in the Americas from the wild ancestor *I. trífida* (Roullier et al. 2013; Srisuwan, Sihachakr, and Siljak-Yakovlev 2006). In the 16th century, it was introduced in Europe and later spread to Asia (Loebenstein and Thottappilly 2009).

Taxonomically, *I. batatas* belongs to the genus *Ipomoea* within the *Convolvulaceae* family. Botanically, the plant is a herbaceous perennial vine with heart-shape or palmately-lobed simple leaves, sympetalous flowers and an edible tuberous root (Mohanraj and Sivasankar 2014). This storage root has a smooth skin and its flesh colour can be white, red, pink, violet, yellow, orange, or purple (Mohanraj and Sivasankar 2014). From the genetic point of view, sweet potato presents a large and hexaploid genome (Ozias-Akins and Jarret 1994). Curiously, it has been recently reported as a natural transgenic plant, in view of the presence of *A. tumefaciens* regions inserted in its genome (Kyndt et al. 2015).

From the agronomical point of view, sweet potato is grown as an annual plant mainly propagated by vegetative means using stem cuttings or storage roots. It has a fast growing cycle, needs little care and presents tolerance to severe hot weather (Loebenstein and Thottappilly 2009). Due to its easy management, sweet potato is among the major food crops, especially in developing countries. According to FAOSFAT data, in 2014 the worldwide sweet potato production was 104 million tonnes. The main producer was Asia with 76% of the production followed by Africa with 20%. In Figure I4, the production per country is represented. Sweet potato cultivation is poorly technified in developing countries, whereas USA is one of the few countries to grow it extensively (Gibson and Kreuze 2014).

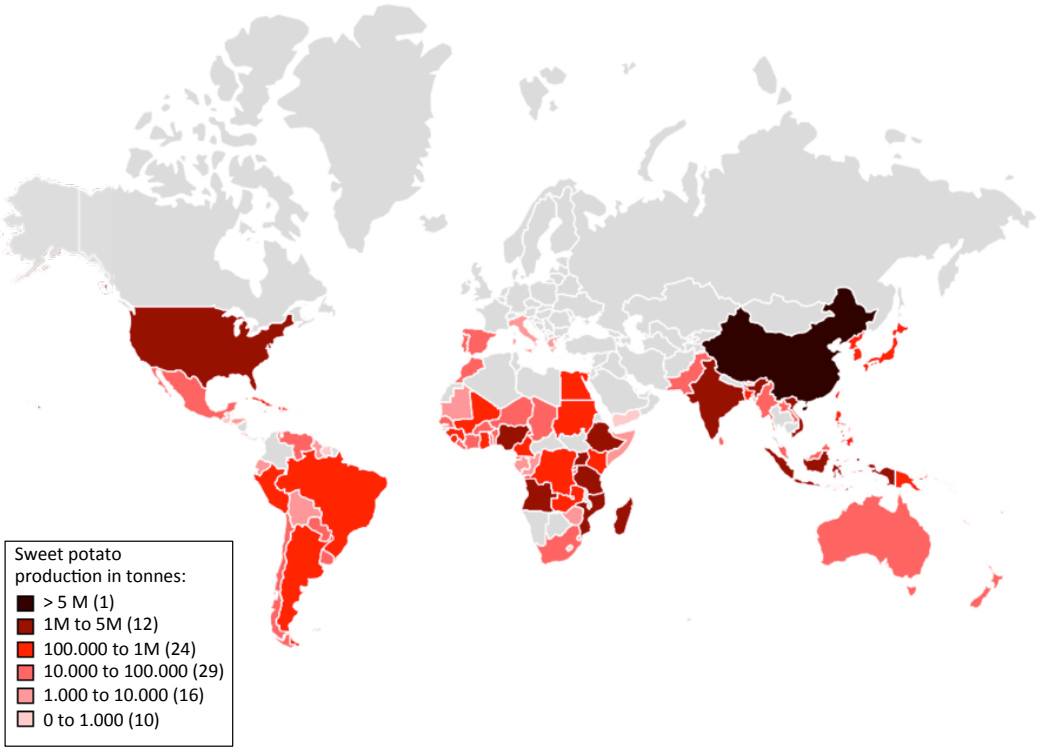

Figure I4: Representation of Sweet potato production worldwide. Data from FAOSFAT, 2014 (http://faostat3.fao.org/download/Q/QC/E). Scale in tonnes.

Sweet potato is mostly used for human consumption and animal feeding. It also has potential to develop bio-processing products like bio-ethanol (El Sheikha and Ray 2015). For humans, it is an important crop for food security and it is used as staple food thanks to its high nutritional value. The root is rich in carbohydrates, dietary fiber, vitamins and minerals (Laurie et al. 2015). Moreover, the high beta-carotene (vitamin A precursor) content of orange-fleshed roots converts this crop in a highly valuable mean to fight malnutrition and vitamin A deficiency (Burri 2011). Finally, sweet potato possesses some pharmacological properties that can contribute to fight against important diseases such as ulcers, diabetes and even cancer (Mohanraj and Sivasankar 2014).

Viral diseases affecting sweet potato crops

Because sweet potato plants are vegetatively propagated in most cases, it is not a surprise that viruses cause the principal diseases of this crop. As a further consequence of this, most viruses are widespread all over the world, being found frequently in every region. The recent advances in molecular techniques have allowed to identify over 30 different sweet potato infecting viruses (Clark et al. 2012) (Table I2). The presence of CMV, a virus with very wide host range, has been found in Egypt and Israel (Clark et al. 2012; Cohen and Loebenstein 1991). Recently, several DNA viruses belonging to *Geminiviridae* and *Caulimoviridae* families have been identified (Kreuze et al. 2009; Lotrakul et al. 2002; Lozano et al. 2009; De Souza and Cuellar 2011). However, they are mostly symptomless and their effects on growth and yield are in many cases unknown. Another common family is the *Potyviridae* one, where the potyvirus SPFMV and the ipomovirus SPMMV are the most relevant viruses (Colinet, Kummert, and Lepoivre 1996; Liao et al. 1979; Qin et al. 2013; Untiveros, Fuentes, and Kreuze 2008). Finally, the crinivirus SPCSV is considered the most damaging virus of sweet potato when combined with other viruses, showing peculiar synergistic effects during mixed infections with unrelated viruses (Kreuze, Savenkov, and Valkonen 2002; Mukasa, Rubaihayo, and Valkonen 2006). In fact, and despite the rather long list of viruses infecting sweet potato plants, only a few produce important economical losses in this crop. This is the case of Sweet potato viral disease (SPVD), a synergism between the crinivirus SPCSV and the potyvirus SPFMV (Gibson et al. 1998). This disease has been reported that can cause yield losses of up 80 to 90% in sweet potato fields (Karyeija, Gibson, and Valkonen 1998).

Nowadays, there are not control strategies adequate to eliminate completely viral infections in sweet potatoes. However, some management approaches are carried out in fields to reduce the impact of viral diseases:

a) Sanitation and use of virus-free propagation materials, usually obtained by meristem-tip culture (Alconero et al. 1975), coupled sometimes to thermotherapy treatments (Walkey and Cooper 1975). Recently, a novel therapy based on cryotherapy of shoot tips has been introduced (Wang et al. 2009). Normally, almost virus-free material is obtained with these treatments. However, they are expensive and the plants can be re-infected once they are exposed to field conditions (Gibson and Kreuze 2014). Although China and developed countries frequently tend to use virus-free material to start their crops, in many places in Africa and other developing countries the governments do not have well-established programs. In this case, even if farmers intuitively try to select healthy-looking cuttings as a starting material, the presence of viruses is rather frequent (Clark et al. 2012).

b) Quarantine programs avoid the introduction and prevent the dissemination of viruses between countries. For sweet potato viruses, the programs adopted are the Technical Guidelines for the Safe Movement of Sweetpotato Germplasm (FAO publication), International Board for Plant Genetic Resources (IBPGR) and CIP-Sweetpotato Action for Security and Health in Africa (SASHA) guidelines (Clark et al. 2012).

c) Breeding programs. The search for cultivars with natural viral resistance has been especially focused in the causal agents of SPVD. For example, a sweet potato breeding program in Uganda have obtained different cultivars with a high yield and SPVD resistance (Mwanga et al. 2003).

d) Engineered resistance. Although some approaches have been adopted to obtain transgenic plants with viral resistance, the partial resistance achieved is in most cases superated in fields by resistant-breaking virus strains (Cipriani et al. 2000; Kreuze et al. 2008).

Sweet potato viral disease (SPVD)

As aforementioned, SPVD is the most important viral disease of sweet potato, resulting of a synergism between SPFMV (Fam. *Potyviridae*, Genus *Potyvirus*) and SPCSV (Fam. *Closteroviridae*, Genus *Crinivirus*). Sweet potato plants infected by both viruses present severe symptoms characterized by leaf distortion and crinkling, general chlorosis, and severe stunting of their development. As a consequence, SPVD causes several damage in sweetpotato crops and significantly reduces yield production (Gutiérrez, Fuentes, and Salazar 2007).

Usually, *Potyviruses* synergize with other unrelated viruses, causing an increase in the viral titers of the unrelated virus, most likely thanks to the effect on suppression of RNA silencing by the potent HCPro protein of potyviruses (González-Jara et al. 2005; Pruss et al. 1997). However, in the SPVD the synergism works in the opposite direction, being the potyvirus partner SPFMV the one that shows tremendous increases in titer, that can reach up to a 600 fold increase in accumulation (Gibson et al. 1998; Karyeija et al. 2000). Some data suggests that the beneficial effect on SPFMV accumulation is due to the action of the SPCSV RNase III. This RNase III is a viral product with nuclease activity, able to cleave viral small interfering RNAs (vsiRNAs) in order to suppress RNA silencing (Cuellar et al. 2009). Further or this, a similar kind of synergism has been reported between SPCSV and several other viruses like the ipomovirus SPMMV and even with sweet potato begomoviruses (Cuellar et al. 2015; Mukasa et al. 2006; Untiveros, Fuentes, and Salazar 2007) (Table I2).

Table I2: Description of viruses that infect sweet potato (Adaptation of Clark *et al*. 2012)

Family	Genus	Virus	Acronym	Vector	Synergism with SPCSV
Bromoviridae	*Cucumovirus*	*Cucumber mosaic virus*	CMV	Aphid	Yes[1]
Potyviridae	*Potyvirus*	*Sweet potato feathery mottle virus*	SPFMV	Aphid	Yes[2, 3]
Potyviridae	*Potyvirus*	*Sweet potato latent virus*	SPLV	Aphid	Yes[1]
Potyviridae	*Potyvirus*	*Sweet potato virus 2*	SPV2	Aphid	Yes[4]
Potyviridae	*Potyvirus*	*Sweet potato virus C*	SPVC	Aphid	Yes[4]
Potyviridae	*Potyvirus*	*Sweet potato virus G*	SPVG	Aphid	Yes[4]
Potyviridae	*Potyvirus*	*Sweet potato mild speckling virus*	SPMSV	Aphid	Yes[1]
Potyviridae		Sweet potato vein mosaic virus	SPVMV	Aphid	
Potyviridae	*Ipomovirus*	*Sweet potato mild mottle virus*	SPMMV	Whitefly?	Yes[1, 5]
Potyviridae	*Ipomovirus*	Sweet potato yellow darf virus	SPYDV		
Closteroviridae	*Crinivirus*	*Sweet potato chlorotic stunt virus*	SPCSV	Whitefly	
Geminiviridae	*Begomovirus*	*Ipomoea yellow vein virus*	IYVV	Whitefly	
Geminiviridae	*Begomovirus*	*Sweet potato leaf curl virus*	SPLCV	Whitefly	Yes[6]
Geminiviridae	*Begomovirus*	*Sweet potato leaf curl Canary virus*	SPLCCaV	Whitefly	
Geminiviridae	*Begomovirus*	*Sweet potato leaf curl China virus*	SPLCV-CN		
Geminiviridae	*Begomovirus*	*Sweet potato leaf curl Georgia virus*	SPLCGV	Whitefly	Yes[6]
Geminiviridae	*Begomovirus*	*Sweet potato leaf curl Lanzarote virus*	SPLCLaV	Whitefly	
Geminiviridae	*Begomovirus*	*Sweet potato leaf curl Spain virus*	SPLCESV	Whitefly	
Geminiviridae	*Begomovirus*	Sweet potato leaf curl South Carolina virus	SPLCSCV	Whitefly	Yes[6]
Geminiviridae	*Begomovirus*	Sweet potato leaf curl Uganda virus	SPLCYV	Whitefly	
Geminiviridae	*Begomovirus*	Sweet potato mosaic associated virus	SPMaV		
Geminiviridae	*Mastrevirus*	*Sweet* potato symptomless virus 1	SPSMV-1		
Caulimoviridae	*Badnavirus*	Sweet potato papakuy virus= Sweet potato badnavirus A/B	SPPV		
Caulimoviridae	*Cavemovirus*	Sweet potato collusive virus= Sweet potato caulimo-like virus	SPCV		Yes[7]
Caulimoviridae	*Solendovirus*	Sweet potato vein clearing virus	SPVCV		
Flexiviridae	*Carlavirus*	*Sweet potato chlorotic fleck virus*	SPCFV		Yes[8]
Others	Others	Sweet potato virus C-3 and C-6, *Sweet potato chlorotic fleck virus, Sweet potato leaf speckling virus,* Sweet potato ringspot virus			

[1](Untiveros et al. 2007) [2](Gibson et al. 1998) [3](Karyeija et al. 2000) [4](Kokkinos and Clark 2006) [5](Mukasa et al. 2006) [6](Cuellar et al. 2015) Isolates with sequence similarity to these begomoviruses. [7](Cuellar et al. 2011) Members of the *Cavemovirus* genus. [8](Cuellar et al. 2009)

Sweet potato feathery mottle virus (SPFMV)

SPFMV belongs to the *Potyvirus* genus. It has been found infecting sweet potato plants in almost all regions where they are cultivated (Clark et al. 2012). The first reports of the presence of the virus dates from the 50s in East African countries (Sheffield 1957). The host range of SPFMV seems to be limited to members of the *Convolvulaceae* family. Apart from sweet potato crops, a set of wild species has been identified as susceptible to the virus. These wild species may act as SPFMV reservoirs in Africa (Tugume, Mukasa, and Valkonen 2008). *Nicotiana benthamiana* and *Chenopodium quinoa* can be used as experimental hosts. In single infections, SPFMV titers are generally low, and the virus can induce only mild symptoms, or even no symptoms at all, affecting more severely the old leaves, and only in some specific strains can affect also the roots (Clark et al. 2013). Nevertheless, as it was mentioned above, the symptoms are exacerbated greatly when SPFMV is in co-infection with SPCSV. SPFMV is transmitted by different aphids in a non-persistent manner, requiring short periods of time for acquisition and inoculation (Sheffield 1957; Stubbs and McLean 1958). The aphids normally do not colonize sweet potato plants, and vector specificity exists between different SPFMV strains (Byamukama et al. 2004; Wosula, Clark, and Davis 2012).

Initially, SPFMV isolates were grouped into 4 different strains: East African (EA), russet crack (RC), ordinary (O) and common (C) (Kreuze et al. 2000). Recently, C strains have been reclassified as a new virus specie named SPVC (Untiveros, Quispe, and Kreuze 2010). Together with SPFMV; SPVC, SPVG, SPV2 are considered distinct potyviruses that share a high sequence homology. They have been proposed to comprise the separated SPFMV phylogenetic lineage (Li et al. 2012; Untiveros et al. 2008). Recombination is frequent between SPFMV lineage species, as well as between SPFMV strains (Tugume et al. 2010; Untiveros et al. 2008).

The reference genome of SPFMV (NC_001841.1) is 10820 nucleotides long with an ORF that encodes the typical potyviral polyprotein: P1 (74K), HCPro (52K), P3 (46K), 6K1, CI (72K), 6K2, NIa-VPg (22K), NIa-Pro (28K), NIb (60K) and CP (35K) (Sakai et al. 1997). The P1 region has 664 amino acid residues, resulting in one of the largest proteins in the *Potyvirus* genus, only superated by similar products in the ipomovirus SPMMV and the brambyvirus BVY. While the C-terminal part of P1 (P1-C) is similar to other potyviruses, the N-terminal part (P1-N) only shows homology with the P1-N of the ipomovirus SPMMV (Untiveros et al. 2010). This similarity has been also confirmed in the other members of SPFMV-lineage, whereas this “unique” P1-N is not found in other sweet potato potyvirus such as SPLV (Clark et al. 2012; Li et al. 2012; Wang et al. 2013). Furthermore, a new overlapping short ORF termed PISPO (Pretty Interesting Sweet potato Potyviral ORF) was predicted by bioinformatic analysis within the P1-coding sequence of a few members of the *Potyvirus* genus, all related to SPFMV,

including SPVG and SPV2, with the notable exception of SPLV (Clark et al. 2012; Li et al. 2012; Wang et al. 2013). In the reference genome of SPFMV, the PISPO sequence is nested in the -1 frame (relative to the polyprotein ORF) within the P1-coding region (positions 118 to 2109), which corresponds to the first N-terminal gene product of the large polyprotein (ORF from position 118 to 10599). The PISPO sequence begins at position 1382 and spans 690 nucleotides from the GGAAAAAA (G_2A_6) motif. This motif is identical to the conserved consensus sequence for the PIPO frameshifting, which in SPFMV gives rise to a shorter coding sequence, also in the -1 frame (Fig. I5).

Figure I5: Genomic organization of the SPFMV genome with the three ORFs corresponding to the polyprotein, PISPO, and PIPO depicted as boxes (details of the conserved G_2A_6 motifs are shown). Boxes with names represent the different gene products.

P1 of SPMMV has been characterized as a silencing suppressor. Actually, the suppressor activity was associated to the presence in the N-terminal part of 3 WG/GW motifs that mediate the interaction with Argonaute 1 (AGO1) (Giner et al. 2010). A later report showed that SPFMV P1, which contains less WG/GW in the N-terminal part, lacked silencing suppressor activity but it could be transformed into a RSS by the introduction of two extra WG/GW motifs (Szabó et al. 2012). Curiously, the translation of PISPO would provide extra WG/GW motifs to the alternative trans-frame product, as noted by the authors that proposed its presence (Clark et al. 2012; Li et al. 2012).

Expression of viral overlapping reading frames

The size of viral genomes is considered limited by different constraints, such as the volume available in viral particles, and other considerations of efficiency and economy of resources. Consequently, viruses are under strong selective pressure to optimize their coding capacity in their small genomes. To achieve this, viruses often use overlapping reading frames to express multiple proteins from a single nucleic acid sequence. Two different mechanisms have been proposed to change the ORF and to express trans-framed proteins overlapping in the genome. While Ribosomal frameshifting occurs at translational level (Fig. I6A), Polymerase slippage takes place during transcription (Fig. I6B).

Ribosomal frameshifting (RF) consists in redirecting the ribosomes to shift into an alternative reading frame in the 5' (-1 frameshifting) or 3' (+1 frameshifting) positions relative to the main ORF, resulting in the translation of trans-framed proteins (Dinman 2012). The elements required for an efficient -1 RF are: a slippery site where the ribosome shifts, a downstream stimulatory structure and a short sequence (<12nt) to create space between them (Firth and Brierley 2012). In viruses, the slippery site is often a heptameric motif with X_XXY_YYZ sequence(Brierley, Jenner, and Inglis 1992). The stimulatory structure, usually an mRNA pseudoknot, provides a barrier to pause ribosomes and tRNAs over the slippery site (Giedroc and Cornish 2009). The -1 RF has been identified in several animal viruses as well as in positive strand RNA plant viruses (Barry and Miller 2002; Brierley et al. 1992; Jacks et al. 1988). On the other hand, the +1 RF is not so common and its mechanism is less understood. Some reports suggest that +1 RF is stimulated by the presence of rare codons that cause a pause in decoding, slowing down the speed of translation allowing the ribosomal frameshifting (Dinman 2012). Only a few cases have been reported for +1 RF in viruses (Auzat et al. 2008; Jagger et al. 2012).

Polymerase slippage results in the synthesis of a heterogeneous RNA population. The polymerase slips in a region of repeated nucleotides, preferentially 'A's or 'U's, introducing extra nucleotides or deleting them in just a portion of RNA transcripts. In viruses, this mechanism leads to the translation of different proteins with different proportions from a given RNA (Baranov et al. 2005). Monopartite negative-strand RNA viruses from *Paramyxovirinae* subfamily use this strategy to introduce one or more extra Gs at the 3'-U*n*C*m*-5' specific site of phosphoprotein mRNA (Kolakofsky et al. 2005). Polymerase slippage has been also well characterized in RNA viruses affecting mammals such *Ebolavirus* (EBOV) (Shabman et al. 2014; Volchkov et al. 1995) or *Hepatitis C virus* (HCV) (Ratinier et al. 2008), where extra 'A's are inserted in motifs with repeated 'A's.

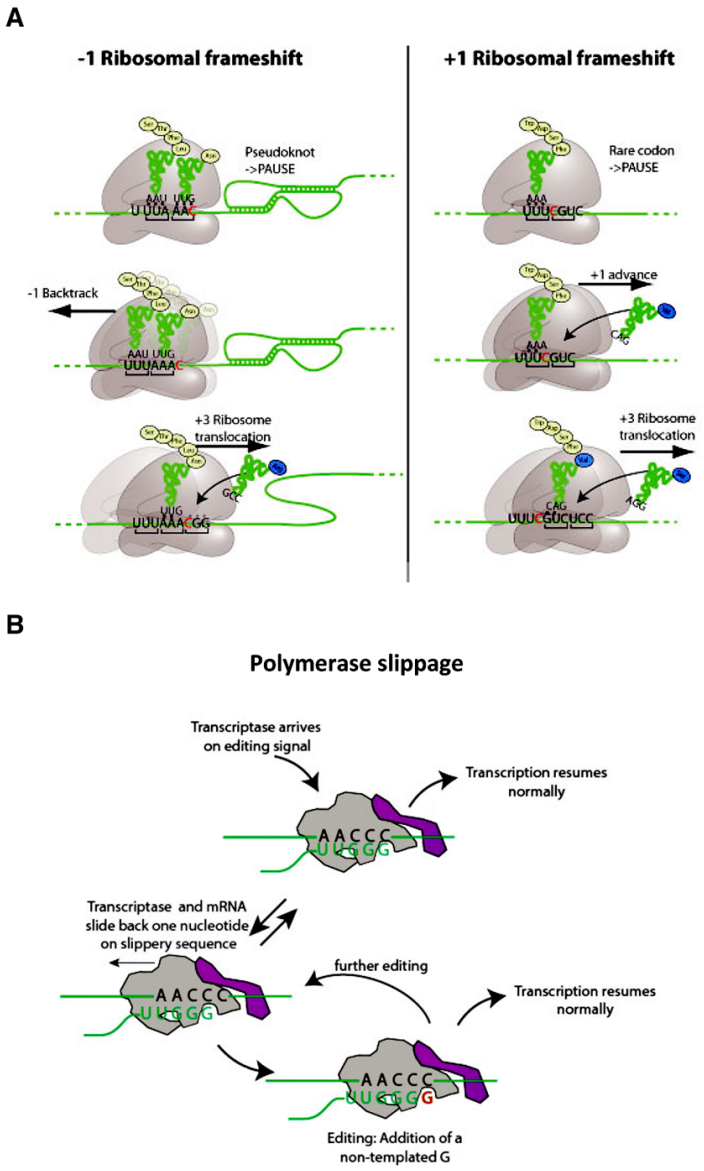

Figure I6: Mechanism to express trans-framed proteins from overlapping reading frames. A) Ribosomal frameshifting B) Polymerase slippage. Pictures from Viral Zone web http://viralzone.expasy.org).

When the work of this thesis was initiated, the mechanism leading to expression of trans-frame ORFs in potyviruses was unknown, and the two alternatives (ribosomal frameshifting or polymerase slippage) were mentioned as equally possible in the paper describing the presence of P3N-PIPO during TuMV infection (Chung et al. 2008).

Induction and suppression of silencing by plant viruses

RNA silencing refers to an evolutionary conserved system that controls gene expression through sequence-specific RNA neutralization by smallRNAs. This system is present in most eukaryotic organisms, playing important roles in different biological processes such as development genome integrity and host defence against viruses and transposons (Valli, López-Moya, and García 2009; Vargason, Burch, and Wilson 2013).

The antiviral function of RNA silencing was discovered in plants (Hamilton and Baulcombe 1999), but it is also present in insects (Li, Li, and Ding 2002), nematodes (Lu et al. 2005; Wilkins et al. 2005), fungi (Segers et al. 2007), and under certain circumstances it has been also proposed in mammals (Li et al. 2013; Maillard et al. 2013). This defensive strategy relies on the accumulation of viral small interference RNAs (vsiRNAs) originated from the infecting virus, which have the ability to degrade the complementary viral RNA (Valli et al. 2009). Viruses, in turn, have developed a counter-defensive strategy based on viral suppressors of RNA silencing (RSSs) able to block or interfere with the host-silencing pathway (Csorba, Kontra, and Burgyán 2015).

This part of the introduction is focussed on plant viruses, providing an overview of the plant antiviral silencing pathway and summarizing the current knowledge about the viral strategies used to overcome this defence strategy during their infectious cycles.

Antiviral RNA silencing pathway in plants

All RNA silencing pathways, including the antiviral one, share a core machinery with several essential components, with their actions being triggered by the presence of double-stranded RNAs (dsRNAs) precursors. These dsRNAs are processed by RNase III-like enzymes belonging to the Dicer family (DCLs) that produce short RNA duplexes (21-24 nt). Moreover, a second round of these duplexes might derive from new dsRNAs, synthetized by RNA-dependent RNA polymerases (RDRs). The processed sRNA duplexes are recruited by Argonaute proteins (AGOs), assembling into complexes able to target complementary RNA/DNA sequences by different mechanisms (Bologna and Voinnet 2014). Figure I7 shows a schematic view of the plant antiviral RNA silencing pathway and its components.

The core components of the silencing machinery are DCL, RDR and AGO proteins, with some accessory factors participating as well. In the model plant *Arabidopsis thaliana,* 4 DCLs, 10 AGOs and 6 RDRs are present in the genome and they play roles in the different pathways in a specific or redundant way (Csorba et al. 2015). Next, we will

detail the roles of these that are involved in the different phases of antiviral silencing pathway.

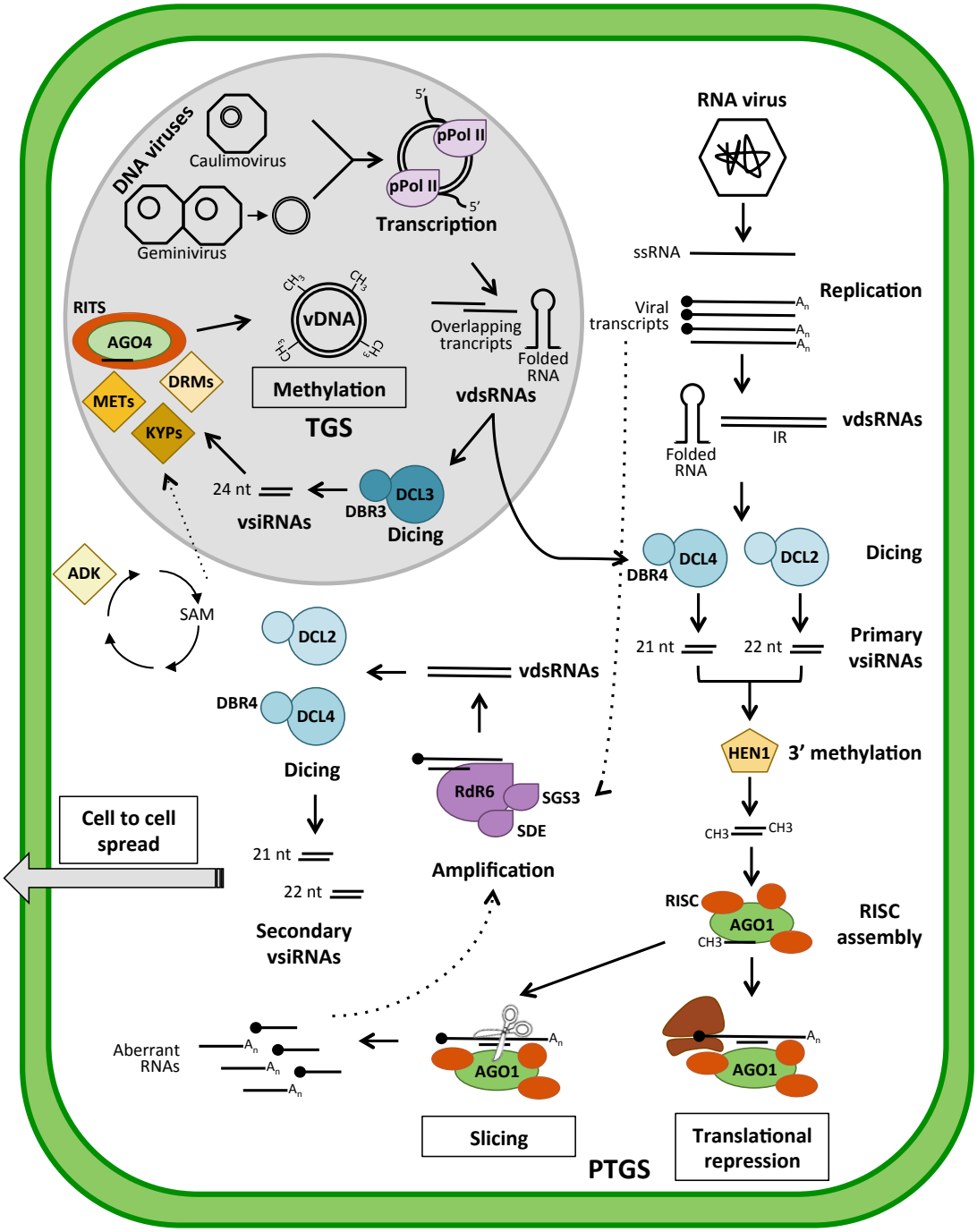

Figure I7: Schematic representation of the antiviral silencing pathway in plant cells. The main components involved in the different steps of the general pathway are represented, as well as some of their predicted functions against RNA and DNA plant viruses.

vsiRNAs biogenesis

The biogenesis of viral small RNAs (vsiRNAs) is analogous to that of endogenous plant small RNAs, consisting in two well-differentiated phases. The initiation phase gives rise to the production of primary vsiRNAs through DCLs action. After viral replication, the amplification phase, mediated by RDRs and DCLs enzymes, result in a secondary production of vsiRNAs (Zhang et al. 2015).

Initiation phase (DCLs, recognition and processing)

Upon virus infection, viral dsRNA molecules are present in the infected cell and can be used as a source substrate for DCLs to generate primary vsiRNAs. In the case of single positive strand RNA (+ssRNA) viruses the origin of dsRNAs could rely on replicative intermediates (Ahlquist 2002), and also most likely in highly specific folded regions of the viral RNA (Donaire et al. 2008, 2009; Molnár et al. 2005; Szittya et al. 2010; Xu et al. 2012). For DNA viruses, dsRNAs might have their origin in overlapping bidirectional transcripts (Aregger et al. 2012; Chellappan et al. 2004), or in highly structured regions, as in the case of the 35S major RNA transcript of *Cauliflower mosaic virus* (Blevins et al. 2011).

DCLs, helped by Double-stranded RNA binding proteins (DBRs), recognize viral dsRNAs in a hierarchical manner and process them into vsiRNAs of different lengths (DCL4 mainly produces siRNAs of 21 nt, DCL2 of 22nt, and DCL3 of 24 nt) (Zhang et al. 2015). During infections of viruses with +ssRNA genomes, DCL4 appears to be the main producer of vsiRNAs, whereas DCL2 can replace DCL4 when its activity is reduced or suppressed (Bouché et al. 2006; Deleris et al. 2006; Du et al. 2007; Fusaro et al. 2006; Garcia-Ruiz et al. 2010; Qu, Ye, and Morris 2008). Furthermore, DCL2 can be the responsible of vsiRNAs generation from specific viral regions (Donaire et al. 2008). Although DCL3 can act in some particular cases, its role seems to be less relevant (Azevedo et al. 2010; Diaz-Pendon et al. 2007; Donaire et al. 2008; Qu et al. 2008). Finally, DCL1 can act as negative regulator of DCL3 and DCL4 expression, repressing the antiviral silencing response (Qu et al. 2008). Regarding viruses with DNA genomes, all four DCLs seem to be involved in the vsiRNA production. DCL2, DCL3 and DCL4 are direct generators of siRNAs, whereas DCL1 can only process viral dsRNAs in some particular cases. Moreover, DCL1 can play an additional role, facilitating the other DCLs tasks (Akbergenov et al. 2006; Aregger et al. 2012; Blevins et al. 2006).

Others actors are involved in vsiRNAs production. The interaction between DCLs and DBRs enzymes is necessary to reach an optimal production. The DBR4/DCL4 pair has been reported in infections of both DNA/RNA viruses (Haas et al. 2008; Qu et al. 2008) and the cooperation of DBR3 with DCL3 seems to be relevant during the geminiviruses

genome methylation (Raja et al. 2014). Interestingly, a recent report suggests a possible role of Rnase three-like 1 (RTL1) enzyme during the initiation phase. RTL1, a RNase-III enzyme without DCL-specific domains, could act degrading dsRNA intermediates of viral replication (Shamandi et al. 2015).

Once vsiRNAs are generated, HUA enhancer 1 (HEN 1) is the responsible of their methylation and stabilization at their 3' end (Blevins et al. 2006; Boutet et al. 2003; Lózsa et al. 2008; Zhang et al. 2012). Then, they will trigger one of two different silencing responses. The vsiRNAs produced by DCL2 and DCL4 will lead a Post-transcriptional gene silencing (PTGS) response, whereas vsiRNAs derived from DCL3 are involved in Transcriptional gene silencing (TGS) (Raja, Wolf, and Bisaro 2010; Rodríguez-Negrete, Carrillo-Tripp, and Rivera-Bustamante 2009).

Amplification phase (RDRs + DCLs)

During the amplification phase, plant RDRs polymerases trigger the synthesis of viral dsRNAs precursors, which will act as a DCLs substrates for the secondary vsiRNAs production (Zhang et al. 2015).

To generate viral dsRNAs precursors, RDRs used as template aberrant viral RNAs that lacked features like the 5' cap or the polyA tail (Donaire et al. 2008; Gazzani et al. 2004; Luo and Chen 2007; Moreno et al. 2013; Voinnet 2008). Some reports suggest that aberrant RNAs come from cleaved viral fragments, targeted by primary vsiRNAs loaded in AGO proteins (Mallory and Vaucheret 2009; Moissiard et al. 2007). On the other hand, primary vsiRNAs could be acting as primers in the amplification event (Moissiard et al. 2007). In RNA viruses, it has been well demonstrated the implication of RDR1, RDR2 and RDR6 in the amplification (Diaz-Pendon et al. 2007; Donaire et al. 2008; Garcia-Ruiz et al. 2010; Lee et al. 2016; Qu et al. 2008; Schwach et al. 2005; Wang et al. 2010; Xie et al. 2001; Yu et al. 2003), whereas in DNA viruses it seems that viral transcripts appear to be poor templates for RDRs (Aregger et al. 2012). The efficient action of RDRs requires interaction with cofactors such as trafficking proteins (SDE3, SDE5) and blockers of RNA degradation (SGS3) (Dalmay et al. 2001; Kumakura et al. 2009; Mourrain et al. 2000; Wang et al. 2011). Afterwards, DCL4 and DCL2 might process these dsRNAs, generating a batch of secondary vsiRNAs (Parent et al. 2015; Wang et al. 2010).

From the point of view of biological relevance, it is thought that the amplification phase might lead to a systemic response, immunizing non-infected tissues and therefore preventing the spread of the infection (Qu et al. 2005; Ruiz-Ferrer and Voinnet 2009; Schwach et al. 2005).

Effector phase (AGOs + RISC complex)

DCLs action has an impact in the directly degradation of viral RNAs, thus the vsiRNAs produced are required to develop the effector phase and avoid the spread of the infection (Carbonell and Carrington 2015; Valli et al. 2009). During the effector phase, a vsiRNA strand is loaded into an Argonaute protein. The 5' terminal nucleotides and thermodynamical properties of the siRNA duplex appear to determine the loading of the guide strand into an specific Argonaute (Mi et al. 2008; Schuck et al. 2013; Schwarz et al. 2003). The RISC activated complexes generated are able to target for degradation and/or silence the translation of the viral complementary RNA in a sequence specific manner (Carbonell and Carrington 2015).

RNA induced silencing complexes (RISCs) mediate a post-transcriptional gene silencing (PTGS) response through endonucleotydic cleavage (slicing) or translational repression of RNA (Martínez de Alba, Elvira-Matelot, and Vaucheret 2013). In plants, the slicing of viral RNAs seems to be the main PTGS mechanism, whereas translational repression has been reported only in the AGO1 silencing response against ToRSV, and also suggested in potyviral infections (Ghoshal and Sanfaçon 2014; Ivanov et al. 2016). The capacity to recruit vsiRNAs has been reported for *Arabidopsis* AGO1, AGO2, AGO5, AGO7 and AGO10 (Carbonell, Fahlgren, et al. 2012; Garcia-Ruiz et al. 2015; Qu et al. 2008; Takeda et al. 2008) and rice AGO1 and AGO18 (Du et al. 2011 a; Wu et al. 2015). AGO1 has been described as the main antiviral slicer against many RNA viruses (Carbonell, Fahlgren, et al. 2012; Morel et al. 2002; Qu et al. 2008; Wang et al. 2011), being itself controlled by the action of miR168 (Rhoades et al. 2002; Vaucheret et al. 2004). Although AGO2 acts as a second antiviral layer in the absence of AGO1, recent observations have confirmed that AGO2 can adopt the role of the main slicer in viruses where AGO1 activity is compromised (Garcia-Ruiz et al. 2015; Harvey et al. 2011; Ma et al. 2015; Scholthof et al. 2011; Wang et al. 2011; Zhang et al. 2012). The other Argonaut proteins (AGO5, AGO7 and AGO10) contribute to the antiviral defence as minor players. For example, AGO7 targets less structured RNAs than AGO1, AGO5 can restrict specifically PVX infection and AGO10 can act in some specific tissues (Brosseau and Moffett 2015; Garcia-Ruiz et al. 2015; Qu et al. 2008). Taken all together, these results suggest that AGO proteins work coordinately and cooperatively during viral infection.

In the other hand, transcriptional gene silencing (TGS) consists on the methylation of histone or the homologous DNA by RNA induced transcriptional silencing (RITS) complexes (Creamer and Partridge, 2011). These complexes contain AGO4 and a viral guide strand processed by DCL3/DBR3 (Raja et al. 2014). Together with other components and enzymes of the methylation pathways (DRMs, METs, KYPs, ADKs…), RITS complexes can guide the methylation of DNA viral genomes (Raja et al. 2010). This

epigenetic component of the defence response has been reported in several geminiviruses (Raja et al. 2008, 2014; Rodríguez-Negrete et al. 2009).

Induction of silencing to indirectly promote defence responses

Plants can directly use the silencing pathway to inactivate viral genomes. However, the silencing machinery can be associated as well with endogenous small RNAs to regulate gene expression and indirectly promote antiviral defence, among other processes (Carbonell and Carrington 2015).

In the defence against CMV, the association of endogenous siRNAs with AGO4 was proposed. More recently, this hypothesis has been supported by the identification of virus-activated small interfering RNAs (vasiRNAs), a new class of sRNAs present during CMV infection as well as TuMV infection (Cao et al. 2014). Viruses induce the production of a vasiRNAs population that largely map in genes related with stress responses, among others. They are active in directing the widespread silencing of certain target genes (Cao et al. 2014).

In rice, it has been proposed that viral infection by RSV and RDV can be regulated through the accumulation of AGO18. In turn, AGO18 sequesters mir168 and triggers the accumulation of AGO1. This plant mechanism confers a broad-spectrum viral resistance (Wu et al. 2015).

Viral counter-defence strategy against the host plant defences

Plant viruses have co-evolved establishing strategies to fight against the antiviral silencing pathway. Nowadays, the best well-known strategy is the suppression of this pathway through viral RNA silencing suppressors (RSSs). During more than a decade, plant virologists have identified many RSSs and studied their mechanisms of action. Indeed, they can interfere with almost all pathway steps, sometimes specifically or even at multiple levels, being AGO proteins and vsiRNAs the most frequently targeted elements. In this part, we will try to summarize all the knowledge that has been described so far in different viral pathosystems. We will describe the RSSs and their mode of action for several viruses (Fig. I8). Also, we will include a revision of the viral capacity to silence other plant transcripts. Table I3 list all the viruses described in this part and Table I4 contains a summary of the different RSSs and their modes of action.

Table I3: List of viruses and their acronyms, which RSS are described in the text. The list is ordered alphabetically.

Acronym	Virus
BCTV	*Beet curly top virus*
BMYV	*Beet western yellows virus*
BSCTV	*Beet severe curly top virus*
BYV	*Beet yellows virus*
CABYV	*Cucurbit aphid-borne yellow virus*
CaLCuV	*Cabbage Leaf Curl Virus*
CaMV	*Cauliflower mosaic virus*
CIRV	*Carnation Italian ringspot virus*
CMV	*Cucumber mosaic virus*
CMV Y-sat	*Cucumber mosaic virus Y satellite*
CVYV	*Cucumber vein yellow virus*
CymRSV	*Cymbidium ringspot virus*
GFkV	*Grapevine fleck virus*
GRSPaV	*Grapevine rupestris steem pitting-associated virus*
GVA	*Grapevine virus A*
LNYV	*Lettuce necrotic yellows virus*
PEMV-1	*Pea enantion mosaic virus-1*
PFBV	*Pelargonium flower break virus*
PIAMV	*Plantago asiatica mosaic virus*
PLMVd	*Peach latent mosaic viroid*
PLPV	*Pelargonium line pattern virus*
PoLV	*Photos latent virus*
PRSV	*Papaya ringspot virus*
PSTVd	*Potato spindle tuber viroid*
PVA	*Potato virus A*
PVX	*Potato virus X*
RCNMV	*Red clover necrotic mosaic virus*
RDV	*Rice dwarf phytoreovirus*
RHBV	*Rice hoja blanca virus*
RSV	*Rice stripe virus*
RYSV	*Rice yellow stunt rhabdovirus*
SCMV	*Sugarcane mosaic virus*
SPCSV	*Sweet potato chlorotic stunt virus*
SPFMV	*Sweet potato feathery mottle virus*
SPMMV	*Sweet potato mild mottle virus*
TAV	*Tomato aspermy virus*
TBSV	*Tomato bushy stunt virus*
TCV	*Turnip crinckle virus*
TEV	*Tobacco etch virus*
TGMV	*Tomato golden mosaic virus*
TMV	*Tobacco mosaic virus*
ToCV	*Tomato chlorosis virus*
ToMV	*Tomato mosaic virus*
ToRSV	*Tomato ringspot virus*
TuMV	*Turnip mosaic virus*
TYLCCNV	*Tomato yellow leaf curl China virus*
TYLCV	*Tomato yellow leaf curl virus*
ZYMV	*Zucchini yellow mosaic virus*

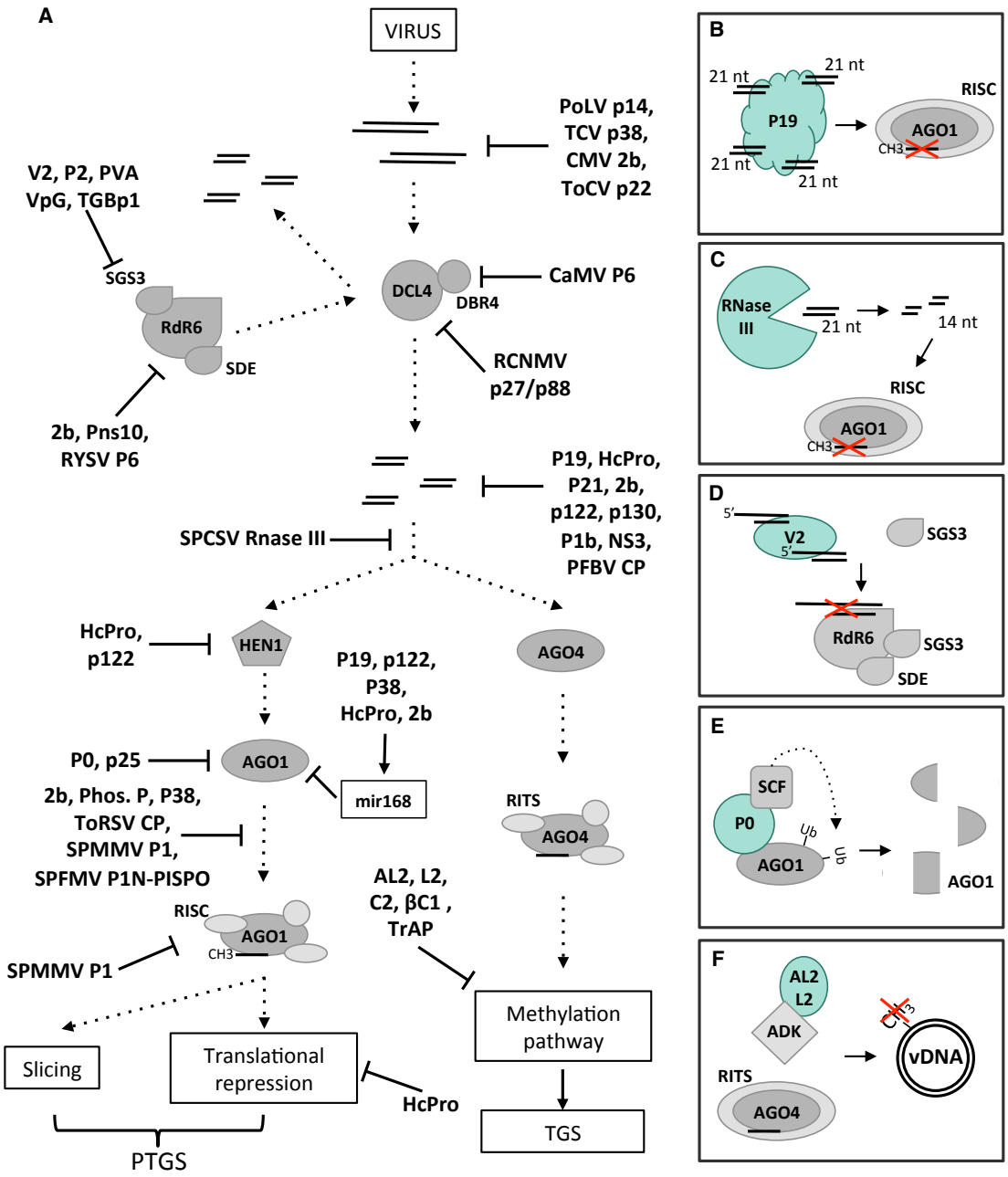

Figure I8: Selection of known viral RNA silencing suppressors, and their modes of action A) The main steps of the silencing pathway are depicted, indicating the RSSs which can interfere them. B-F) Examples of specific RSSs and their modes of action: B) Sequestration of vsiRNAs by P19-vsiRNAs; C) Degradation of vsiRNAs by Rnase III; D) Competition of interaction with dsRNAs by V2; E) AGO degradation by P0; F) Interference with methylation by AL2/L2.

Suppression of silencing pathway: RNA silencing suppressors

Suppressors targeting the initiation phase (DCLs)

The production of vsiRNAs during the initiation phase plays a key role during the plant silencing response against viruses. For this reason, it is not surprising that several RSSs are able to block this step. To achieve this objective, they can prevent the cleavage of dsRNAs into vsiRNA or they can sequester and/or modify vsiRNAs before the loading into AGO proteins.

Just a few viral suppressors have been reported as inhibitors of DCLs proteins. For RNA viruses, some evidences point that the p27 and p88 proteins of RCNMV disrupt DCLs activity (Mine et al. 2010; Takeda et al. 2005). Although the same hypothesis was proposed for the p38 of TCV (Deleris et al. 2006; Qu, Ren, and Morris 2003), a later study attributed this DCL dysfunction to an indirect effect derived from AGO blocking (Azevedo et al. 2010). In addition, this mechanism has been indirectly described in CaMV, where the P6 protein of this DNA virus inactivates DBR4, a DCL4 cofactor (Haas et al. 2008; Love et al. 2007; Shivaprasad et al. 2008).

Another group of viral suppressors are able to interact with long dsRNAs precursors. The PoLV p14, TCV p38, CMV 2b and ToCV p22 viral suppressors bind long dsRNAs, preventing its cleavage by DCLs thus they avoid the vsiRNAs formation (Goto et al. 2007; Landeo-Ríos et al. 2016; Mérai et al. 2005, 2006).

Finally, the most widespread strategy is based in the interaction with vsiRNAs, through diverse mechanisms. The capacity to sequester vsiRNAs and, therefore, to prevent the incorporation into AGO proteins has been reported in several cases (such as for the Tombusviral P19, potyviral HCPro, BYV p21, CMV 2b, tobamoviral TMV p122 and ToMV p130, CVYV P1b, RHBV NS3, PFBV CP) (Chapman et al. 2004; Csorba et al. 2007; Goto et al. 2007; Hemmes et al. 2007; Kurihara et al. 2007; Lakatos et al. 2006; Martínez-Turiño and Hernández 2009; Mérai et al. 2006; Silhavy et al. 2002; Valli, Dujovny, and García 2008). Although all these viral suppressors share the ability to bind vsiRNAs, they present some peculiarities. For example, the length specificity of the small RNA targeted is determined for the protein structure in the case of P19 (Vargason et al. 2003; Ye, Malinina, and Patel 2003). Also, they may have or not have affinity for the 2nt-long 3’ overhangs typical of Dicer-derived small RNAs (Csorba et al. 2007; Hemmes et al. 2007; Lakatos et al. 2006; Valli et al. 2011). Even in certain cases like CVYV P1b, TEV HCPro, and CMV 2b, specific motifs in their sequences have been proposed to be required for vsiRNA binding (Dong et al. 2016; Sahana et al. 2014; Valli et al. 2011). Curiously, GW motifs have been implicated in the binding between the PLPV p37 and vsiRNAs, although these motifs were initially described as AGO interactors (Pérez-Cañamás and Hernández 2015).

In addition, two different mechanisms have been described for the blocking of vsiRNAs action. The first one corresponds to SPCSV RNase III, an endonuclease able to degrade vsiRNAs through their cleavage into 14 bp duplexes (Cuellar et al. 2009; Kreuze et al. 2005; Weinheimer et al. 2014). The second one is used by viral suppressors such as potyviral HCPro and TMV p122, which block the vsiRNAs maturation because they inhibit its 3' methylation by HEN1 (Csorba et al. 2007; Ebhardt et al. 2005; Jamous et al. 2011; Lózsa et al. 2008; Vogler et al. 2007).

Suppressors targeting the amplification phase (RDRs)

During the amplification phase, the secondary vsiRNA synthesis is indirectly related to the availability of both primary vsiRNAs and AGO proteins. Therefore, the inactivation of these essential components by some RSSs may have a subsequent inhibitory effect on the subsequent amplification steps (Csorba et al. 2007). Besides, the suppression of RNA silencing induced by sense RNAs and not by intermediate replicatives, as well as the down-regulation of secondary vsiRNAs without any effect in the amount of primary vsiRNAs, are all suggesting a direct action of RSSs against this phase (Chen et al. 2004; Diaz-Pendon et al. 2007; Mlotshwa et al.2008; Moissiard et al. 2007; Takeda et al. 2002; Voinnet, Lederer, and Baulcombe 2000).

RDR6 and its cofactor SGS3 have been reported as direct targets in several RSSs. The SCMV HCPro, TAV 2b, RDV Pns10 and RYSV P6 are able to decrease RDR6 mRNA levels (Guo et al. 2013; Ren et al. 2010; Zhang et al. 2008). Different studies have demonstrated that SGS3 interacts with TYLCV V2, RSV P2 and PVA VPg silencing suppressors, indicating a mode of action related with this cofactor (Du et al. 2011 b; Glick et al. 2008; Rajamäki, Streng, and Valkonen 2014). Actually, a later study showed that the relationship between SGS3 and the geminiviral V2 is associated with the competition by dsRNA substrates (Fukunaga and Doudna 2009). Finally, the PIAMV TGBp1 coaggregates in the cytoplasm with both RdR6 and SGS3, and can inhibit their activities (Okano et al. 2014).

Suppressors targeting the effector phase (AGOs + RISC)

The action of RSSs against the effector phase has been widely studied during last years. These viral proteins operate in different ways: destabilizing the activity of Argonaute proteins, interfering with the single strand loaded in RISC/RITS complexes or even blocking activities downstream of these complexes.

Several viral suppressors target Argonaute proteins through acting in the gene regulation expression, or the protein degradation pathways. As aforementioned, AGO1 homeostasis depends on the mir168 activity (Rhoades et al. 2002; Vaucheret et al. 2004). The induction of mir168 levels associated with the down-regulation of AGO1

has been demonstrated in different RSSs (p19, p122, p38, HCPro and 2b) (Várallyay and Havelda 2013; Várallyay et al. 2010). These findings suggest a general additional mechanism to alleviate the action of RNA silencing during the infection, complementing other activities of the RSSs. However, the other mentioned manner to affect Argonaute through its degradation seems to be related to specific RSSs with a more dedicated activity specific to this phase. The F-box motif of the poleoviral and enamoviral P0 RSS interacts with AGO1 as well as with SCF ubiquitin ligases (Bortolamiol et al. 2007; Fusaro et al. 2012; Pazhouhandeh et al. 2006). Consequently, P0-type RSSs might promote the degradation of AGO proteins through an ubiquitination autophagy process, and then preventing *de novo* formation of RISC complex (Baumberger et al. 2007; Csorba et al. 2010; Derrien et al. 2012). This is not the case for the PVX p25, which acts as a silencing suppressor degrading almost all AGOs via the proteasome pathway (Chiu et al. 2010).

Another group of RSSs can inhibit AGO activity through a physical interaction. This could be the case of CMV 2b and LNYV Phosphoprotein P, which interact with different AGO proteins (Duan et al. 2012; Hamera et al. 2012; Mann et al. 2016; Zhang et al. 2006). A similar mechanism is found in RSSs with WG/GW motifs in their sequences. GW motifs have been identified in different host-proteins and they mediate the interaction with AGOs, being required for RISC assembly and function (El-Shami et al. 2007; Eulalio, Tritschler, and Izaurralde 2009). The TCV P38 and ToRSV CP RSSs have been able to mimic this strategy to supress RNA silencing (Azevedo et al. 2010; Karran and Sanfaçon 2014). This was also revealed in the ipomovirus SPMMV, where the P1 acts as a silencing suppressor. The binding of P1 to AGO1 through 3 WG/GW motifs prevents de novo RISC formation, thus it inhibits AGO1 function once RISC is assembled (Giner et al. 2010). This was further evidenced when the SPFMV P1, without clear silencing suppressor activity, was transformed into a RSS by the introduction of additional WG/GW motifs, which also enhance the AGO binding capacity of the product (Szabó et al. 2012). Interestingly, the PVA HCPro and AGO1 interact with each other, when they are both associated with ribosomes in planta. This finding suggests a role of HCPro in PTGS translational repression (Ivanov et al. 2016).

Moreover, the block of RISC/RITS complexes could be achieved through targeting of the guide strand RNA. This fact is supported by the capacity to bind single-strand siRNAs of GVA P10 and RSV NS3 (Zhou et al. 2006; Xiong et al. 2009).

Finally, some suppressors of DNA viruses may inactive the antiviral silencing pathway downstream of RITS (Bisaro 2006). This is the case of the TGMV AL2, BCTV L2, TYLCCNV βC1, BSCTV C2, and CaLCuV TrAP, which affect the methylation process somehow (Buchmann et al. 2009; Castillo-González et al. 2015; Yang et al. 2011; Zhang et al. 2011).

Summarizing, viral silencing suppressors can block almost all the steps of silencing pathway through diverse mechanisms. Moreover, specific suppressors (like potyviral HCPro, cucumoviral 2b, and tombusviral P19) present multiple modes of action. The capacity of a single RSS to act through different modes of action may lead to a strong suppression of plant defence. But it is important to keep in mind that sometimes a strong suppression can be detrimental for viruses. The suppression activity of RNA silencing needs to be tightly regulated to allow viral replication and dissemination without interfering too extremely with crucial plant physiological processes that could compromise the survival of the host, and subsequently of the viral pathogen. In other words, the damage on plants could not be too extreme for the host, or otherwise the viral propagation cycle would be compromised. To reach an equilibrium, viruses most likely have evolved to use different strategies aiming to modulate RSS activity. Such strategies can be for instance the control of RSSs sub-cellular localization, or the accumulation of mutated forms with different suppressor strength (Du et al. 2014; Haas et al. 2008; Torres-Barceló et al. 2008). Considering all these situations, the induction and suppression of silencing response needs to be considered as a very precise spatio-temporal regulated mechanism during plant viral infection.

Table I4: Summary of RSSs described in this work and their mode/s of action. RSSs are classified by kind of viral genome, viral family and genus. (1/4)

Genome	Family	Genus	Virus	Acronym	RSS	Mode of action	Ref.
+ssRNA	*Alphaflexiviridae*	*Potexvirus*	*Plantago asiatica mosaic virus*	PlAMV	TGBp1	RdR6/SGS3 interaction	(Okano et al. 2014)
+ssRNA	*Alphaflexiviridae*	*Potexvirus*	*Potato virus X*	PVX	P25	AGO1 degradation	(Chiu et al. 2010; Voinnet et al. 2000)
+ssRNA	*Betaflexiviridae*	*Vitivirus*	*Grapevine virus A*	GVA	P10	Single and dúplex siRNA binding	(Zhou et al. 2006)
+ssRNA	*Bromoviridae*	*Cucumovirus*	*Cucumber mosaic virus*	CMV	2b	dsRNA binding siRNA sequestration. AG01 homeostasis. AGO1 and AGO4 interaction.	(Brigneti et al. 1998; Dong et al. 2016; Duan et al. 2012; Goto et al. 2007; Hamera et al. 2012; Várallyay and Havelda 2013; Zhang et al. 2006)
+ssRNA	*Bromoviridae*	*Cucumovirus*	*Tomato aspermy virus*	TAV	2b	RDR6 down-regulation	(Li et al. 1999; Zhang et al. 2008)
+ssRNA	*Closteroviridae*	*Closterovirus*	*Beet yellows virus*	BYV	p21	siRNA sequestration	(Chapman et al. 2004; Reed et al. 2003)
+ssRNA	*Closteroviridae*	*Crinivirus*	*Sweet potato chlorotic stunt virus*	SPCSV	Rnase III	siRNA cleavage	(Cuellar et al. 2009; Kreuze et al. 2005; Weinheimer et al. 2014)
+ssRNA	*Closteroviridae*	*Crinivirus*	*Tomato chlorosis virus*	ToCV	P22	dsRNA binding	(Cañizares, Navas-Castillo, and Moriones 2008; Landeo-Ríos et al. 2016)
+ssRNA	*Luteoviridae*	*Enamovirus*	*Pea enantion mosaic virus-1*	PEMV-1	P0	AG01 degradation	(Fusaro et al. 2012)
+ssRNA	*Luteoviridae*	*Poleovirus*	*Beet western yellows virus*	BMYV	P0	AGO1 degradation	(Baumberger et al. 2007; Bortolamiol and Pazhouhandeh M, Marrocco K, Genschik P 2007; Csorba et al. 2010; Derrien et al. 2012; Pazhouhandeh M, Dieterle M, Marrocco K, Lechner E, Berry B, Brault V, Hemmer O, Kretsch T, Richards KE, Genschik P 2006; Pfeffer et al. 2002)
+ssRNA	*Luteoviridae*	*Poleovirus*	*Cucurbit aphid-borne yellow virus*	CABYV	P0	AGO1 degradation	(Bortolamiol and Pazhouhandeh M, Marrocco K, Genschik P 2007; Pazhouhandeh M, Dieterle M, Marrocco K, Lechner E, Berry B, Brault V, Hemmer O, Kretsch T, Richards KE, Genschik P 2006; Pfeffer et al. 2002)
+ssRNA	*Potyviridae*	*Ipomovirus*	*Cucumber vein yellow virus*	CVYV	P1b	siRNA sequestration	(Valli et al. 2006, 2011, 2008)

Table I4: Summary of RSSs described in this work and their mode/s of action. RSSs are classified by kind of viral genome, viral family and genus. (2/4)

Genome	Family	Genus	Virus	Acronym	RSS	Mode of action	Ref.
+ssRNA	*Potyviridae*	*Ipomovirus*	*Sweet potato mild mottle virus*	SPMMV	P1	AGO1 interaction	(Giner et al. 2010)
+ssRNA	*Potyviridae*	*Potyvirus*	*Papaya ringspot virus*	PRSV	HCPro	siRNA sequestration	(Sahana et al. 2014)
+ssRNA	*Potyviridae*	*Potyvirus*	*Potato virus A*	PVA	HCPro VPg	AGO1 interaction SGS3 interaction	(Ivanov et al. 2016; Rajamäki et al. 2014; Rajamäki and Valkonen 2009)
+ssRNA	*Potyviridae*	*Potyvirus*	*Tobacco etch virus*	TEV	HCPro	siRNA sequestration. interference with HEN1 methylation. AGO1 homeostasis.	(Ebhardt et al. 2005; Kasschau and Carrington 1998; Lakatos et al. 2006; Lózsa et al. 2008; Mérai et al. 2006; Várallyay and Havelda 2013)
+ssRNA	*Potyviridae*	*Potyvirus*	*Turnip mosaic virus*	TuMV	HCPro	siRNA sequestration	(Garcia-Ruiz et al. 2015; Kasschau et al. 2003)
+ssRNA	*Potyviridae*	*Potyvirus*	*Sugarcane mosaic virus*	SCMV	HCPro	RdR6 down-regulation	(Zhang et al. 2008)
+ssRNA	*Potyviridae*	*Potyvirus*	*Zucchini yellow mosaic virus*	ZYMV	HCPro	interference with HEN1 methylation.	(Jamous et al. 2011)
+ssRNA	*Secoviridae*	*Nepovirus*	*Tomato ringspot virus*	ToRSV	CP	AGO1 interaction	(Karran and Sanfaçon 2014)
+ssRNA	*Tombusviridae*	*Aureusvirus*	*Photos latent virus*	PoLV	p14	dsRNA binding	(Mérai et al. 2005)
+ssRNA	*Tombusviridae*	*Carmovirus*	*Pelargonium flower break virus*	PFBV	CP	siRNA sequestration	(Martínez-Turiño and Hernández 2009)
+ssRNA	*Tombusviridae*	*Carmovirus*	*Pelargonium line pattern virus*	PLPV	P37 (CP)	siRNA sequestration	(Pérez-Cañamás and Hernández 2015a)
+ssRNA	*Tombusviridae*	*Carmovirus*	*Turnip crinckle virus*	TCV	P38 (CP)	dsRNA binding. AGO1 and AGO2 interaction. AGO1 homeostasis.	(Azevedo et al. 2010; Deleris et al. 2006; Mérai et al. 2006; Qu et al. 2003; Várallyay and Havelda 2013; Zhang et al. 2012)
+ssRNA	*Tombusviridae*	*Dianthovirus*	*Red clover necrotic mosaic virus*	RCNMV	p27 p88	Unknown	(Mine et al. 2010; Takeda et al. 2005)
+ssRNA	*Tombusviridae*	*Tombusvirus*	*Carnation italian ringspot virus*	*CIRV*	P19	siRNA sequestration	(Vargason et al., 2003)

Table I4: Summary of RSSs described in this work and their mode/s of action. RSSs are classified by kind of viral genome, viral family and genus. (3/4)

Genome	Family	Genus	Virus	Acronym	RSS	Mode of action	Ref.
+ssRNA	*Tombusviridae*	*Tombusvirus*	*Cymbidium ringspot virus*	*CymRSV*	P19	siRNA sequestration. AGO1 homeostasis.	(Lakatos et al. 2004, 2006; Várallyay et al. 2010)
+ssRNA	*Tombusviridae*	*Tombusvirus*	*Tomato bushy stunt virus*	*TBSV*	P19	siRNA sequestration	(Silhavy et al. 2002; Voinnet, Pinto, and Baulcombe 1999; Ye et al. 2003)
+ssRNA	*Virgaviridae*	*Tobamovirus*	*Tobacco mosaic virus*	TMV	p126=p122	siRNA sequestration. interference with HEN1 methylation. AGO1 homeostasis.	(Csorba et al. 2007; Ding et al. 2004; Kurihara et al. 2007; Várallyay and Havelda 2013; Vogler et al. 2007)
+ssRNA	*Virgaviridae*	*Tobamovirus*	*Tomato mosaic virus*	ToMV	p130	siRNA sequestration	(Kubota et al. 2003; Kurihara et al. 2007)
-ssRNA	*Rhabdoviridae*	*Cytorhabdovirus*	*Lettuce necrotic yellows virus*	LNYV	Phosphoprotein P	AGO1, AGO2 and AGO4 interaction. RdR6 and SGS3 interaction.	(Mann et al. 2016; Mann, Johnson, and Dietzgen 2015)
-ssRNA	*Rhabdoviridae*	*Nucleorhabdovirus*	*Rice yellow stunt rhabdovirus*	RYSV	P6	RdR6 down-regulation	(Guo et al. 2013)
-ssRNA	Unassigned	*Tenuivirus*	*Rice hoja blanca virus*	RHBV	NS3	siRNA sequestration	(Bucher et al. 2003; Hemmes et al. 2007)
-ssRNA	Unassigned	*Tenuivirus*	*Rice stripe virus*	RSV	NS3 P2	Single and dúplex siRNA binding. SGS3 interaction.	(Z. Du et al. 2011; Xiong et al. 2009)
dsRNA	*Reoviridae*	*Phytoreovirus*	*Rice dwarf phytoreovirus*	RDV	Pns10	RdR6 down-regulation	(Cao et al. 2005; Ren et al. 2010)
dsDNA	*Caulimoviridae*	*Caulimovirus*	*Cauliflower mosaic virus*	CaMV	P6	DBR4 inactivation	(Haas et al. 2008; Love et al. 2007; Shivaprasad et al. 2008)
ssDNA	*Geminiviridae*	*Begomovirus*	*Tomato yellow leaf curl virus*	TYLCV	V2	SGS3 interaction (competition by dsRNA)	(Fukunaga and Doudna 2009; Glick et al. 2008; Zrachya et al. 2007)
ssDNA	*Geminiviridae*	*Begomovirus*	*Tomato yellow leaf curl China virus*	TYLCCNV	βC1	SAHH inhibition	(Yang et al. 2011)
ssDNA	*Geminiviridae*	*Begomovirus*	*Beet severe curly top virus*	BSCTV	C2	SAMDC1 degradation	(Zhang et al. 2011)
ssDNA	*Geminiviridae*	*Begomovirus*	*Cabbage Leaf Curl Virus*	CaLCuV	TrAP	KYP inactivation	(Castillo-González et al. 2015)

Table I4: Summary of RSSs described in this work and their mode/s of action. RSSs are classified by kind of viral genome, viral family and genus. (4/4)

Genome	Family	Genus	Virus	Acronym	RSS	Mode of action	Ref.
ssDNA	*Geminiviridae*	*Begomovirus*	*Tomato golden mosaic virus*	TGMV	AL2=TrAP	ADK inactivation. KYP inactivation.	(Buchmann et al. 2009; Castillo-González et al. 2015)
ssDNA	*Geminiviridae*	*Curtovirus*	*Beet curly top virus*	BCTV	L2	ADK inactivation	(Buchmann et al. 2009)

Silencing of plant transcripts by viral siRNAs

Occasionally, some specific siRNAs derived from viral sequences induce host transcripts silencing when there is a near specific complementarity (Table I5). For instance, some plant symptoms might be the consequence of this down-regulation of gene expression in the host. A specific small RNA coming from CMV Y satellite is able to target the chlorophyll biosynthetic gene (CHLI), leading to a yellow mosaic in the host plant (Shimura et al. 2011; Smith, Eamens, and Wang 2011). In the PLMVd viroid, two different siRNAs trigger the cleavage of the chloroplastic heat-shock protein 90 (cHSP90) mRNA. The lack of cHSP90 causes an albino phenotype in infected leaves (Navarro et al. 2012). Another example has been reported in genes related to pathogen infection. Some callose synthase genes are degraded by the action of a PSTVd siRNA during tomato infection (Adkar-Purushothama et al. 2015). Finally, many genes in grapevine hosts were identified as putative target of viral derived small RNAs, although the mRNA cleavage was only validated for a small fraction of them (Miozzi et al. 2013). According to these results, regulation of plant gene expression by vsiRNAs might only occur rarely, not being a widespread strategy, and only contributing to pathogenicity in a few pathosystems.

Table I4: Summary of vsiRNAs with demonstrated activities to target host plant genes.

Genome	Family	Genus	*Virus*	Acronym	Plant gene targeted by vsiRNAs	Ref.
satRNA			*Cucumber mosaic virus Y satellite*	CMV Y-sat	Chlorophyll biosynthetic gene (CHLI)	(Shimura et al. 2011; Smith et al. 2011)
Circular ssRNA	*Avsunviroidae*	*Pelamoviroid*	*Peach latent mosaic viroid*	PLMVd	Chloroplastic heat-shock protein 90 (cHSP90)	(Navarro et al. 2012)
Circular ssRNA	*Pospiviroidae*	*Pospiviroid*	*Potato spindle tuber viroid*	PSTVd	Callose synthase genes	(Adkar-Purushothama et al. 2015)
+ssRNA	*Tymoviridae*	*Maculavirus*	*Grapevine fleck virus*	GFkV	Ribosomal biosynthetic and stress-related genes	(Miozzi et al. 2013)
+ssRNA	*Betaflexiviridae*	*Foveavirus*	*Grapevine rupestris steem pitting-associated virus*	GRSPaV	Ribosomal biosynthetic and stress-related genes	(Miozzi et al. 2013)

Final remarks about RNA silencing suppression in SPFMV

When this thesis was initiated, there was no specific information about the case of SPFMV in their natural hosts. By analogy with other potyviruses, it was assumed that HCPro might be acting as RSS. However, the peculiarities of the synergism with other viruses, with the potyviral partner being beneficiated, contrarily to the most frequent responses in which the potyviruses tend to enhance the unrelated partners, and the predicted presence of a putative new gene product deriving from the out-of-frame PISPO, leave many uncertainties to be explained. In this context, the experimental work was planned to try to answer some of those questions.

OBJECTIVES

OBJECTIVES

The presence of a new overlapping open reading frame, named PISPO, had been noticed earlier within the P1 coding region of the potyvirus *Sweet potato feathery mottle virus* (SPFMV) and the members of its lineage (Clark et al. 2012; Li et al. 2012). The unique conservation of PISPO in such specific viruses and the possible existence and function of the derived P1N-PISPO gene product (in the form of a protein with the C-terminal part in a different coding frame) during viral infection could have special interest to better understand the complexity of viral functions in members of the *Potyviridae* family.

The general goal of this thesis is to elucidate if the predicted P1N-PISPO gene product is expressed during the virus infectious cycle, and characterize some aspects of its production and function. To achieve this goal, we raised the following specific objectives:

A) Characterization of a SPFMV isolate containing the predicted PISPO and confirmation of its behavior during co-infection with the unrelated crinivirus *Sweet potato chlorotic stunt virus* (SPCSV).

B) Analysis of the mechanism of expression of the P1N-PISPO gene product in SPFMV and related potyviruses, as well as of the more general and well-characterized P3N-PIPO gene product, present in all potyvirids.

C) Determination of the presence of P1N-PISPO gene product during SPFMV infection.

D) Functional characterization of P1N-PISPO as a RNA silencing suppressor (RSS).

MATERIAL & METHODS

MATERIAL & METHODS

Plants and virus material

Commercial sweet potato (*Ipomea batatas*) roots were acquired in a local food market in Barcelona, and were planted on soil to produce fresh aerial tissue (stems and leaves) that was further propagated through cuttings at CRAG plant growth facilities. The identification of virus isolates (corresponding to the potyvirus species SPFMV, SPVC and SPV2, and to a begomovirus and a badnavirus) infecting these plants was performed by RT-PCR and RNA-Seq analysis (see result for detailed descriptions). The SPFMV isolate, denoted AM-MB2, was used in further experiments.

To obtain sweet potato plants super-infected with a crinivirus (to reproduce the sweet potato viral disease SPVD), virus transmission experiments were performed with *Bemisia tabaci* whiteflies as insect vectors and the isolate Can181-9 of the crinivirus SPCSV strain West Africa. This isolate was kindly provided by Dr. Jesús Navas-Castillo (IHSM La Mayora, CSIC-UMA, Málaga, Spain) in an *Ipomea setosa* plant, also propagated through cuttings. Groups of adult insects raised on tobacco plants were collected and allowed to acquire SPCSV during 48 h on infected plants before being transfered to AM-MB2 plants for inoculation during an additional 48 h period, and later were eliminated with insecticide treatment.

Samples of *Nicotiana tabacum* var. Xanthy plants infected by SPMMV were used in high-throughput sequencing experiments. The isolate 130 originated from Tanzania for SPMMV was inoculated in *N. tabacum* plants from an *Ipomoea batata* plant provided by Prof. Jari Valkonen (University of Helsinki, Finland). This isolate was used in previous projects in our laboratory (Giner et al. 2010).

The primers used for RT-PCR detection of SPMFV, SPCSV and SPMMV infections are listed in the Table MM1.

Transient expression of viral proteins by agro-infiltration were performed in *Nicotiana benthamiana*, either wild type or transgenic line 16c expressing constitutively the GFP reporter gene (Ruiz, Voinnet, and Baulcombe 1998).

Extraction of total RNA, construction and utilization of RNA sequencing (RNA-seq) libraries, and preliminary data processing

Samples of symptomatic tissue of infected plants were collected for RNA extraction with TRIzol reagent. Contaminating DNA was removed from RNA samples with Turbo DNase (Ambion), and RNA was further purified using the RNeasy minikit (Qiagen). The insert P1HCPro in pENTR was mobilized using Gateway to the destination vector pDEST17 (ThermoFisher scientific), under the control of the T7 promoter. mRNAs were produced by *in vitro* transcription using the mMESSAGE mMACHINE® T7 Transcription Kit (ThermoFisher scientific) and purified by RNeasy minikit (Qiagen).

RNA libraries were constructed with the ScripSeq complete kit (plant leaf) (Epicenter, Illumina), including barcoding elements to identify the different samples, according to the provider's protocols. Libraries were submitted to BGI (Hong Kong) for Illumina sequencing on a HiSeq 2000 platform, and 100-bp (average) paired-end reads were generated. Sequences with an average quality below 20, as well as sequences with more than 10 nt with quality below 15, were removed using the FASTX toolkit (HannonLab 2014). The quality process was driven with FASTQC (Babraham-Bioinformatics 2014)

Alignments and indel analysis

Filtered sequences were mapped versus the references with Bowtie2 (Langmead and Salzberg 2012), allowing a maximum of 3 mismatches, insertions, or deletions (indels) per read. To reduce the number of sequencing errors, only the central part of reads (80 nt) was used, and only paired alignments were considered (Wright et al. 2011). Alignments were analyzed with SAMtools to create a list of variants in which only indels were included. Reads that presented fewer than 3 nonredundant sequences and reads in which the frameshift caused by the indel was cancelled out by another indel in the same sequence were discarded. To reduce false positives caused by sequencing errors or random errors, the expected indel error was modeled as a Poisson distribution, which was calculated from Illumina indel calling-error rate, PCR error rate, and sample indel frequency. Indels with a false discovery rate (FDR) higher than 0.05 were removed. Analysis was performed with in-house R scripts.

Phylogenetic and recombination analysis

Initial phylogenetic analysis of the SPFMV, SPVC, and SPV2 isolates found in AM-MB2 was performed with data sets created with the full genome sequences corresponding to 9 SPFMV, 7 SPVC, and 6 SPV2 isolates found in the NCBI nucleotide database, with no filter by identity redundancy. Also, sequences of complete CP regions of all other SPFMV, SPVC, and SPV2 isolates available in the NCBI nucleotide database were

considered, after exclusion of partial CP sequences and application of a filter at 97% of identity to reduce redundancy, leading to data sets of 63 SPFMV, 46 SPVC, and 6 SPV2 annotated sequences. Phylogenetic trees were created using the maximum-likelihood algorithm implemented in MEGA6 software (Tamura et al. 2013). The bootstrapping test was driven with 1,000 replicates. CP sequence-based trees were used to estimate putative recombination events (see below).

The assembly of SPFMV genome was driven with Quasirecomb (Töpfer et al. 2013). The same procedure was applied to SPVC and SPV2. The reconstruction of sequences used coverage of >10.000 to reduce errors, thereby excluding both extremes, and the option to reduce the false positives were activated. The sequences obtained were used to search for putative recombination events with the software RDP (Martin et al. 2010) version 3.45, using a threshold of a *P* value equal or less than 0.05 with the methods RDP (Martin and Rybicki 2000), BootScan (Martin et al. 2005), Geneconv (Martin et al. 2005), and MaxChi (Smith 1992). The recombination points were identified using the SBP and GARD algorithms (Kosakovsky Pond et al. 2006) implemented in the Datamonkey webserver (Delport et al. 2010).

Presence of A_6 motifs

Expected events with AAAAAA (A_6) motif (E) are calculated as $E= P(A)^6 \times M$, where P(A) is the probability of an adenine and M is the average of the coding regions of the genomes minus the motif length plus one. E was calculated assuming that the probability of nucleotide appearance is statistically independent. P(A) was calculated from the frequency of which this nucleotide appears in the coding regions of the viral family. Viral sequences were extracted from NCBI Genome database.

Constructs of viral gene products for *in vitro* translation and for transient expression of viral proteins by agroinfiltration

Cloning and plasmid production were performed using *Escherichia coli* strain DH5α and standard procedures. Viral products were RT-PCR amplified with appropriate primers, and the products were cloned directionally into pENTR/D-TOPO (Life Technologies). Primers are listed in Table MM1, which includes information about their use for the modifications required to direct and/or force or avoid the expression of certain gene products in the different frames. Recombinant products with mutations introduced by PCR with appropriate primers were generated and were confirmed by sequencing the pENTR clones. The multiple mutant with the 4 WG/GWs motifs altered was synthesized as follows. A fragment flanked by NcoI and AscI restriction enzyme sites engineered upstream and downstream from position 1 to 1964 (Met to Stop) in the P1N-PISPO sequence, with replacement of W with A residues in the WG/GW motifs

located at positions 73, 1465, 1795, and 1918 (relative to the initial Met codon), was ordered from GeneScript (USA) and inserted using the unique restriction sites into the pENTR plasmid, linearized with the same enzymes, and ligated with T4 DNA ligase. Clones containing inserts were selected and sequenced to confirm the presence of the mutated motifs. The inserts in pENTR were mobilized using Gateway into the different destination vectors with LR Clonase II enzyme mix (Life Technologies). Reactions were performed, and two clones of the different plasmids were verified. For expression in plants, the pGWB7XX destination plasmid series was used (Nakagawa et al. 2007; Tanaka et al. 2011), which placed the construct under control of appropriate regulatory elements.

In vitro translation

pENTR-P1 was used as the template for PCR amplifications of all constructs used for *in vitro* translation, including unmodified wild-type P1 and variants with P1 interrupted by a stop codon after the slippage site (P1Δ) and P1 with the PISPO sequence interrupted (P1N-PISPOΔ) generated by site-directed mutagenesis with the primers FMP1ΔF and Δ1PMFR for P1Δ and FMPISPOΔF and ΔOPSIPMFR for P1N-PISPOΔ (Table MM1). T7 promoter, 5' untranslated region (5'UTR), and 3'UTR fragments were prepared as described previously (Pasin, Simón-Mateo, and García 2014). mRNAs were produced by *in vitro* transcription using the T7-Scribe Standard RNA IVT kit (Cellscript) and purified by organic extraction and ammonium acetate precipitation, and their quality and amount were assessed by NanoDrop (Thermo Fisher Scientific) and gel electrophoresis. The final concentration was adjusted to 1 g/liter, and *in vitro* translation was carried out using wheat germ extract (Promega) according to the manufacturer's instructions. Labeling of the synthesized proteins was done by including in the reaction mixture L-[^{35}S]methionine and L-[^{35}S]cysteine (PerkinElmer). Samples were resolved by 12% SDS-PAGE and detected with a PhosphorImager.

Agrobacterium tumefaciens infiltration of Nicotiana benthamiana leaves

N. benthamiana leaves (fully expanded, from 3- to 4-week-old plants grown in a greenhouse) were agroinfiltrated as described previously (Valli et al. 2006), using *A. tumefaciens* cultures of strain C58C1 or EHA105 transformed with the relevant plasmids. Growth of bacteria was monitored by assessing the optical density at 600 nm (OD_{600}) until it reached 0.5 units. Cultures were induced by acetosyringone and infiltrated with a needleless syringe. For sampling material to be analyzed by LC-tandem MS (LC- MS/MS) (see below), the agroinfiltration was performed with mixed cultures incorporating a construct expressing P1b of CVYV (Valli et al. 2006) to increase expression of SPFMV proteins. For silencing suppression experiments (see below),

negative (empty vector, delta) and positive (CVYV P1b) controls were included, following previously described procedures (Carbonell, Dujovny, et al. 2012; Valli et al. 2008). The delta control was previously obtained by A. Valli (CNB, CSIC) replacing through gateway recombination the selection region in the destination vectors by a random non-coding sequence, resulting in a plasmid not expressing any product (empty vector).

SDS-PAGE and fractionation of protein products

Plant samples were collected, deep-frozen, and homogenized in extraction buffer. (62,5 mM Tris-HCl pH 7,5, 2% SDS and 2% beta-mercaptoethanol). After boiling for 5 min, aliquots were separated by 10% SDS-PAGE. Following staining with Coomassie blue G-250 (SimplyBlue safe stain; Life Technologies), the portion above the RuBisCO was excised and processed.

MS and protein identification by LC-MS/MS analysis

Gel-excised fragments containing protein samples were washed with 25 mM NH_4HCO_3 and acetonitrile (ACN), reduced for 60 min at 60°C with 20 mM dithiothreitol (DTT), and alkylated for 30 min at 30°C with 55 mM iodoacetamide in the dark before being digested for 16 h at 37°C with 0.9 µg trypsin (porcine sequence-grade modified trypsin; Promega). Peptides were extracted from the gel matrix with 10% formic acid and ACN, dyed, and desalted with a C_{18} Top-tip (PolyLC), following the procedure of the provider. Dried-down tryptic peptides mixtures resuspended in 1% formic acid were injected for chromatographic separation in a nanoAcquity liquid chromatograph (Waters) coupled to an LTQ-Orbitrap Velos (Thermo Scientific) mass spectrometer. Peptides were trapped on a Symmetry C_{18} trap column (5 µm by 180 µm by 20 mm; Waters) and separated with a C_{18} reverse-phase capillary column (75 µm, 10 cm nanoAcquity; 1.7-µm BEH column; Waters). The gradient for elution was prepared with 0.1% formic acid in ACN and consisted of 1 to 30% for 60 min, 35to45% for 10 min, and 45 to 85% for 5min, with a flow rate of 250 nl/min. Eluted peptides were subjected to electrospray ionization in an emitter needle (PicoTip; New Objective) with 2,000 V applied. Peptide masses (*m/z* 350 to 1700) were analyzed in full-scan MS data-dependent mode in the Orbitrap with 60,000 full width at half maximum (FWHM) resolution at 400 *m/z*. Up to the 10 most abundant peptides (minimum intensity of 500 counts) were selected for each MS scan and fragmented using collision-induced dissociation in a linear ion trap with helium as the collision gas and 38% normalized collision energy. The targeted mode was used to analyze the presence of predicted peptides in the ORF that contains PISPO (the seven peptides underlined in the sequence LVWEKTGRTIGHKERDQKRSQSKMEVGTLQTSQEDQEGQPKTAPTEAHGEGTAIIDGYATSSSDG HLHCWGSIGESGNDSNSEWEDFLHAFHEEEENFKISQINTRENSRAHAGSSENCVQEKDEHRIGG

QEVHKRAVQEISRSKLFVPSFKTYGRLKRVSGFKNSHNNSKPRTSSCQGWSMEKTCKDNNVVQRF KWHGAESRQTVGPKRSCTTRNARGAWGFTRSAIRRTNETW) or in the C-terminal part of the P1 (the three peptides underlined in the sequence KLDEQLATRNEIRKGLKVKWRWGLYRLVKKTRKDNQRQRRQRRMEKEQQLLMAMPPQVLTGISI AGGPSASLEMTPTPNGKIFCTPSMKKKKTLKSPKLTQEKIHELTQAVLKIACRKRMSIELVGKKSTKG QYRKFQGANYLFLHLKHMEGLRESVDLRIHTTTQNLVLQAAKVGAWKRPVKTTMLSKGSSGMVL NPDKLLGPRGHAPHGM LVVRGALRGVLYDARMKLGRSVLPYIIQY). Generated raw data were collected with Thermo Xcalibur (v.2.2). For database searching, custom databases were created merging all UniProt entries (as of December 2014) for *I. batatas* plus the predicted list of mature protein sequences from SPFMV plus a list of predicted mature gene products deriving from viruses present in the AM-MB2 sample or for *N. benthamiana* and *A. tumefaciens* plus P1 and P1N-PISPO. Entries from common laboratory contaminants were also added. Sequest search engine searches were performed with Thermo Proteome Discoverer software (v.1.3.0.339), using a target and a decoy database to obtain a false-discovery rate (FDR) (strict, 0.01; relaxed, 0.05) and to estimate the number of incorrect pep- tide spectrum matches exceeding a given threshold (peptide tolerances of 10 ppm and 0.6 Da, respectively, for MS and MS/MS), with parameters for trypsin allowing up to 2 missed cleavages, considering cysteine carbam- idomethylation as fixed and methionine oxidation as variable modifications. Validation was based on FDR, using Percolator (a semisupervised learning machine) to discriminate peptide spectrum matches. Only proteins identified with at least 2 high-confidence peptides (FDR of ≤0.01) were considered.

RNA silencing suppression activity assays: GFP imaging, Northern blotting, and RT-qPCR analysis

Leaves of *N. benthamiana* and *N. benthamiana 16c* plants were coagroinfiltrated with a green fluorescent protein (GFP)-expressing construct together with constructs of the different viral products or adequate controls. The infiltrated patches were visualized under UV light with a Black Ray B 100 AP lamp, and photographs were taken with a Nikon D7000 digital camera.

Total RNA from *N. benthamiana* tissue was isolated using TRIzol and treated with Turbo DNase (Ambion) to remove contaminating DNA. For Northern blot analysis of mRNAs and small interfering RNAs (siRNAs), approximately 10 and 15 µg of total RNA were resolved on 1.2% agarose (containing 2% formaldehyde) or 15% denaturing polyacrylamide (containing 7 M urea) gels, respectively, and transferred to nylon Hybond-N+ membranes (Amersham) by capillary blotting for the agarose gels or using a transfer apparatus (XCell SureLock; Invitrogen) for the acrylamide gels. Ethidium bromide staining was used to verify equal loading of lanes and monitor the transference processes. After UV cross-linking and prehybridization in UltraHyb buffer

(Ambion), blots were hybridized in the same solution with probes specific to the GFP sequence, using a ^{32}P-labeled DNA probe (Valli et al. 2006) in the case of mRNAs or a ^{32}P-labeled RNA probe (Valli et al. 2011) in the case of small RNAs. Hybridization signals were detected with a PhosphorImager.

For quantitative real-time reverse transcription-PCR (RT-qPCR) analysis, 1 µg of total RNA was reverse transcribed using the SuperScript III first-strand synthesis system (Invitrogen), and RT-PCRs were performed in a 20-µl volume with gene-specific primers and LightCycler 480 SYBR green I master mix (Roche). A 102-bp GFP fragment was amplified with primers described by Leckie and Stewart (Leckie and Neal Stewart 2011). Ubiquitin was selected as a reference gene, amplifying a 88-bp fragment using the primers described by Lacomme and coworkers (Lacomme, Hrubikova, and Hein 2003) (see Table MM1 for primer sequences). The average cycle threshold (C_T) value for triplicate PCRs was normalized to the average C_T value for the reference gene, yielding the ΔC_T value. An analysis of variance (ANOVA) for at least three independent biological replicates was performed using the Tukey-Kramer test.

RNA silencing suppression activity assays: Western-blot analysis

Constructs HCPro, P1 only and P1N-PISPOmut were cloned in the destination vector pGWB718, which contains 4xMyc tag at the 5'end, transferred to *A. tumefaciens* cultures, induced and used to agroinfiltrate plants. Tissue of *N. benthamiana* agroinfiltrated leaves was collected at different time points and ground under liquid nitrogen. Total proteins were extracted using a urea extraction buffer (125 mM Tris-HCl pH 7,5, 6 M Urea, 2% SDS and 5% beta-mercaptoethanol) (1 ml/mg). Protein extracts were boiled for 5 minutes, resolved on SDS-PAGE (8% acrylamide), electroblotted to a nitrocellulose membrane (Amersham Protan 0,45µm, 10600016, GE Healthcare Life Sciences) and subjected to immunoblotting. Anti-Myc tag clone 4A6 (05-724, Millipore) and Anti-mouse IgG-peroxidase (A2304, Sigma) antibodies were used for immunodetection. Proteins reacting with the specific anty-Myc antibody were detected by chemiluminescence using the ECL kit (Amershan Biosciences). Ponceau red staining was used to estimate equal loading of all control and sample lanes.

Nucleotide sequence accession numbers

Data corresponding to viral sequences used and their accession numbers (GenBank) are listed in Table MM2.

Table MM1: List of primers used in this thesis

Primer	Sequence (5'-3')	Application
FMCPFdeg	GCATCATCAAAGGGTG**Y**GAG	Detection of an SPFMV CP amplicon (389bp) with a degeneration (Y=C or T) in order to amplify most SPFMV strains/isolates.
MFRdeg	ACTGCATG**R**TCCAACAATGG	Detection of an SPFMV CP amplicon (389bp) with a degeneration (R=G or A) in order to amplify most SPFMV strains/isolates.
CSCPF	cctctagaATGGCTGATAGCACTAAAG	Detection of an SPCSV CP amplicon (790bp).
PCSCR	ccctcgagTCAACAGTGAAGACCTGTTC	Detection of an SPCSV CP amplicon (790bp).
MMCPF	AGAGATTATCAAGTTAGTATGGA	Detection of an SPMMV CP amplicon (509bp).
PCMMR	GTCCAGTTGAGCTCCTCTCAGAC	Detection of an SPMMV CP amplicon (509bp).
FMP1seqF	GAATGCGTACCTTAGTGATG	Sequencing of the different transframed P1 versions.
FMP1F	ccacATGGCAACTGTAATGGC	Directional cloning of P1wt/P1HCPro in pENTRY-D-TOPO.
1PMFR	CTAATACTGGATGATGTATGGTAG	Cloning of SPFMV P1wt in pENTRY-D-TOPO.
FMHCF	caccATGAGCTCTACTATGGAAAG	Directional cloning of SPFMV HCPro in pENTRY-D-TOPO.
CHMFR	CTAGCCTACTATGTAGTGTTTCAT	Cloning of SPFMV HCPro/P1HCPro in pENTRY-D-TOPO.
FMPISPOF	caccATGGAAAAAACTGGACGAACAAT**A**G	Directional cloning of SPFMV PISPO in pENTRY-D-TOPO with stop in P1 frame.
OPSIPMFR	CTACCAAGTTTCATTCGTGCG	Cloning of SPFMV PISPO in pENTRY-D-TOPO.
FMP1onF	GGAAAAAACT**T**GACGAACAATTGG	Site-directed mutagenesis of SPFMV P1 in order to stop the PISPO frame.
no1PMFR	CCAATTGTTCGTC**A**AGTTTTTTCC	Site-directed mutagenesis of SPFMV P1 in order to stop the PISPO frame.
FMP1NPISPOF	GG**(+G)**AAAAAACTGGACGAACAAT**A**G	Site-directed mutagenesis of SPFMV P1 in order to force the PISPO frame and to stop the P1 frame.
OPSIPN1PMFR	C**T**ATTGTTCGTCCAGTTTTTT**(**+**C)**CC	Site-directed mutagenesis of SPFMV P1 in order to force the PISPO frame and to stop the P1 frame.
FMP1ΔF	CAAT**A**GGCCACAAGGAAC	Site-directed mutagenesis of SPFMV P1 in order to generate a truncated P1.
Δ1PMFR	GTTCCTTGTGGCC**T**ATTG	Site-directed mutagenesis of SPFMV P1 in order to generate a truncated P1.
FMPISPOΔF	GGGGGTCC**TAGC**GCGAGTC	Site-directed mutagenesis of SPFMV P1 in order to generate a truncated P1N-PISPO.
ΔOPSIPMFR	GACTCGC**GCTA**GGACCCCC	Site-directed mutagenesis of SPFMV P1 in order to generate a truncated P1N-PISPO.
GFP1F	CAACTTCAAGACCCGCCACA	qRT-PCR for GFP.
1PFGR	TCTGGTAAAAGGACAGGGCCA	qRT-PCR for GFP.
UBIF	TCCAGGACAAGGAGGGTATCC	qRT-PCR for Ubiquitin.
IBUR	TAGTCAGCCAAGGTCCTTCCAT	qRT-PCR for Ubiquitin

Table MM 1: List of viral sequences and accession numbers

Potyvirus	Acronym/Isolate	Accession number
Sweet potato feathery mottle virus	SPFMV	NC_001841
Sweet potato feathery mottle virus	SPFMV AM-MB2 isolate	KU511268
Sweet potato virus C	SPVC AM-MB2 isolate	KU511269
Sweet potato virus 2	SPV2 AM-MB2 isolate	KU511270
Sweet potato begomovirus	Begomovirus AM-MB2 isolate	KU511271
Sweet potato badnavirus	Badnavirus AM-MB2 isolate	KU511272
Sweet potato virus G	SPVG GWB isolate	JN613807
Sweet potato chlorotic stunt virus	SPCSV Can 181-9 isolate	FJ807784
Sweet potato mild mottle virus	SPMMV isolate 130	GQ353374
Sweet potato latent virus	SPLV	KC443039
Potato virus Y	PVY	NC_001616
Tobacco etch virus	TEV	NC_001555
Turnip mosaic virus	TuMV	NC_002509
Pea seed borne mosaic virus	PSbMV	NC_001671
Plum pox virus	PPV	NC_001445
Sweet potato latent virus	SPLV	NC_020896
Potato virus A	PVA	NC_004039
Tobacco vein mosaic virus	TVMV	NC_001768
Zucchini yellow mosaic virus	ZYMV	NC_003224

RESULTS

RESULTS

Sweet potato viruses

Identification of a new isolate of SPFMV

The identification of a new SPFMV isolate was performed in naturally infected plant material. Four commercial sweet potato (*Ipomea batatas*) roots, named AM-MB, were germinated at Centre for Research in Agricultural Genomics facilities. Once the plants grew, they were further propagated vegetatively through cuttings.

The presence of SPFMV on sweet potato plants was confirmed by reverse transcription-PCR (RT-PCR) of total RNA. The primers (FMCPF, PCMFR) were designed to amplify a 389 bp fragment within the CP-coding region. Both primer sequences corresponded to specific regions for the SPFMV reference genome (NC_001841), selected for not being present in the other members of SPFMV-lineage species (SPVC, SPVG and SPV2). Moreover, they were degenerated in some nucleotides in order to amplify all known SPFMV strains (EA, RC and O) (Table MM1).

The presence of SPFMV was detected by RT-PCR in AM-MB1 and AM-MB2 plants (Fig. R1A). These two plants showed occasional viral symptoms (weak mosaic, leaf spots, and distortions), being those slightly more severe in the AM-MB2 plant (Fig. R1B). The AM-MB2 CP amplicon was sequenced, showing a 94% of similarity with the 9898-10185 positions of the SPFMV reference sequence (Fig. R1C). AM-MB2 plant was selected, further propagated and used in all the subsequent experiments of the present work.

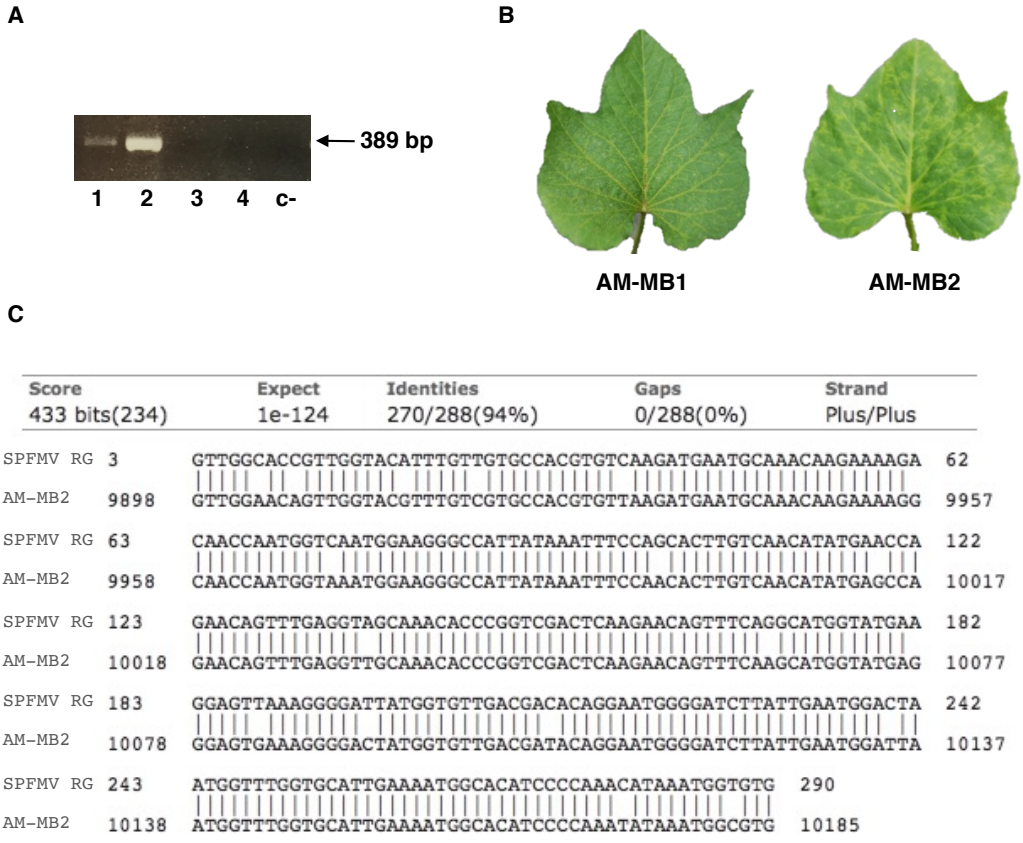

Figure R1: Identification of a new SPFMV isolate in AM-MB plants A) Detection by RT-PCR of a SPFMV CP amplicon in AM-MB plants (Lines 1-4: Sweet potato AM-MB plants, C-: Negative control corresponding to an RT-PCR in the absence of biological template). B) Detail of viral symptoms on AM-MB1 and AM-MB2 plants. C) Alignment of the sequence corresponding to a fragment of the CP region in SPFMV. The SPFMV reference genome (NC_001841) is compared to SPFMV AM-MB2 (BLAST: Basic Local Alignment Search tool, NCBI).

Super-infection with SPCSV

As mentioned in the introduction, it has been reported that SPFMV causes more severe damages in sweet potato plants when synergized with the unrelated crinivirus SPCSV, producing a notable increase in the potyvirus titer (Karyeija et al. 2000). With the aim to reproduce the superinfection in our AM-MB2 plants, and consequently to boost the SPFMV titer, we performed vector transmission assays of SPCSV to independent vegetatively propagated AM-MB2 progeny plants. SPCSV is transmitted by *Bemisia tabaci* whiteflies in a semi-persistent manner. Groups of around 50 viruliferous whiteflies that had acquired SPCSV during 48 h in an infected *Ipomea setosa* plant were caged on fully expanded leaves of AM-MB2 cuttings for a 48-h inoculation period. After insect removal and insecticide treatment, plants were sampled and tested for detection of both SPFMV and SPCSV, in the later case with oligonucleotides CSCPF and PCSCR, which amplify a 790-nt fragment from the CP-

coding sequence of SPCSV (Table MM1). Five plants from a total of 10 were positive for both viruses (Fig. R2A), resulting in a transmission rate of 50% for SPCSV. As shown in Fig. R2B, the superinfection of AM-MB2 plants with SPCSV resulted in a strong enhancement of disease symptoms.

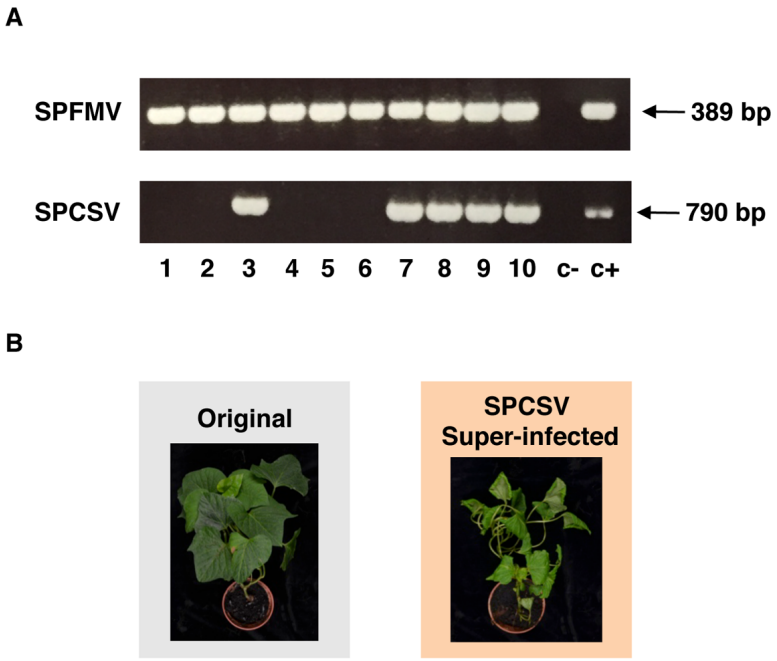

Figure R2: Super-infection of AM-MB2 plants with SPCSV A) Detection by RT-PCR of amplicons corresponding to SPFMV and SPCSV CP in samples from individual plants after insect inoculation of the crinivirus (Lines 1-10: Sweet potato AM-MB plants inoculated with SPCSV with *B. tabaci*; Negative control (C-) corresponding to an RT-PCR in absence of biological template; Positive controls (C+): for SPFMV, an AM-MB2 plant original; for SPCSV, an *I. setosa* infected plant. B) Appearance of AM-MB2 plants propagated vegetatively, with a representative original plant (top) and another superinfected with SPCSV (bottom). Pictures were taken 4 months after whitefly-mediated inoculation of the crinivirus.

Virome of AM-MB2 plant

It is rather frequent that sweet potato plants are naturally infected with several viruses. With the aim to find the putative presence of other viruses in AM-MB2 plants, as well as to obtain the complete sequence of our SPFMV isolate, a high-throughput sequence analysis was performed. Total RNA isolated from samples of the plants coinfected with SPCSV and SPFMV was analyzed by RNA-seq using Illumina technology and compared to equivalent samples deriving from AM-MB2 plants not superinfected with the crinivirus. Abundant SPFMV-derived reads were found in the analysis of sequences, together with a smaller number of reads from two additional potyviruses, SPV2 and SPVC. In addition, reads corresponding to a begomovirus and a badnavirus were identified, but in insufficient number to obtain complete coverage of the genomes of these viruses. Total or partial assemblies of the different viruses were

deposited in GenBank, and their preliminary annotations and accession numbers are provided in Tables R1-R5. SPCSV reads derived from coinfected plants were also used to reconstruct SPCSV complete genome. The reads were divided between both SPCSV RNAs, where 819 reads belonged to RNA1 while 1236 reads corresponded to RNA2 (Tables R6-R7).

As expected, the number of reads for potyviruses increased notably after superinfection with SPCSV, as shown in Figure R3, whereas no major change in the accumulation of reads was observed for the begomovirus and badnavirus.

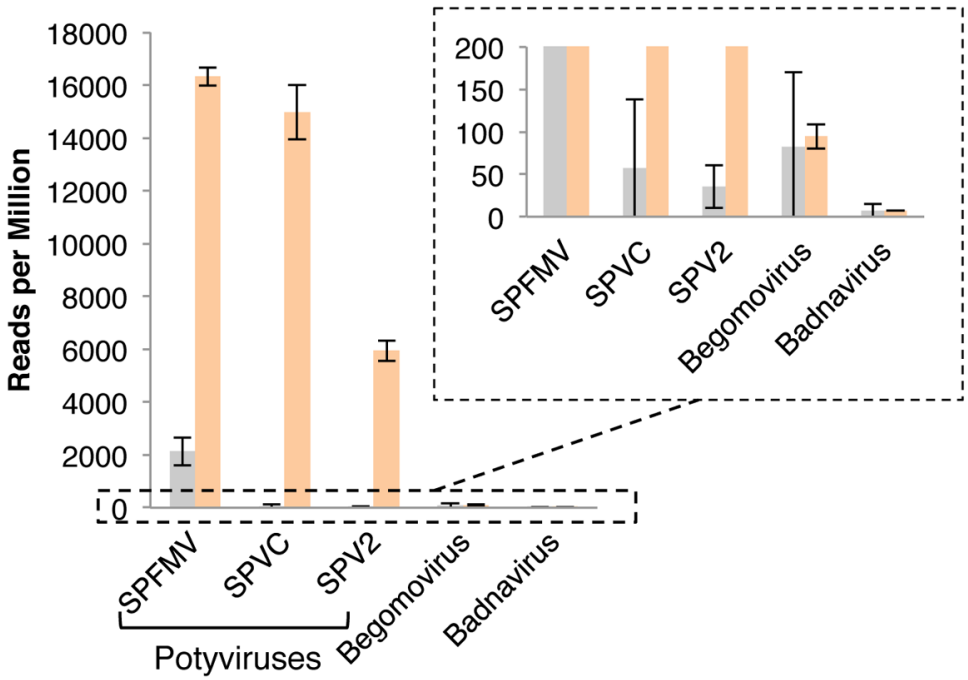

Figure R3: Virome of AM-MB2 plants. Normalized number of virus-derived RNA-seq reads in AM-MB2 plants (gray bars) compared to those plants superinfected with SPCSV (salmon bars). Individual viruses are indicated, and for each one the average and standard deviation values are plotted. The inset with an extended scale was included to accommodate the large differences between the two conditions, without or with SPCSV coinfection.

The assembly of the genomic sequence from SPFMV (Table R1) spanned 10,814 nt, representing almost all of its genome, except for a short region at the 5' end of 6 nt. The sequence of SPFMV AM-MB2 encoded the canonical potyvirus gene products in the polyprotein, i.e., P1, HCPro, P3, 6K1, CI, 6K2, VPg/NIaPro, NIb, and CP, as well as the predicted P1N-PISPO and P3N-PIPO, in both cases preceded by G_2A_6 motifs. The genomic organization is summarized in Figure R4. Positions in the genome were numbered after alignment with other published SPFMV sequences to facilitate comparison of regions with the reference genome (95.12% identity) (Sakai et al. 1997).

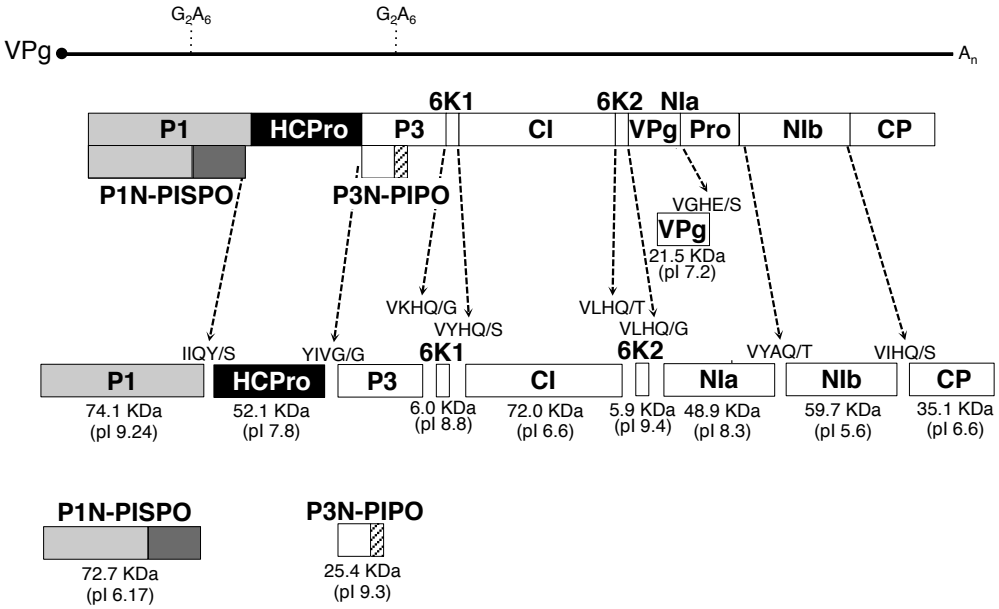

Figure R4: Genomic organization of the SPFMV genome assembled from the RNA-seq data. The RNA genome of SPFMV is represented as a solid line flanked by a covalently linked VPg (solid circle) and the poly(A) tail, with the three ORFs corresponding to the polyprotein, PISPO, and PIPO depicted as boxes (details of the conserved G_2A_6 motifs are shown). Boxes with names represent the different gene products. For the different mature products, the predicted sizes (in kDa), the isoelectric points and details of the cleavage sequences are indicated.

Table R1: Expected gene products deriving from SPFMV isolate AM-MB2[1]

Predicted Gene Product	Genome position (first)	Genome position (last)	Size (aas)	MW (Da)	pI (calc.)	Sequence
P1	118	2103	664	74107,71	9,24	MATVMASAKPAGKRKLTWKECCNKWGRAAMEQQQQQQSKKTVHLGRDHLAAYLLAFVPETEWHKYYYGSRGGPSPALLILKGAIEHGEVYKWESELTFCAECD DVLDGHNCDSCGHRHIKRDDNIADNMNAIARALGGYDAYYASNWAVYETAKYELDQVAPTAGMLYKQAKEAEKLLGKRPTRREIQEVEDLWAEYEEAAAREAVEA SEASNGHATSEVANKNAYLSDEEDDEEFPPLVVTVEKVVPTTTIIESTPEVGKTIEVQTPLEPVPEVLAATTFVEATIEGKDAPTGSIQFGTIVCALEPIKASEAGIVKEP TTGFFFGTIPAIVPLPTIPLLKLEPTIVEPIATPVVEVTSSEIVKVPIATPTEVEKASKAPLPKHLYPWTAKTQTPGEVHHKMVRKWVQKTQQAAAEKEKLVWKKLDEQL ATRNEIRKGLKVKWRWGLYRLVKKTRKDNQRQRRQRRMEKEQQLLMAMPPQVLTGISIAGGPSASLEMTPTPNGKIFCTPSMKKKKTLKSPKLTQEKIHELTQAVL KIACRKRMSIELVGKKSTKGQYRKFQGANYLFLHLKHMEGLRESVDLRIHTTTQNLVLQAAKVGAWKRPVKTTMLSKGSSGMVLNPDKLLGPRGHAPHGMLVVRG ALRGVLYDARMKLGRSVLPYIIQY
P1N-PISPO	118	2072 (+1)	654	72726,52	6,17	MATVMASAKPAGKRKLTWKECCNKWGRAAMEQQQQQQSKKTVHLGRDHLAAYLLAFVPETEWHKYYYGSRGGPSPALLILKGAIEHGEVYKWESELTFCAECD DVLDGHNCDSCGHRHIKRDDNIADNMNAIARALGGYDAYYASNWAVYETAKYELDQVAPTAGMLYKQAKEAEKLLGKRPTRREIQEVEDLWAEYEEAAAREAVEA SEASNGHATSEVANKNAYLSDEEDDEEFPPLVVTVEKVVPTTTIIESTPEVGKTIEVQTPLEPVPEVLAATTFVEATIEGKDAPTGSIQFGTIVCALEPIKASEAGIVKEP TTGFFFGTIPAIVPLPTIPLLKLEPTIVEPIATPVVEVTSSEIVKVPIATPTEVEKASKAPLPKHLYPWTAKTQTPGEVHHKMVRKWVQKTQQAAAEKEKLVWKK**TGRTI GHKERDQKRSQSKMEVGTLQTSQEDQEGQPKTAPTEAHGEGTAIIDGYATSSSDGHLHCWGSIGESGNDSNSEWEDFLHAFHEEEENFKISQINTRENSRAHA GSSENCVQEKDEHRIGGQEVHKRAVQEISRSKLFVPSFKTYGRLKRVSGFKNSHNNSKPRTSSCQGWSMEKTCKDNNVVQRFKWHGAESRQTVGPKRSCTTR NARGAWGFTRSAIRRTNETW**
HCPro	2020	3477	488	52149,48	7,86	SSTMERFLSGFDNKFKQMRQTDLNHVCESSYDAEQAGSVAAISHHMLYPMGRTTCKFCINNVEDMSRDEWCEYVRSFISRNKILCQSEYKNFVHLPQIMDFLSDSL VNTNKNLKAFNEIQNLIGDRTDAPFTSVCEVNKVLVKGGRAKSDELIKASENLLEVARYLKNRTENIKKGSLQSFRNKISQKSSVNLALMCDNQLDKNGNLIWGERGY HSKRFFANYFDVIDPSQGYEKYVIRENPNGSRKLAIGKLIVSTNFSVFREQMKGEPIQKQKLDNHCTSLRDGNFVYPCCCVTLDDGQPLESEFKLPTKNHLVIGNSG DPKYVDMPPEISKNMYIAKDGYCYVNIFLAMLVNVNEAEAKDFTKQVRDVLMEKLGKWPTMFDVATACAFMSVFYPETRNAELPRILVDHSTKTMHVVDSFGSLST GYHVLKANTVSQLIQFSSSSLESEMKHYIVG
P3	3484	4533	352	39639,25	8,52	GVTALPDVQERCIRTIIKGVYKPDVMYTILSEDPYALLLSVMSPRILLALLNSGSLDRSMEAWITEDQEVAVIIGTLQELAKKVSTSRVLEKQLKVIESQAHTLLFDPAFV RSRTPSFALSQKIIRGLAEGRESNRVLYEQGHSIASYAASHELMEKIWDRLLKEEYEGLPWHGKCAQIMRSSKRACGLLSIPTWPKIGALSDRATDLCTTLHTKSVTF KNTCRNGVVQRIADAHIKCVRTIMRTSLAAIKFAIPDVLKFVNMLLVINLLLQIAKVARDMSMKHRQAQIDLNAYLFDQEIDKVNVIYDAYCLKIGGEPTMDEFLGHVEYI NPTLSGTAKWLCYTADMEVKHQ
P3N-PIPO	3484	4145 (+1)	223	25461,58	9,35	GVTALPDVQERCIRTIIKGVYKPDVMYTILSEDPYALLLSVMSPRILLALLNSGSLDRSMEAWITEDQEVAVIIGTLQELAKKVSTSRVLEKQLKVIESQAHTLLFDPAFV RSRTPSFALSQKIIRGLAEGRESNRVLYEQGHSIASYAASHELMEK**NLGSSFKGGIRRTALAWKMCTNHAIIKTCMWFTKYSNMAKNRRFKRQSNRLMYYLTHEE CHIQEYL**
6K1	4540	4689	52	6048,15	8,87	GKSRKEMQYERIIAFVSLLLMIVDSEKSDCVYKILQKLKGLMGTINNDVYHQ
CI	4696	6618	643	72047,24	6,62	SLDDITNVLEEKNLTVDFELQSGEHPTNPCTDSTFDEWWRRQIETNNTITHYRTEGVFIEFTRSNAVSVVNNIATIDAKDILIRGAVGSGKSTGLPFYLSRKGRVLLLEP TRPLAENVHRQLGGEPFMVQATLRMRGLTVFGSHPINIMTTGFAFHYYANNPEQIGEYDFIMFDECHVHDAQAMAFRCLLKEHEFKGKILKTSATPPGREVEFTTQY PVQIKVEERLSFKAFVEAQGTGSNADVVTIADNILVYVASYNEVDELSRMLVEANYKVTKVDGRTMKVGNVEIQTCGSPQKKHFIVATNIIENGVTLDIEAVVDFGTKV TAYLDVDLRALHMSKGPISYGERIQRLGRVGRNKAGVALRIGFTEKGLTEIPQTTATEAAFLCFAYGLPVMTPNVSTSLLSTCTVKQARTMLQFELTPFYMVNMVRY DGSMHPAIHSILKKYKLRDAETDLNKMAIPNRGVTGWLSVGEYAKSGKRMDIDDSVRIPFLNPSMPERLHVDIWDAITKYKHEAGFGRISCINSCKVAYTLQTDLYAIP RTIKIIDALIADEMRKKEHYKTITGRTVSSSSFTLNSIATLWRNRYAQDYTSENIAVLSSVRSQLLEFENLSVDSSFNSMGEAALRAYVRETGATSCVLHQ
6K2	6625	6777	53	5929,98	9,4	TKDSLSKHLRLKGVWNKSVITQDLFILAGVFAGGLWMIMAGLKESFDQTVLHQ
NIa	6784	8082	435	48985,93	8,29	GKEKRQMQKLKFRKARDNKLGFEVHADDGTIEHFFGSAYTKKGKQKGKVTGMGSKNRKFINMYGFDPTEYSFVRFVDPLTGAVMDDSPYTDILLVQEKIGEARLNA IKEDELSREKVAQNPGIHAYYINEITNAALKVDLTPHNPLLACERHSTIAGHPEYEGVLRQTGPPIKMTLNDVPVNPEEASLVGHESKSLFRGLRDYNPIASVICHLMN EADGRTSDCFGIGYGGLIITNRHLFKRNNGTLTIKSRHGEFVIKNTTQLGMKPCADRDILIIRMPKDIPPFPQRIKFRVPKENERICLVGSNFQDKSITSTISETSVTCHV PNSHFWKHWIDTKDGHCGLPLVSTTDGALLGVHSLSNLTNTQNFFASFPENFEVDYLKTPEAMDWIKKWSYNPDEICWGTLELKTGQPVAPFKVSKLITDLEGIQVY AQ
VPg	6784	7353	192	21543,47	7,23	GKEKRQMQKLKFRKARDNKLGFEVHADDGTIEHFFGSAYTKKGKQKGKVTGMGSKNRKFINMYGFDPTEYSFVRFVDPLTGAVMDDSPYTDILLVQEKIGEARLNA IKEDELSREKVAQNPGIHAYYINEITNAALKVDLTPHNPLLACERHSTIAGHPEYEGVLRQTGPPIKMTLNDVPVNPEEASLVGHE
NIb	8089	9645	521	59773,15	5,59	TRSDRWVQDRLYGNLKAVGQCPAQLVTKHVVKGKCMLFDLYLQQDQSEREYFKPLMGAYGKSRLNKEAYNKDLFKYATQIQAGDVQVDTFELAERSVVSMLTSK GFEKCNYITDPEEILRALNMKAAVGAMYSGKKKDYFEGMSDHDVEDHLFHSCKRLFMGHKGLWNGSLKAELRPMEKVELNKTRTFTAAPLDTLLGGKVCVDDFNN MFYNHHLKCPWTVGITKFYQGWDRLLTSLPEGWVYCDADGSQFDSSLSPYLINSVLNIRREFMEDWDVGDQMLRNLYTEIVYTPILTPDGTIVKKFKGNNSGQPST VVDNTLMVVLAVHYTLLKLGIQESEFDKCCVFFANGDDLLLAMRPDTAHLLDEFGGCFSELGLNYDFSSRTNKKEDLWFMSHCGVKRDGIFIPKLEPERIVSILEWDR SHEPIHRLEAICAAMVESWGYDELLHHIRKFYAWVLDQAPYNELARNGKAPYIAETALKALYTGVQPNASELSAYTRVLKEMYDDSVLQENDLEVYHQ
CP	9652	10590	315	35146,61	6,66	SSESTEFKNAGADPPAPKPKNIPPPPTITEITDPEDPKQAALKAARAKQPAVIPESYGRDTSKERESIVGASSKGVKDKDVNVGTVGTFVVPRVKMNANKKRQPMVN GRAIINFQHLSTYEPEQFEVANTRSTQEQFQAWYEGVKGDYGVDDTGMGILLNGLMVWCIENGTSPNINGVWTMMDGDEQVTYPIKPLLDHAVPTFRQIMTHFSD VAEAYIEMRNRTKAYMPRYGLQRNLTDMSLARYAFDFYELHSTTPARAKEAHLQMKAAALKNARNRLFGLDGNVSTQEEDTERHTTTDVTRNIHNLLGMRGVQ

[1] Prediction of the SPFMV protein products based on the preliminary nucleotide annotated sequence deposited in GeneBank (Accession Number: KU511268).

Table R2: Expected gene products deriving from SPV2 isolate AM-MB2[1]

Predicted Gene Product	Genome position (first)	Genome position (last)	Size (aas)	MW (Da)	pI (calc.)	Sequence
P1	118	1971	618	70385,46	9,33	MACVTNGTAFARKKKMTWKECCNKWGRAAMEQQQGKGSAYTTEVSRDQLAANIFAFIPTTEWHSYYVARVGLSANALKLKYAISFGEKYEHGANFNRCPECDCAI DEHYCDECEIRFKKADDNIIKNMNGTAKALGGWDNYYAATWKQFEAAKYDMEQIAPTAGMLERRAKEAEKLLGKKAKKHEIAEVQQLWEEFEAAKELEAEEETFFE HEASLSSIPEPTTYEEAFPQLKVTSDVSTNTSQASGVVEDNLGFFFGEIPAKIALPTIPILEILPAAPILNLNGELNDITEVKQPEVIDEVCVTTQPKETDIIQSGLKKYELV NGKFQKVKKLPKTLYPWGDRKTTPGKTQHAMVTKWVRKKMSEEADKEEKIWSAWEHTKKQQLEKRLDLKVKWRYGMFRLAKKTRKDNQRQRLKQRAMLEQKKL EMMPQQIVSTISIGGGLAPSHMEEATQKSGMIFCTPSMKKRKLFKPLVISNGNLDNLTQAVLKIACKKEMNVEFIGKRVIKGDYTRKENVRHLRLQLKHMKGLRHSID LRIPSDLQALIVKAAHVAAWKKIYNTQNVVKGMSGFVLNPQRLQGKTGHAPQGIFVVRGAFKGVLYDARMKIGRSILPYMEQF
P1N-PISPO	118	1919 (+1)	601	68297,56	6,61	MACVTNGTAFARKKKMTWKECCNKWGRAAMEQQQGKGSAYTTEVSRDQLAANIFAFIPTTEWHSYYVARVGLSANALKLKYAISFGEKYEHGANFNRCPECDCAI DEHYCDECEIRFKKADDNIIKNMNGTAKALGGWDNYYAATWKQFEAAKYDMEQIAPTAGMLERRAKEAEKLLGKKAKKHEIAEVQQLWEEFEAAKELEAEEETFFE HEASLSSIPEPTTYEEAFPQLKVTSDVSTNTSQASGVVEDNLGFFFGEIPAKIALPTIPILEILPAAPILNLNGELNDITEVKQPEVIDEVCVTTQPKETDIIQSGLKKYELV NGKFQKVKKLPKTLYPWGDRKTTPGKTQHAMVTKWVRKKMSEEADKEEK**NLECVGTHKETATREAIGPESEMALWDVSPRQKDTKGQPKTTSETACNARAEET RNDAPTDSLNNINWGWSSTESYGGSHSEEWDDFLHAFYEEEEAFQTTSNFEWELRQSHTSSSKDRLQERNERGVHWKTCDKRRLHAQGKCKASSPSVEAYE RLAPLHRSKNPFRPTSSHCKGSTRGSVEKDLQHAKCCKRNERVCLKPSATARENRTRTTRNFRGTWSFQRRPV****
HCPro	1972	3375	458	52595,4	7,9	SQTGDRFWNGYDQMYRDLRGNEQDHICKSDLDVSEAGKLAAVMQHLCLPMNRITCLTCANKILEMSSSEWVEHIRMFVNSKLEFIRKECPNYKHVHWMIETMTKN LVHENKNLKAFNEIQQLIGDRTDAPFSTVNEINKILVKGGKIKAEEFLQASEHLLEVARYLKNRTENIKKGSLVSFRNKISQKAHLNLSLMCDNQLDKNGNLIWGDRGY HSKRFLSNYFEVVDPEQGYEKHIIRQNPNGARKLAIGKLIVSTNFSVFREQMKGEPIPKLKLDNHCTSLREGNFVYPCCCVTMDDGTPIESEFKLPTKNHLVIGNSGD PKYVDMPPEVDKKMYIAKEGYCYVNIFLAMLVNINESDAKDFTKQVRDILMEKLGKWPSMYDVATACAWISIFYPETRNAELPRILVDHNTKTMHVIDSFGSLTTGYH VLKANTVSQLIQFSSNSLDSEMKHYLVG
P3	3346	4401	352	40115,96	8,42	GIVGVSKDEERCLRSIIKSVFKPELMHQILEEDPYVLLLSILSPRVLLALFNSGSLDRSLEKWLTKDQEVSTILGILIELSRKVTVARTLDEQLNVIEGHASYLIDNLWIEG RKTVAHALSYKIARGLSEKREANKVLYEQGHRITAFISSHEMMEKIWDQLLLEAWNELSWQEKCCSMMRSLKYAKPLQGGFPQVNIGGLKDKVGESLTTLHTKSAVI GKECKKSVIDNVASLYKSMIRNTINVTLSTVRLLMPDILKFVNILLVINLLLQIAKTAKSMNQKTKQMKIDLGEFMLDQEIDKINVIYNSMCSKEGKLPTKEEFLEKVEYLN PQLLGTAKWLVYAYDSDVFHQ
P3N-PIPO	3346	4004(+1)	220	25320,43	9,43	GIVGVSKDEERCLRSIIKSVFKPELMHQILEEDPYVLLLSILSPRVLLALFNSGSLDRSLEKWLTKDQEVSTILGILIELSRKVTVARTLDEQLNVIEGHASYLIDNLWIEG RKTVAHALSYKIARGLSEKREANKVLYEQGHRITAFISSHEMMEK**NLGSTFAGSMERVKLAGKVLFNDALVKVCKTFTRRFSPSKYRRFERQSRRITYYITHKECC DR**
6K1	4402	4557	52	5733,7	8,14	AKSAKESSYERIIAFIALVLMVIDAERSDCVYKSLNKLKGLMGTIGDGVYHQ
CI	4558	6486	643	72285,5	7,04	SLDDISNEFEEKKLTIDFELQSDESHINSESDSTFGDWWKKQLETNNVIPHYRTEGHFMEFTRANAVSVANTIAMSPHKDLLIRGAVGSGKSTGLPFYLSRKGRVLLV EPTRPLAENVHRQLAGEPFMIQSTLRMRGLSVFGSAPISIMTSGFAFNYYAHNPDQLREYEFVIFDECHVNDAHAMAFRCLLHEHAFNGKVLKVSATPPGREVEFST QYPVKIKTEERLSFQAFVDAQGTGSNSDVISSADNILVYVASYNEVDELSKMLIDRGHKVTKVDGRTMKVGNVEIITSGTSNKKHFIVATNIIENGVTLDIEAVVDFGTK VTVYLDVDSRMIRPCKGPITYGERIQRLGRVGRNKAGIALRIGFTERGLCEIPQTVATEAAFLSFAYGLPVMTNNVSTSLLSTCTVRQARTVLQFELTPFYTVNLVRYD GSMHQAIHNLLKKYKLRDSEIVLNKLAIPNRGITGWLSVCDYIRIGQRMDLDDSIRIPFLNNAMPVRLHQEIWDVIQKYKHEAGFGRLSCISACKIAFTLQTDMYAIPRTI KILDALIESEMRKKEHFKTVTGRTTSSHHFTLNSIATMWRARYAQDYTSENIAILTAAKSQLLEFANLSTDVSFNEMSESMLSSYIRDSGAVSCVQHQ
6K2	6487	6645	53	5889,02	7,92	SAEAMAKHLKLKGIWCKSLMTQDLLVLAGVFIGGIWMIMQGAKDAFDETVRHQ
NIa	6646	7956	437	49625,31	8,52	GKDKRQRQKLKFREARDKKMGFEVTADDGTIEHFFGEAYTKKGKQKGKTTGMGSKNRRFINMYGFDPTEYSLVRYVDPLTGKIIDDSIYTDVLLVQEQFTKARREAI NDDLLSNEKVAQNPGIVAYFIKEGANAALKVDLTPHNPLKACDRINTIAGFPERESELRQTGQPIQISKNQVPHNPETSDSSVVTHESKSLFRGLRDYNPIASVICHLV NTSDGRTTDVFGLGFGGLIITNRHLFKRNNGELLIKSRHGEFTIKNTTQLHMMPCSERDILVIKMPKDIPPFPQKLRFRVPKENERICLVGSNFQEKSITSTVSETSVTC RVDRSHFWKHWVDTKDGHCGLPIVSTTDGAILGLHSLSTMTNSQNFFAAFPESFEEDYLRSPESLEWVRKWSYNPDEVCWGSLELQWSQPGEPFKPTKLMSDLN AIPVYAQ
VPg	6646	7227	194	21935,72	8,84	GKDKRQRQKLKFREARDKKMGFEVTADDGTIEHFFGEAYTKKGKQKGKTTGMGSKNRRFINMYGFDPTEYSLVRYVDPLTGKIIDDSIYTDVLLVQEQFTKARREAI NDDLLSNEKVAQNPGIVAYFIKEGANAALKVDLTPHNPLKACDRINTIAGFPERESELRQTGQPIQISKNQVPHNPETSDSSVVTHE
NIb	7957	9519	521	59520,24	5,24	AKHDTWVRDRLNGNLKAVGVCPSQLVTKHVVKGKCMLFELFLQTFPDEKSFFKPLMGAYGKSKLNKEAYTKDLFKYATPISAGEVDTEVFEQAETLVIEMLREKGF TECNYVTDTDEIIEALNMKAAVGALYSGKKKEYFQDLNADDRDDLLFHSCKRLYMGRKGLWNGSLKAELRPMEKINANKTRTFTAAPLDTLLGGKVCVDDFNNMFY NHHLKCPWTVGITKFYKGWDTLLNKLPEGWLYCDADGSQFDSSLSPYLINAVLNIRLAFMEDWEIGAQMLKNLYTEIVYTPILTPDGTIVKKVKGNNSGQPSTVVDNT LMVVLAMTYSLCKLNIKPENHDQVCIYFANGDDLLLAIDPTYEWILDSLGKLFRELGLNYDFSSRTNDKEELWFMSHRGMKRDGIYIPKLEPERIVSILEWDRASEPVH RLEAICAAMVEAWGYDDLLQHIRKFYAWILDQAPYSELARVGKAPYIAETALKALYTCVEPSAEDLSEYVRVLNLMYDDAVESNDCEPVYHQ
CP	9520	10515	332	37117,62	6,2	SGTEEIKDAGTPTPAKSVKTRTGQTQPLKAPEGSTNPTDPPPPTVEEIIEEETPAQKALREARGKQPATQPSYTYGRDTGPRSPRQVTTTSRVRDRDVNAGTVGTFI VPRLQITSSKKRLPIVDGRPVINLDHLA?YDPEQTNLANTRSTQEQFKAWYEGVNGDYGVSDDEMSILLNGLMVWCIENGTSPNINGMWVMMDGEEQVTYPIKPLL DHAVPTFRQIMTHFSDIAEAYIEKRNRIKAYMPRYGLQRNLTDMSLARYAFDFYELHSNTPVRAREAHMQMKAAALKNAQNRLFGLDGNVSTQEEDTERHTTTDVT RNIHNLLGMRGVQ

[1] Prediction of the SPV2 protein products based on the preliminary nucleotide annotated sequence deposited in GeneBank (Accession Number: KU511270).

Table R3: Expected gene products deriving from SPVC isolate AM-MB2[1]

Predicted Gene Product	Genome position (first)	Genome position (last)	Size (aas)	MW (Da)	pI (calc.)	Sequence
P1	157	2118	654	73232,81	8,95	MASATVSVKPAGKRKLTWKECCNKWGRAAMEQQQAAHSRRRVELSRNQLAANIFAFVPETEWHKYYFGNRGGPSPQLEVLSNAIQYGEAFKYKFDFTFCPDCDE FLEGHKCEECGTTFRKTDDNLADNMNVVARELGGYDAYYASTWSEFEQAKLELEEVAPTAGQLRKQAQAAEKLLDKRSTRKEKEYVNSLWEAVEEAEATETGEA SDASEKAAELSGIPSSATAGEMFPPLVGHKNTEVITATSDVVVSECSNIQFGQITEFMPEENKDEKVVESLIEEVENATASAVMPIETGFFFGTIPAIIPLPVVVPQQGS MGVLQPAFMQVGTMPVNGIALADTHLETKETAVKEIEPAKEDIDVGAQKSTSLPAHLYPWAPRSKNSGATHHQMVRKWVKKTQEAEEMKQRAVVKKLDEQLAAR NEARKDLKVKWRWGLYRLVKKTRKDNQRQRQKKRMEKEQQLLLAMPPQILTGISIAGGPVASLQETPTVNGKISSTPSMKRKRILKSPTLSSDKIQELIKATLKIACK QGLQVEIINKKTVKGVYRRHGGTNHLFLHLKHMEGWRKPVDLHIHQEDIELVTMAARVGAWNKRFRTSQLCKGTSGLVLNPDKLTGPRGHAPKGLFVVRGALAEV VYDARMRLGRSTLPYIEQF
P1N-PISPO	157	2087(+1)	644	71988,27	5,98	MASATVSVKPAGKRKLTWKECCNKWGRAAMEQQQAAHSRRRVELSRNQLAANIFAFVPETEWHKYYFGNRGGPSPQLEVLSNAIQYGEAFKYKFDFTFCPDCDE FLEGHKCEECGTTFRKTDDNLADNMNVVARELGGYDAYYASTWSEFEQAKLELEEVAPTAGQLRKQAQAAEKLLDKRSTRKEKEYVNSLWEAVEEAEATETGEA SDASEKAAELSGIPSSATAGEMFPPLVGHKNTEVITATSDVVVSECSNIQFGQITEFMPEENKDEKVVESLIEEVENATASAVMPIETGFFFGTIPAIIPLPVVVPQQGS MGVLQPAFMQVGTMPVNGIALADTHLETKETAVKEIEPAKEDIDVGAQKSTSLPAHLYPWAPRSKNSGATHHQMVRKWVKK**TGRTIGSS ERSKERPQSEMEVGPLQAGQKDQKGQPKAAAEETNGKGATTAPCNATSDFNGHFNSWWPSSESAGDSYSEWKDFIDAFYEAEKDFKISNPIIRQDTRVDKSNF KDCLQTRTSSGDYQQENRERSLQTTRRNKPFVPSFKTHGRMEEACGSAYPPRRYRACNNGSSRRCMEQEIPYKPTMQRYQWVSSQSGQIDRSARSRAQGAL RGSWGFSRSSIRRADAAW**
HCPro	2119	3492	458	52382,02	8,11	SSTMERFLRGFDEKFKQLRQVDSDHVCESTYDAEQAGAVAAILHHMVCPMNRTTCKHCSNKIEDLSKDEWCDYVRDFTNKNRLPLQLEFKDFKHLPLIMDFIAESL VQTNKDVRAFNEIQTLIGNRIDAPFTTVCEVNKVLVKGGRAKGTEFTKASEALLELARYLKNRTENIKKGSLQSFRNKISQKAAMNLALMCDNQLDKNGNLIWGERG YHSKRFFSNYFDEINPEEGYSRYIVRNNPNGTRKLAIGKLIVSTNFSVFREQMKGEPIHKQKLDNHCTSTLDGNFIYPCCCVTYDDGQPMESEFKLPTKNHLVIGNSG DPKYVDMPPEISKKMYIAKEGYCYINIFLAMLVNVNEAEAKDFTKQVRDVLMEKLGKWPTMFDVATACAFMSVFYPETRNAELPRILIDHTTKTMHVIDSFGSLSTGY HILKANTVSQLIKFANSSLDSEMKHYLVG
P3	3493	4548	352	39955,17	7,25	GLTALPANEERCVRTVIKGVYRPKILYEILSEDPYMLMLSVISPCIILALFNSGSLDRAMDTWITKDQEVAVIIGTLSELARKVSTSRVLEQQLQIIESQSHTLLFDDSTAR RRTPSFALSQRVIRSLSERRETNRVLHEQGHTVSAYATSHELMEKIWDTLLKQEYAELALLEKCSLIMRSSRYMRCIQGTYLRQSIDDFKGRVDASYTALHTKSVALS NTCKEGFVSRVAGAHARCVRTIVQTSLSAIRFAVPDILKFVNLLLVVNLILQIAHVARNMVQKHQQAQIDLNAYLFDQEIDKINVIYDSFCKKIGGEPTMDEFLAHIEYIN PTLLGTAKWLCYTADVEVEHQ
P3N-PIPO	3478	4145(+1)	223	25598,61	9,58	GLTALPANEERCVRTVIKGVYRPKILYEILSEDPYMLMLSVISPCIILALFNSGSLDRAMDTWITKDQEVAVIIGTLSELARKVSTSRVLEQQLQIIESQSHTLLFDDSTAR RRTPSFALSQRVIRSLSERRETNRVLHEQGHTVSAYATSHELMEK**NLGHSFKAGVRRTCLVGKMLTNHAIIQVYALYTRYVSATKYRRFQRQSRRILYCITHKECSI EQHL**
6K1	4549	4704	52	5933,02	8,73	GKSRKEVQYERIIAFISLLLMVIDSERSDCVYKILSKLRGLMGCIDGGVYHQ
CI	4705	6633	643	72287,37	6,8	SLDDITNILEEKNLTVDFELQGDEQLSNAMTDATFDEWWRKQLETNRTITHYRTEGTFIEFTRSNAVSVANNIATLPANDILVRGAVGSGKSTGLPFYLSRKGRVLLLE PTRPLAENVHRQLGGDPFMVQTTLRMRGLTVFGSHPINIMTTGFAFHYYANNPEQLREYEFIIFDECHVNDAQAMAFRCLLKEHEFSGKIIKASATPPGREVEFTTQ HPVQIKVEEESLSFKAFVEAQGTGSNADVVAVADNILVYVASYNEVDELSRLLVEANHKVTKVDGRTMKVGNVEIKTTGTSNKKHFIVATNIIENGVTLDIEAVVDFGTK VTAYLDVDLRMIRTSKGPISYGERIQRLGRVGRNKAGTALRIGYTEKGLVDIPQTVATEAAFLCFAYGLPVMTPNVSTSLLGSCTVRQARTMLQFELTPFYMVNMVR FDGSMHHAIHQLLKRYKLRDAETTLNKLAIPNRGITGWMSAADYRKVGQRLDIEDQIRIPFYHQSMPEKLHSDIWEAIQRYKHEAGFGRVSCINSCKIAYTLQTDVYAI PRTIKILDALIADEMRKKEHYKTITGRTVSSSSFTLNSIATLWRNRYAQDYTSENIAVLSSARAQLLEFENLSMDASYNEMSKGILETYVRESGATTCVLHQ
6K2	6634	6792	53	5843,78	8,11	TKSDLAKHLQLKGIWNKSVITQDLLVLAGVFVGGVWMVFSGAKESFEQTVTHQ
NIa	6793	8097	435	48917,56	8,5	GKEKRQRQKLKFRQARDRKLGFEVHADDGTIEHYFGSAYTAKGKQKGKVTGMGVKNRKFINMYGFDPTEYSFVRFVDPLTGLVFDDSPYTDIQLVQEKIGDARHK AILEDKLSRERVSYNPGVSAYYINEITNAALKVDLTPHNPLLACERHSTIAGHPDHEGELRQTGAAVKVDIKDVPENPEEASLVGHESKSLFRGLRDYNPIASVICHLV NEADGRTSDSYGIGYGGLIITNRHLFKRNNGTLTIRSRHGEFVIKNTTQLGMKPCADRDILIIKMPKDIPPFPQRLQFRIPKENERICLVGSNFQDKSITSTVSETSVTCH VPNSHFWKHWIDTKDGHCGLPLVSTVDGAILGVHSLSNLTNTQNFFAAVPANFEVDYLKTPEATEWIKKWSYNPSEICWGTLELKTGQPVAPFKVTKLITDLDSMQV YAQ
VPg	6793	7368	192	21627,34	7,26	GKEKRQRQKLKFRQARDRKLGFEVHADDGTIEHYFGSAYTAKGKQKGKVTGMGVKNRKFINMYGFDPTEYSFVRFVDPLTGLVFDDSPYTDIQLVQEKIGDARHK AILEDKLSRERVSYNPGVSAYYINEITNAALKVDLTPHNPLLACERHSTIAGHPDHEGELRQTGAAVKVDIKDVPENPEEASLVGHE
NIb	8098	9660	521	59582,23	5,52	ARSDRWVLDRLYGNLKAVGQCPAQLVTKHVVKGKCMLFDLYLQQDCDVRSFFKPLMGAYGKSRLNKEAYNKDLFKYATPINAGDVCHKTFEQAELAVVDMLKAN GFHKCNYITDPEEIVKALNMKAAVGAMYSGKKKDYFDGMDDKDIENLLFHSCKRLYMGQKGLWNGSLKAELRPMAKVELNKTRTFTAAPLDTLLGGKTCVDDFNN MFYNNHLKCPWTVGITKFYQGWDRLLTSLPEDWIYCDADGSQFDSSLSPYLINAVLNIRREFMEEWDIGDQMLRNLYTEIVYTPILTPDGTIVKKFKGNNSGQPSTVV DNTLMVVLAVFYTLLKLGVSEFEISERCVFFANGDDLLIAMRPDTAHLLDNFSECFAELGLNYDFSSRTTKKEELWFMSHCGIKRDGIYIPKLEPERIVSILEWDRSHE PIHRLEAICAAMVEAWGYDELLHQIRKFYAWVLGQAPYSELARTGKAPYIAETALKSLYTGVQPSADDLSEYTRVLNEMYDDSLLQDNELSVYHQ
CP	9661	10599	313	34986,39	6,83	SGNPPEFKDAGANPPAPKPKGPFAAPEITEVTEPEDPKQAALREARQKQPAVTPESYGRDTGEKSMRSVSPQRVKDKDVNVGTTGTFVVPRVKLHTGKMRQPRV NGISVVNLQHLATYEPEQHNIGNTRSTQEQFRAWYEGVKGDYGVDDAGMAILLNGLMVWCIENGTSPNINGVWTMMDGDEQVTYPIKPLLDHAVPTFRQIMTHFS DVAEAYIEMRNRTKAYMPRYGLQRNLTDMSLARYAFDFYELHSTTPARAKEAHMQMKAAALKNAHNRLFGLDGNVSTQEEDTERHTATDVTRNIHNLLGMRGVH

[1] Prediction of the SPVC protein products based on the preliminary nucleotide annotated sequence deposited in GeneBank (Accession Number: KU511269).

Table R4: Expected gene products deriving from unknown Sweet potato begomovirus isolate AM-MB2[1]

Predicted Gene Product	Genome position (first)	Genome position (last)	Size (aas)	MW (Da)	pI (calc.)	Sequence
V2/MP	43	441	132	15454,85	8,11	MMTLLYKDQSGCRAWRPSMAEMWDPLQNPLPDTLYGFRCMLSVKYLQGILKKYEPGTLGFELCSELIRIFRVRQYDRANSRFAEISSLWGETGKTEAELRDSYRALHWECCPNCCPKLCPGFKRRPDEEKEG*
V1/CP	266	1030	254	29476,86	10,04	MTGRIRVSPRFHPYGGRQVRRRLNFETAIVPYTGNAVPIAARSYVPVSRGVRMKRRRGDRIPKGCVGPCKIQDYEFKMDVPHTGTFVCVSDFTRGTGLTHRLGKRVCIKSMGIDGKVWMDDNVAKRDHTNIITYWLIRDRRPNKDPLNFGQIFTMYDNEPTTAKIRMDLRDRMQVLKKFSVTVSGGPYSHKEQALIRKFFKGLYNHVTYNHKEEAKYENQLENALMLYSASSHASNPVYQTLRCRAYFYDSHNN*
C3/REn	1480	1049	144	16864,56	9,5	MDSRTGESLSHAQTTRAVEFNTNPISVGRTAPFHLRIMYVHESTQGRTILKFQLRVNHRERRQLGFHKIFLQFRILTTRLTGAIHSWTGILERLKWHICNELANLGLFSLINLVFVIRYLPRVCSWIDEIDTIDCNDDVKVLLY*
C2/TrAp	1643	1200	148	16560,58	8,08	MSNPLSGYKRKCPIQEPLHTEAKKAKRKVPEQRTRIVWK?CGCSAFITTNCKYQHGFTHRGITKSCSDYESSRIQHQPHLCGSDCTIPS?NHVCPREHTGENHPQIPTESQPQGKEAAGIPQDLPPIQDLDDPSNWCYSQLDWYFGTP*
C1/Rep	2646	1555	364	40830,69	6,32	MPRAGRFNIKAKNYFLTYPQCSLTKEEALDQLLHLNTPTNKKFIKICRELHENGEPHLHVLLQFEGNYQCTNQRFFDLVSPSRSSHFHPNIQRAKSSSDVKSYVDKDGDTIEWGEFQVDGRSARGGQQTANDAAAEALNSGSKEAALQIIREKLPEKFIFQYHNLCGNLDRIFSPPPSVYSSPFSSSSFNAVPDIISDWAAENVMDSAARPDRPISIVIEGPSRIGKTVWARSLGPHNYLCGHLDLSPKVYSNSAWYNVIDDVNPQYLKHFKEFMGAQKDWQSNCKYGKPVQIKGGIPTIFLCNPGEGSSFKLWLDKPEQGALKNWATANAIFCDVQSPFWVQEEVSHSGATAHRGEEGQEESS*
C4	2495	2235	87	9533,85	9,6	MKMGNLISTCCCSSKGTTNARIRDSSTLFPHQGHHTFTLISRELNPAPMSSPTSIRTVTQLNGVSSRSTADLLEEASRLLMTQQQRP*

[1] Prediction of the Sweet potato begomovirus protein products based on the preliminary nucleotide annotated sequence deposited in GeneBank (Accession Number: KU511271).

Table R5: Expected gene products deriving from unknown Sweet potato badnavirus isolate AM-MB2[1]

Predicted Gene Product	Genome position (first)	Genome position (last)	Size (aas)	MW (Da)	pI (calc.)	Sequence
ORF1	(703)	(1131)	ND	ND	ND	MSERWEKSLQNWYDSRRSHLEYLDLETVSKPSLSQLAHNLSIV[...]YVLEEKLEEQSLLIKRLEKGLEALTEEFLSSRPLTA[...]
ORF2	ND	ND	ND	ND	ND	[...]
ORF3a	(1486)	(4999)	ND	ND	ND	[...]QGANLLITRGMVGRLSNTPNVGFNYNISAVTDYLASRGVRTLPGRRYSTADLQGLRWNIRRPREVIPRHPTEMISRNLLGGGFSLSFREYQPITTEQRRAAQHPEEDSLEEEVLGVLNVEVLDWDGLDFPEPDPTLVNFEIPEPEPQQQHPEQVVEPVSDEILEFRREYSSIWDYGSEEEALLEFVYYSTTPDDSNYWSYSNAYRELAAALEGNVSPNDVEGLEEVEGGTSTHFSGGGEVVPPSEPNCCIMCNKRGIPEDKILCQNCMDITDDSDDEREVERQERKRMQKQKEKRVTPSTSKQTSQEEIIGAIEGDPWEEFEEMVERLHAQVTQQQPNPPADPQASNTRGQSAQSPYRPPEDTTMGQPSYAPARPTVETVSGPPSFRTDSRFLKRGTNNENWSLPPAQQQGGVLLTLPEQMGLLNDVFMRWETTTLNHMSLMNIQDTQEKVDYMENLLGETAKLAWIQWRTVYEDEYKAIVAQAEGRMGTQNVISQVRRILTLSDPVQGSTAIQDQAYRDLERLQCHDVKDMVKFLNDYMRLATKTGRLYIGRELSDKLWIKMPGDLGTKIKEEFDKKHPGAEIAVIPRIFFAHKYLEDRCKEAAFTRSLKSVSFCKDIPIQGYYGSDKPKYTPRKAKTYKGKPHETHVRIDRRKNLDRNSHCKCFICEEPGHYARDCPNQKRNIKRVMMFNQVNIPDNYDIVSVQENEEDSDAIYSLTEGEEGDEIAFGIVQESVHMISHQVIGSWRAHIDMSEVQKVCRHQWQDHQEIEAPGEDTCLWCKHHINIRTRSHCPACLLTTCNICSLRYLGREVPPKAQERPLPFPDQTALIQQQQLYMNWADQDRARLKQEVEDEKRRGQLLFEAERRRTERLGEEIAQQKLRIESMEEEQKLKNDLHAHTERDLQKKIKELKRLLREEKIKRRSLRNGKDVRTGSSEDDASSEEASGSEN*
ORF3b	(5166)	(7481)	771	85643,35	9,45	MRVSIRIRGCPEFNVNAILDTGATVCCIEEERVPKEGLEESRMTAQFTGLNSTQQTRKKLKEGYMIIADHTFPLPFVYALNPMRIGRGIQFIIGCNFIRRMKGGLRIEGPTVTFYRNVSTIETQEKSTVAAAIGNINEERTMVFPRFRKEVARLIQEGYIGENPLRHWSKNKVECTLRIKNPDLVIQDPPLKHVTPAAREFFQNQVSSLIKAQLIRPSRSRHRTTAFMVESGTSVDPKTGKEVRGKQRMVLNYKRLNDNTEKDQYSLPGINTIISRVAGKKVFSKFDLKSGFHQIRMSKESIPWTAFWTPDGLYEFLVMPFGLVNAPADFQRKMDNAFRGTEAFIAVYIDDILIFSETEEDHEQHLLKFAQIVEKNGLILSPTKMKIGVKSVDFLGVKIHQNKVQLQEHILKKIGDFREEDLLTKKGLRSWLGILNYARQHIPNLGKMLGPLYGKTSPTGEIRFNAQDWKLVREIKRKIQQLPPLEIPPKDCCIVLEADGCMDGWGAICKWKQFAYDPRSKERITAYASGKFQPIKSTIDAEIFAIMNAMEAFKIYYLDKKEMVIRTDCQAIVSFFNKSASNKPSRARWISFTDYITGTGIKIRIEHIDGKDNTLADYLSRLVFSLIIAEWKTQGRRSTAHHQAQSMAQTIGSCSKQQEPLLLREPPLKQEQEGTGEGPWGIEQLTLPLERLLKGLKTGPYKNKLIIGTGLMNSLKIALRILDLSPEVIISTYKLKEGYSEMGSQEMSVHNL*LIDSPYCMKRPRRPGEAS*
ORF4	(7055)	(7636)	193	22065,72	6,99	MENARQEINSPPSSPVNGPNHRVMQQAARAFALERATVEAGARRNRGRPMGHRAVNPATRTPAQRFEDWSLQEQTYHRDWINEQFEDSLANLGPLARGYNFNIQIERRLFRDGLSGDVGTQLVANRLSLLHEAAQEARRSVMTLQRMIRDRAEHNERFVTRDNAYMDLRQPYAEAQAQIEAAAIILMACIEDL*

[1] Prediction of the Sweet potato badnavirus protein products based on the preliminary nucleotide annotated sequence deposited in GeneBank (Accession Number: KU511272). ND, not determined [...] indicates gaps in the sequencing of the isolate AM-MB2. Provisional numbers (in brackets) are given to estimate positions, using the sequence of a Badnavirus B isolate (FJ560944.1) for the alignment.

Table R6: Expected gene products deriving from the RNA1 of SPCSV isolate Can 181-9[1]

Predicted Gene Product	Genome position (first)	Genome position (last)	Size (aas)	MW (Da)	pI (calc.)	Sequence
Polyprotein1a	94	6057	1987	226890,84	9,01	MATVCSSAINSGSLASNATKTGFFDPILNQHINVFLSKTNNASPPNKTDVMAVKNNRFGRMGPAVPKIPFKVRMALYPNNPTVEVVDSNNVVSYINKRRVNVEDRLD VLRKICNIPYCKFNRLPKAVVRVLGYDFYNINKAIDTVLYGKVGHKNNTPLVPDDKISGCTKYNLGYELRFFQPQSRIDIFFKFGGYIVDSYDFKVSMQALYLHGRTIHD FKVMAHVCQSKTVTSPFCSSFNLKDKLNFRQFSTKVLISSVIGLFDEYVYYTNLYFGKAFREFYSVASKSIQENQKKYCEYVSRLSTKGAKIGTDSNKGKTSENRTSF KDVVNKPELTFGSLKGVKLVHNSVATPSRPTPSIPLVTFVVDDKGHESFIIKEKNGFTKKITNDERALVTLFNATLTDRKYNLHPKCKVGKHGRLEDFPNDFCWIDAFA CAGKKMPVDLQPYPQISIAYLFRCGLSRVIQKHSRETGWRLFHFDRRQVVNLKRLPHGAVLGVKGDMNIPNITRNIDILFDDLVGNVIEQTSLKADNLLLSNVVNRLS DRVNRMCERPKQLTIKTTLDSNQKRKLTKLFPEVTMNFEDSTYSSHPLQTAMRTCENFVMDRKCGGREYIDVGGDVVSLLCKESKDVHLCCPVVDVKDAHRHITR SNIIDRMKGFDESITICDKLTQDCDVSYPNIVAVEVYDMSLEDMARSILSHKAKRFDLSLIIPPEICDSYCDVLLFDDSMRVFVREGVVNYEYGSSGECYRHDLKTLQDI LRVQLFVVDGVVFKKTLECSREQLHFYSIVPCVNMKPGVYNLTSHYSKSRNDKVEMIIPVREFDGGLRNVRVSVDKYVTMHLIEYAMNTTLKVEDKAAEYLISQFRS RKSVSISGGKVVQKEFDLPDELHAGYLAVIMAEGARRREKVVNLARVSYFKHYAPTVIQVLFNIFYELYGFAKRMCYKAFISAMSLVMSEDFLEKVVVGERRIFEVQE VVHFDQEIVLVGKQGSMNVLQESLNNFTVENEKRAVDISQIVYANRDSFADDELDTMKELFQTGGGSKFRRFTSNLERCTYGFYSKVWNFASFYVKDVKMVRLVT NFFVSLCDFFRQCGISTWEYIRSVFKEFVGFVRGGLKGSFPNMWSEMKKAAKFMKEKFNAQSEDLKSLLQDFYTRQTGLDNDGNELFWQDLTYDLGTRRLFSEEK KNRLVAGMKRTYKNFLGMTSKLLSKIMMVYKYMKFIFTYVRDQFKGEDLINTIDHIIKGVSFFFVHALSLCAMGSFSFTGLVAAVSTYLGLKFTGIEKKYLGSSIVSQHL ITACSVSSPAALMTLPVRSAITKCVEIGLKKKLSKCEGLTSTMQTVIAKDAIGMKWYSHVTPYRIRMTIYTSLVLVFFFPRLAIALMLTTILVAEHKKYFDKFAIVANVNLS FASVLNRTQPTKRMTTLKRLLKEKFLTAKIKEQNEDGASTVDGEPSQDAMLGGDIELRDDEIDVEFDYDGSYVERHGKLSASKLVVEEDLKPSAADGLNFYQLKISG KGNFMQFNVPFKVSAAMTQYAFRDIPSIVYVGDEKLDTLNEYYYLEKKKTFMELGKLDNVVDMYLSQLDNKSSFDKVVFHLRQRFDDSTLYVSEDGVRWHKLKIGS KSIVSLDHKCKYDCNRVLMAYDSECKNFQVTSDELAGMYSNERCLALEYLTVDKIPQLARDLTHKVKFFNKPPGAGKTTTIVNEFSRLHNEGKRCLALTCTKAGKIEI AEKLKARGIKSVFSNCLTYDAFLMKNMYRDVDYVFCDEIFMIHAGLWLAITCNLEFSSMSCYGDVNQIPYINRVPNTICTKSMNHFYAYEMFHDNISYRCPVDVCKLL STLTDNTGKLIYPKGVYPVGDNANVLRSLQIVPIYSPEDAMDDQNVKIVTFTQPEKEEMIKATRMRNGVSSSVNTVNEVQGGTFSKVDVYRLKPYDNPIYSDLNQFV VSISRHTQLMRYRVVSSKMSDKIANNISSMDNVSDFILKEFAAKRCV*
RdRP	6056	7570	505	58534,48	5,35	DVYNLQVEEFLLPQTFSRPPASTLVAVNEFMMLINPGIIDHEFLHRTLISEYSMFELPPVGDLTIDLSKSKPYISGEFVTSGVLGKGERSRPDTWRQAIASLSHRNFSA PRVNERLDTFKTAELLCESLLKAFDMSRLFENYDYIIPDIYKIDQWLSDRDVSKFNRIKRDMNHNLMYEQFSTMKMMIKGDMKPKMDLSCYTTYAPPANIIYYKHIVS MFFSPLFLEVFDRITYCLSNKVVMYSGMNLETLSRVVKSKLPLPLDSYYTLEIDFSKFDKSQGCVFKLYEGMIYRFLKFSEEAYVNIETTEYFCRFKSASGITGELGAQ RRTGSPNTWLSNTLVTMGMLLNVYDLDDIDLMLVSGDDSLIFSKKQLENKTNELNINFGFEAKFIENSVPYFCSKFIIDDRGSIKVVPDPVRFFEKLSVPVRLSDFLSET TLRERFTSYKDLMSEYDNDSVCLLVDSLISKRYSLPLMTSYAALCFIHCLCANFSSFRKIFDEFFVVDI
RNase3	7587	8276	229	26390,56	6,91	MMIPIYSDVSEESKLTIFGSRHRLDSIIQSICTSEDRDKYEILGDWAITTYVTSMLTDLFKHDADAESLSLLRAHNISNFMFAKVMVESRFYEDFSIWLTPDQLQLCRMT FGGGKNVYEVNVKFLANYFERVVGWLVVHDNSESIKMFLDLFLKPLMSFRIKKPARSILLEWAVKNNKKLDIYTGEYNVNSVVYVLVDGKEISRANDLISKKRAISKAV IFAVQALNLN*
p7	8281	8445	55	6574,98	8,86	MDYSAIFNECCKECALYNPKKCRLDVALLWFGIGFFALSILLFLLFPFLIFRFRR

[1] Prediction of the SPCSV protein products based on the nucleotide sequences obtained from RNA-Seq analysis. The complete sequence of SPCSV isolate Can 181-9 has been already deposited in GenBank (Accession number: FJ807784) by Dr. Jesús Navas-Castillo.

Table R7: Expected gene products deriving from the RNA2 of SPCSV isolate Can 181-9[1]

Predicted Gene Product	Genome position (first)	Genome position (last)	Size (aas)	MW (Da)	pI (calc.)	Sequence
p5.2	192	326	45	5200,74	10,42	MRYKNQKHKNITSSPREVSTNISSSAHQTEQNFLSNNRITPLGRE
p5	333	464	44	5027,77	4,75	MFSVVSFKTTSPYKESYDPPVPPTHEFDSFCPSVVCMSLSYIYI
p5.1	406	531	42	5074,15	7,66	MNLIVFAQVWYVCRCRIFIFDSALWCTVDFKEVRLVINNLCM
HSp70h	880	2544	554	60959,91	6,62	MEAKAGLDFGTTFSTISAYVGGTMKVLRINGSEFIPTCLSITKSGDVIVGGAAQVLDASQLPHCYFYDLKRWVGVDRLSFEEIKRKIAPQYSVKLEGNDVLITGIDKGY TCTYTVKQLILLYVDTLVRLFSNVEKLKILSLNVSVPADYKTKQRMFMKSVCESLGFPLRRIINEPSAAAIYSISKHPGFDYFLVYDFGGGTFDTSLIAKDGKFVTVADTL GDSFLGGRDIDKAILAFITRTNNLVSPLSADSLAAIKEEVNSTGKSSFNVLDTTGNIVFVKFSSEDLDKIVSKFTSKSLKILKAIADRNKITSGALFLVGGSSLLRKVQSDV SNFAKSIGLTPIIDKDLRSAVSYGCSMMHAQEDSGSMIYIDCNSHPLMDISLFANPRVIIRKPMSVPFSYKTTRTIKQHINTAINVYEGSSLFVLDNDWLVSANVNTQDF VQSGQDLSFVYKYNVDGILDLFVRNETTGVESLLPNSFALTEKVNKLDLNLTQLSSVDELATVVSILSHFDSSFSDLLKLVNTPSIFEASCSKFGDLRSLYDRLISFNTN FS*
p60	2566	4122	518	60322,51	9,26	MAQPIYHSDFVKETFKYAFKKNDVREYLQRLNEVMLSKCDIINGKSYKFNFQGKTFSLNSKYYVRGGDVYVNTEDPLEVLKLLSVYLYYVEPKYIELSPYSPESLFGN PNYMKAVKTWKPYYDKSMNEYLSDRSEVGCIYTMDGHRLRLNSMNETRKITLYRVCNSLGKLIDLKELSSGTLKAFEVKTSDVGQAVMTTTSSNALFAECVKVFKD YIVLNSTKAGREKIEVNRKFLNSFLRCLSPKEELGNLGENPLLIAWFMREFTDRTRTSSGFRDNYKAVVELSRPMLKFLKDVFLKNLSLDEDSLFITFPKNSVVEIVDQ VIPLANFHRNQTLPTPMSNSCDLPREIDAIVSESIIKYLSKFIKTDGDLLLDAFLFVLGRSTTNQQRWTSGFEIDFKVIGSRIRFDSRDLWSYLNDAVKTKRPKFRTHNII RQWANNRGDRARVMFKICGYKPGLFGTIPRIDEHMRFDFFKLMNLRMMSESEKVSYYTLRLMTESKSNNSDKDFCKLISWISAS*
p8	4104	4322	73	8458,83	5,56	MDFSELIEQHGIEKISNLVSRLVEIRRTGRGLTNLLLDIINDSFVHFDSKRSPCGFEKEDYILVLQIITLLRV
CP	4353	5126	257	28781,34	6,17	MADSTKVEEKNFDSDSDLETNPKNKLQSEYASRRDVQTEGTAGLGRRDMELTSGILTSDQLALARLGKIQVYSNSPDIMSKSQEDEFKRHMENFAKVVTGEATITP EIFAAFYASLIQAWANQSTSEKNASNVNLENMFMVDGKEYSWKTHNFINHIQSNMPDVKNAIRKWARAHANDYKVLVGMGIVKPDYHLQAKQGVLPEYWHLATDF MRGNDLATTADGLAATLMMKRNALCNKDSKNSVYNVTQLTGTGLHC*
mCP	5129	7183	684	78122,02	7,86	MEELDDSVSNTIVDNYSDDEQSVVARASGCELNQDYLLPYKDKEQVDLSISYSSALRTKPVSVKLYFHIGKGFVVYSCKPVENFNQKVYESNLGAFFSSFTNLVTPR KPRGTNAFRFGYLRAGNDCFILVEGWRIVQIPNAEKIVGVTLRLTLDIDEVQFSKSGKLVGNIIDLPSCLNSTRPSDLFSNLKPSSVTLFSLSTKDSVNVQPSKTIPLSKI ESAVDLDLKPFRNDGETNPDKNLTEIDTLKKTMGAEEDKEKIFRIYYSNFLDSGFNGSLSYQIMWPNISCDGMSVNHQFWLGDRDDMLEGGVQYIHTEPAHRLFFV HRRGDVSEYYKTDEASVNKVLNSLPTELRFVLTRGSDGKFVVSVNEIVFLTTVLPKVGSKVQIGWEMKIFKEKFKGFNRERLSTFETVPRESQVKSNGELVNLRKYD FEMTESDACGWNLKRKSGLRLRNIRNVTEMLAQDDVKEPPVDNNNMKPDRESIPEKKVELEELTERVDNQKEKFEEFALKAIVYQPISKIDDERIFNSIIKHYVSKGLS SWQAELVVYQMGVSFCTSVNSCANSNLNLIVTKSDGSFLRVSKADHVMRLQLLCNKYCNVERTLLRNRSDKIFRLLKAGILTPPFRHARNRGLKSDMAHMACDFM DYSTIPLSDEENLALTSIQRYVLMKNKHRRSIVNVNQLY*
p28	7188	7916	242	27857,76	6,22	MSGWDDLPVNNSYAMSTNRSDDDIARICARTFNRAINLLTEYSQHTVPELRESRFELGCIRSLCENDDFSINLGADNSNLFQGLNKLGVRSDSLRVNSERFFPSISS KVMTNVIDSISSVLEFVIDLNHSGFSTLWVGEIMTIYDVTSFEKLVDAIYRFLVYTYNFPEEVQFHMTLNLFNDDILKILNKAKRKLRPLTDSERIAMAKSITKGLHFEFHF TYRSLGLYLPKVTNSIMICNKNR*

[1] Prediction of the SPCSV protein products based on the nucleotide sequences obtained from RNA-Seq analysis. The complete sequence of SPCSV isolate Can 181-9 has been already deposited in GenBank (Accession number: FJ807784) by Dr. Jesús Navas-Castillo.

Phylogenetic analysis of SPFMV AM-MB2

Phylogenetic analyses were performed with all potyviral sequences in AM-MB2 using whole-genome sequences (Fig. R5) and selected CP sequences of individual potyviruses (Figures R6, R7 and R8). In the case of the SPFMV isolate, a comparison of trees constructed with whole-genome and CP sequences suggested that it can be placed in the group of recombinant isolates, a frequent occurrence among SPFMV isolates (Tugume et al. 2010; Untiveros et al. 2008). Comparison of our sequence with those of two selected isolates (Piu3 and RC-ARg, accession numbers FJ155666.1 and KF386014.1, respectively) is illustrated in Fig. R9, where a crosspoint upstream from the CP region is noticeable. Application of adequate analysis tools predicted a recombination site located at position 7227 in the NIa region, further confirming the putative recombinant nature of the SPFMV AM-MB2 isolate.

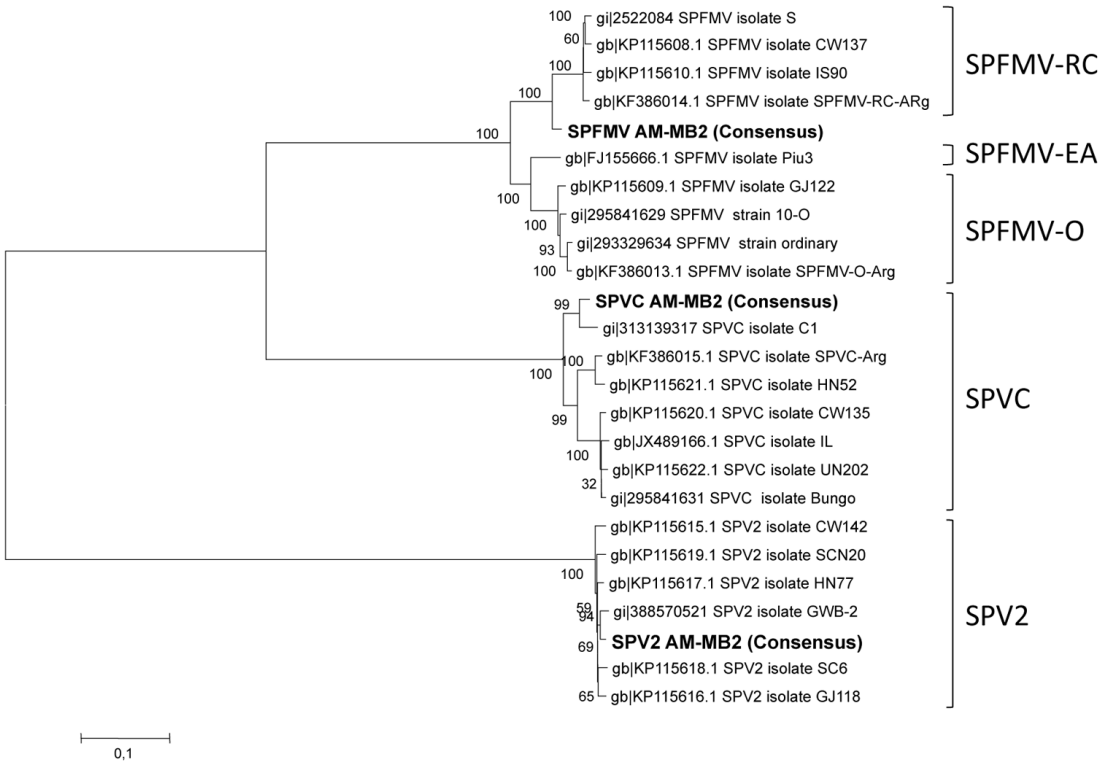

Figure R5: Phylogenetic analysis of the complete nucleotide sequences corresponding to the three potyviruses found in AM-MB2 (highlighted in bold), compared to full-length sequences of SPFMV, SPVC, and SPV2 available in GenBank, using alignments and the maximum-likelihood algorithm to generate a tree with 1,000 replications for the bootstrapping test.

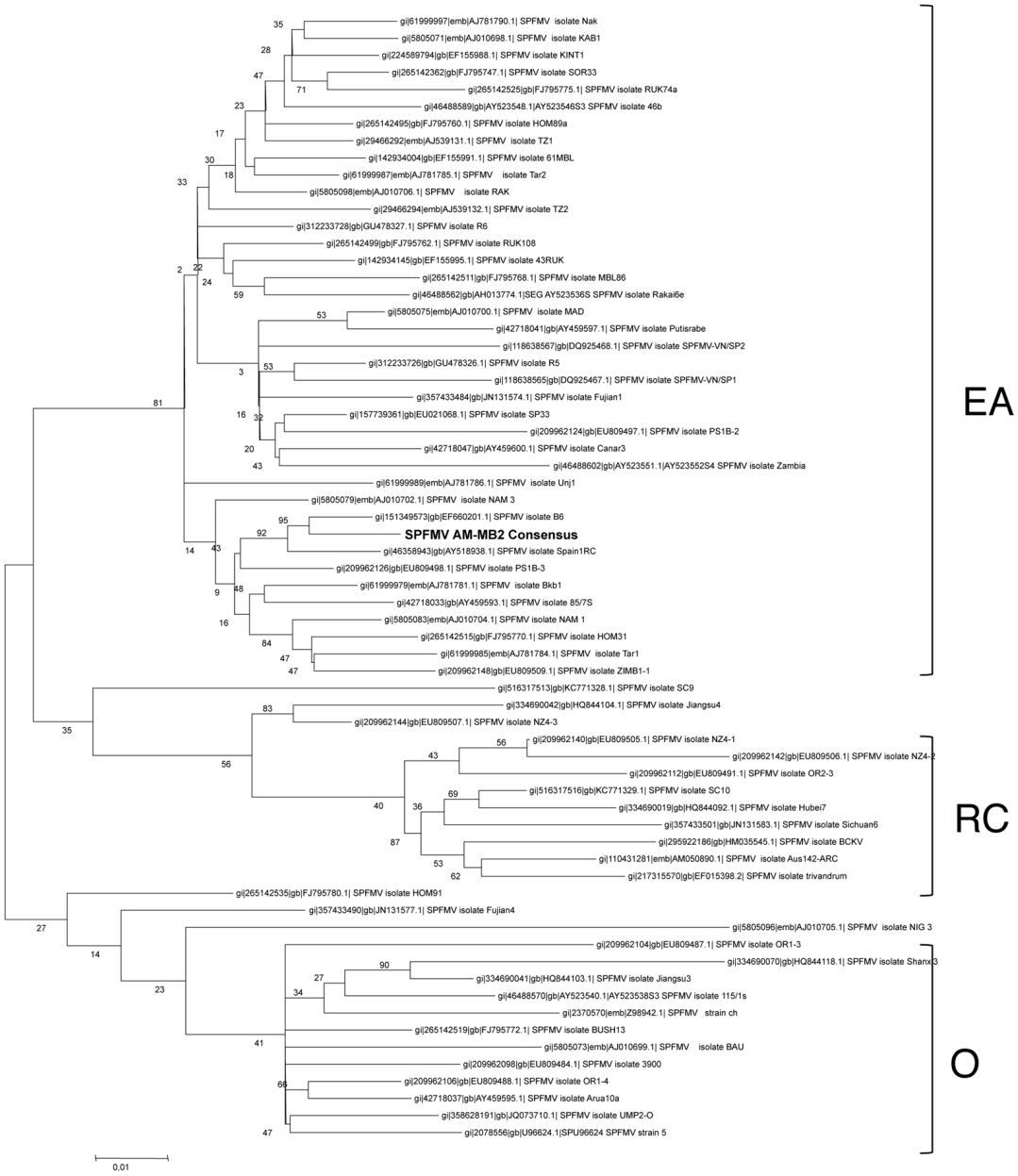

Figure R6: Phylogenetic analysis of the nucleotide sequence corresponding to the CP of SPFMV isolate AM-MB2 compared to the CP of selected SPFMV isolates.

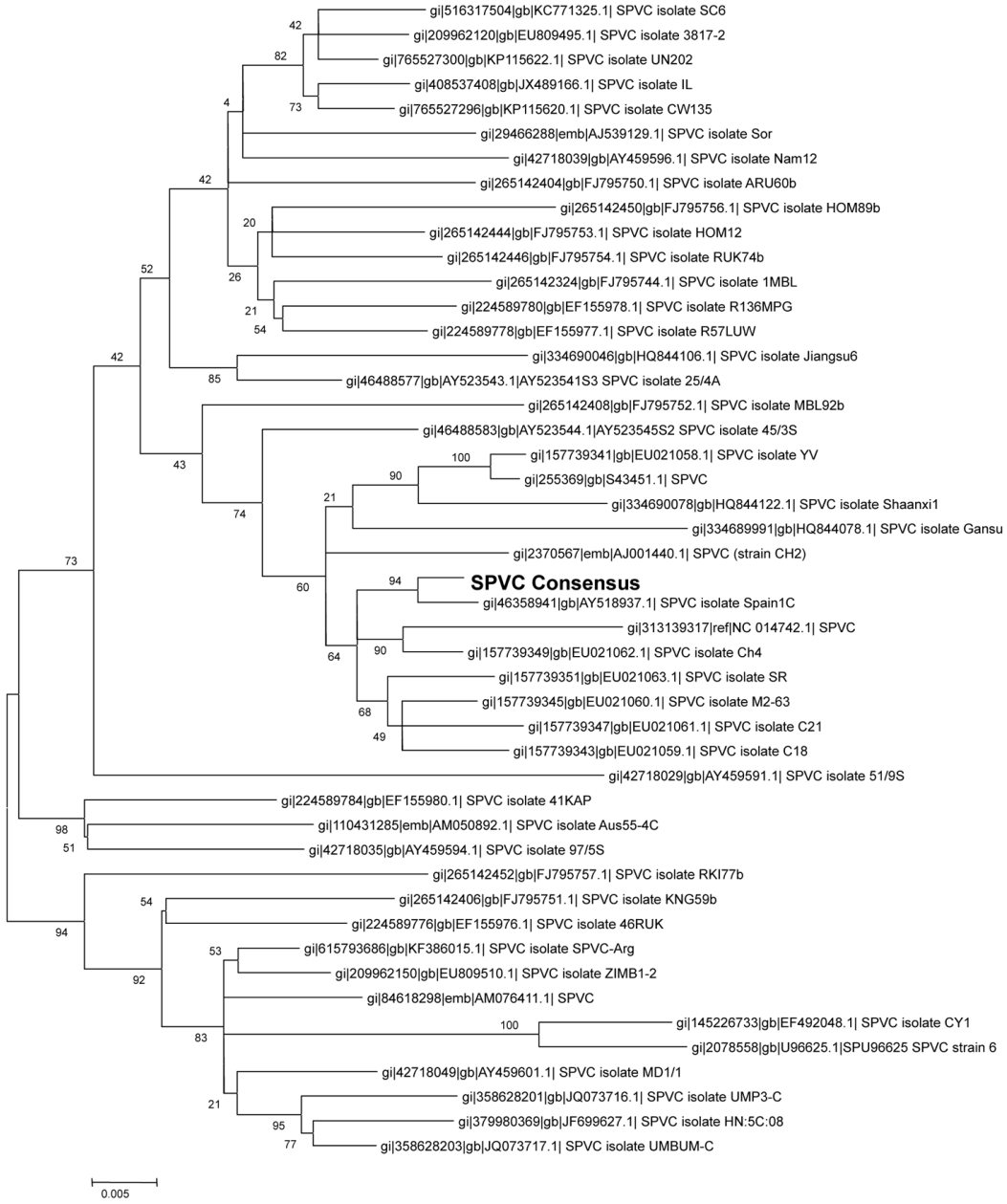

Figure R7: Phylogenetic analysis of the nucleotide sequence corresponding to the CP of SPVC isolate AM-MB2 compared to the CP of selected SPVC isolates.

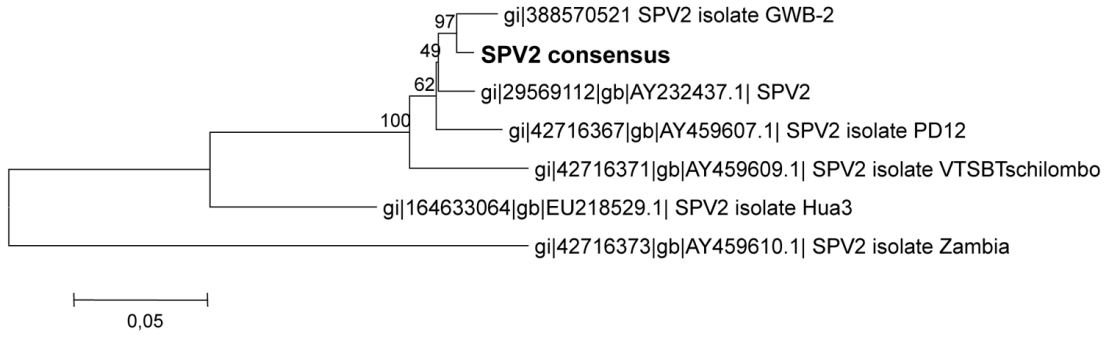

Figure R8: Phylogenetic analysis of the nucleotide sequence corresponding to the CP of SPV2 isolate AM-MB2 compared to the CP of selected SPV2 isolates.

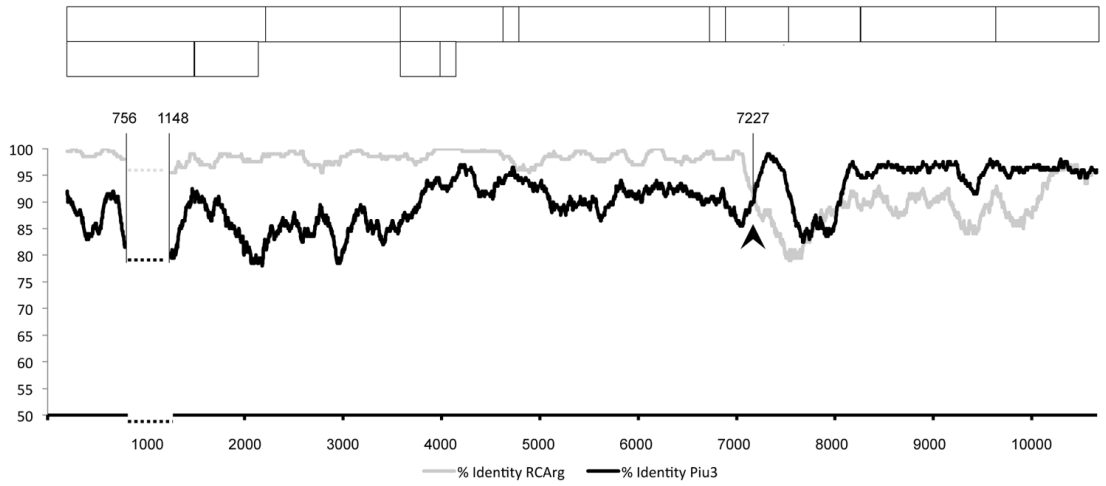

Figure R9: Plot of nucleotide identities between SPFMV isolate AM-MB2 and isolates Piu3 (EA strain) and RC-ARg (RC strain), after comparison with a sliding window of 100 nt. The recombination site detected by the SBP and GARD analysis is indicated with an arrowhead and the position number in the viral genome. The dashed horizontal lines correspond to a highly divergent region (between the indicated positions in the viral genome) with abundant gaps, which was eliminated to facilitate the global comparison. A schematic drawing of the expected gene products of SPFMV is shown above the plot to facilitate comparison of the recombination site.

P1N-PISPO expression during viral infection

Sequence analysis of PISPO overlapping reading frame embedded in P1 region

The SPFMV/SPVC/SPV2 AM-MB2 nucleotide sequences determined in this thesis (Tables R1-R3), as well as an available SPVG sequence (Accession number: JN613807) were translated and aligned in all 3+ reading frames. The conserved presence of the overlapping reading frame PISPO in the P1 region, previously described in these viruses (Clark et al. 2012; Li et al. 2012; Wang et al. 2013), was confirmed in all cases, including the new viral isolates described here. PISPO ORF starts in the G_2A_6 domain in all the cases (Fig. R10A). The position of triplets for the polyprotein ORF is GG_AAA_AAA in SPFMV and SPVC isolates and G_GAA_AAA_A in SPV2 and SPVG, whereas PISPO ORF is found in the -1 reading frame in all the cases. PISPO ORF has a length of 230 aminoacids in SPFMV and SPVC, and 228 aminoacids in SPV2 and SPVG. The translation of this ORF harbors the possibility of producing a frameshifted P1N-PISPO gene product, whose existence was still to be determined experimentally at the beginning of the present work.

The alignment also showed the presence of PIPO overlapping reading frame in our SPFMV/SPVC/SPV2 AM-MB2 isolates. P3N-PIPO partially trans-framed protein is supposed to be expressed in all potyviruses, and it has been involved in cell-to-cell movement during viral infection (Chung et al. 2008; Vijayapalani et al. 2012; Wei et al. 2010; Wen and Hajimorad 2010). PIPO starts at a similar highly conserved motif, being G_2A_6 in the viruses of the SPFMV-lineage but presenting minor changes in the range of $G_{1\text{-}2}A_{6\text{-}7}$ in some other potyviruses (Fig. R10B).

The presence of other GA_6 motifs in potyviral genomes was investigated. Interestingly, GA_6 and other A_n motifs (n= 6) are clearly underrepresented among members of the *Potyviridae* family (1.2 A_6 motifs in the coding region per viral genome versus the expected 8.1 motifs, according to the average genome size).

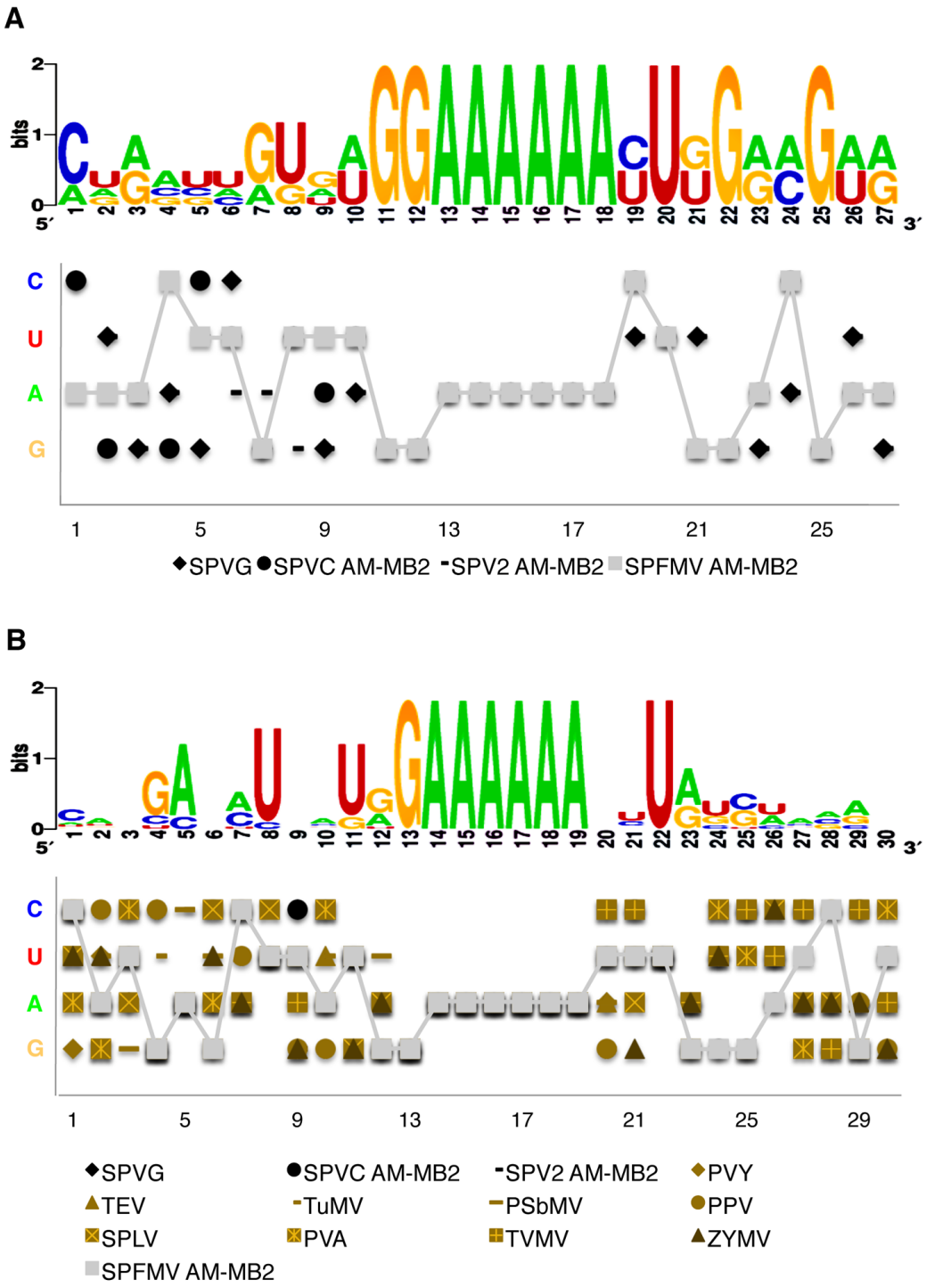

Figure R10: Representation of sequence conservation around PISPO and PIPO $G_{1\text{-}2}A_{6\text{-}7}$ motifs between different potyviruses A) Sequence conservation around PISPO G_2A_6 motif for SPFMV and the members of its lineage. The sequences used for the alignment belong to SPFMV/SPV2 and SPVC AM-MB2 isolates and the reference genome of SPVG. B) Sequence conservation around PIPO $G_{1\text{-}2}A_{6\text{-}7}$ motif for SPFMV, the members of its lineage and others potyviruses (see table MM2). Alignments were done using ClustalOmega, logos were created with the WebLogo tool (available in http://weblogo.berkeley.edu) and linear graphics were done with Excel tools.

Identification of the mechanism which contributes to P1N-PISPO expression

The expression of viral proteins from overlapping reading frames in viral genomes has been described in a few cases. Two different mechanisms have been proposed in other viruses: Ribosomal frameshifting and Polymerase slippage (Fig. I6). Although these two mechanisms were considered for the translation of P3N-PIPO in potyviruses, neither of them could be demonstrated nor discarded at the time of its first description (Chung et al. 2008). To identify which mechanism was the main responsible of P1N-PISPO expression, we performed a series of dedicated experiments described in the following sections.

Polymerase slippage in P1N-PISPO (SPFMV)

To explore the possibility of P1N-PISPO synthesis through polymerase slippage, we analysed our RNA sequencing (RNA-seq) data of *Ipomoea batata* plants infected with SPFMV AM-MB2. The bioinformatic analysis was performed by our collaborator David San León (CNB, Madrid, Spain). After data filtering (Babraham-Bioinformatics 2014; HannonLab 2014) sequences were mapped versus the references (Langmead and Salzberg 2012) allowing a maximum of three mismatches per read. The expected indel error was modeled as a Poisson distribution calculating from the Illumina indel calling error rate, PCR error rate, and sample indel frequency.

This analysis revealed the presence of a high proportion of molecules (11.8%) with a single A nucleotide addition in the G_2A_6 motif right upstream PISPO, which is indicative of polymerase slippage (Fig. R11). This change would result in the production of a variant of RNA changing to the -1 frame, and thus leading to the translation of the hypothetical P1N-PISPO gene product. Therefore, these results strongly support the existence of this alternative product, simply deriving of canonical translation of the near 12% of variant RNA molecules. Interestingly, the presence of an additional A residue in this motif was also detected in the domain before PIPO, where 1,8% of the sequences were variants with an extra A residue (Fig. R11).

To test if other RNA polymerases might slip at the PISPO region, we analysed a RNA-Seq library from a RNA sample derived from *in vitro* transcription. First, a fragment of the P1HCPro coding region in SPFMV was clonated into a plasmid vector under the control of the T7 promoter. The plasmid was subjected to a T7 polymerase driven *in vitro* transcription, and the generated transcripts were purified; a RNA-Seq library was constructed and submitted to the same sequencing platform already described. The analysis revealed a 2,7% of transcripts with an extra A in the PISPO slip region.

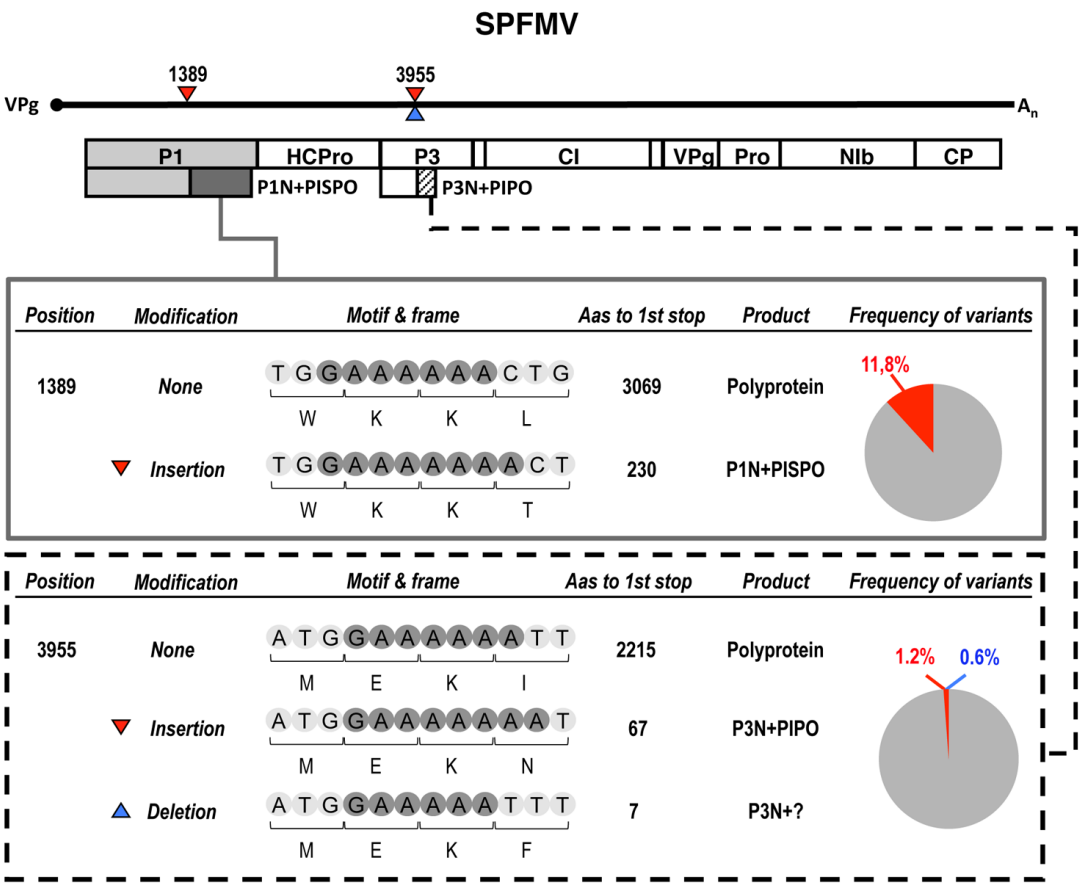

Figure R11: RNA slippage frequencies in SPFMV PISPO and PIPO G_2A_6 motifs. Data obtained from a RNA-Seq library of an *Ipomoea batata* AM-MB2 plant infected by SPFMV, but not superinfected with SPCSV. The genomes of SPFMV are depicted schematically. Mature gene products are shown as boxes. Additional ORFs corresponding to out-of-frame PIPO and PISPO regions are also depicted. In A sites where indels were detected after RNA-seq analysis are shown with red (insertion) or blue (deletion) triangles. Details of the motif, the resulting frame for the modifications, and the length of the expected products, as well as the RNA slippage percentages, are indicated for each modification. Color codes in the pie charts refer to insertions and deletions compared to the genomic sequence. Percentages showed the average for two independent samples proceeded of a single plant used for RNA-seq analysis.

Evaluation of changes in the slippage frequency between samples of SPFMV and of SPFMV super-infected with SPCSV

To test whether the presence of SPCSV in plants infected with SPFMV affects to the proportion of slippage events at the PISPO and PIPO regions, we analysed the RNA-Seq libraries from *I. batata* AM-MB2 super infected with SPCSV.

Our data showed that superinfection with SPCSV resulted in a decrease in the relative proportion of RNA-seq reads with an additional A in the G_2A_6 motifs at the PISPO site in SPFMV (from 10,5-13,2% to 6,5-6,8%) (Fig. R12). However, in the PIPO site, where a less frequent A insertion was observed, almost no changes in the proportion between

super-infected and not super-infected plant were observed (from 1,1-1,4% to 0,9-1%) (Fig. R12).

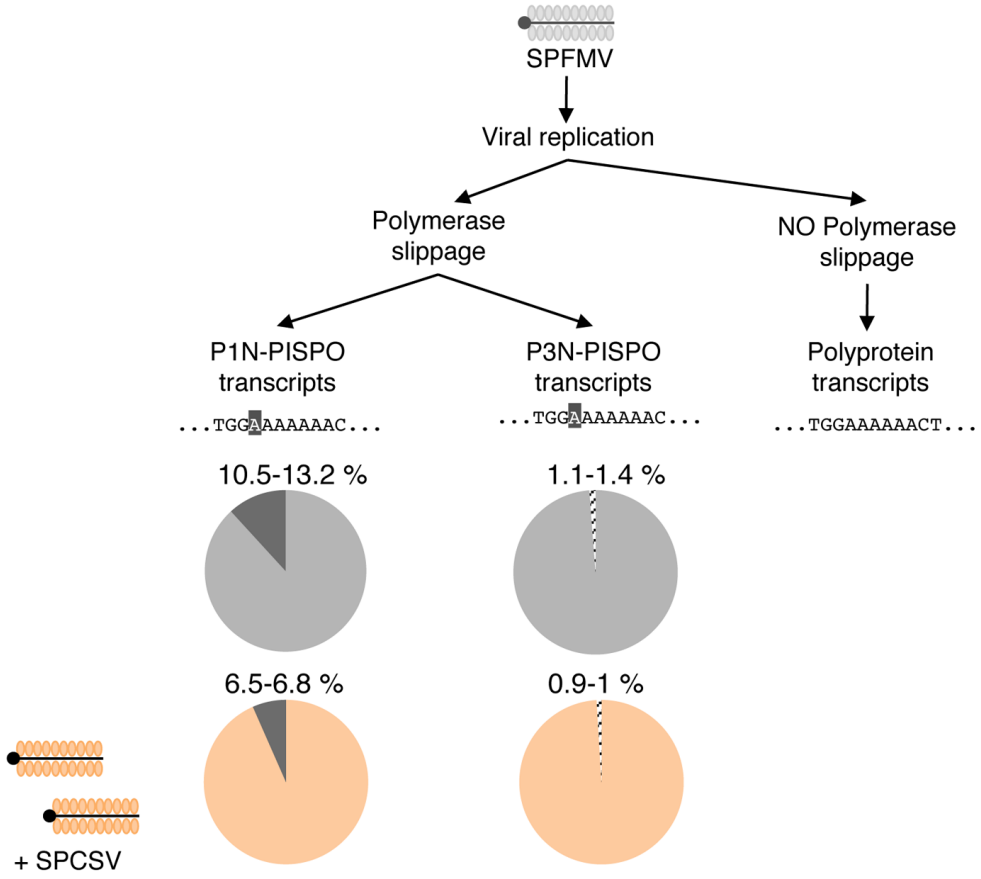

Figure R12: Comparison of RNA slippage percentages between SPFMV AM-MB2 infected *I. batata* plants (gray circles) and SPFMV AM-MB2 super-infected with SPCSV *I. batata* plants (salmon circles). The virus SPFMV is represented by a gray schematic virion. The bipartite SPCSV is represented with two salmon virions. Two variants of viral RNAs with the G_2A_6 or G_2A_7 motifs are indicated. The slide section graphics represents the percentages (see Table R8) of RNA-seq reads with insertion of an extra A nucleotide at the slippage sites corresponding to PISPO (left) and PIPO (right).

We could not repeat the same kind of analysis in the case of SPV2 and SPVC viruses, because the number of reads for these viruses in AM-MB2 infected plants was insufficient to perform the bioinformatic analysis with the same statistical significance. However, boosting of SPV2 and SPVC accumulation in the crinivirus-superinfected samples allowed us to analyze the presence of insertions at PISPO and PIPO G_2A_6 conserved motifs. As in the case of SPFMV, transcripts with A insertions were found in the G_2A_6 motifs upstream of *trans*-frame PISPO and PIPO (Table R8).

Analysis of polymerase slippage events in other potyvirids

To assess the scope among the *Potyviridae* family of the presence of an extra A at the PIPO junction, we analyzed available RNA sequencing (RNA-seq) data of two isolates of the potyvirus *Plum pox virus* (PPV) (Rodamilans et al. 2014). The presence of A residue additions in the PIPO GA_6 motif was found in 1.6% of the reads. Besides, published data on another potyvirus, *Zucchini yellow mosaic virus*, showed a minor variant with an extra A in all samples of a *Cucurbita pepo* vine studied by deep sequencing of long RNAs (Dunham et al. 2014), and our analysis located this modification in the PIPO GA_6 motif as well. Finally, the analysis of a sample of N. *tabacum* infected with SPMMV revealed a group of transcripts with an extra A in the PIPO motif of this ipomovirus (Table R8).

Curiously, the presence of an A deletion in the PIPO GA_6 motif were also detected in SPFMV, SPV2 and SPMMV samples. The percentage of reads with an A deletion in PIPO motif ranged from 0,5% to 2,57% in these viruses (Table R8). The deletion would result in a very short overlapping reading frame downstream of P3N. However, SPFMV reads with similar deletions affecting the PISPO motif were not found in our analysis.

To evaluate if polymerase slippage might occur in repetitive A motifs in other unrelated viruses with RNA genomes in the *Picornaviridae* family, we analysed available highthroughput sequence data from the enterovirus *Human rhinovirus C* (SRR363436). The analysis of an A_6 motif at 6036 position showed a 2,7% of transcripts with insertions at this location.

Altogether, these data strongly suggest that P1N-PISPO as well as P3N-PIPO can be produced, at least partially, through a polymerase slippage mechanism. The analysis of available data also suggests that this mechanism of polymerase slippage could occur in other picornaviruses, and also can be observed in transcripts generated *in vitro* with a bacteriophage-derived T7 RNA polymerase.

Table R8: Detailed indel data on selected positions in the genome of members of the *Potyvirus, Ipomovirus* and *Enterovirus* genera

Genus	Virus	Sample[1]	Position	Indel	ORF	%	Coverage
Potyvirus	**SPFMV**	AM-MB2 (sample 1)	1377	A insertion	PISPO	13,21%	2172
			3943	A insertion	PIPO	1,02%	1541
			3943	A deletion	PIPO	0,65%	3944
		AM-MB2 (sample 2)	1377	A insertion	PISPO	10,47%	1175
			3943	A insertion	PIPO	1,38%	799
			3943	A deletion	PIPO	0,50%	799
		AM-MB2 + SPCSV (sample 1)	1377	A insertion	PISPO	6,82%	13444
			3943	A insertion	PIPO	1,02%	9837
			3943	A deletion	PIPO	0,53%	9837
		AM-MB2 + SPCSV (sample 2)	1377	A insertion	PISPO	6,48%	12564
			3943	A insertion	PIPO	0,88%	11415
			3943	A deletion	PIPO	0,68%	11415
	SPV2	AM-MB2 + SPCSV (sample 1)	1231	A insertion	PISPO	3,61%	7754
			3811	A insertion	PIPO	2,61%	3406
			3811	A deletion	PIPO	1,05%	3406
		AM-MB2 + SPCSV (sample 2)	1231	A insertion	PISPO	2,72%	8497
			3811	A insertion	PIPO	2,57%	3153
			3811	A deletion	PIPO	2,57%	3153
	SPVC[2]	AM-MB2 + SPCSV (sample 1)	3953	A insertion	PIPO	2,58%	10183
		AM-MB2 + SPCSV (sample 2)	3953	A insertion	PIPO	2,38%	5751
	PPV-D	JOJOW+PPV	2911	A insertion	PIPO	1,93%	881
	PPV-Rec	JOJOW+PPV	2911	A insertion	PIPO	1,23%	408
Ipomovirus	**SPMMV**	SPMMV 130	4115	A insertion	PIPO	3,37%	3498
			4115	A deletion	PIPO	0,51%	
Enterovirus	**HRV-C**		6036	A insertion		2,40%	333

[1] Two samples of the same plant material were processed in parallel as independent libraries, and the data was analysed separately.

[2] Not enough sequences to analyse PISPO region.

Absence of detectable production of P1N-PISPO by frameshifting in *in vitro* translation experiments

To evaluate the putative contribution of translational frameshifting to the production of P1N-PISPO, our collaborator Bernardo Rodamilans (CNB, Madrid, Spain) performed *in vitro* translation experiments in wheat germ extracts using as starting material to program the reactions a set of SPFMV constructs deriving from the original materials generated in our laboratory.

The SPFMV P1-coding region was cloned after RT-PCR amplification (P1 construct), and appropriate mutations were designed to express truncated proteins in each of the frames. In the P1Δ construct, a stop codon interrupted the main ORF of the polyprotein downstream of the G_2A_6 motif to generate a 54-kDa variant, whereas in the P1N-PISPOΔ construct, the corresponding stop codon was introduced in the PISPO sequence (-1 frame), leading to a putative 47-kDa product without altering the P1-coding sequence. P1, P1Δ, and P1N-PISPOΔ, together with a luciferase gene control, were used for *in vitro* transcription. The analysis showed a band with a mobility corresponding to around 70 kDa in the P1 sample, roughly compatible with both P1 and P1N-PISPO (expected sizes of 74.1 kDa and 72.7 kDa, respectively) (Table R9). However, major protein products derived from translational frameshifting were not detected in the analysis of the two other constructs designed to yield products of different sizes in the P1 and PISPO frames: in P1Δ, the major band was compatible with the expected size of the truncated P1 (54 kDa), while in P1N-PISPOΔ, the pattern was similar to that for the unaltered P1 and not any other evident products were present at the expected region for the truncated 47-kDa protein (results are summarized in Table R9). The results of this experiment support the hypothesis that viral RNA polymerase slippage is the main mechanism that produces the out-of-frame product, and that the hypothetical contribution of translational frameshift was apparently below the detection limit of the *in vitro* assay.

Table R1: *In vitro* expression of P1-related products.[1]

Construct	Expected products	Expected size (kDa)	Detection of expressed products
P1	P1	74,1	Yes, a band of ≈ 70 kDa compatible with both P1 and P1N-PISPO products.
	P1N-PISPO	72,7	
P1Δ	P1Δ	54	Yes
	P1N-PISPO	72,7	No clear product
P1N-PISPOΔ	P1	74,1	Yes
	P1N-PISPOΔ	47	No clear product
Luciferase	Luciferase	61	Yes

[1] Constructs were designed to express selected proteins. Wheat germ extract was programmed with RNA transcripts, including a luciferase mRNA and water as controls. The proteins synthetized after *in vitro* translation were subjected to an SDS-PAGE analysis and detected by autoradiography.

Detection of P1N-PISPO protein during viral infection

Although the identification of polymerase slippage in the PISPO G_2A_6 motif supports the expression of the P1N-PISPO gene product, and consequently the existence of this alternative protein during viral infection, no experimental evidence was available at that point of the project. To test if the expected gene product was indeed present in infected tissues, proteins samples of *N. benthamina* plants agroinfiltrated with P1 and P1N-PISPO constructs as well as *I. batata* plants infected with SPFMV were subjected to a mass-spectrometry analysis. The use of agroinfiltrated controls programmed to overexpress forced variants was intended to facilitate the identification of true peptides which could be later searched for in the virus infected samples.

Identification of virus-derived proteins in agroinfiltrated plant tissue by LC-MS/MS analysis

A construct containing the wild-type P1-coding sequence and a construct designed to produce only P1N-PISPO (by insertion of a nucleotide in the G_2A_6 motif) were expressed by agroinfiltration in *N. benthamiana* leaves in the presence of P1b RSS from the unrelated ipomovirus *Cucumber vein yellowing virus* (CVYV) (Valli et al. 2006). The P1b RSS was included to further enhance (and maintain on time, avoiding gene silencing phenomenon) the protein expression levels, already expected to be high by the use of a strong constitutive 35S promoter. Total proteins present in the infiltrated patches were extracted and separated by SDS-PAGE, and the fraction above 50 kDa (to avoid the highly abundant RuBisCO) was excised and analyzed by LC-MS/MS.

The analysis identified more than 180 and 200 proteins in samples expressing the wild-type P1 and the mutant forced to produce P1N-PISPO, respectively. Most of the proteins corresponded to the host plant or to the *A. tumefaciens* bacteria used as the expression vector. In each sample, the overexpressed viral gene products were readily identified with high scores and coverages: for P1, a score of 97.38, with 13 unique peptides, and 31.33% coverage; for P1N- PISPO, a score of 173.38, with 25 unique peptides, and 46.02% coverage. The detected peptides corresponded to the transiently expressed viral gene products; their distributions along the amino acid sequences are shown in Fig. 13A and B, and complete details of each unique peptide are provided in Table R10.

Intriguingly, no peptides corresponding to the PISPO frame were found in the sample that expressed the wild-type P1 gene products, even after applying a targeted approach for PISPO-derived peptides. In addition, it also confirmed the identity of the expressed P1N-PISPO protein in the corresponding construct, as an identified peptide overlapped the frameshifted region and showed the amino acid introduced to force the frameshift (sequence, LVW**E**K [mutation in bold] (Table R10).

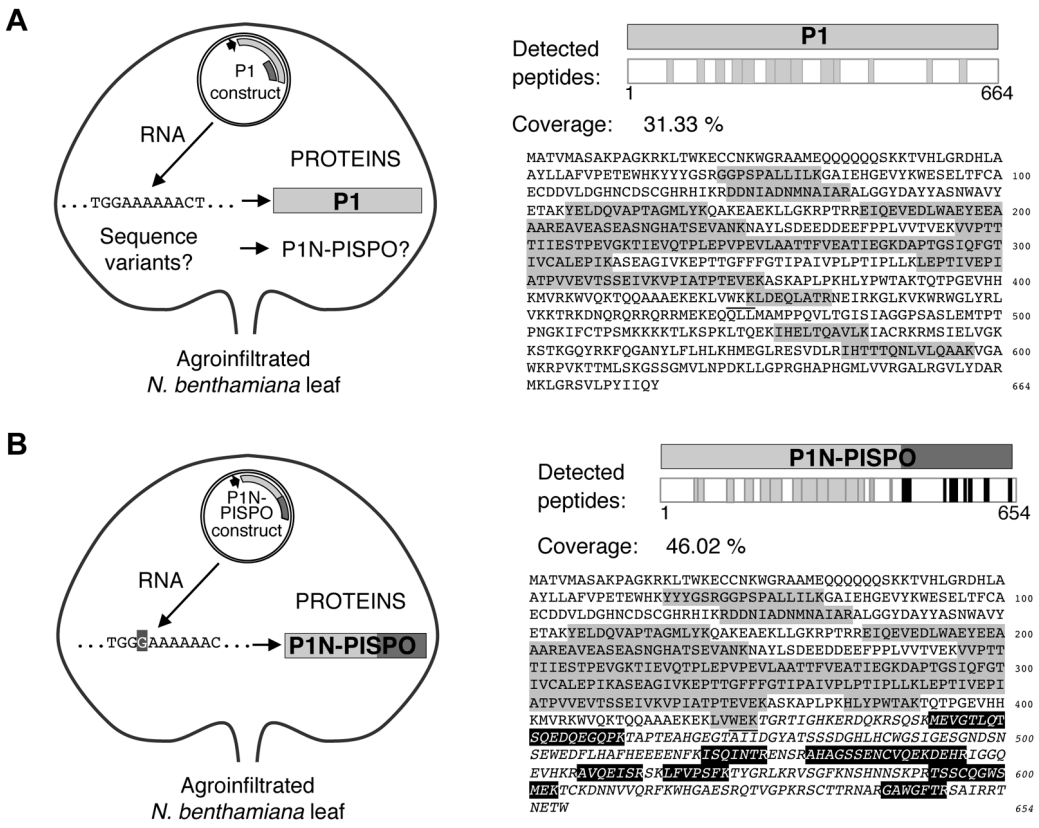

Figure R13: Identification of viral proteins by LC-MS/MS in agroinfiltrated samples. (A) Detection of peptides corresponding to proteins transiently expressed in *N. benthamiana* leaves agroinfiltrated with a construct that contains the wild-type P1 sequence of SPFMV under control of the appropriate promoter for overex- pression. The plasmid construct is schematically drawn inside a leaf outline, with a detail of the expected RNA sequence corresponding to the G_2A_6 motif upstream of the PISPO starting point and the detected protein P1. A question mark besides the P1N-PISPO name indicates that no peptides corresponding to the PISPO domain were found in the analysis. The peptides detected are shown (as gray boxes) distributed along the P1 protein sequence in the right panel, and the percentage of coverage is indicated. The sequences of the detected peptides are shaded in gray on the sequence of the P1 gene product, and the frameshift point is underlined. (B) Detection of peptides as in panel A but in the sample agroinfiltrated with the P1N-PISPO construct, which ensures expression of the *trans*-frame product. The PISPO region is highlighted and is depicted in italic lettering in the sequence, starting at the underlined frameshift point. Peptides found in the analysis are shown as boxes (gray for P1N and black for PISPO) in the graphic and shaded in the sequence below, using a gray background in the case of peptides corresponding to the P1N or a black background with white letters for the PISPO region.

Detection of SPFMV P1N-PISPO in infected sweet potato plants

Total proteins were extracted from plants infected with SPFMV AM-MB2, and the fraction corresponding to protein products of above 50 kDa was subjected to LC-MS/MS analysis. The list of peptides corresponding to viral proteins included several large size gene products expected to accumulate during infection, such as P1, HCPro, CI, and NIb (all of them with sizes above the exclusion limit selected >50 kDa, and translated from the long viral ORF). Detection was also positive for 4 peptides corresponding exclusively to the PISPO region of P1N-PISPO, and thus likely derived

from a *trans*-frame protein that incorporated PISPO (21.3% coverage). Along with these peptides, peptides corresponding to the P1 protein were detected from upstream of the polymerase slippage signal (11 different peptides, 39% coverage of the P1N region), and therefore common to P1 and P1N-PISPO, and from the C-terminal part (2 peptides, 10% coverage). Scores were 116.56 (13 peptides, 28.46% coverage) for P1 and 196.2 (15 peptides, 32.72% coverage) for P1N-PISPO.

Figure R14 summarizes the coverage and location of the peptides corresponding to the two alternative gene products from the P1 region, P1 and P1N-PISPO, which were present in infected sweet potato samples. Details on all identified virus-derived proteins and the individual peptides found in the analysis are provided in Table R11. Considering the exclusion limit (>50 kDa) used for sampling and that no smaller viral proteins, including the abundant CP (35.1 kDa), were detected by this analysis, our results are compatible with the simultaneous expression and accumulation of both P1 and P1N-PISPO (predicted to be 74.1 and 72.7 kDa, respectively) during SPFMV infection.

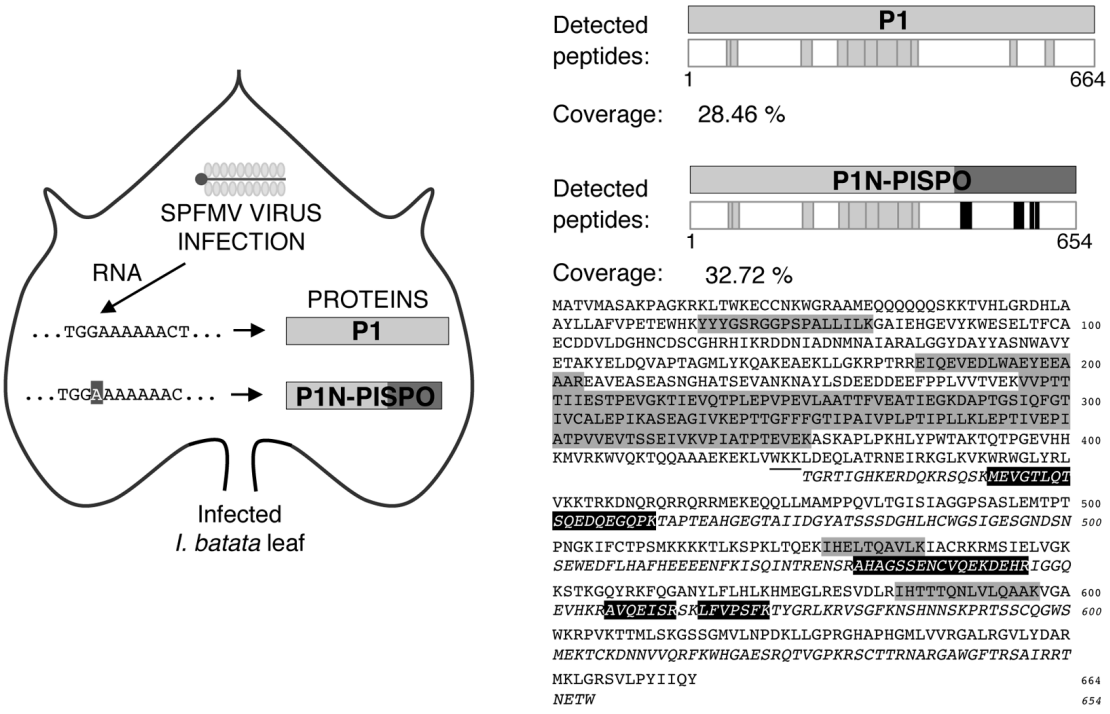

Figure R14: Identification of viral proteins by LC-MS/MS in AM-MB2 *I. batata* plant infected with SPFMV. The virus SPFMV is represented by a schematic virion inside the outline of the sweet potato leaf, and two variants of viral RNAs with the G_2A_6 or G_2A_7 motifs are indicated. Peptides deriving from the common P1N region, from the P1 C-terminal region, and from PISPO are shown in the protein schemes, using gray for the common P1N part and the rest of P1, while the peptides found in the PISPO frame are represented by black boxes. The sequences of peptides are also highlighted in the sequence, with the two variants shown after the frameshift point (underlined), represented in the upper lines for P1 or in the lower (in italic) for PISPO and using as above a gray or black background in the sequence detail,respectively.

Table R10: SPFMV viral gene products transiently expressed on *N. benthamiana* plant tissue and detected by LC-MSMS analysis

Sample	Viral protein	Score[1]	Coverage	Unique Peptides[2]	PSMs[3]	Size	MW [kDa]	calc. pI	Peptides							
									Sequence[4]	Size	Initial[5]	Final	Missed Cleavages	MH+ [Da][6]	PSMs	PEP[7]
Agroinfiltrated P1 construct	P1	97,38	31,33	13 (10 + **3**)	26	664	74,1	9,17	GGPSPALLILK	11	71	81	0	1065,67009	2	0,02370553
									DDNIADNmNAIAR	13	122	134	0	1448,64372	1	0,002282131
									DDNIADNMNAIAR	13	122	134	0	1432,65166	1	0,000296073
									YELDQVAPTAGmLYK	15	155	169	0	1714,84661	2	4,98689E-07
									YELDQVAPTAGMLYK	15	155	169	0	1698,84929	2	1,07017E-06
									EIQEVEDLWAEYEEAAAR	18	186	203	0	2150,99516	2	1,30644E-05
									EAVEASEASNGHATSEVANK	20	204	223	0	2000,91977	1	0,009433393
									VVPTTTIIESTPEVGK	16	246	261	0	1670,92717	2	5,91988E-05
									TIEVQTPLEPVPEVLAATTFVEATIEGK	28	262	289	0	2982,59946	1	0,001826707
									DAPTGSIQFGTIVcALEPIK	20	290	309	0	2117,09990	3	4,50031E-07
									LEPTIVEPIATPVVEVTSSEIVK	23	342	364	0	2450,36716	4	0,000277995
									VPIATPTEVEK	11	365	375	0	1183,65911	2	0,002508105
									KLDEQLATR	9	424	432	1	1073,59978	1	0,01176776
									IHELTQAVLK	10	527	536	0	1151,67961	1	0,03467921
									IHTTTQNLVLQAAK	14	584	597	0	1537,87314	1	0,000769235
Agroinfiltrated P1N-PISPO construct	P1N-PISPO	173,38	46,02	25 (17 + **8**)	58	654	72,7	6,47	YYYGSR	6	65	70	0	808,36339	2	0,05871485
									GGPSPALLILK	11	71	81	0	1065,67095	2	0,01128503
									RDDNIADNmNAIAR	14	121	134	1	1604,74381	1	0,001550777
									DDNIADNmNAIAR	13	122	134	0	1448,64348	2	8,56681E-05
									YELDQVAPTAGmLYK	15	155	169	0	1714,83550	2	2,69142E-05
									YELDQVAPTAGMLYK	15	155	169	0	1698,84050	2	0,00018226
									EIQEVEDLWAEYEEAAAR	18	186	203	0	2150,98906	5	4,48992E-07
									EAVEASEASNGHATSEVANK	20	204	223	0	2000,91300	3	0,002131125
									VVPTTTIIESTPEVGK	16	246	261	0	1670,92192	4	0,0003182
									TIEVQTPLEPVPEVLAATTFVEATIEGK	28	262	289	0	2982,59671	5	0,02217205
									DAPTGSIQFGTIVcALEPIK	20	290	309	0	2117,09770	4	6,45506E-06
									ASEAGIVKEPTTGFFFGTIPAIVPLPTIPLLK	32	310	341	1	3324,89353	2	0,00897333
									ASEAGIVK	8	310	317	0	774,43566	1	0,02094499
									EPTTGFFFGTIPAIVPLPTIPLLK	24	318	341	0	2569,48111	2	0,000227663
									LEPTIVEPIATPVVEVTSSEIVKVPIATPTEVEK	34	342	375	1	3615,00620	2	0,008460695
									LEPTIVEPIATPVVEVTSSEIVK	23	342	364	0	2450,37339	5	3,8468E-06
									VPIATPTEVEK	11	365	375	0	1183,65825	2	0,008864285
									HLYPWTAK	8	384	391	0	1015,53710	1	0,1502403
									LVWEK	**5**	***420***	***424***	0	674,38786	1	0,14696
									mEVGTLQTSQEDQEGQPK	**18**	***443***	***460***	0	2020,91570	1	9,41641E-07
									ISQINTR	**7**	***519***	***525***	0	831,46898	2	0,02658513
									AHAGSSENcVQEKDEHR	**17**	***530***	***546***	1	1953,85525	2	2,32708E-07
									AVQEISR	**7**	***556***	***562***	0	802,44304	1	0,02908999
									LFVPSFK	**7**	***565***	***571***	0	837,48924	1	0,08113639
									TSScQGWSmEK	**11**	***593***	***603***	0	1316,52410	1	0,005354153
									GAWGFTR	**7**	***598***	***604***	0	794,39562	2	0,1082382

[1] Sum of the SEQUEST scores of the individual peptides

[2] Number of identified peptide sequences (peptide spectrum matches) for the protein, including those redundantly identified. In brackets are indicated the number of common peptides (corresponding to the N-terminal part of the protein, upstream of the G_2A_6 motif) followed by the differential ones (in white letters on grey or black background for the alternative C-terminal part of P1 or PISPO sequences, respectively)

[3] Protonated monoisotopic mass of the peptides, in daltons

[4] Modifications displayed as lowercase letters (m: oxidation, c: carbamidomethyl). White letters on grey or black background indicate the alternative C-terminal part of P1 or PISPO sequences, respectively.

[5] Positions in the predicted genomic frame polyprotein. Numbers in italics corresponded to the +2frame of PISPO continuing P1N

[6] Protonated monoisotopic mass of the peptides, in daltons

[7] Posterior error probability. Probability that the observed PSM is incorrec

Table R11: SPFMV viral gene products identified by LC-MSMS analysis of sweet potato tissue samples infected with SPFMV AM-MB2

Sample	Viral protein	Score[1]	Coverage	Unique Peptides[2]	PSMs[3]	Size	MW [kDa]	calc. pI	Peptides							
									Sequence[4]	Size	Initial[5]	Final	Missed Cleavages	MH+ [Da][6]	PSMs	PEP[7]
AM-MB2	P1N-PISPO	196,22	32,72	15 (11 + **4**)	70	654	72,7	6,47	YYYGSR	6	65	70	0	808,36315	1	0,05593261
									GGPSPALLILK	11	71	81	0	1065,66899	1	0,004198602
									EIQEVEDLWAEYEEAAAR	18	186	203	0	2150,99101	2	3,99548E-09
									VVPTTTIIESTPEVGK	16	246	261	0	1670,91252	3	3,90719E-05
									TIEVQTPLEPVPEVLAATTFVEATIEGK	28	262	289	0	2982,58792	7	3,90915E-06
									DAPTGSIQFGTIVcALEPIK	20	290	309	0	2117,08965	2	5,44594E-08
									ASEAGIVKEPTTGFFFGTIPAIVPLPTIPLLK	32	310	341	1	3324,87595	4	0,000152128
									ASEAGIVK	8	310	317	0	774,43645	1	0,03614698
									EPTTGFFFGTIPAIVPLPTIPLLK	24	318	341	0	2569,46390	6	6,45971E-06
									LEPTIVEPIATPVVEVTSSEIVK	24	342	365	0	2450,36588	1	2,7674E-05
									VPIATPTEVEK	11	365	375	0	1183,65666	3	0,01060038
									mEVGTLQTSQEDQEGQPK	18	*443*	*460*	0	2020,91277	15	4,60753E-10
									AHAGSSENcVQEKDEHR	17	*530*	*546*	1	1953,84780	9	5,28656E-08
									AVQEISR	7	*556*	*562*	0	802,44170	3	0,2101074
									LFVPSFK	7	*565*	*571*	0	837,48723	12	0,007931116
	P1	116,56	28,46	13 (11 + **2**)	35	664	74,1	9,17	YYYGSR	6	65	70	0	808,36315	1	0,05593261
									GGPSPALLILK	11	71	81	0	1065,66899	1	0,004198602
									EIQEVEDLWAEYEEAAAR	18	186	203	0	2150,99101	2	3,99548E-09
									VVPTTTIIESTPEVGK	16	246	261	0	1670,91252	3	3,90719E-05
									TIEVQTPLEPVPEVLAATTFVEATIEGK	28	262	289	0	2982,58792	7	3,90915E-06
									DAPTGSIQFGTIVcALEPIK	20	290	309	0	2117,08965	2	5,44594E-08
									ASEAGIVKEPTTGFFFGTIPAIVPLPTIPLLK	32	310	341	1	3324,87595	4	0,000152128
									ASEAGIVK	8	310	317	0	774,43645	1	0,03614698
									EPTTGFFFGTIPAIVPLPTIPLLK	24	318	341	0	2569,46390	6	6,45971E-06
									LEPTIVEPIATPVVEVTSSEIVK	24	342	365	0	2450,36588	1	2,7674E-05
									VPIATPTEVEK	11	365	375	0	1183,65666	3	0,01060038
									IHELTQAVLK	10	527	536	0	1151,67827	2	0,1482055
									IHTTTQNLVLQAAK	14	584	597	0	1537,86948	2	0,2301637
	CI	45,28	19,75	9	21	643	72,2	7,25	STGLPFYLSR	10	1617	1626	0	1140,60686	3	5,92849E-05
									VLLLEPTRPLAENVHR	16	1630	1645	0	1857,07461	5	1,30016E-05
									EVEFTTQYPVQIK	13	1735	1747	0	1581,81047	3	5,24599E-06
									VGNVEIQTcGSPQKK	15	1810	1824	1	1644,83823	2	0,023518
									GPISYGER	8	1867	1874	0	878,43834	3	0,004448509
									GVTGWLSVGEYAK	13	1991	2003	0	1366,70268	1	0,000104976
									YKHEAGFGR	9	2038	2046	1	1064,52701	2	3,29513E-05
									IScINScK	8	2047	2054	0	981,45098	2	0,02123955
									VAYTLQTDLYAIPR	14	2055	2068	0	1623,87663	1	4,87008E-05
									TVSSSSFTLNSIATLWR	17	2094	2110	0	1869,97112	3	3,39834E-08

[1] Sum of the SEQUEST scores of the individual peptides. The different viral proteins are listed according to their scores.
[2] Number of identified peptide sequences (peptide spectrum matches) for each protein, including those redundantly identified. In brackets are indicated the number of common peptides (corresponding to the N-terminal part of the protein, upstream of the G_2A_6 motif) followed by the differential ones (in white letters on black or grey background for the alternative PISPO or C-terminal part of P1 sequences, respectively)
[3] Protonated monoisotopic mass of the peptides, in daltons
[4] Modifications displayed as lowercase letters (m: oxidation, c: carbamidomethyl). White letters on grey or black background indicate the alternative for PISPO or the alternative C-terminal part of P1 sequences, respectively).
[5] Positions in the predicted genomic frame polyprotein. Numbers in italics corresponded to the +2 frame of PISPO continuing P1N
[6] Protonated monoisotopic mass of the peptides, in daltons
[7] Posterior erro probability. Probability that the observed PSM is incorrect.

P1N-PISPO as a RSS

Identification of P1N-PISPO as a RNA silencing suppressor and interference with the silencing systemic response

Once we determined that P1N-PISPO is produced in plants infected with SPFMV, we investigated putative functions for the novel gene product. Based on our previous experience with proteins encoded at the 5' ends of potyviral genomes, we tested whether P1N-PISPO exhibits RNA silencing suppression activity.

The standard silencing assay is based on the co-overexpression of GFP mRNA with viral products in *N. benthamiana* plants. The overexpression of GFP induces sense-mediated silencing of GFP and results in a red leaf patch under UV light, unless the test viral product suppresses silencing in which case the leaf patch will show enhanced green fluorescence under UV light for a prolongued period of time, compared with the negative control.

A useful variation of the analysis can be performed if *N. benthamiana* 16c plants, which express constituvely GFP, are used in the assay. In this case, the spread of the GFP silencing signal to the rest of the cells can be monitored, since it will cause first the shutting down of the GFP expression in the patch neighboring cells, (visible as a red halo) and eventually later in the rest of the plant after its systemic dissemination (Voinnet and Baulcombe 1997).

A construct to produce only P1N-PISPO (by insertion of a nucleotide in the G_2A_6 motif) was cloned in a binary vector under the 35S promoter and the TMV omega sequence acting as enhancer of expression (Fig. R16A). P1N-PISPO was coagroinfiltrated with a GFP-expressing construct in *N. benthamiana* 16c plants. Both positive and negative controls, using the CVYV P1b silencing suppressor as a positive control, and delta as a negative control, were included side-to-side with the tested constructs in the same leaves. The design of the silencing assay is depicted in the Fig. R15A. Monitoring of GFP fluorescence over time under UV light showed that P1N-PISPO presented clear RNA silencing suppression activity at 3 and 5 days post-agroinfiltration (Fig. R15B).

All the P1N-PISPO coagroinfiltrated patches manifested a red halo surrounding the patch at 5 days postagroinfiltration, indicating a short distance spread of the silencing signal (Fig. R15B). At that time the read halo was not present in the P1b agroinfiltraded patches, as it had been reported previously (Valli et al. 2006). At 1-month postagroinfiltration, the upper leaves of plants co-agroinfiltrated with P1N-PISPO showed a reduction of the GFP expression. However, this reduction was lower than the ones coagroinfiltrated with the negative control (Fig R15C). This observation indicates

a delay of the long distance silencing spreading.

Altogether, these results suggest that P1N-PISPO has silencing suppressor activity but apparently it fails to block the silencing signal spread.

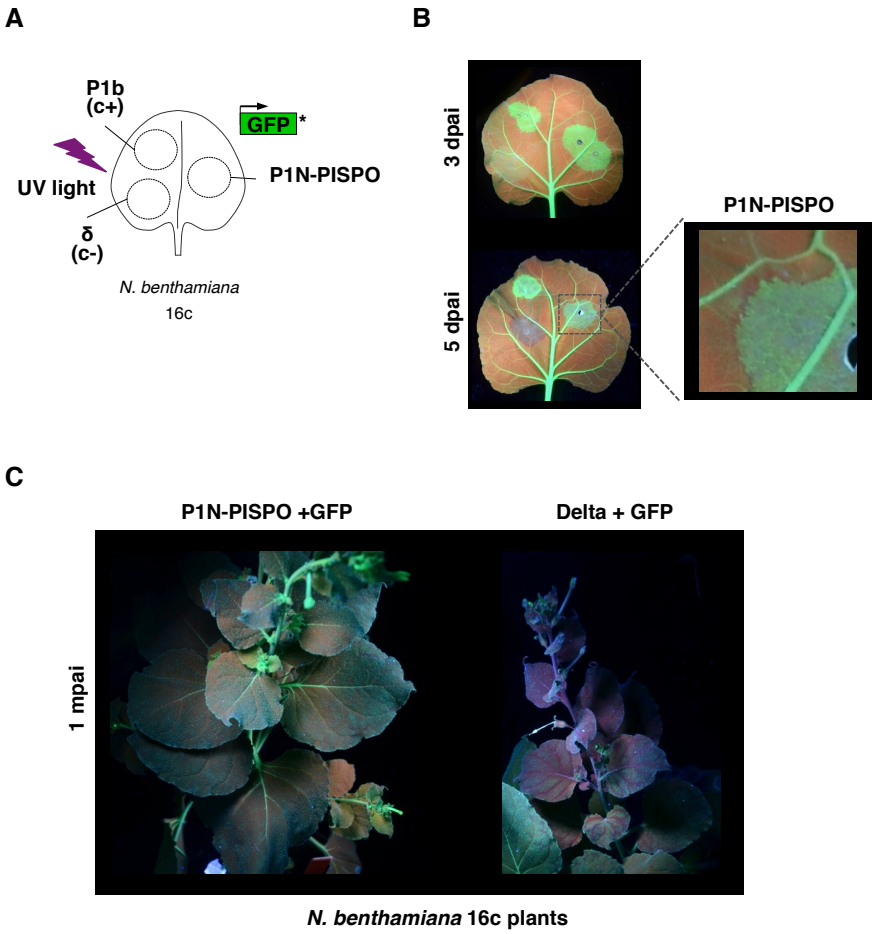

Figure R15: RNA silencing suppression activity of SPFMV P1N-PISPO and effect on systemic GFP silencing. A) Patch design used for coagroinfiltration in *N. benthamiana* 16c leaves of a GFP-expressing construct together with P1N-PISPO SPFMV product, CVYV P1b positive control (c+), or empty vector (δ, c-) B) Pictures of GFP fluorescence in agroinfiltrated leaves at 3 (top) or 5 (bottom) days postagroinfiltration (dpai) under UV light. Detail of a red halo surrounding the P1N-PISPO agroinfiltrated patch at 5 dpai. C) Pictures for whole plants of *N. benthamiana* 16c at 1-month post-agroinfiltration, showing GFP fluorescence under UV light. The left picture was taken from a plant co-agroinfiltrated with GFP together with P1N-PISPO. The right picture was taken from a plant co-agroinfiltrated with GFP together with the empty vector.

Assays to corroborate the anti-silencing activity of P1N-PISPO and evaluation of this activity in other individual SPFMV proteins

To verify whether P1N-PISPO acts as a RNA silencing suppressor (RSS) and to compare in parallel this capacity in other SPFMV viral proteins (P1 and HCPro), we performed a standard silencing assay in *N. benthamiana* plants.

The P1, HCPro and a P1 variant with the ORF corresponding to PISPO interrupted by a stop codon (P1 only) were cloned into the same binary vector that P1N-PISPO (see above, Fig. R16A). All the constructs, including P1N-PISPO were coagroinfiltrated in *N. benthamiana* leaves with a GFP-expressing construct, side-to-side with the same controls described above (Fig. R16B). The GFP fluorescence was monitored over time under UV light. The experiment was repeated several times, using at least three independent *Agrobacterium* cultures for each construct.

Compared to other individual SPFMV gene products, only P1N-PISPO showed clear RNA silencing suppression activity at 3 and 5 days postagroinfiltration (dpai) in the visual assay (Fig. R16C), which correlated with higher accumulation of GFP mRNA as observed by Northern blotting (Fig. R16D) and RT-qPCR (Fig. R16E). Differences in GFP fluorescence and accumulation of GFP mRNA between the CVYV P1b positive control and P1N-PISPO suggested that the last one was a weaker RSS compared with P1b. This was confirmed by the RT-qPCR analysis, which showed around 5-times-higher levels of GFP mRNA in the presence of P1b (Fig. R16E).

Constructs expressing P1 (wild-type P1 sequence) and P1 only (P1 with an out-of-frame stop codon precluding any expression of PISPO, as described) failed to exhibit enough noticeable RNA silencing suppression activity in our assays. Interestingly, the construct expressing HCPro also failed to exhibit RSS activity, with quantitative values always below those obtained for P1 (Fig. R16C, D, and E).

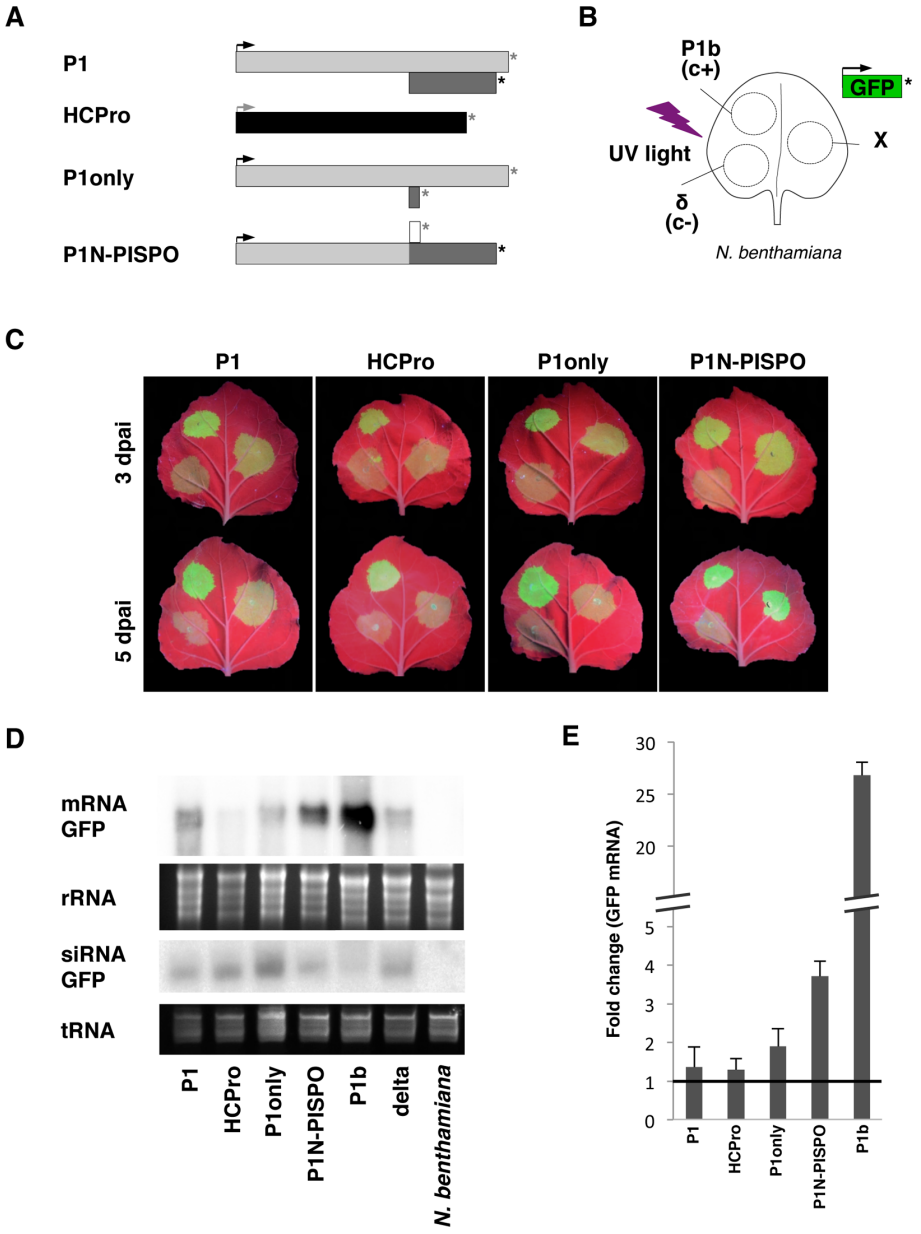

Figure R16: RNA silencing suppression activity of SPFMV P1N-PISPO. (A) The constructs used are represented with the same conventions as in the other figures for AUG and stop codons. (B) Patch design used for coagroinfiltration in *N. benthamiana* leaves of a GFP-expressing construct together with other constructs expressing SPFMV products (indicated by X), a CVYV P1b positive control (c+), or an empty vector (δ, c-). (C) Pictures of representative agroinfiltrated leaves taken at 3 (top row) or 5 (bottom row) days postagroinfiltration (dpai) under UV light. (D) Northern blot analysis of GFP mRNA extracted from agroinfiltrated tissue patches at 3 dpai, comparing the different constructs indicated above each lane. The bottom panel show the ethidium bromide staining of the gel as loading controls. (E) Relative accumulation of GFP mRNAs measured by specific RT-qPCR and normalized against the mean value corresponding to the negative control. The average values ± standard deviations from several experiments, each performed with at least three independent *Agrobacterium* cultures are plotted. Significant difference in pairwise comparisons and after applying the Tukey-Kramer test were found only for the positive control CVYV P1b (shown with a broken axis to accommodate the large difference) and for the P1N-PISPO samples.

The same P1 and P1N-PISPO constructs tested for RSS activity were used in the LC-MS/MS experiments described above. Although it is not a quantitative assay, the detection of similar numbers of specific peptides in both cases (Table R10) suggests that P1 and P1N-PISPO accumulated at comparable levels in agroinfiltrated leaves in the presence of a heterologous RSS. Hence, these results support the idea that the absence of noticeable silencing suppression activity by the P1 construct is not due to problems in protein expression, accumulation, or stability. To evaluate if some of these problems were interfering with the other negative constructs (HCPro, P1 only), we tested their expression in agroinfiltrated leaves by Western-blot. A Myc tag was added at the N-terminal part of HCPro and P1 only. Myc-P1b and *N.benthamiana* were used, respectively, as positive and negative controls. In the case of HCPro, the presence of a band of the expected size (52 kDa) was detected (Fig. R17). For P1 only a band of around 100 kDa was present (Fig. R17). This molecular weight was higher than the expected one (74 kDa), indicating that some post-trancriptional modifications might have occurred in these proteins.

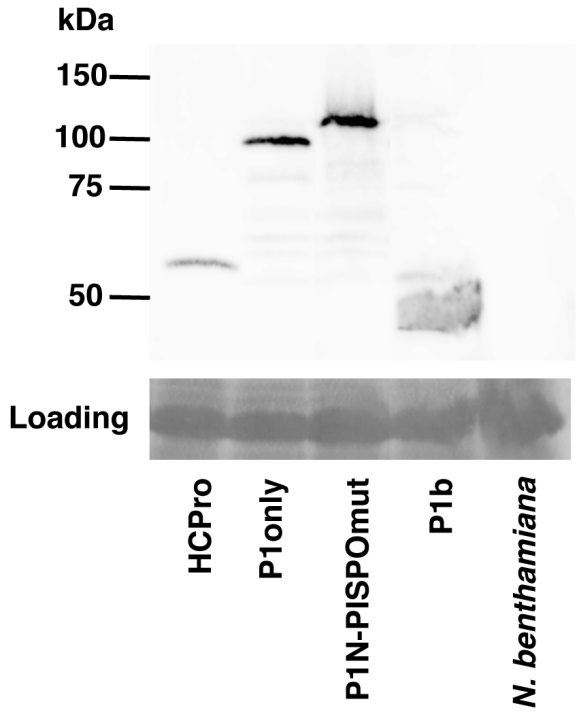

Figure R17: Protein expression of HCPro, P1 only and a mutated version (P1N-PISPOmut) in agroinfiltrated leaves, measured by Western-blot analysis using specific anti-myc antibody. Molecular weight (kDa) of the mobility of ladder bands is indicated at the left of the picture.

Altogether, these results confirmed that P1N-PISPO showed RNA silencing suppressor activity. Moreover, the assays showed that the individual P1 and HCPro SPFMV proteins did not presented a clear anti-silencing activity, at least in the standard procedures used for characterization of RSS.

Preliminary evaluation of anti-silencing activity in constructs co-expressing P1 and HCPro

As aforementioned, P1 and HCPro did not presented clear anti-silencing activity when they were co-agroinfiltrated individually. To test if these two proteins showed silencing suppression activity when they were co-expressed in cis, a construct corresponding to the complete P1HCPro region of SPFMV AM-MB2 isolate (Fig. R18A) was co-agroinfiltrated with GFP in *N. benthamiana* plants (Fig. R18B). Visual observations under UV showed that P1HCPro presented some noticeable silencing suppression activity at 3dpai, whereas at 5dpai this activity was still visible but was reduced to an even lower degree, compared with the positive control (Fig. R18C). The quantification of GFP mRNA by RT-PCR supported the visual observations at 3dpai, where the GFP mRNA levels were similar to that showed by P1N-PISPO (Fig. R16E and R18D).

Two additional P1HCPro variants were also constructed and co-agroinfiltrated (Fig. R18A). In the first P1HCPro variant, the frame of P1N-PISPO was stopped (P1onlyHCPro). In the second one, the conserved reported FRNK box (Shiboleth et al. 2007) involved in HCPro anti-silencing activity was mutated to FANA, replacing charged residues by Alanines (P1HCPromut). Although visual observations (Fig R18C) and GFP mRNA values (Fig R18D) showed a slightly decrease of silencing suppression activity in both variants compared to the non-mutated construct, the results were not conclusive due to the high variability between replicates. In fact, the measurements of GFP mRNAs were too close to the discrimination limit of the assay to attribute a clear activity in any of the two variants. Therefore, to elucidate if P1 or HCPro contributed to counteract the antiviral silencing pathway, or alternatively if HCPro could be involved in the generation of P1N-PISPO, further experiments will be needed.

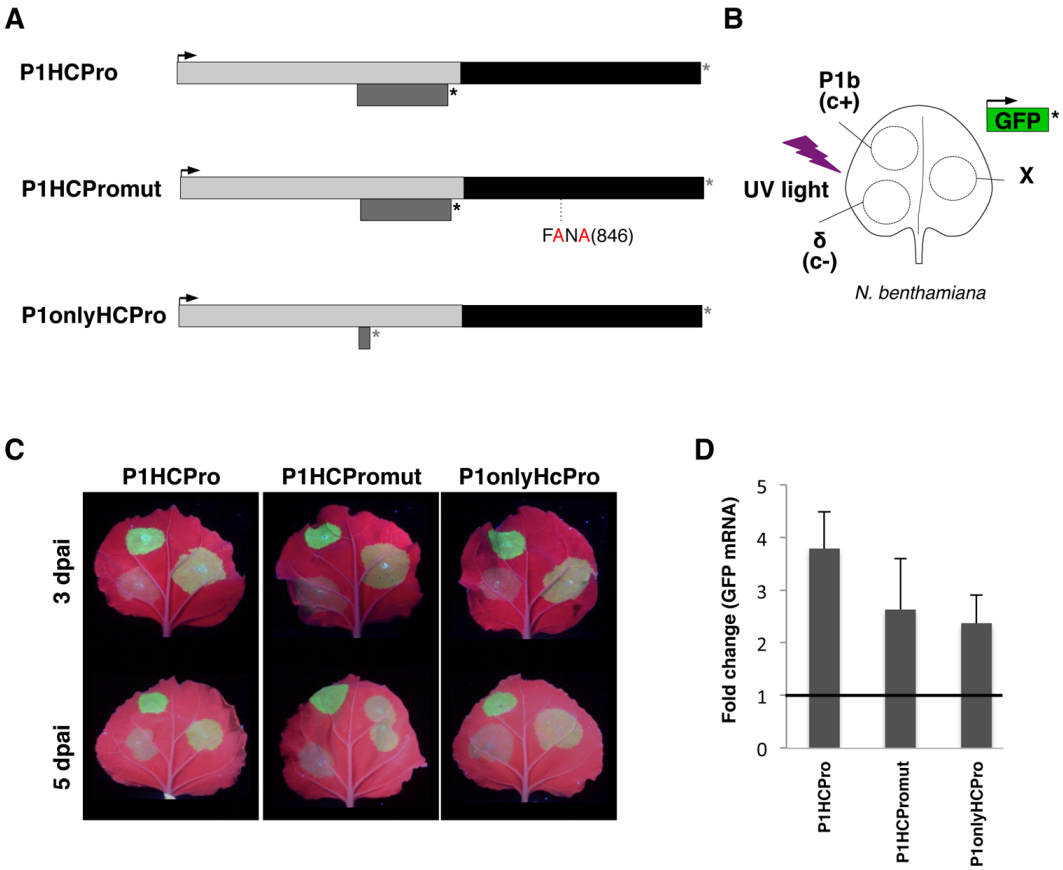

Figure R18: RNA silencing suppression activity of SPFMV P1-HCPro. (A) The constructs used are represented with the same conventions as in the other figures for AUG and stop codons. The localization of the FRNK present in the sequence (positions in parentheses) in the mutant in which the R and K residues were replaced by A residues is indicated. (B) Patch design used for coagroinfiltration in *N. benthamiana* leaves of a GFP-expressing construct together with other constructs expressing SPFMV products (indicated by X), a CVYV P1b positive control (c+), or an empty vector (δ, c-). (C) Pictures of representative agroinfiltrated leaves taken at 3 (top row) or 5 (bottom row) days postagroinfiltration (dpai) under UV light. (D) Relative accumulation of GFP mRNAs measured by specific RT-qPCR and normalized against the mean value corresponding to the negative control. The average values ± standard deviations from several experiments, each performed with at least three independent *Agrobacterium* cultures are plotted.

Approximations to the mode of action involved in the silencing suppression capacity of P1N-PISPO

Once we confirmed that P1N-PISPO counteracted the plant antiviral silencing defence we were interested to determine the mode of action involved in this capacity. In order to evaluate that, we performed some experiments described in the following sections.

Presence of WG/GWs motifs in PISPO aminoacid sequence

In some RSS found in plant viruses, tryptophan-glycine/glycine-tryptophan (WG/GW) motifs can act as key functional motifs. They have been described to play essential roles in interactions with Argonaute (Ago) proteins, and in some cases with small RNAs, their presence being necessary to preserve suppressor activity (Azevedo et al. 2010; Chattopadhyay et al. 2015; Giner et al. 2010; Pérez-Cañamás and Hernández 2015).

The analysis of sequences in SPFMV and in the members of its lineage (SPV2, SPVC and SPVG) showed that in all these viruses the PISPO sequence contained, respectively, three, one, one and one WG/GW motifs. While SPVC had 3 WG/GWs motifs in the P1 coding sequence versus 2 in P1N-PISPO, SPVG and SPV2 presented the same number of motifs in both proteins (P1 and P1N-PISPO) (Fig. R19).

Interestingly, the P1 of SPFMV AM-MB2 only presents 2 WG/GWs motifs compared to the 4 motifs found in the P1N-PISPO protein variant (Fig. R19). Szabo and co-workers have recently showed that the P1 of another SPFMV isolate only recovered measurable RNA silencing suppressor activity when 2 extra WG/GWs motifs were artificially added to its sequence (Szabó et al. 2012). These observations suggested that the WG/GWs of SPFMV P1N-PISPO could be involved in its silencing suppressor activity.

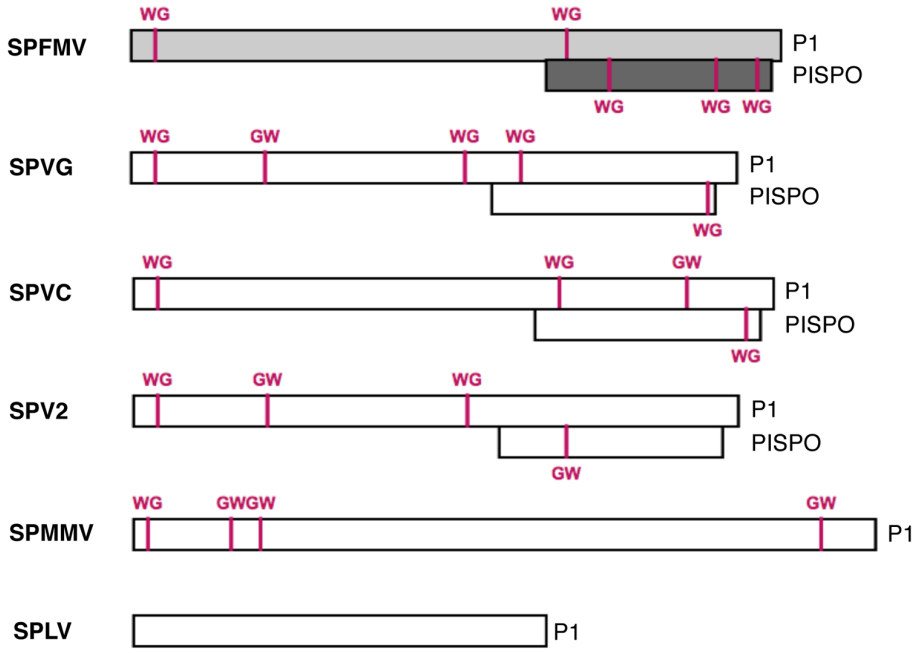

Figure R19: Localization of WG/GW motifs in P1 and P1N-PISPO proteins of sweet potato viruses. P1 and P1N-PISPO are represented with boxes. The positions of WG/GWs motifs correspond with vertical purple lines. The viral isolates represented are SPFMV AM-MB2, SPVG GWB (JN613807), SPVC AM-MB2, SPV2 AM-MB2, SPMMV 130 (GQ353374) and SPLV (KC443039). The scale schemes were created with IBS: Illustrator for biological sequences (available in http://ibs.biocuckoo.org).

Analysis of P1N-PISPO WG/GWs mutant

In order to evaluate the contribution of WG/GWs motifs in P1N-PISPO activity, we generated a mutated variant of P1N-PISPO. In this mutant (P1N-PISPOmut), the tryptophan (W) of all four WG/GW motifs was replaced by alanine (A) (Fig. R20A).

The mutated variant was agroinfiltrated in *N. benthamiana* leaves, along with the GFP-expressing construct, to evaluate its activity as an RSS. The mutated product failed to counteract the RNA silencing, as shown by GFP fluorescence under UV light (Fig. R20B). This observation was confirmed by GFP mRNA Northern blot and RT-qPCR quantification of GFP mRNA (Fig. R20B and C). The levels of GFP mRNA in leaves co-agroinfiltrated with P1N-PISPOmut were even lower that the ones determined in the empty vector sample (delta).

To discard a problem of expression in P1N-PISPOmut, the level of a myc-P1N-PISPOmut product was detected in agroinfiltrated samples by Western blotting. While the expected size of this variant is around 73 kDa, a band of around 100 kDa was detected (Fig. R17). As in the case of P1 only, we attributed this difference in size to possibly the same kind of post-translational modifications, still pending to be determined.

In conclusion, this assay indicates that the WG/GWs motifs found in the P1N-PISPO coding sequence are positively correlated with its capacity to counteract the plant silencing defence.

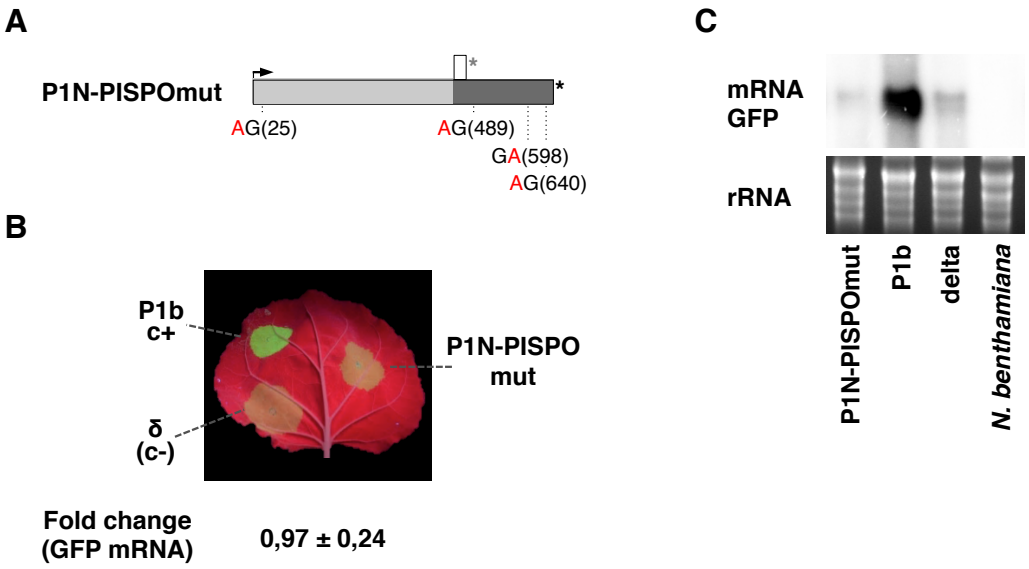

Figure R20: Involvement of WG/GWs motifs in P1N-PISPO silencing activity. A) P1N-PISPOmut construct is represented with the same conventions as in the other figures for AUG and stop codons. The distribution of the four WG/GW motifs in the sequence (positions in parentheses) is indicated in the mutant in which the four W residues were replaced by A residues. B) Picture of representative leave co-agroinfiltrated with GFP and the indicated construct (P1-PISPOmut) and the corresponding controls taken at 3 days postagroinfiltration (dpai) under UV light. The average of GFP mRNAs relative accumulation ± standard deviation measured by specific RT-qPCR and normalized against the mean value corresponding to the negative control is indicated below the picture. Three different samples were collect at 3dpai and analysed. C) Northern blot analysis of GFP mRNA extracted from agroinfiltrated tissue patches at 3 dpai, comparing the different constructs indicated above each lane. The bottom panel shows the ethidium bromide staining of the gel as loading controls. The control lanes were the same used in figure R16, since all samples were tested in the same blot to facilitate comparisons.

Interference of P1N-PIPSO with siRNAs generation

As aforementioned, WG/GWs motifs can be related with the anti-silencing activities of some RSS with different modes of action. For example the WG/GWs motifs of SPMMV P1 mediated the interaction with AGO1 (Giner et al. 2010), whereas the unique WG motif of PLPV p37 also is involved in binding to siRNAs (Pérez-Cañamás and Hernández 2015).

To test if P1N-PISPO inhibits siRNAs generation and to evaluate if WG/GWs are related with this mode of action, the GFP siRNAs levels of co-agroinfiltrated tissue with the different constructs (Fig. 11A) were analysed by Northern blotting. As expected from previous results (Giner et al. 2010; Valli et al. 2011) CVYV P1b prevented to certain extent the generation of GFP-derived siRNAs, while a clear similar effect was not observed for P1N-PISPO (Fig. R21) and no differences were observed between P1N-PISPO and the WG/GW mutants.

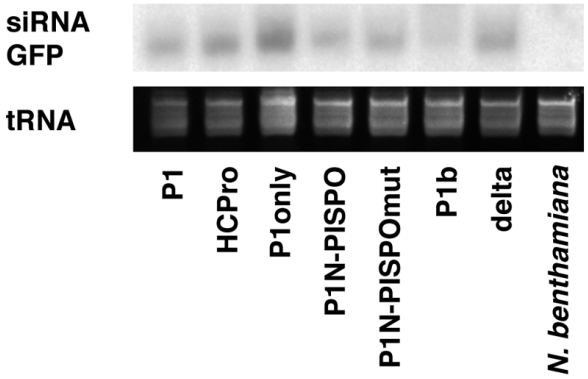

Figure R21: Interference of P1N-PISPO with siRNAs generation. Northern blot analysis of GFP siRNAs extracted from agroinfiltrated tissue patches at 3 dpai, comparing the different constructs indicated above each lane. The bottom panel shows the ethidium bromide staining of the gel as loading controls

This result suggested that P1N-PISPO might use a mode of action different than the inhibition of siRNAs generation. To evaluate different modes of action, as for example the interference with Argonaute proteins, further experiments will be needed.

DISCUSSION

DISCUSSION

Among all the known members of the *Potyvirus* genus (158 species according to the International Committee of Taxonomy of Viruses [ICTV] [2014] release), SPFMV presents several peculiarities. First, its genome is the largest, with an extraordinarily long P1 region (664 to 724 aa), which is surpassed in the *Potyviridae* family only by the equivalent P1 product of the ipomovirus SPMMV (758 aa), which shares some similarity with SPFMV P1 in the N-terminal region (Valli, López-Moya, and García 2007). The bioinformatic prediction of the additional ORF PISPO within the P1-coding sequence (Clark et al. 2012; Li et al. 2012) added a further peculiarity, although it was unknown until now whether PISPO was expressed. Our results shed light on these aspects of SPFMV biology, first by finding the occurrence of RNA slippage events in the PISPO G_2A_6 conserved motif, and then by confirmation that the predicted *trans*-framed P1N-PISPO product was indeed expressed during SPFMV infection. Moreover, our results demonstrated that P1N-PISPO contributed to counteract the RNA silencing-based plant defence to viral infection.

P1N-PISPO a new gene product expressed through polymerase slippage as an out-of-frame ORF

The novel potyviral gene product P1N-PISPO (654 aa, 72.7 kDa) combines a P1N part shared with the canonical P1 (N-terminal portion of 422 aa, equivalent to a 46.5-kDa protein fragment) and the PISPO sequence (232 aa, fragment of 26.1 kDa). The product is similar in size to P1 (664 aa, 74.1 kDa) but with notable differences, including, for instance, the predicted isoelectric points of the two proteins: 9.24 for P1 and 6.17 for P1N-PISPO. Interestingly, an isoelectric point of slightly below 7 is a hallmark of P1s displaying RNA silencing suppression activity in other potyvirids (Valli et al. 2007). Regarding the P1N-PISPO sequence, the P1N part is quite conserved between the members of the SPFMV-lineage, and even is related to the homologous P1N region of the ipomovirus SPMMV. Instead, alignment of PISPO sequences revealed a high variability between them. This lack of conservation may indicate that PISPO has evolved recently, as it has been observed in other viral overlapping reading frames (Sabath, Wagner, and Karlin 2012). The fact that P3N-PIPO is expressed in all the potyvirids whereas P1N-PISPO is restricted to SPFMV-lineage members also supports the recent emergence of P1N-PISPO.

The expression of P1N-PISPO is likely to derive from the translation of RNA variants with a G_2A_7 sequence, generated by polymerase slippage in the G_2A_6 conserved motif situated upstream of PISPO. This mechanism of expression is supported by examination of sequences corresponding to different potyviruses present in the

virome of the AM-MB2 plant, which showed results consistent with polymerase slippage in equivalent G_2A_6 motifs for SPV2 and SPVC (Table R8).

Polymerase slippage as a general mechanism to express potyviral out-of-frame proteins

Analysis of sequence variants around the P3N-PIPO gene product in several potyviruses revealed the presence of polymerase slippage events in the $G_{1-2}A_{6-7}$ motif located upstream of PIPO, suggesting that P3N-PIPO is expressed by the same mechanism. In our data, a percentage of transcripts with an extra A in the PIPO $G_{1-2}A_{6-7}$ motif, lower than the one for SPFMV PISPO G_2A_6 motif, has been identified for SPFMV, SPVC, SPV2, PPV and SPMMV. Although this possibility could not be demonstrated when P3N-PIPO was first identified in *Turnip mosaic virus* (Chung et al. 2008), the same group of researchers from the University of Cambridge has recently reported that polymerase slippage also occurs at the PIPO motif of this virus (Olspert et al. 2015).

On the other hand, a low but significant number of transcripts with a deletion of one nucleotide in the PIPO motif, but not in the PISPO one, were identified in SPFMV, SPV2 and SPMMV samples. This finding suggests that two variants in addition to the in-frame P3 product (frame 0) can be produced: the P3N-PIPO variant (frame -1), and another in the third frame (frame +1), characterized by the presence of a very short overlapping sequence after the PIPO slippage motif, which would lead to the expression of a truncated form of P3. The existance of this theorically predicted product has been recently demonstrated in the case of the potyvirus *Clover yellow vein virus* (ClYVV). This new gene product (named P3N-ALT by the authors describing it) was also produced by a polymerase slippage event, and it has been proposed to be involved in cell-to-cell movement function, along with P3N-PIPO (Hagiwara-Komoda et al. 2016).

All these data strongly suggest that P1N-PISPO and P3N-PIPO are produced, at least partially, through polymerase slippage and lead us to propose that this polymerase slippage is a mechanism adopted by viruses in certain situations to rapidly produce new protein variants deriving from the same sequence, and thus boosting the coding capacity of the compact genomes of viruses. However, several aspects remains unclear about the mechanism and its regulation, and further work will be necessary to propose a complete model to better explain how the polymerase slippage works in potyvirids and other viruses, and what are the biological, pathological and evolutive consequences of its adoption.

For example, the regulation of polymerase slippage events is still mostly unknown. The tendency of polymerases to stutter when encountering repetitive motifs has been demonstrated in EBOV, HCV, *Vaccinia virus*, T7 bacteriophage or paramyxoviruses

(Baulcombe 2004; Kulkarni et al. 2009; Revers and García 2015; Valli et al. 2015). Repetitive motifs, however, are not the rule but the exception, probably because of selective negative pressure supported by nonsense-mediated decay (Garcia, Garcia, and Voinnet 2014) or other mechanisms. Nonetheless, the slipping frequency of EBOV polymerase, as well as the paramyxoviral one, has been associated to the surrounding sequences and the secondary structures of each specific repetitive motif (Hausmann et al. 1999; Kulkarni et al. 2009; Mehedi et al. 2013; Shabman et al. 2014). In SPFMV, our data reveals that viral polymerase slips more efficiently in PISPO than in PIPO domain, but no clear hallmark elements have been identified that can explain these differences. Further investigations will be required to elucidate if sequences surrounding the $G_{1\text{-}2}A_{6\text{-}7}$ motifs or other aspects in the virus sequence context are involved in the regulation of potyviral polymerase slippage.

One consequence of the use of polymerase slippage mechanisms to expand the potyviral protein coding capacity is that it leads to the accumulation of modified viral genomes in the infected hosts. The risks derived from this accumulation of genome variants diverging from the master genome, such as genomic modifications in the viral progeny (Olspert et al. 2015; Shabman et al. 2014) or those derived from mRNA decay (Garcia et al. 2014), may have important consequences during viral infection. Thus, understanding how potyvirids counteract problems derived from this peculiar gene expression mechanism will certainly deserve further experimental work.

Considering the evolutionary relationship of polymerases between members of the families *Picornaviridae* and *Potyviridae* (Olspert et al. 2015), it is reasonable to envision similar behaviors in both viral families and, consistent with that idea, the six-adenine repetition motif is underrepresented in picornaviruses (0.67 motif in the coding region per viral genome versus the expected 1.9 motifs), as it was the case in the family *Potyviridae*. There is no previous report of polymerase slippage in the *Picornaviridae* family; nonetheless, when an A_6 motif was present, as in the case of the enterovirus *Human rhinovirus C* (SRR363436), there were 2,7% A residue insertions at this location. These data suggest that polymerase slippage can occur in both *Picorna*-like families but that *Potyviridae* take more frequent advantage of this mechanism. Again, the important differences in the two pathosystems deserve a careful examination to dilucidate the balance of advantages and disadvantages that leads to the divergent strategies adopted.

Detection of P1N-PISPO protein during viral infection and mass-spectometry assays as a method to detect new viral proteins

Our experiments designed to identify translational frameshifting in WGE failed to show a noticeable production of truncated frameshifted protein products. However, the presence of minor products compatible in size with P1N-PISPO was also detected. It is well-known that the T7 polymerase is prone to slip (Molodtsov, Anikin, and McAllister 2014; Olspert et al. 2015; Wons, Furmanek-Blaszk, and Sektas 2015) and our results revealed that T7 is also able to slip at the PISPO region. Thus, the minor products detected in WGE experiments may be the result of T7 polymerase slippage. Consistent with our view that viral RNA polymerase slippage is the most likely mechanism of production of out-of-frame products in potyviruses during infection, the transient expression of wild-type P1 sequence out of the viral infection context resulted in the production only of P1-derived peptides when analyzed with the sensitive mass spectrometry technique (Fig. R13A). Altogether, a strong case can be proposed for viral polymerase transcriptional slippage as the mechanism used to produce the *trans*-frame P1N-PISPO, and likely the same conclusion can be expanded to P3N-PIPO proteins found in all other potyvirids. The combination of our analysis with SPFMV, SPVC, and SPV2 suggests that polymerase slippage might occur in all sweet potato potyviruses where the PISPO sequence was predicted (Clark et al. 2012).

When facing the challenge of detecting a previously unknown gene product that was predicted bioinformatically, we decided to adopt a straightforward approach using mass spectrometry. Similar techniques have been used previously to identify viral infections in plants, including those produced for potyviruses (Luo, Wylie, and Jones 2010), but to our knowledge, this is the first time that it serves to demonstrate that an out-of-frame gene product is being expressed in infected plant tissues. We believe that this new method is a convenient approach that gives fast and unequivocal proof of protein translation without the need of obtaining specific antibodies, which is a time-consuming procedure that may fail depending on the antigenicity of the target protein. In fact, we learnt after generating our results that an independent team was also searching for P1N-PISPO in a different SPFMV isolate, but their strategy based on the generation of peptide-specific antibodies failed to show the presence of the out-of-frame variant in their analysis (Untiveros et al. 2016, and personal communication by Kreuze, Firth and Valkonen). On the other hand, the Mass spectrometry strategy used in our assays allowed unambiguous detection of both P1 and P1N-PISPO together in the same sample, showing that the two gene products coexist in infected plants. Although the methodology is not quantitative, the abundance and number of peptides might provide some indication of the expression levels and the stability of the mature proteins. For example, compared to another large viral product, CI, the high coverage obtained for P1 and P1N-PISPO suggests that these two proteins are quite stable.

While we have shown mass spectrometry to be a useful method for identifying novel gene products, further research is required to determine the turnover and subcellular localization of P1N-PISPO during the infection cycle and to evaluate its impact in pathogenicity.

P1N-PISPO as a RNA silencing suppressor

The functions of potyviral P1s have remained elusive for many years, but recent results are revealing the importance of P1 during potyvirus infection (Martínez and Daròs 2014; Pasin et al. 2014). In the case of SPFMV and other potyviruses infecting sweet potato, the presence of P1N-PISPO adds a further layer of complexity to the efforts to unravel the role(s) of these gene products in the infection context (Ivanov et al. 2014). To start addressing this, our experiments show a clear role for P1N-PISPO as an RSS. Interestingly, for all the members of the *Potyvirus* genus tested so far, the essential RNA silencing suppression activity was found associated with HCPro, which was the first characterized RSS (Anandalakshmi et al. 1998; Kasschau and Carrington 1998). In other members of the *Potyviridae* family, however, the RNA silencing suppression function is often shifted to P1 products, as has been observed in ipomoviruses (Giner et al. 2010; Mbanzibwa et al. 2009; Valli et al. 2006), tritimoviruses (Young et al. 2012), and poaceviruses (Tatineni et al. 2012). These RSSs belong to a distinct group of P1 proteins that appears to be evolutionarily separated from typical P1 proteins of members of the genus *Potyvirus* (Rodamilans, Valli, and García 2013; Valli et al. 2007). Our finding that the P1N-PISPO product acts as an RSS would serve to expand this list of known P1-related sources of RNA silencing suppression activity in the family *Potyviridae* and might help to understand the evolutionary acquisition of this important viral function.

Whereas the P1b protein of the ipomovirus CVYV displays a strong RSS activity that depends on its ability to bind small RNAs (Valli et al. 2011), the P1 protein of SPMMV suppresses RNA silencing by interfering with RISC activity, specifically through blocking Ago binding via WG/GW hooks (Giner et al. 2010). In SPFMV, the P1 present two WG/WGs in its sequence whereas 4 WG/GWs motifs are found in the P1N-PISPO coding sequence (Fig. R19). Interestingly, a recent study showed that the native SPFMV P1, which shares noticeable sequence similarity with SPMMV P1 (Valli et al. 2007), does not work as an RSS but can gain this functionality when mutations are introduced to create additional WG/GW motifs in positions nearly matching the ones present in SPMMV P1 (Szabó et al. 2012). In our experiments, P1 also failed to show a clear RSS activity, confirming the observations of Szabó and coworkers (Szabó et al. 2012).

Our result that an SPFMV P1N-PISPO variant in which all the WG/GW motifs have been mutated loses RNA silencing suppression activity suggests that P1N-PISPO might disrupt the RNA silencing machinery by a mechanism involving Ago hooks, similar to

that described for SPMMV P1 (Giner et al. 2010). The fact that the silencing activities of SPFMV P1N-PISPO and SPMMV P1 are both quite weak further supports the hypothesis that these suppressors share a similar mechanism of action. However, we cannot rule out that the correlation between functionality and presence of WG/GW in SPFMV P1N-PISPO could correspond to Ago-independent disturbances caused, for instance, by conformational alterations derived from mutations of W residues, as might be the case in other RSSs (Pérez-Cañamás and Hernández 2015).

Giner and coworkers suggested that the expression of a weak RSS in SPMMV could be a viral strategy to cause only mild damage in the host, allowing sweet potato potyvirids to survive in infected perennial plants for an extended period of time (Giner et al. 2010). This idea will be also in agreement with the weak RSS activity observed in SPFMV P1N-PISPO. We can also speculate that sweet potato potyvirids might not depend exclusively on the weak RNA silencing suppression activities of their P1N-PISPO variants, and that other viral products could also help to counteract RNA silencing during infection. In this regard, for instance, the VPg of the potyvirus PVA has been found to counteract RNA silencing (Cuellar et al. 2009; Rajamäki et al. 2014). Additionally, the levels of expression of HCPro in other potyviruses were reported to be regulated by P1 (Tena Fernández et al. 2013). In the case of SPFMV, although our transient agroinfiltration experiments with individual gene products showed no clear anti-silencing activity for P1 or HCPro, preliminary results suggested that P1-HCPro might display some activity. Indeed, a recent report based on the analysis of another SPFMV isolate has showed that both P1 and P1N-PISPO have RNA silencing suppressor activity (Untiveros et al. 2016). Thus, despite our negative results with P1 and HCPro constructs, the contribution of P1 and/or HCPro to silencing suppression during SPFMV infection cannot be ruled out. Differences in behavior during natural virus infection in the original hosts, and the functional analysis of individual gene products in experimental conditions are quite frequent, and therefore, caution needs to be applied before discarding any contribution of P1 and HCPro to the RSS activity of SPFMV. Also, the use of different isolates of SPFMV in our work and in the experiments of Untiveros and coworkers might reflect the natural variability. Another possibility to explain the somehow conflicting results can be the modulation of P1N-PISPO production during P1HCPro expression. Although the expression of the P1 wild type construct by agroinfiltration does not produce P1N-PISPO in a detectable amount by the highly sensitive LC-MS/MS assay (Fig. R13A), a contribution of HCPro to the regulation of the polymerase slippage mechanism can not be discarded. To elucidate the mechanism used by the cis construct P1HCPro to act as a weak RNA silencing suppressor, a P1HCPro variant with the frame of P1N-PISPO interrupted by a mutated stop codon, and a P1HCPro variant with a mutation in the FRNK box involved in HCPro anti-silencing activity (Shiboleth et al. 2007) were tested (Fig. R18). Unfortunately, the preliminary analysis of these variants does not allow us to exclude any possibility,

because the level of activities were too weak and variable, and too close to the thresholds used to discriminate the negative controls of the experiments.

Taking into account these results, and knowing that the context of the viral infection is most likely quite different from that in the transient agroinfiltration assays, further work will be needed to fully understand the modes of action and the relationships of all viral factors that might be participating in counteracting the RNA silencing-based host defences.

The switch of the anti-silencing role from established suppressors such as HC-Pro or P1 (the strength of which could be adjusted through regular mutation/selection processes) (Torres-Barceló, Daròs, and Elena 2010) to P1N-PISPO with its rather peculiar expression mechanism deserves some attention from an evolutionary point of view. As mentioned above, whereas the main RNA silencing suppression activity lies with HCPro in members of the genus *Potyvirus*, it is supplied by a P1-type protein in ipomoviruses, tritimoviruses, and poaceviruses, likely highlighting two evolutionary lineages in the family *Potyviridae*. Thus, we can speculate that the existence of a P1-related RNA silencing suppressor in the potyvirus SPFMV could be the result of a recombination event between a potyvirus and an ipomovirus in sweet potato, which is supported by the notable similarity between the N termini of the P1 proteins from SPFMV and the ipomovirus SPMMV (Valli et al. 2007).

Importance of P1N-PISPO during Sweet potato viral disease (SPVD)

The knowledge generated in this work about P1N-PISPO might be especially relevant in the context of the devastating and widespread sweet potato viral disease (SPVD) (Clark et al. 2012; Karyeija et al. 2000). In contrast to many other synergisms involving potyviruses (Syller and Grupa 2015; Syller 2012), sweet potato viral disease is considered atypical because the potyvirus is the partner with a boost in its accumulation. Although we have confirmed this previous observation with our plant material, many important aspects still remain to be explained. For instance, further research is needed to elucidate whether the rather peculiar RNase3 RSSs from SPCSV (Cuellar et al. 2009; Tugume et al. 2013; Weinheimer et al. 2015) and P1N-PISPO are involved in the outcome of this complex interaction. In line with that, another interesting but unexpected observation of our work is related to this unusual synergism: we have noticed a specific reduction in RNA slippage frequency at the PISPO site, but not in PIPO, in plants superinfected with SPCSV (Fig. R12). The different roles of P1N-PISPO and P3N-PIPO during viral infection, named suppression of RNA silencing (this report) or viral movement (Vijayapalani et al. 2012; Wei et al. 2010; Wen and Hajimorad 2010), respectively, might provide clues not only to explain this

observation but also to understand how changes in the relative amounts of these two gene products could affect the outcome of SPVD in the coinfected plants. It will be certainly most interesting to elucidate the mechanisms that regulate the slippage frequency, and how the virus is adapting such complex systems to regulate the amount required for each particular gene product.

To summarize, our results highlight the enormous genomic flexibility of viruses, which allows them to take profit from particular biochemical features of their genomes and gene products, such as the slippage capacity of the RNA polymerase in certain motif sequences, in order to expand their gene dotation, and consequently explore alternative pathways to improve their adaptation to a variety of hosts, vectors and environmental conditions.

CONCLUSIONS

CONCLUSIONS

1. A new isolate of the virus *Sweet potato feathery mottle virus* (SPFMV) was characterized from AM-MB2 plants. The complete sequence of SPFMV AM-MB2 was obtained, and its analysis suggested that it might correspond to a recombination event between two SPFMV strains from the RC and the EA groups. SPFMV AM-MB2 complete sequence presented all the gene products of potyviruses plus two overlapping open reading frames PIPO and PISPO.

2. SPFMV AM-MB2 largely increased its titer when the plant was super-infected with the unrelated virus *Sweet potato chlorotic stunt virus* (SPCSV), as it has been already reported for other potyviruses in sweet potatoes. The increase in titer was also confirmed for the two related potyvirus isolates of SPVC and SPV2 infecting the AM-MB2 plants, whereas apparently the titers of a begomovirus and a badnavirus found in these plants was not altered by the presence of SPCSV.

3. An average of 11,8% of transcripts with an extra A were detected in the G_2A_6 motif upstream of PISPO during SPFMV viral infection, a feature compatible with polymerase slippage events occurring in the indicated motif that can lead to expression of an out-of-frame gene product. This percentage decreased to an average of 6,6% when SPCSV was present. The polymerase slippage frequency for the G_2A_6 motif upstream of PIPO in SPFMV was considerably lower, with only 1,25% of transcripts with extra A, and this value was not modified in the case of co-infection with SPCSV.

4. The insertion of an extra A in $G_{1\text{-}2}A_{6\text{-}7}$ motifs was also verified in the motifs upstream of PISPO in SPVC and SPV2, and in the motifs upstream of PIPO in SPVC, SPV2, PPV and SPMMV. Polymerase slippage is proposed as the main mechanism involved in the production of PISPO and PIPO out-of-frame potyviral products.

5. Ribosomal frameshifting did not seem to contribute to the synthesis of P1N-PISPO, at least as detectable products in the wheat germ extract *in vitro* translation system.

6. The P1N-PISPO gene product was not detected in *N. benthamiana* leaves agroinfiltrated with the P1 wild-type construct. This suggested that the plant RNA polymerases were not able to slip efficiently at the SPFMV G_2A_6 motif.

7. In mass-spectometry assays PISPO specific peptides were identified in sweet potato plants infected with the SPFMV AM-MB2 isolate. This finding revealed that the P1N-PISPO gene product was an additional viral protein synthetised, expressed and accumulated in a detectable form during SPFMV infection.

8. P1N-PISPO exhibited RNA silencing suppression activity in transient expression experiments in *Nicotiana benthamiana* leaves. No interfere with the dispersion of the systemic silencing signal was observed in GFP-expressing 16c transgenic plants. Regarding other gene products, no activity was observed for P1 or HCPro individually expressed, although their expression in *cis* resulted in a measurable anti-silencing activity.

9. While P1N-PISPO seemed not to interfere with the generation of siRNAs, a variant with mutated WG/GWs motifs failed to maintain its silencing suppression activity, suggesting that these motifs might participate in the mode of action of P1N-PISPO.

BIBLIOGRAPHY

BIBLIOGRAPHY

Adkar-Purushothama, C. R., Brosseau, C., Giguère, T., Sano, T., Moffett, P., & Perreault, J.-P. (2015). Small RNA Derived from the Virulence Modulating Region of the Potato spindle tuber viroid Silences callose synthase Genes of Tomato Plants. *The Plant Cell*, *27*(8), 2178–94.

Ahlquist, P. (2002). RNA-dependent RNA polymerases, viruses, and RNA silencing. *Science (New York, N.Y.)*, *296*(5571), 1270–3.

Akbergenov, R., Si-Ammour, A., Blevins, T., Amin, I., Kutter, C., Vanderschuren, H., … Pooggin, M. M. (2006). Molecular characterization of geminivirus-derived small RNAs in different plant species. *Nucleic Acids Research*, *34*(2), 462–71.

Alconero, R., Santiago, A. G., Morales, F., & Rodriguez, F. (1975). Meristem tip culture and virus indexing of sweet potatoes. *Phytopathology*, *65*, 769–773.

Anandalakshmi, R., Pruss, G. J., Ge, X., Marathe, R., Mallory, A. C., Smith, T. H., & Vance, V. B. (1998). A viral suppressor of gene silencing in plants. *Proceedings of the National Academy of Sciences of the United States of America*, *95*(22), 13079–84.

Aregger, M., Borah, B. K., Seguin, J., Rajeswaran, R., Gubaeva, E. G., Zvereva, A. S., … Pooggin, M. M. (2012). Primary and secondary siRNAs in geminivirus-induced gene silencing. *PLoS Pathogens*, *8*(9), e1002941.

Auzat, I., Dröge, A., Weise, F., Lurz, R., & Tavares, P. (2008). Origin and function of the two major tail proteins of bacteriophage SPP1. *Molecular Microbiology*, *70*(3), 557–69.

Azevedo, J., Garcia, D., Pontier, D., Ohnesorge, S., Yu, A., Garcia, S., … Voinnet, O. (2010). Argonaute quenching and global changes in Dicer homeostasis caused by a pathogen-encoded GW repeat protein. *Genes & Development*, *24*(9), 904–15.

Babraham-Bioinformatics. (2014). FASTQC, a quality tool for high throughput sequence data.

Baranov, P. V, Hammer, A. W., Zhou, J., Gesteland, R. F., & Atkins, J. F. (2005). Transcriptional slippage in bacteria: distribution in sequenced genomes and utilization in IS element gene expression. *Genome Biology*, *6*(3), R25.

Barry, J. K., & Miller, W. A. (2002). A -1 ribosomal frameshift element that requires base pairing across four kilobases suggests a mechanism of regulating ribosome and replicase traffic on a viral RNA. *Proceedings of the National Academy of Sciences of the United States of America*, *99*(17), 11133–8.

Baulcombe, D. (2004). RNA silencing in plants. *Nature*, *431*(7006), 356–63.

Baumberger, N., Tsai, C.-H., Lie, M., Havecker, E., & Baulcombe, D. C. (2007). The Polerovirus silencing suppressor P0 targets ARGONAUTE proteins for degradation. *Current Biology : CB*, *17*(18), 1609–14.

Bisaro, D. M. (2006). Silencing suppression by geminivirus proteins. *Virology*, *344*(1), 158–68.

Blanc, S., López-Moya, J. J., Wang, R., García-Lampasona, S., Thornbury, D. W., & Pirone, T. P. (1997). A specific interaction between coat protein and helper component correlates with aphid transmission of a potyvirus. *Virology*, *231*(1), 141–7.

Blevins, T., Rajeswaran, R., Aregger, M., Borah, B. K., Schepetilnikov, M., Baerlocher, L., … Pooggin, M. M. (2011). Massive production of small RNAs from a non-coding region of Cauliflower mosaic virus in plant defense and viral counter-defense. *Nucleic Acids Research*, *39*(12), 5003–14.

Blevins, T., Rajeswaran, R., Shivaprasad, P. V, Beknazariants, D., Si-Ammour, A., Park, H.-S., … Pooggin, M. M. (2006). Four plant Dicers mediate viral small RNA biogenesis and DNA virus induced silencing. *Nucleic Acids Research*, *34*(21), 6233–46.

Bologna, N. G., & Voinnet, O. (2014). The diversity, biogenesis, and activities of endogenous silencing small RNAs in Arabidopsis. *Annual Review of Plant Biology*, *65*, 473–503.

Bortolamiol, D., & Pazhouhandeh M, Marrocco K, Genschik P, Z.-G. V. (2007). The Polerovirus F box protein P0 targets ARGONAUTE1 to suppress RNA silencing. - PubMed - NCBI. *Current Biology : CB*, *17*(18), 1615–1621.

Bouché, N., Lauressergues, D., Gasciolli, V., & Vaucheret, H. (2006). An antagonistic function for Arabidopsis DCL2 in development and a new function for DCL4 in generating viral siRNAs. *The EMBO Journal*, *25*(14), 3347–56.

Boutet, S., Vazquez, F., Liu, J., Béclin, C., Fagard, M., Gratias, A., … Vaucheret, H. (2003). Arabidopsis HEN1: a genetic link between endogenous miRNA controlling development and siRNA controlling transgene silencing and virus resistance. *Current Biology : CB*, *13*(10), 843–8.

Brierley, I., Jenner, A. J., & Inglis, S. C. (1992). Mutational analysis of the "slippery-sequence" component of a coronavirus ribosomal frameshifting signal. *Journal of Molecular Biology*, *227*(2), 463–79.

Brosseau, C., & Moffett, P. (2015). Functional and Genetic Analysis Identify a Role for Arabidopsis ARGONAUTE5 in Antiviral RNA Silencing. *The Plant Cell*, *27*(6), 1742–1754.

Buchmann, R. C., Asad, S., Wolf, J. N., Mohannath, G., & Bisaro, D. M. (2009). Geminivirus AL2 and L2 proteins suppress transcriptional gene silencing and cause genome-wide reductions in cytosine methylation. *Journal of Virology*, *83*(10), 5005–13.

Burri, B. J. (2011). Evaluating Sweet Potato as an Intervention Food to Prevent Vitamin A Deficiency. *Comprehensive Reviews in Food Science and Food Safety*, *10*(2), 118–130.

Byamukama, E., Gibson, R. W., Aritua, V., & Adipala, E. (2004). Within-crop spread of sweet potato virus disease and the population dynamics of its whitefly and aphid vectors. *Crop Protection*, *23*(2), 109–116.

Cao, M., Du, P., Wang, X., Yu, Y.-Q., Qiu, Y.-H., Li, W., … Ding, S.-W. (2014). Virus infection triggers widespread silencing of host genes by a distinct class of endogenous siRNAs in Arabidopsis. *Proceedings of the National Academy of Sciences of the United States of America*, *111*(40), 14613–8.

Carbonell, A., & Carrington, J. C. (2015). Antiviral roles of plant ARGONAUTES. *Current Opinion in Plant Biology*, *27*, 111–7.

Carbonell, A., Dujovny, G., García, J. A., & Valli, A. (2012). The Cucumber vein yellowing virus silencing suppressor P1b can functionally replace HCPro in Plum pox virus infection in a host-specific manner. *Molecular Plant-Microbe Interactions : MPMI*, *25*(2), 151–64.

Carbonell, A., Fahlgren, N., Garcia-Ruiz, H., Gilbert, K. B., Montgomery, T. A., Nguyen, T., … Carrington, J. C. (2012). Functional analysis of three Arabidopsis ARGONAUTES using slicer-defective mutants. *The Plant Cell*, *24*(9), 3613–29.

Castillo-González, C., Liu, X., Huang, C., Zhao, C., Ma, Z., Hu, T., … Zhang, X. (2015). Geminivirus-encoded TrAP suppressor inhibits the histone methyltransferase SUVH4/KYP to counter host defense. *eLife*, *4*, e06671.

Chapman, E. J., Prokhnevsky, A. I., Gopinath, K., Dolja, V. V, & Carrington, J. C. (2004). Viral RNA silencing suppressors inhibit the microRNA pathway at an intermediate step. *Genes & Development*, *18*(10), 1179–86.

Chattopadhyay, M., Stupina, V. A., Gao, F., Szarko, C. R., Kuhlmann, M. M., Yuan, X., … Simon, A. E. (2015). Requirement for Host RNA-Silencing Components and the Virus-Silencing Suppressor when Second-Site Mutations Compensate for Structural Defects in the 3' Untranslated Region. *Journal of Virology*, *89*(22), 11603–18.

Chellappan, P., Vanitharani, R., & Fauquet, C. M. (2005). MicroRNA-binding viral protein interferes with Arabidopsis development. *Proceedings of the National Academy of Sciences of the United States of America*, *102*(29), 10381–6.

Chellappan, P., Vanitharani, R., Pita, J., & Fauquet, C. M. (2004). Short interfering RNA accumulation correlates with host recovery in DNA virus-infected hosts, and gene silencing targets specific viral sequences. *Journal of Virology*, *78*(14), 7465–77.

Chen, J., Li, W. X., Xie, D., Peng, J. R., & Ding, S. W. (2004). Viral virulence protein suppresses RNA silencing-mediated defense but upregulates the role of microrna in host gene expression. *The Plant Cell*, *16*(5), 1302–13.

Chiu, M.-H., Chen, I.-H., Baulcombe, D. C., & Tsai, C.-H. (2010). The silencing suppressor P25 of Potato virus X interacts with Argonaute1 and mediates its degradation through the proteasome pathway. *Molecular Plant Pathology*, *11*(5), 641–9.

Chung, B. Y.-W., Miller, W. A., Atkins, J. F., & Firth, A. E. (2008). An overlapping essential gene in the Potyviridae. *Proceedings of the National Academy of Sciences of the United States of America*, *105*(15), 5897–902.

Cipriani, G., Fuentes, S., Bello, V., Salazar, L. F., Ghislain, M., & Zhang, D. P. (2000). Transgene Expression of Rice Cysteine Proteinase Inhibitors for the Development of Resistance against Sweetpotato Feathery Mottle Virus. *CIP Program Report*, 267–271.

Clark, C. A., Ferrin, D. M., Smith, T. P., & Holmes, G. J. (2013). *Compendium of Sweetpotato Diseases, Pests, and Disorders, Second Edition*. American Phytopathological Society.

Clark, C., Davis, J., Abad, J., Mukasa, S., Cuellar, W. J., Fuentes, S., … Kingdom, U. (2012). Recent Progress in Virus Characterization. *Plant Disease*, *96*(2), 168–185.

Cohen, J., & Loebenstein, G. (1991). Role of a whitefly-transmitted agent in infection of sweetpotato by cucumber mosaic virus. *Plant Disease*, *75*, 291–292.

Colinet, D., Kummert, J., & Lepoivre, P. (1996). Molecular evidence that the whitefly-transmitted sweetpotato mild mottle virus belongs to a distinct genus of the Potyviridae. *Archives of Virology*, *141*(1), 125–35.

Creamer, K. M., & Partridge, J. F. (2011). RITS-connecting transcription, RNA interference, and heterochromatin assembly in fission yeast. *Wiley Interdisciplinary Reviews. RNA*, *2*(5), 632–46.

Csorba, T., Bovi, A., Dalmay, T., & Burgyán, J. (2007). The p122 subunit of Tobacco Mosaic Virus replicase is a potent silencing suppressor and compromises both small interfering RNA- and microRNA-mediated pathways. *Journal of Virology*, *81*(21), 11768–80.

Csorba, T., Kontra, L., & Burgyán, J. (2015). viral silencing suppressors: Tools forged to fine-tune host-pathogen coexistence. *Virology*, *479-480*, 85–103.

Csorba, T., Lózsa, R., Hutvágner, G., & Burgyán, J. (2010). Polerovirus protein P0 prevents the assembly of small RNA-containing RISC complexes and leads to degradation of ARGONAUTE1. *The Plant Journal : For Cell and Molecular Biology*, *62*(3), 463–72.

Cuellar, W. J., De Souza, J., Barrantes, I., Fuentes, S., & Kreuze, J. F. (2011). Distinct cavemoviruses interact synergistically with sweet potato chlorotic stunt virus (genus Crinivirus) in cultivated sweet potato. *The Journal of General Virology*, *92*(Pt 5), 1233–43.

Cuellar, W. J., Galvez, M., Fuentes, S., Tugume, J., & Kreuze, J. (2015). Synergistic interactions of begomoviruses with Sweet potato chlorotic stunt virus (genus Crinivirus) in sweet potato (Ipomoea batatas L.). *Molecular Plant Pathology*, *16*(5), 459–71.

Cuellar, W. J., Kreuze, J. F., Rajamäki, M.-L., Cruzado, K. R., Untiveros, M., & Valkonen, J. P. T. (2009). Elimination of antiviral defense by viral RNase III. *Proceedings of the National Academy of Sciences of the United States of America*, *106*(25), 10354–10358.

Dalmay, T., Horsefield, R., Braunstein, T. H., & Baulcombe, D. C. (2001). SDE3 encodes an RNA helicase required for post-transcriptional gene silencing in Arabidopsis. *The EMBO Journal*, *20*(8), 2069–78.

De Souza, J., & Cuellar, W. J. (2011). Sequence analysis of the replicase gene of "sweet potato caulimo-like virus" suggests that this virus is a distinct member of the genus Cavemovirus. *Archives of Virology*, *156*(3), 535–7.

Deleris, A., Gallego-Bartolome, J., Bao, J., Kasschau, K. D., Carrington, J. C., & Voinnet, O. (2006). Hierarchical action and inhibition of plant Dicer-like proteins in antiviral defense. *Science (New York, N.Y.)*, *313*(5783), 68–71.

Delport, W., Poon, A. F. Y., Frost, S. D. W., & Kosakovsky Pond, S. L. (2010). Datamonkey 2010: a suite of phylogenetic analysis tools for evolutionary biology. *Bioinformatics (Oxford, England)*, *26*(19), 2455–7.

Derrien, B., Baumberger, N., Schepetilnikov, M., Viotti, C., De Cillia, J., Ziegler-Graff, V., … Genschik, P. (2012). Degradation of the antiviral component ARGONAUTE1 by the autophagy pathway. *Proceedings of the National Academy of Sciences of the United States of America*, *109*(39), 15942–6.

Diaz-Pendon, J. A., Li, F., Li, W.-X., & Ding, S.-W. (2007). Suppression of antiviral silencing by cucumber mosaic virus 2b protein in Arabidopsis is associated with drastically reduced accumulation of three classes of viral small interfering RNAs. *The Plant Cell*, *19*(6), 2053–63.

Dinman, J. D. (2012). Mechanisms and implications of programmed translational frameshifting. *Wiley Interdisciplinary Reviews. RNA*, *3*(5), 661–73.

Donaire, L., Barajas, D., Martínez-García, B., Martínez-Priego, L., Pagán, I., & Llave, C. (2008). Structural and genetic requirements for the biogenesis of tobacco rattle virus-derived small interfering RNAs. *Journal of Virology*, *82*(11), 5167–77.

Donaire, L., Wang, Y., Gonzalez-Ibeas, D., Mayer, K. F., Aranda, M. A., & Llave, C. (2009). Deep-sequencing of plant viral small RNAs reveals effective and widespread targeting of viral genomes. *Virology*, *392*(2), 203–14.

Dong, K., Wang, Y., Zhang, Z., Chai, L.-X., Tong, X., Xu, J., … Wang, X.-B. (2016). Two amino acids near the N-terminus of Cucumber mosaic virus 2b play critical roles in the suppression of RNA silencing and viral infectivity. *Molecular Plant Pathology*, *17*(2), 173–83.

Du, P., Wu, J., Zhang, J., Zhao, S., Zheng, H., Gao, G., … Li, Y. (2011) a. Viral infection induces expression of novel phased microRNAs from conserved cellular microRNA precursors. *PLoS Pathogens*, *7*(8), e1002176.

Du, Q.-S., Duan, C.-G., Zhang, Z.-H., Fang, Y.-Y., Fang, R.-X., Xie, Q., & Guo, H.-S. (2007). DCL4 targets Cucumber mosaic virus satellite RNA at novel secondary structures. *Journal of Virology*, *81*(17), 9142–51.

Du, Z., Chen, A., Chen, W., Liao, Q., Zhang, H., Bao, Y., … Carr, J. P. (2014) b. Nuclear-cytoplasmic partitioning of cucumber mosaic virus protein 2b determines the balance between its roles as a virulence determinant and an RNA-silencing suppressor. *Journal of Virology*, *88*(10), 5228–41.

Du, Z., Xiao, D., Wu, J., Jia, D., Yuan, Z., Liu, Y., … Xie, L. (2011). p2 of rice stripe virus (RSV) interacts with OsSGS3 and is a silencing suppressor. *Molecular Plant Pathology*, *12*(8), 808–14.

Duan, C.-G., Fang, Y.-Y., Zhou, B.-J., Zhao, J.-H., Hou, W.-N., Zhu, H., … Guo, H.-S. (2012). Suppression of Arabidopsis ARGONAUTE1-mediated slicing, transgene-induced RNA silencing, and DNA methylation by distinct domains of the Cucumber mosaic virus 2b protein. *The Plant Cell*, *24*(1), 259–74.

Dunham, J. P., Simmons, H. E., Holmes, E. C., & Stephenson, A. G. (2014). Analysis of viral (zucchini yellow mosaic virus) genetic diversity during systemic movement through a Cucurbita pepo vine. *Virus Research*, *191*, 172–9.

Ebhardt, H. A., Thi, E. P., Wang, M.-B., & Unrau, P. J. (2005). Extensive 3' modification of plant small RNAs is modulated by helper component-proteinase expression. *Proceedings of the National Academy of Sciences of the United States of America*, *102*(38), 13398–403.

El Sheikha, A. F., & Ray, R. C. (2015). Potential Impacts of Bio-processing of Sweet Potato: Review. *Critical Reviews in Food Science and Nutrition*.

El-Shami, M., Pontier, D., Lahmy, S., Braun, L., Picart, C., Vega, D., … Lagrange, T. (2007). Reiterated WG/GW motifs form functionally and evolutionarily conserved ARGONAUTE-binding platforms in RNAi-related components. *Genes & Development*, *21*(20), 2539–44.

Eskelin, K., Hafrén, A., Rantalainen, K. I., & Mäkinen, K. (2011). Potyviral VPg enhances viral RNA Translation and inhibits reporter mRNA translation in planta. *Journal of Virology*, *85*(17), 9210–21.

Eulalio, A., Tritschler, F., & Izaurralde, E. (2009). The GW182 protein family in animal cells: new insights into domains required for miRNA-mediated gene silencing. *RNA (New York, N.Y.)*, *15*(8), 1433–42.

Firth, A. E., & Brierley, I. (2012). Non-canonical translation in RNA viruses. *The Journal of General Virology*, *93*(Pt 7), 1385–409.

Fukunaga, R., & Doudna, J. A. (2009). dsRNA with 5' overhangs contributes to endogenous and antiviral RNA silencing pathways in plants. *The EMBO Journal*, *28*(5), 545–55.

Fusaro, A. F., Correa, R. L., Nakasugi, K., Jackson, C., Kawchuk, L., Vaslin, M. F. S., & Waterhouse, P. M. (2012). The Enamovirus P0 protein is a silencing suppressor which inhibits local and systemic RNA silencing through AGO1 degradation. *Virology*, *426*(2), 178–87.

Fusaro, A. F., Matthew, L., Smith, N. A., Curtin, S. J., Dedic-Hagan, J., Ellacott, G. A., … Waterhouse, P. M. (2006). RNA interference-inducing hairpin RNAs in plants act through the viral defence pathway. *EMBO Reports*, *7*(11), 1168–75.

Gabrenaite-Verkhovskaya, R., Andreev, I. A., Kalinina, N. O., Torrance, L., Taliansky, M. E., & Mäkinen, K. (2008). Cylindrical inclusion protein of potato virus A is associated with a subpopulation of particles isolated from infected plants. *The Journal of General Virology*, *89*(Pt 3), 829–38.

Garcia-Ruiz, H., Carbonell, A., Hoyer, J. S., Fahlgren, N., Gilbert, K. B., Takeda, A., … Carrington, J. C. (2015). Roles and programming of Arabidopsis ARGONAUTE proteins during Turnip mosaic virus infection. *PLoS Pathogens*, *11*(3), e1004755.

Garcia-Ruiz, H., Takeda, A., Chapman, E. J., Sullivan, C. M., Fahlgren, N., Brempelis, K. J., & Carrington, J. C. (2010). Arabidopsis RNA-dependent RNA polymerases and dicer-like proteins in antiviral defense and small interfering RNA biogenesis during Turnip Mosaic Virus infection. *The Plant Cell*, *22*(2), 481–96.

Garcia, D., Garcia, S., & Voinnet, O. (2014). Nonsense-mediated decay serves as a general viral restriction mechanism in plants. *Cell Host & Microbe*, *16*(3), 391–402.

Gazzani, S., Lawrenson, T., Woodward, C., Headon, D., & Sablowski, R. (2004). A link between mRNA turnover and RNA interference in Arabidopsis. *Science (New York, N.Y.)*, *306*(5698), 1046–8.

Ghoshal, B., & Sanfaçon, H. (2014). Temperature-dependent symptom recovery in Nicotiana benthamiana plants infected with tomato ringspot virus is associated with reduced translation of viral RNA2 and requires ARGONAUTE 1. *Virology*, *456-457*, 188–97.

Gibson, R. W., & Kreuze, J. F. (2014). Degeneration in sweetpotato due to viruses, virus-cleaned planting material and reversion: A review. *Plant Pathology*, 1–15.

Gibson, R. W., Mpembe, I., Alicai, T., Carey, E. E., Mwanga, R. O. M., Seal, S. E., & Vetten, H. J. (1998). Symptoms, aetiology and serological analysis of sweet potato virus disease in Uganda. *Plant Pathology*, *47*(1), 95–102.

Giedroc, D. P., & Cornish, P. V. (2009). Frameshifting RNA pseudoknots: Structure and mechanism. *Virus Research*, *139*(2), 193–208.

Giner, A., Lakatos, L., García-Chapa, M., López-Moya, J. J., & Burgyán, J. (2010). Viral protein inhibits RISC activity by argonaute binding through conserved WG/GW motifs. *PLoS Pathogens*, *6*(7), e1000996.

Glick, E., Zrachya, A., Levy, Y., Mett, A., Gidoni, D., Belausov, E., … Gafni, Y. (2008). Interaction with host SGS3 is required for suppression of RNA silencing by tomato yellow leaf curl virus V2 protein. *Proceedings of the National Academy of Sciences of the United States of America*, *105*(1), 157–61.

Gómez de Cedrón, M., Osaba, L., López, L., & García, J. A. (2006). Genetic analysis of the function of the plum pox virus CI RNA helicase in virus movement. *Virus Research*, *116*(1-2), 136–45.

González-Jara, P., Atencio, F. A., Martínez-García, B., Barajas, D., Tenllado, F., & Díaz-Ruíz, J. R. (2005). A Single Amino Acid Mutation in the Plum pox virus Helper Component-Proteinase Gene Abolishes Both Synergistic and RNA Silencing Suppression Activities. *Phytopathology*, *95*(8), 894–901.

Goto, K., Kobori, T., Kosaka, Y., Natsuaki, T., & Masuta, C. (2007). Characterization of silencing suppressor 2b of cucumber mosaic virus based on examination of its small RNA-binding abilities. *Plant & Cell Physiology*, *48*(7), 1050–60.

Guo, H., Song, X., Xie, C., Huo, Y., Zhang, F., Chen, X., … Fang, R. (2013). Rice yellow stunt rhabdovirus protein 6 suppresses systemic RNA silencing by blocking RDR6-mediated secondary siRNA synthesis. *Molecular Plant-Microbe Interactions : MPMI*, *26*(8), 927–36.

Gutiérrez, D. L., Fuentes, S., & Salazar, L. F. (2007). Sweetpotato Virus Disease (SPVD): Distribution, Incidence, and Effect on Sweetpotato Yield in Peru.

Haas, G., Azevedo, J., Moissiard, G., Geldreich, A., Himber, C., Bureau, M., … Voinnet, O. (2008). Nuclear import of CaMV P6 is required for infection and suppression of the RNA silencing factor DRB4. *The EMBO Journal*, *27*(15), 2102–12.

Hagiwara-Komoda, Y., Choi, S., Sato, M., Atsumi, G., Abe, J., Fukuda, J., … Naito, S. (2016). Truncated yet functional viral protein produced via RNA polymerase slippage implies underestimated coding capacity of RNA viruses. - PubMed - NCBI. *Scientific Reports*, *6*.

Hamera, S., Song, X., Su, L., Chen, X., & Fang, R. (2012). Cucumber mosaic virus suppressor 2b binds to AGO4-related small RNAs and impairs AGO4 activities. *The Plant Journal : For Cell and Molecular Biology*, *69*(1), 104–15.

Hamilton, A. J., & Baulcombe, D. C. (1999). A species of small antisense RNA in posttranscriptional gene silencing in plants. *Science (New York, N.Y.)*, *286*(5441), 950–2.

HannonLab. (2014). FASTX toolkit. Cold Spring Harbor Laboratory, Cold Spring Harbor, NY.

Harvey, J. J. W., Lewsey, M. G., Patel, K., Westwood, J., Heimstädt, S., Carr, J. P., & Baulcombe, D. C. (2011). An antiviral defense role of AGO2 in plants. *PloS One*, *6*(1), e14639.

Hausmann, S., Garcin, D., Morel, A. S., & Kolakofsky, D. (1999). Two nucleotides immediately upstream of the essential A6G3 slippery sequence modulate the pattern of G insertions during Sendai virus mRNA editing. *Journal of Virology*, *73*(1), 343–51.

Hemmes, H., Lakatos, L., Goldbach, R., Burgyán, J., & Prins, M. (2007). The NS3 protein of Rice hoja blanca tenuivirus suppresses RNA silencing in plant and insect hosts by efficiently binding both siRNAs and miRNAs. *RNA (New York, N.Y.)*, *13*(7), 1079–89.

Hong, Y., & Hunt, A. G. (1996). RNA polymerase activity catalyzed by a potyvirus-encoded RNA-dependent RNA polymerase. *Virology*, *226*(1), 146–51.

Ivanov, K. I., Eskelin, K., Bašić, M., De, S., Lõhmus, A., Varjosalo, M., & Mäkinen, K. (2016). Molecular insights into the function of the viral RNA silencing suppressor HCPro. *The Plant Journal*, *85*(1), 30–45.

Ivanov, K. I., Eskelin, K., Lõhmus, A., & Mäkinen, K. (2014). Molecular and cellular mechanisms underlying potyvirus infection. *The Journal of General Virology*, *95*(Pt 7), 1415–29.

Jacks, T., Power, M. D., Masiarz, F. R., Luciw, P. A., Barr, P. J., & Varmus, H. E. (1988). Characterization of ribosomal frameshifting in HIV-1 gag-pol expression. *Nature*, *331*(6153), 280–3.

Jagger, B. W., Wise, H. M., Kash, J. C., Walters, K.-A., Wills, N. M., Xiao, Y.-L., … Digard, P. (2012). An overlapping protein-coding region in influenza A virus segment 3 modulates the host response. *Science (New York, N.Y.)*, *337*(6091), 199–204.

Jamous, R. M., Boonrod, K., Fuellgrabe, M. W., Ali-Shtayeh, M. S., Krczal, G., & Wassenegger, M. (2011). The helper component-proteinase of the Zucchini yellow mosaic virus inhibits the Hua Enhancer 1 methyltransferase activity in vitro. *The Journal of General Virology*, *92*(Pt 9), 2222–6.

Karran, R. A., & Sanfaçon, H. (2014). Tomato ringspot virus coat protein binds to ARGONAUTE 1 and suppresses the translation repression of a reporter gene. *Molecular Plant-Microbe Interactions : MPMI*, *27*(9), 933–43.

Karyeija, R. F., Gibson, R. W., & Valkonen, J. P. T. (1998). The Significance of Sweet Potato Feathery Mottle Virus in Subsistence Sweet Potato Production in Africa. *Plant Disease*, *82*(1), 4–15.

Karyeija, R. F., Kreuze, J. F., Gibson, R. W., & Valkonen, J. P. (2000). Synergistic interactions of a potyvirus and a phloem-limited crinivirus in sweet potato plants. *Virology*, *269*(1), 26–36.

Kassanis, B., & Govier, D. A. (1971). The Role of the Helper Virus in Aphid Transmission of Potato Aucuba Mosaic Virus and Potato Virus C. *Journal of General Virology*, *13*(2), 221–228.

Kasschau, K. D., & Carrington, J. C. (1998). A counterdefensive strategy of plant viruses: suppression of posttranscriptional gene silencing. *Cell*, *95*(4), 461–70.

Kokkinos, C. D., & Clark, C. A. (2006). Interactions Among Sweet potato chlorotic stunt virus and Different Potyviruses and Potyvirus Strains Infecting Sweetpotato in the United States. *Plant Disease*, *90*(10), 1347–1352.

Kolakofsky, D., Roux, L., Garcin, D., & Ruigrok, R. W. H. (2005). Paramyxovirus mRNA editing, the "rule of six" and error catastrophe: a hypothesis. *The Journal of General Virology*, *86*(Pt 7), 1869–77.

Kosakovsky Pond, S. L., Posada, D., Gravenor, M. B., Woelk, C. H., & Frost, S. D. W. (2006). GARD: a genetic algorithm for recombination detection. *Bioinformatics (Oxford, England)*, *22*(24), 3096–8.

Kreuze, J. F., Karyeija, R. F., Gibson, R. W., & Valkonen, J. P. (2000). Comparisons of coat protein gene sequences show that East African isolates of Sweet potato feathery mottle virus form a genetically distinct group. *Archives of Virology*, *145*(3), 567–74.

Kreuze, J. F., Klein, I. S., Lazaro, M. U., Chuquiyuri, W. J. C., Morgan, G. L., Mejía, P. G. C., … Valkonen, J. P. T. (2008). RNA silencing-mediated resistance to a crinivirus (Closteroviridae) in cultivated sweet potato (Ipomoea batatas L.) and development of sweet potato virus disease following co-infection with a potyvirus. *Molecular Plant Pathology*, *9*(5), 589–98.

Kreuze, J. F., Perez, A., Untiveros, M., Quispe, D., Fuentes, S., Barker, I., & Simon, R. (2009). Complete viral genome sequence and discovery of novel viruses by deep sequencing of small RNAs: a generic method for diagnosis, discovery and sequencing of viruses. *Virology*, *388*(1), 1–7.

Kreuze, J. F., Savenkov, E. I., Cuellar, W., Li, X., & Valkonen, J. P. T. (2005). Viral class 1 RNase III involved in suppression of RNA silencing. *Journal of Virology*, *79*(11), 7227–38.

Kreuze, J. F., Savenkov, E. I., & Valkonen, J. P. T. (2002). Complete genome sequence and analyses of the subgenomic RNAs of sweet potato chlorotic stunt virus reveal several new features for the genus Crinivirus. *Journal of Virology*, *76*(18), 9260–70.

Kulkarni, S., Volchkova, V., Basler, C. F., Palese, P., Volchkov, V. E., & Shaw, M. L. (2009). Nipah virus edits its P gene at high frequency to express the V and W proteins. *Journal of Virology*, *83*(8), 3982–7.

Kumakura, N., Takeda, A., Fujioka, Y., Motose, H., Takano, R., & Watanabe, Y. (2009). SGS3 and RDR6 interact and colocalize in cytoplasmic SGS3/RDR6-bodies. *FEBS Letters*, *583*(8), 1261–6.

Kurihara, Y., Inaba, N., Kutsuna, N., Takeda, A., Tagami, Y., & Watanabe, Y. (2007). Binding of tobamovirus replication protein with small RNA duplexes. *The Journal of General Virology*, *88*(Pt 8), 2347–52.

Kyndt, T., Quispe, D., Zhai, H., Jarret, R., Ghislain, M., Liu, Q., … Kreuze, J. F. (2015). The genome of cultivated sweet potato contains Agrobacterium T-DNAs with expressed genes: An example of a naturally transgenic food crop. *Proceedings of the National Academy of Sciences*, *112*(18), 201419685.

Lacomme, C., Hrubikova, K., & Hein, I. (2003). Enhancement of virus-induced gene silencing through viral-based production of inverted-repeats. *The Plant Journal : For Cell and Molecular Biology*, *34*(4), 543–53.

Laín, S., Martín, M. T., Riechmann, J. L., & García, J. A. (1991). Novel catalytic activity associated with positive-strand RNA virus infection: nucleic acid-stimulated ATPase activity of the plum pox potyvirus helicaselike protein. *Journal of Virology*, *65*(1), 1–6.

Laín, S., Riechmann, J. L., & García, J. A. (1990). RNA helicase: a novel activity associated with a protein encoded by a positive strand RNA virus. *Nucleic Acids Research*, *18*(23), 7003–6.

Lakatos, L., Csorba, T., Pantaleo, V., Chapman, E. J., Carrington, J. C., Liu, Y.-P., … Burgyán, J. (2006). Small RNA binding is a common strategy to suppress RNA silencing by several viral suppressors. *The EMBO Journal*, *25*(12), 2768–80.

Landeo-Ríos, Y., Navas-Castillo, J., Moriones, E., & Cañizares, M. C. (2016). The p22 RNA silencing suppressor of the crinivirus Tomato chlorosis virus preferentially binds long dsRNAs preventing them from cleavage. *Virology*, *488*, 129–136.

Langmead, B., & Salzberg, S. L. (2012). Fast gapped-read alignment with Bowtie 2. *Nature Methods*, *9*(4), 357–9.

Laurie, S., Faber, M., Adebola, P., & Belete, A. (2015). Biofortification of sweet potato for food and nutrition security in South Africa. *Food Research International*, *76*, 962–970.

Le Gall, O., Christian, P., Fauquet, C. M., King, A. M. Q., Knowles, N. J., Nakashima, N., … Gorbalenya, A. E. (2008). Picornavirales, a proposed order of positive-sense single-stranded RNA viruses with a pseudo-T = 3 virion architecture. *Archives of Virology*, *153*(4), 715–27.

Leckie, B. M., & Neal Stewart, C. (2011). Agroinfiltration as a technique for rapid assays for evaluating candidate insect resistance transgenes in plants. *Plant Cell Reports*, *30*(3), 325–34.

Lee, W.-S., Fu, S.-F., Li, Z., Murphy, A. M., Dobson, E. A., Garland, L., … Carr, J. P. (2016). Salicylic acid treatment and expression of an RNA-dependent RNA polymerase 1 transgene inhibit lethal symptoms and meristem invasion during tobacco mosaic virus infection in Nicotiana benthamiana. *BMC Plant Biology*, *16*(1), 15.

Li, F., Xu, D., Abad, J., & Li, R. (2012). Phylogenetic relationships of closely related potyviruses infecting sweet potato determined by genomic characterization of Sweet potato virus G and Sweet potato virus 2. *Virus Genes*, *45*(1), 118–25.

Li, H., Li, W. X., & Ding, S. W. (2002). Induction and suppression of RNA silencing by an animal virus. *Science (New York, N.Y.)*, *296*(5571), 1319–21.

Li, W., Hilf, M. E., Webb, S. E., Baker, C. A., & Adkins, S. (2008). Presence of P1b and absence of HC-Pro in Squash vein yellowing virus suggests a general feature of the genus Ipomovirus in the family Potyviridae. *Virus Research*, *135*(2), 213–9.

Li, Y., Lu, J., Han, Y., Fan, X., & Ding, S.-W. (2013). RNA interference functions as an antiviral immunity mechanism in mammals. *Science (New York, N.Y.)*, *342*(6155), 231–4.

Liao, C.-H., Chien, I.-C., Chung, M.-L., Chiu, R.-J., & Han, Y.-H. (1979). A study of sweet potato virus disease in Taiwan I. Sweet potato yellow spot virus disease. *Journal of Agricultural Research of China*, *28*(3), 127–137.

Loebenstein, G., & Thottappilly, G. (2009). *The Sweetpotato*. *Springer Sciences Business Media BV, Dordrecht, The Netherlands.*

López-Moya, J. J., Wang, R. Y., & Pirone, T. P. (1999). Context of the coat protein DAG motif affects potyvirus transmissibility by aphids. *The Journal of General Virology*, *80 (Pt 12*, 3281–8.

Lotrakul, P., Valverde, R. A., Clark, C. A., Hurtt, S., & Hoy, M. W. (2002). Sweetpotato leaf curl virus and related geminiviruses in sweetpotato. *Acta Horticulturae*.

Love, A. J., Laird, J., Holt, J., Hamilton, A. J., Sadanandom, A., & Milner, J. J. (2007). Cauliflower mosaic virus protein P6 is a suppressor of RNA silencing. *The Journal of General Virology*, *88*(Pt 12), 3439–44.

Lozano, G., Trenado, H. P., Valverde, R. A., & Navas-Castillo, J. (2009). Novel begomovirus species of recombinant nature in sweet potato (Ipomoea batatas) and Ipomoea indica: taxonomic and phylogenetic implications. *The Journal of General Virology*, *90*(Pt 10), 2550–62.

Lózsa, R., Csorba, T., Lakatos, L., & Burgyán, J. (2008). Inhibition of 3' modification of small RNAs in virus-infected plants require spatial and temporal co-expression of small RNAs and viral silencing-suppressor proteins. *Nucleic Acids Research*, *36*(12), 4099–107.

Lu, R., Maduro, M., Li, F., Li, H. W., Broitman-Maduro, G., Li, W. X., & Ding, S. W. (2005). Animal virus replication and RNAi-mediated antiviral silencing in Caenorhabditis elegans. *Nature*, *436*(7053), 1040–3.

Luo, H., Wylie, S. J., & Jones, M. G. K. (2010). Identification of plant viruses using one-dimensional gel electrophoresis and peptide mass fingerprints. *Journal of Virological Methods*, *165*(2), 297–301.

Luo, Z., & Chen, Z. (2007). Improperly terminated, unpolyadenylated mRNA of sense transgenes is targeted by RDR6-mediated RNA silencing in Arabidopsis. *The Plant Cell*, *19*(3), 943–58.

Ma, X., Nicole, M.-C., Meteignier, L.-V., Hong, N., Wang, G., & Moffett, P. (2015). Different roles for RNA silencing and RNA processing components in virus recovery and virus-induced gene silencing in plants. *Journal of Experimental Botany*, *66*(3), 919–32.

Maillard, P. V, Ciaudo, C., Marchais, A., Li, Y., Jay, F., Ding, S. W., & Voinnet, O. (2013). Antiviral RNA interference in mammalian cells. *Science (New York, N.Y.)*, *342*(6155), 235–8.

Mallory, A. C., & Vaucheret, H. (2009). ARGONAUTE 1 homeostasis invokes the coordinate action of the microRNA and siRNA pathways. *EMBO Reports*, *10*(5), 521–6.

Mann, K. S., Johnson, K. N., Carroll, B. J., & Dietzgen, R. G. (2016). Cytorhabdovirus P protein suppresses RISC-mediated cleavage and RNA silencing amplification in planta. *Virology*, *490*, 27–40.

Martin, D. P., Lemey, P., Lott, M., Moulton, V., Posada, D., & Lefeuvre, P. (2010). RDP3: a flexible and fast computer program for analyzing recombination. *Bioinformatics (Oxford, England)*, *26*(19), 2462–3.

Martin, D. P., Posada, D., Crandall, K. A., & Williamson, C. (2005). A modified bootscan algorithm for automated identification of recombinant sequences and recombination breakpoints. *AIDS Research and Human Retroviruses*, *21*(1), 98–102.

Martin, D., & Rybicki, E. (2000). RDP: detection of recombination amongst aligned sequences. *Bioinformatics (Oxford, England)*, *16*(6), 562–3.

Martínez de Alba, A. E., Elvira-Matelot, E., & Vaucheret, H. (2013). Gene silencing in plants: a diversity of pathways. *Biochimica et Biophysica Acta*, *1829*(12), 1300–8.

Martínez-Turiño, S., & Hernández, C. (2009). Inhibition of RNA silencing by the coat protein of Pelargonium flower break virus: distinctions from closely related suppressors. *The Journal of General Virology*, *90*(Pt 2), 519–25.

Martínez, F., & Daròs, J.-A. (2014). Tobacco etch virus protein P1 traffics to the nucleolus and associates with the host 60S ribosomal subunits during infection. *Journal of Virology*, *88*(18), 10725–37.

Mbanzibwa, D. R., Tian, Y., Mukasa, S. B., & Valkonen, J. P. T. (2009). Cassava brown streak virus (Potyviridae) encodes a putative Maf/HAM1 pyrophosphatase implicated in reduction of mutations and a P1 proteinase that suppresses RNA silencing but contains no HC-Pro. *Journal of Virology*, *83*(13), 6934–40.

Mehedi, M., Hoenen, T., Robertson, S., Ricklefs, S., Dolan, M. A., Taylor, T., … Feldmann, H. (2013). Ebola virus RNA editing depends on the primary editing site sequence and an upstream secondary structure. *PLoS Pathogens*, *9*(10), e1003677.

Mérai, Z., Kerényi, Z., Kertész, S., Magna, M., Lakatos, L., & Silhavy, D. (2006). Double-stranded RNA binding may be a general plant RNA viral strategy to suppress RNA silencing. *Journal of Virology*, *80*(12), 5747–56.

Mérai, Z., Kerényi, Z., Molnár, A., Barta, E., Válóczi, A., Bisztray, G., … Silhavy, D. (2005). Aureusvirus P14 is an efficient RNA silencing suppressor that binds double-stranded RNAs without size specificity. *Journal of Virology*, *79*(11), 7217–26.

Mi, S., Cai, T., Hu, Y., Chen, Y., Hodges, E., Ni, F., … Qi, Y. (2008). Sorting of small RNAs into Arabidopsis argonaute complexes is directed by the 5' terminal nucleotide. *Cell*, *133*(1), 116–27.

Mine, A., Hyodo, K., Takeda, A., Kaido, M., Mise, K., & Okuno, T. (2010). Interactions between p27 and p88 replicase proteins of Red clover necrotic mosaic virus play an essential role in viral RNA replication and suppression of RNA silencing via the 480-kDa viral replicase complex assembly. *Virology*, *407*(2), 213–24.

Miozzi, L., Gambino, G., Burgyan, J., & Pantaleo, V. (2013). Genome-wide identification of viral and host transcripts targeted by viral siRNAs in Vitis vinifera. *Molecular Plant Pathology*, *14*(1), 30–43.

Mlotshwa S, Pruss GJ, Peragine A, Endres MW, Li J, Chen X, Poethig RS, Bowman LH, V. V. (2008). DICER-LIKE2 plays a primary role in transitive silencing of transgenes in Arabidopsis. - PubMed - NCBI. *PloS One*, *3*(3).

Mohanraj, R., & Sivasankar, S. (2014). Sweet potato (Ipomoea batatas [L.] Lam) - A valuable medicinal food: A review. *J. Med. Food*, *17*(7), 733–741.

Moissiard, G., Parizotto, E. A., Himber, C., & Voinnet, O. (2007). Transitivity in Arabidopsis can be primed, requires the redundant action of the antiviral Dicer-like 4 and Dicer-like 2, and is compromised by viral-encoded suppressor proteins. *RNA (New York, N.Y.)*, *13*(8), 1268–78.

Molnár, A., Csorba, T., Lakatos, L., Várallyay, E., Lacomme, C., & Burgyán, J. (2005). Plant virus-derived small interfering RNAs originate predominantly from highly structured single-stranded viral RNAs. *Journal of Virology*, *79*(12), 7812–8.

Molodtsov, V., Anikin, M., & McAllister, W. T. (2014). The presence of an RNA:DNA hybrid that is prone to slippage promotes termination by T7 RNA polymerase. *Journal of Molecular Biology*, *426*(18), 3095–107.

Morel, J.-B., Godon, C., Mourrain, P., Béclin, C., Boutet, S., Feuerbach, F., … Vaucheret, H. (2002). Fertile hypomorphic ARGONAUTE (ago1) mutants impaired in post-transcriptional gene silencing and virus resistance. *The Plant Cell*, *14*(3), 629–39.

Moreno, A. B., Martínez de Alba, A. E., Bardou, F., Crespi, M. D., Vaucheret, H., Maizel, A., & Mallory, A. C. (2013). Cytoplasmic and nuclear quality control and turnover of single-stranded RNA modulate post-transcriptional gene silencing in plants. *Nucleic Acids Research*, *41*(8), 4699–708.

Mourrain, P., Béclin, C., Elmayan, T., Feuerbach, F., Godon, C., Morel, J. B., … Vaucheret, H. (2000). Arabidopsis SGS2 and SGS3 genes are required for posttranscriptional gene silencing and natural virus resistance. *Cell*, *101*(5), 533–42.

Mukasa, S. B., Rubaihayo, P. R., & Valkonen, J. P. T. (2006). Interactions between a crinivirus, an ipomovirus and a potyvirus in coinfected sweetpotato plants. *Plant Pathology*, *55*(3), 458–467.

Mwanga, R. O. M., Odongo, B., Turyamureeba, G., Alajo, A., Yencho, G. C., Gibson, R. W., … Carey, E. E. (2003). Release of six sweetpotato cultivars ('NASPOT 1' to "NASPOT 6") in Uganda. *HortScience: A Publication of the American Society for Horticultural Science*, *38*(3), 475–476.

Nakagawa, T., Suzuki, T., Murata, S., Nakamura, S., Hino, T., Maeo, K., … Ishiguro, S. (2007). Improved Gateway binary vectors: high-performance vectors for creation of fusion constructs in transgenic analysis of plants. *Bioscience, Biotechnology, and Biochemistry*, *71*(8), 2095–100.

Navarro, B., Gisel, A., Rodio, M. E., Delgado, S., Flores, R., & Di Serio, F. (2012). Small RNAs containing the pathogenic determinant of a chloroplast-replicating viroid guide the degradation of a host mRNA as predicted by RNA silencing. *The Plant Journal : For Cell and Molecular Biology*, *70*(6), 991–1003.

Okano, Y., Senshu, H., Hashimoto, M., Neriya, Y., Netsu, O., Minato, N., … Namba, S. (2014). In Planta Recognition of a Double-Stranded RNA Synthesis Protein Complex by a Potexviral RNA Silencing Suppressor. *The Plant Cell*, *26*(5), 2168–2183.

Olspert, A., Chung, B. Y.-W., Atkins, J. F., Carr, J. P., & Firth, A. E. (2015). Transcriptional slippage in the positive-sense RNA virus family Potyviridae. *EMBO Reports*, *16*(8), 995–1004.

Ozias-Akins, P., & Jarret, R. L. (1994). Nuclear DNA Content and Ploidy Levels in the Genus Ipomoea. *J. Amer. Soc. Hort. Sci.*, *119*(1), 110–115.

Parent, J.-S., Bouteiller, N., Elmayan, T., & Vaucheret, H. (2015). Respective contributions of Arabidopsis DCL2 and DCL4 to RNA silencing. *The Plant Journal : For Cell and Molecular Biology*, *81*(2), 223–32.

Pasin, F., Simón-Mateo, C., & García, J. A. (2014). The hypervariable amino-terminus of P1 protease modulates potyviral replication and host defense responses. *PLoS Pathogens*, *10*(3), e1003985.

Pazhouhandeh M, Dieterle M, Marrocco K, Lechner E, Berry B, Brault V, Hemmer O, Kretsch T, Richards KE, Genschik P, Z.-G. V. (2006). F-box-like domain in the polerovirus protein P0 is required for silencing suppressor function. - PubMed - NCBI. *PNAS*, *103*(6), 1994–1999.

Pérez-Cañamás, M., & Hernández, C. (2015). Key importance of small RNA binding for the activity of a glycine-tryptophan (GW) motif-containing viral suppressor of RNA silencing. *The Journal of Biological Chemistry*, *290*(5), 3106–20.

Pruss, G., Ge, X., Shi, X. M., Carrington, J. C., & Bowman Vance, V. (1997). Plant viral synergism: the potyviral genome encodes a broad-range pathogenicity enhancer that transactivates replication of heterologous viruses. *The Plant Cell*, *9*(6), 859–68.

Puustinen, P., & Mäkinen, K. (2004). Uridylylation of the potyvirus VPg by viral replicase NIb correlates with the nucleotide binding capacity of VPg. *The Journal of Biological Chemistry*, *279*(37), 38103–10.

Qin, Y., Zhang, Z., Qiao, Q., Zhang, D., Tian, Y., & Wang, Y. (2013). Molecular variability of sweet potato chlorotic stunt virus (SPCSV) and five potyviruses infecting sweet potato in China. *Archives of Virology*, *158*(2), 491–5.

Qu, F., Ren, T., & Morris, T. J. (2003). The coat protein of turnip crinkle virus suppresses posttranscriptional gene silencing at an early initiation step. *Journal of Virology*, *77*(1), 511–22.

Qu, F., Ye, X., Hou, G., Sato, S., Clemente, T. E., & Morris, T. J. (2005). RDR6 has a broad-spectrum but temperature-dependent antiviral defense role in Nicotiana benthamiana. *Journal of Virology*, *79*(24), 15209–17.

Qu, F., Ye, X., & Morris, T. J. (2008). Arabidopsis DRB4, AGO1, AGO7, and RDR6 participate in a DCL4-initiated antiviral RNA silencing pathway negatively regulated by DCL1. *Proceedings of the National Academy of Sciences of the United States of America*, *105*(38), 14732–7.

Raja, P., Jackel, J. N., Li, S., Heard, I. M., & Bisaro, D. M. (2014). Arabidopsis double-stranded RNA binding protein DRB3 participates in methylation-mediated defense against geminiviruses. *Journal of Virology*, *88*(5), 2611–22.

Raja, P., Sanville, B. C., Buchmann, R. C., & Bisaro, D. M. (2008). Viral genome methylation as an epigenetic defense against geminiviruses. *Journal of Virology*, *82*(18), 8997–9007.

Raja, P., Wolf, J. N., & Bisaro, D. M. (2010). RNA silencing directed against geminiviruses: post-transcriptional and epigenetic components. *Biochimica et Biophysica Acta*, *1799*(3-4), 337–51.

Rajamäki, M.-L., Streng, J., & Valkonen, J. P. T. (2014). Silencing suppressor protein VPg of a potyvirus interacts with the plant silencing-related protein SGS3. *Molecular Plant-Microbe Interactions : MPMI*, *27*(11), 1199–210.

Rajamäki, M.-L., & Valkonen, J. P. T. (2009). Control of nuclear and nucleolar localization of nuclear inclusion protein a of picorna-like Potato virus A in Nicotiana species. *The Plant Cell*, *21*(8), 2485–502.

Ratinier, M., Boulant, S., Combet, C., Targett-Adams, P., McLauchlan, J., & Lavergne, J.-P. (2008). Transcriptional slippage prompts recoding in alternate reading frames in the hepatitis C virus (HCV) core sequence from strain HCV-1. *The Journal of General Virology*, *89*(Pt 7), 1569–78.

Ren, B., Guo, Y., Gao, F., Zhou, P., Wu, F., Meng, Z., … Li, Y. (2010). Multiple functions of Rice dwarf phytoreovirus Pns10 in suppressing systemic RNA silencing. *Journal of Virology*, *84*(24), 12914–23.

Revers, F., & García, J. A. (2015). Molecular biology of potyviruses. *Advances in Virus Research*, *92*, 101–99.

Rhoades, M. W., Reinhart, B. J., Lim, L. P., Burge, C. B., Bartel, B., & Bartel, D. P. (2002). Prediction of plant microRNA targets. *Cell*, *110*(4), 513–20.

Riechmann, J. L., Laín, S., & García, J. A. (1992). Highlights and prospects of potyvirus molecular biology. *The Journal of General Virology*, *73 (Pt 1)*, 1–16.

Rodamilans, B., San León, D., Mühlberger, L., Candresse, T., Neumüller, M., Oliveros, J. C., & García, J. A. (2014). Transcriptomic analysis of Prunus domestica undergoing hypersensitive response to plum pox virus infection. *PloS One*, *9*(6), e100477.

Rodamilans, B., Valli, A., & García, J. A. (2013). Mechanistic divergence between P1 proteases of the family Potyviridae. *The Journal of General Virology*, *94*(Pt 6), 1407–14.

Rodríguez-Negrete, E. A., Carrillo-Tripp, J., & Rivera-Bustamante, R. F. (2009). RNA silencing against geminivirus: complementary action of posttranscriptional gene silencing and transcriptional gene silencing in host recovery. *Journal of Virology*, *83*(3), 1332–40.

Rojas, M. R., Zerbini, F. M., Allison, R. F., Gilbertson, R. L., & Lucas, W. J. (1997). Capsid protein and helper component-proteinase function as potyvirus cell-to-cell movement proteins. *Virology*, *237*(2), 283–95.

Roullier, C., Duputié, A., Wennekes, P., Benoit, L., Fernández Bringas, V. M., Rossel, G., … Lebot, V. (2013). Disentangling the origins of cultivated sweet potato (Ipomoea batatas (L.) Lam.). *PloS One*, *8*(5), e62707.

Ruiz-Ferrer, V., & Voinnet, O. (2009). Roles of plant small RNAs in biotic stress responses. *Annual Review of Plant Biology*, *60*, 485–510.

Ruiz, M., Voinnet, O., & Baulcombe, D. (1998). Initiation and maintenance of virus-induced gene silencing. *The Plant Cell*, *10*(6), 937–46.

Sabath, N., Wagner, A., & Karlin, D. (2012). Evolution of viral proteins originated de novo by overprinting. - PubMed - NCBI. *Molecular Biology and Evolution*, *29*(12), 3767–3780.

Sahana, N., Kaur, H., Jain, R. K., Palukaitis, P., Canto, T., & Praveen, S. (2014). The asparagine residue in the FRNK box of potyviral helper-component protease is critical for its small RNA binding and subcellular localization. *The Journal of General Virology*, *95*(Pt 5), 1167–77.

Sakai, J., Mori, M., Morishita, T., Tanaka, M., Hanada, K., Usugi, T., & Nishiguchi, M. (1997). Complete nucleotide sequence and genome organization of sweet potato feathery mottle virus (S strain) genomic RNA: the large coding region of the P1 gene. *Archives of Virology*, *142*(8), 1553–62.

Schaad, M. C., Lellis, A. D., & Carrington, J. C. (1997). VPg of tobacco etch potyvirus is a host genotype-specific determinant for long-distance movement. *Journal of Virology*, *71*(11), 8624–31.

Scholthof, H. B., Alvarado, V. Y., Vega-Arreguin, J. C., Ciomperlik, J., Odokonyero, D., Brosseau, C., … Moffett, P. (2011). Identification of an ARGONAUTE for antiviral RNA silencing in Nicotiana benthamiana. *Plant Physiology*, *156*(3), 1548–55.

Schuck, J., Gursinsky, T., Pantaleo, V., Burgyán, J., & Behrens, S.-E. (2013). AGO/RISC-mediated antiviral RNA silencing in a plant in vitro system. *Nucleic Acids Research*, *41*(9), 5090–103.

Schwach, F., Vaistij, F. E., Jones, L., & Baulcombe, D. C. (2005). An RNA-dependent RNA polymerase prevents meristem invasion by potato virus X and is required for the activity but not the production of a systemic silencing signal. *Plant Physiology*, *138*(4), 1842–52.

Schwarz, D. S., Hutvágner, G., Du, T., Xu, Z., Aronin, N., & Zamore, P. D. (2003). Asymmetry in the assembly of the RNAi enzyme complex. *Cell*, *115*(2), 199–208.

Segers, G. C., Zhang, X., Deng, F., Sun, Q., & Nuss, D. L. (2007). Evidence that RNA silencing functions as an antiviral defense mechanism in fungi. *Proceedings of the National Academy of Sciences of the United States of America*, *104*(31), 12902–6.

Shabman, R. S., Jabado, O. J., Mire, C. E., Stockwell, T. B., Edwards, M., Mahajan, M., … Basler, F. (2014). Deep Sequencing Identifies Noncanonical Editing of Ebola and Marburg Virus RNAs in Infected Cells, *5*(6), 1–11.

Shamandi, N., Zytnicki, M., Charbonnel, C., Elvira-Matelot, E., Bochnakian, A., Comella, P., … Vaucheret, H. (2015). Plants Encode a General siRNA Suppressor That Is Induced and Suppressed by Viruses. *PLOS Biology*, *13*(12), e1002326.

Sheffield, F. (1957). Virus diseases of sweet potato in East-Africa - Identification of the viruses and their insect vectors. *Phytopathology*, *47*, 582–590.

Shiboleth, Y. M., Haronsky, E., Leibman, D., Arazi, T., Wassenegger, M., Whitham, S. A., … Gal-On, A. (2007). The conserved FRNK box in HC-Pro, a plant viral suppressor of gene silencing, is required for small RNA binding and mediates symptom development. *Journal of Virology*, *81*(23), 13135–48.

Shimura, H., Pantaleo, V., Ishihara, T., Myojo, N., Inaba, J., Sueda, K., … Masuta, C. (2011). A viral satellite RNA induces yellow symptoms on tobacco by targeting a gene involved in chlorophyll biosynthesis using the RNA silencing machinery. *PLoS Pathogens*, *7*(5), e1002021.

Shivaprasad, P. V, Rajeswaran, R., Blevins, T., Schoelz, J., Meins, F., Hohn, T., & Pooggin, M. M. (2008). The CaMV transactivator/viroplasmin interferes with RDR6-dependent trans-acting and secondary siRNA pathways in Arabidopsis. *Nucleic Acids Research*, *36*(18), 5896–909.

Silhavy, D., Molnár, A., Lucioli, A., Szittya, G., Hornyik, C., Tavazza, M., & Burgyán, J. (2002). A viral protein suppresses RNA silencing and binds silencing-generated, 21- to 25-nucleotide double-stranded RNAs. *The EMBO Journal*, *21*(12), 3070–80.

Smith, J. M. (1992). Analyzing the mosaic structure of genes. *Journal of Molecular Evolution*, *34*(2), 126–9.

Smith, N. A., Eamens, A. L., & Wang, M.-B. (2011). Viral small interfering RNAs target host genes to mediate disease symptoms in plants. *PLoS Pathogens*, *7*(5), e1002022.

Srisuwan, S., Sihachakr, D., & Siljak-Yakovlev, S. (2006). The origin and evolution of sweet potato (Ipomoea batatas Lam.) and its wild relatives through the cytogenetic approaches. *Plant Science : An International Journal of Experimental Plant Biology*, *171*(3), 424–33.

Stubbs, L. L., & McLean, D. L. (1958). A note on aphid transmission of a feathery mottle virus of sweetpotato. *Plant Disease Reports*, *42*, 216.

Susaimuthu, J., Tzanetakis, I. E., Gergerich, R. C., & Martin, R. R. (2008). A member of a new genus in the Potyviridae infects Rubus. *Virus Research*, *131*(2), 145–51.

Syller, J. (2012). Facilitative and antagonistic interactions between plant viruses in mixed infections. *Molecular Plant Pathology*, *13*(2), 204–16.

Syller, J., & Grupa, A. (2015). Antagonistic within-host interactions between plant viruses: molecular basis and impact on viral and host fitness. *Molecular Plant Pathology*.

Szabó, E. Z., Manczinger, M., Göblös, A., Kemény, L., & Lakatos, L. (2012). Switching on RNA silencing suppressor activity by restoring argonaute binding to a viral protein. *Journal of Virology*, *86*(15), 8324–7.

Szittya, G., Moxon, S., Pantaleo, V., Toth, G., Rusholme Pilcher, R. L., Moulton, V., … Dalmay, T. (2010). Structural and functional analysis of viral siRNAs. *PLoS Pathogens*, *6*(4), e1000838.

Takeda, A., Iwasaki, S., Watanabe, T., Utsumi, M., & Watanabe, Y. (2008). The mechanism selecting the guide strand from small RNA duplexes is different among argonaute proteins. *Plant & Cell Physiology*, *49*(4), 493–500.

Takeda, A., Sugiyama, K., Nagano, H., Mori, M., Kaido, M., Mise, K., … Okuno, T. (2002). Identification of a novel RNA silencing suppressor, NSs protein of Tomato spotted wilt virus. *FEBS Letters*, *532*(1-2), 75–9.

Takeda, A., Tsukuda, M., Mizumoto, H., Okamoto, K., Kaido, M., Mise, K., & Okuno, T. (2005). A plant RNA virus suppresses RNA silencing through viral RNA replication. *The EMBO Journal*, *24*(17), 3147–57.

Tamura, K., Stecher, G., Peterson, D., Filipski, A., & Kumar, S. (2013). MEGA6: Molecular Evolutionary Genetics Analysis version 6.0. *Molecular Biology and Evolution*, *30*(12), 2725–9.

Tanaka, Y., Nakamura, S., Kawamukai, M., Koizumi, N., & Nakagawa, T. (2011). Development of a series of gateway binary vectors possessing a tunicamycin resistance gene as a marker for the transformation of Arabidopsis thaliana. *Bioscience, Biotechnology, and Biochemistry*, *75*(4), 804–7.

Tatineni, S., Qu, F., Li, R., Morris, T. J., & French, R. (2012). Triticum mosaic poacevirus enlists P1 rather than HC-Pro to suppress RNA silencing-mediated host defense. *Virology*, *433*(1), 104–15.

Tena Fernández, F., González, I., Doblas, P., Rodríguez, C., Sahana, N., Kaur, H., … Canto, T. (2013). The influence of cis-acting P1 protein and translational elements on the expression of Potato virus Y helper-component proteinase (HCPro) in heterologous systems and its suppression of silencing activity. *Molecular Plant Pathology*, *14*(5), 530–41.

Töpfer, A., Zagordi, O., Prabhakaran, S., Roth, V., Halperin, E., & Beerenwinkel, N. (2013). Probabilistic inference of viral quasispecies subject to recombination. *Journal of Computational Biology : A Journal of Computational Molecular Cell Biology*, *20*(2), 113–23.

Torrance, L., Andreev, I. A., Gabrenaite-Verhovskaya, R., Cowan, G., Mäkinen, K., & Taliansky, M. E. (2006). An unusual structure at one end of potato potyvirus particles. *Journal of Molecular Biology*, *357*(1), 1–8.

Torres-Barceló, C., Daròs, J.-A., & Elena, S. F. (2010). Compensatory molecular evolution of HC-Pro, an RNA-silencing suppressor from a plant RNA virus. *Molecular Biology and Evolution*, *27*(3), 543–51.

Torres-Barceló, C., Martín, S., Daròs, J.-A., & Elena, S. F. (2008). From hypo- to hypersuppression: effect of amino acid substitutions on the RNA-silencing suppressor activity of the Tobacco etch potyvirus HC-Pro. *Genetics*, *180*(2), 1039–49.

Tugume, A. K., Amayo, R., Weinheimer, I., Mukasa, S. B., Rubaihayo, P. R., & Valkonen, J. P. T. (2013). Genetic variability and evolutionary implications of RNA silencing suppressor genes in RNA1 of sweet potato chlorotic stunt virus isolates infecting sweetpotato and related wild species. *PloS One*, *8*(11), e81479.

Tugume, A. K., Cuéllar, W. J., Mukasa, S. B., & Valkonen, J. P. T. (2010). Molecular genetic analysis of virus isolates from wild and cultivated plants demonstrates that East Africa is a hotspot for the evolution and diversification of sweet potato feathery mottle virus. *Molecular Ecology*, *19*(15), 3139–56.

Tugume, A. K., Mukasa, S. B., & Valkonen, J. P. T. (2008). Natural Wild Hosts of Sweet potato feathery mottle virus Show Spatial Differences in Virus Incidence and Virus-Like Diseases in Uganda.

Untiveros, M., Fuentes, S., & Kreuze, J. (2008). Molecular variability of sweet potato feathery mottle virus and other potyviruses infecting sweet potato in Peru. *Archives of Virology*, *153*(3), 473–83.

Untiveros, M., Fuentes, S., & Salazar, L. F. (2007). Synergistic Interaction of Sweet potato chlorotic stunt virus (Crinivirus) with Carla-, Cucumo-, Ipomo-, and Potyviruses Infecting Sweet Potato. *Plant Disease*, *91*(6), 669–676.

Untiveros, M., Olspert, A., Artola, K., Firth, A. E., Kreuze, J. F., & Valkonen, J. P. T. (2016). A novel sweet potato potyvirus ORF is expressed via polymerase slippage and suppresses RNA silencing. *Molecular Plant Pathology*.

Untiveros, M., Quispe, D., & Kreuze, J. (2010). Analysis of complete genomic sequences of isolates of the Sweet potato feathery mottle virus strains C and EA: molecular evidence for two distinct potyvirus species and two P1 protein domains. *Archives of Virology*, *155*(12), 2059–63.

Valli, A., Dujovny, G., & García, J. A. (2008). Protease activity, self interaction, and small interfering RNA binding of the silencing suppressor p1b from cucumber vein yellowing ipomovirus. *Journal of Virology*, *82*(2), 974–86.

Valli, A., García, J. A., & López-Moya, J. J. (2015). Potyviridae. In *Encyclopedia of Life Sciences* (pp. 1–10). Chichester, UK: John Wiley & Sons, Ltd.

Valli, A., López-Moya, J. J., & García, J. A. (2007). Recombination and gene duplication in the evolutionary diversification of P1 proteins in the family Potyviridae. *The Journal of General Virology*, *88*(Pt 3), 1016–28.

Valli, A., López-Moya, J. J., & García, J. A. (2009). *RNA Silencing and its Suppressors in the Plant-virus Interplay*. *Encyclopedia of Life Sciences*.

Valli, A., Martín-Hernández, A. M., López-Moya, J. J., & García, J. A. (2006). RNA silencing suppression by a second copy of the P1 serine protease of Cucumber vein yellowing ipomovirus, a member of the family Potyviridae that lacks the cysteine protease HCPro. *Journal of Virology*, *80*(20), 10055–63.

Valli, A., Oliveros, J. C., Molnar, A., Baulcombe, D., & García, J. A. (2011). The specific binding to 21-nt double-stranded RNAs is crucial for the anti-silencing activity of Cucumber vein yellowing virus P1b and perturbs endogenous small RNA populations. *RNA (New York, N.Y.)*, *17*(6), 1148–58.

Várallyay, E., & Havelda, Z. (2013). Unrelated viral suppressors of RNA silencing mediate the control of ARGONAUTE1 level. *Molecular Plant Pathology*, *14*(6), 567–75.

Várallyay, E., Válóczi, A., Agyi, A., Burgyán, J., & Havelda, Z. (2010). Plant virus-mediated induction of miR168 is associated with repression of ARGONAUTE1 accumulation. *The EMBO Journal*, *29*(20), 3507–19.

Vargason, J. M., Burch, C. J., & Wilson, J. W. (2013). Identification and RNA binding characterization of plant virus RNA silencing suppressor proteins. *Methods (San Diego, Calif.)*, *64*(1), 88–93.

Vargason, J. M., Szittya, G., Burgyán, J., & Hall, T. M. T. (2003). Size selective recognition of siRNA by an RNA silencing suppressor. *Cell*, *115*(7), 799–811.

Vaucheret, H., Vazquez, F., Crété, P., & Bartel, D. P. (2004). The action of ARGONAUTE1 in the miRNA pathway and its regulation by the miRNA pathway are crucial for plant development. *Genes & Development*, *18*(10), 1187–97.

Vijayapalani, P., Maeshima, M., Nagasaki-Takekuchi, N., & Miller, W. A. (2012). Interaction of the trans-frame potyvirus protein P3N-PIPO with host protein PCaP1 facilitates potyvirus movement. *PLoS Pathogens*, *8*(4), e1002639.

Vogler, H., Akbergenov, R., Shivaprasad, P. V, Dang, V., Fasler, M., Kwon, M.-O., … Heinlein, M. (2007). Modification of small RNAs associated with suppression of RNA silencing by tobamovirus replicase protein. *Journal of Virology*, *81*(19), 10379–88.

Voinnet, O. (2008). Use, tolerance and avoidance of amplified RNA silencing by plants. *Trends in Plant Science*, *13*(7), 317–28.

Voinnet, O., & Baulcombe, D. C. (1997). Systemic signalling in gene silencing. *Nature*, *389*(6651), 553.

Voinnet, O., Lederer, C., & Baulcombe, D. C. (2000). A viral movement protein prevents spread of the gene silencing signal in Nicotiana benthamiana. *Cell*, *103*(1), 157–67.

Volchkov, V. E., Becker, S., Volchkova, V. A., Ternovoj, V. A., Kotov, A. N., Netesov, S. V, & Klenk, H. D. (1995). GP mRNA of Ebola virus is edited by the Ebola virus polymerase and by T7 and vaccinia virus polymerases. *Virology*, *214*(2), 421–30.

Voloudakis, A. E., Malpica, C. A., Aleman-Verdaguer, M.-E., Stark, D. M., Fauquet, C. M., & Beachy, R. N. (2004). Structural characterization of Tobacco etch virus coat protein mutants. *Archives of Virology*, *149*(4), 699–712.

Walkey, D. G., & Cooper, V. C. (1975). Effect of temperature on virus eradication and growth of infected tissue cultures. *The Annals of Applied Biology*, *80*(2), 185–90.

Wang, M., Abad, J., Fuentes, S., & Li, R. (2013). Complete genome sequence of the original Taiwanese isolate of sweet potato latent virus and its relationship to other potyviruses infecting sweet potato. *Archives of Virology*, *158*(10), 2189–92.

Wang, Q. C., Panis, B., Engelmann, F., Lambardi, M., & Valkonen, J. P. T. (2009). Cryotherapy of shoot tips: a technique for pathogen eradication to produce healthy planting materials and prepare healthy plant genetic resources for cryopreservation. *Annals of Applied Biology*, *154*, 351–363.

Wang, X.-B., Jovel, J., Udomporn, P., Wang, Y., Wu, Q., Li, W.-X., … Ding, S.-W. (2011). The 21-nucleotide, but not 22-nucleotide, viral secondary small interfering RNAs direct potent antiviral defense by two cooperative argonautes in Arabidopsis thaliana. *The Plant Cell*, *23*(4), 1625–38.

Wang, X.-B., Wu, Q., Ito, T., Cillo, F., Li, W.-X., Chen, X., … Ding, S.-W. (2010). RNAi-mediated viral immunity requires amplification of virus-derived siRNAs in Arabidopsis thaliana. *Proceedings of the National Academy of Sciences of the United States of America*, *107*(1), 484–9.

Wei, T., Zhang, C., Hong, J., Xiong, R., Kasschau, K. D., Zhou, X., … Wang, A. (2010). Formation of complexes at plasmodesmata for potyvirus intercellular movement is mediated by the viral protein P3N-PIPO. *PLoS Pathogens*, *6*(6), e1000962.

Weinheimer, I., Boonrod, K., Moser, M., Wassenegger, M., Krczal, G., Butcher, S. J., & Valkonen, J. P. T. (2014). Binding and processing of small dsRNA molecules by the class 1 RNase III protein encoded by sweet potato chlorotic stunt virus. *The Journal of General Virology*, *95*(Pt 2), 486–95.

Weinheimer, I., Jiu, Y., Rajamäki, M.-L., Matilainen, O., Kallijärvi, J., Cuellar, W. J., … Valkonen, J. P. T. (2015). Suppression of RNAi by dsRNA-degrading RNaseIII enzymes of viruses in animals and plants. *PLoS Pathogens*, *11*(3), e1004711.

Wen, R.-H., & Hajimorad, M. R. (2010). Mutational analysis of the putative pipo of soybean mosaic virus suggests disruption of PIPO protein impedes movement. *Virology*, *400*(1), 1–7.

Wilkins, C., Dishongh, R., Moore, S. C., Whitt, M. A., Chow, M., & Machaca, K. (2005). RNA interference is an antiviral defence mechanism in Caenorhabditis elegans. *Nature*, *436*(7053), 1044–7.

Wons, E., Furmanek-Blaszk, B., & Sektas, M. (2015). RNA editing by T7 RNA polymerase bypasses InDel mutations causing unexpected phenotypic changes. *Nucleic Acids Research*, *43*(8), 3950–63.

Wosula, E. N., Clark, C. A., & Davis, J. A. (2012). Effect of Host Plant, Aphid Species, and Virus Infection Status on Transmission of Sweetpotato feathery mottle virus. *Plant Disease*, *96*(9), 1331–1336.

Wright, C. F., Morelli, M. J., Thébaud, G., Knowles, N. J., Herzyk, P., Paton, D. J., … King, D. P. (2011). Beyond the consensus: dissecting within-host viral population diversity of foot-and-mouth disease virus by using next-generation genome sequencing. *Journal of Virology*, *85*(5), 2266–75.

Wu, J., Yang, Z., Wang, Y., Zheng, L., Ye, R., Ji, Y., … Li, Y. (2015). Viral-inducible Argonaute18 confers broad-spectrum virus resistance in rice by sequestering a host microRNA. *eLife*, *4*.

Xie, Z., Fan, B., Chen, C., & Chen, Z. (2001). An important role of an inducible RNA-dependent RNA polymerase in plant antiviral defense. *Proceedings of the National Academy of Sciences of the United States of America*, *98*(11), 6516–21.

Xiong, R., Wu, J., Zhou, Y., & Zhou, X. (2009). Characterization and subcellular localization of an RNA silencing suppressor encoded by Rice stripe tenuivirus. *Virology*, *387*(1), 29–40.

Xu, Y., Huang, L., Fu, S., Wu, J., & Zhou, X. (2012). Population diversity of rice stripe virus-derived siRNAs in three different hosts and RNAi-based antiviral immunity in Laodelphgax striatellus. *PloS One*, *7*(9), e46238.

Yang, X., Xie, Y., Raja, P., Li, S., Wolf, J. N., Shen, Q., … Zhou, X. (2011). Suppression of methylation-mediated transcriptional gene silencing by βC1-SAHH protein interaction during geminivirus-betasatellite infection. *PLoS Pathogens*, *7*(10), e1002329.

Ye, K., Malinina, L., & Patel, D. J. (2003). Recognition of small interfering RNA by a viral suppressor of RNA silencing. *Nature*, *426*(6968), 874–8.

Young, B. A., Stenger, D. C., Qu, F., Morris, T. J., Tatineni, S., & French, R. (2012). Tritimovirus P1 functions as a suppressor of RNA silencing and an enhancer of disease symptoms. *Virus Research*, *163*(2), 672–7.

Yu, D., Fan, B., MacFarlane, S. A., & Chen, Z. (2003). Analysis of the involvement of an inducible Arabidopsis RNA-dependent RNA polymerase in antiviral defense. *Molecular Plant-Microbe Interactions : MPMI*, *16*(3), 206–16.

Zhang, C., Wu, Z., Li, Y., & Wu, J. (2015). Biogenesis, Function, and Applications of Virus-Derived Small RNAs in Plants. *Frontiers in Microbiology*, *6*, 1237.

Zhang, X., Du, P., Lu, L., Xiao, Q., Wang, W., Cao, X., … Li, Y. (2008). Contrasting effects of HC-Pro and 2b viral suppressors from Sugarcane mosaic virus and Tomato aspermy cucumovirus on the accumulation of siRNAs. *Virology*, *374*(2), 351–60.

Zhang, X., Yuan, Y.-R., Pei, Y., Lin, S.-S., Tuschl, T., Patel, D. J., & Chua, N.-H. (2006). Cucumber mosaic virus-encoded 2b suppressor inhibits Arabidopsis Argonaute1 cleavage activity to counter plant defense. *Genes & Development*, *20*(23), 3255–68.

Zhang, X., Zhang, X., Singh, J., Li, D., & Qu, F. (2012). Temperature-dependent survival of Turnip crinkle virus-infected arabidopsis plants relies on an RNA silencing-based defense that requires dcl2, AGO2, and HEN1. *Journal of Virology*, *86*(12), 6847–54.

Zhang, Z., Chen, H., Huang, X., Xia, R., Zhao, Q., Lai, J., … Xie, Q. (2011). BSCTV C2 attenuates the degradation of SAMDC1 to suppress DNA methylation-mediated gene silencing in Arabidopsis. *The Plant Cell*, *23*(1), 273–88.

Zhou, Z. S., Dell'Orco, M., Saldarelli, P., Turturo, C., Minafra, A., & Martelli, G. P. (2006). Identification of an RNA-silencing suppressor in the genome of Grapevine virus A. *The Journal of General Virology*, *87*(Pt 8), 2387–95.

APPENDIX

RNA Polymerase Slippage as a Mechanism for the Production of Frameshift Gene Products in Plant Viruses of the *Potyviridae* Family

Bernardo Rodamilans,[a] Adrian Valli,[b] Ares Mingot,[c] David San León,[a] David Baulcombe,[b] Juan J. López-Moya,[c] Juan A. García[a]

Centro Nacional de Biotecnología CNB, CSIC, Madrid, Spain[a]; Department of Plant Sciences, University of Cambridge, Cambridge, United Kingdom[b]; Center for Research in Agricultural Genomics CRAG, CSIC-IRTA-UAB-UB, Campus UAB Bellaterra, Barcelona, Spain[c]

Downloaded from http://jvi.asm.org/ on July 17, 2015 by UNIVERSITAT AUTONOMA DE BARCELONA

Modifications of RNA sequences by nucleotide insertions, deletions, or substitutions can result in the expression of multiple proteins in overlapping open reading frames (ORFs). In the case of viruses, polymerase slippage results in the alteration of newly synthesized RNA. The mechanism has been well characterized in animal RNA viruses such as *Ebolavirus* (1) (EBOV) or *Hepatitis C virus* (HCV) (2). For plant viruses of the *Potyviridae* family, polymerase slippage has been proposed as a general process of evolution (3), although a lack of experimental systems has precluded confirmatory data, and most pieces of evidence are indirect (4).

Translation of a large ORF that results in a polyprotein, later processed into mature factors, is the canonical strategy of potyviral protein production. Along with this, in all members of this family, an overlapping ORF named PIPO was identified in the middle of the P3 coding region. The translation of PIPO begins at a specific GA_6 motif (5). Interestingly, GA_6 and other A_n motifs ($n = \geq 6$) are misrepresented among members of the *Potyviridae* family (1.2 A_6 motifs in the coding region per viral genome versus the expected 8.1 motifs). This additional ORF of potyviruses produces a P3N-PIPO fusion protein, which was originally identified in *Turnip mosaic virus* (5) and was shown to be essential for cell-to-cell movement during viral infection (6). Recently, another extra ORF located downstream of a GA_6 motif was informatically identified inside the large P1 coding region of sweet-potato-infecting potyviruses (7, 8). This new ORF, named PISPO, harbors the possibility of producing a frameshifted P1N-PISPO gene product, whose existence is still to be determined.

To explore the mechanism by which these additional potyviral proteins can be synthesized, we analyzed available RNA sequencing (RNA-seq) data of two *Plum pox virus* (PPV) isolates (9). After data filtering (10, 11), sequences were mapped versus the references (12) allowing a maximum of three mismatches per read. The expected indel error was modeled as a Poisson distribution calculating λ from the Illumina indel calling error rate, PCR error rate, and sample indel frequency. This analysis revealed the presence of A residue additions in the PIPO GA_6 motif in 1.6% of the reads (Fig. 1A). Interestingly, the presence of an additional A residue in this motif was also detected in libraries of PPV-derived small RNAs (not shown). Besides, published data on another potyvirus, *Zucchini yellow mosaic virus*, showed a minor variant with an extra A in all samples of a *Cucurbita pepo* vine studied by deep sequencing of long RNAs (13), and our analysis located this modification in the PIPO GA_6 motif as well.

To assess the scope among potyviruses of the extra A at the PIPO junction, we subjected a sample of sweet potato (*Ipomea batatas*) infected with the potyvirus *Sweet potato feathery mottle virus* (SPFMV) to RNA-seq analysis. SPFMV reconstruction (SRR1693230 and SRR1693363) showed that there were 1.8% sequence variants in this PIPO ORF, with the insertion of an A residue as the most prominent modification (Fig. 1B).

Altogether, these data strongly suggest that P3N-PIPO is produced, at least partially, through polymerase slippage. This possibility, previously considered by Chung et al. (5), could not be demonstrated at that time, likely because of the low rate of nucleotide insertion into this site.

Reconstruction of the SPFMV genome confirmed the previously described PISPO ORF imbedded in the P1 coding sequence. But more importantly, the RNA-seq data also revealed the presence of a high proportion of molecules (11.8%) with a single A nucleotide addition in the upstream GA_6 motif, which is indicative of polymerase slippage (Fig. 1B). This change would result in the production of the hypothetical P1N-PISPO, and these results not only support the existence of this alternative product but also suggest that this protein might play an important role during sweet potato potyvirus infection.

Considering the evolutionary relatedness of polymerases of the members of the families *Picornaviridae* and *Potyviridae* (14), it is reasonable to envision similar behaviors in both viral families and, consistent with that idea, the six-adenine repetition motif is underrepresented in picornaviruses (0.67 motif in the coding region per viral genome versus the expected 1.9 motifs), as was the case in the family *Potyviridae*. There is no previous report of polymerase slippage in the *Picornaviridae* family; nonetheless, when an A_6 motif was present, as in the case of the enterovirus *Human rhinovirus C* (SRR363436), there were 2.4% A residue insertions at this location. These data suggest that polymerase slippage can occur in both *Picorna*-like families but that *Potyviridae* take more frequent advantage of this mechanism.

A common denominator in RNA slippage is the low fidelity of viral RNA polymerases and their tendency to stutter when encountering repetitive motifs. It is known that polymerases of EBOV, HCV, *Vaccinia virus*, or T7 bacteriophage, given the appropriate contexts, are prone to slippage (1, 2, 15). Repetitive

Accepted manuscript posted online 15 April 2015

Citation Rodamilans B, Valli A, Mingot A, San León D, Baulcombe D, López-Moya JJ, García JA. 2015. RNA polymerase slippage as a mechanism for the production of frameshift gene products in plant viruses of the *Potyviridae* family. J Virol 89:6965–6967. doi:10.1128/JVI.00337-15.

Editor: A. Simon

Address correspondence to Juan A. García, jagarcia@cnb.csic.es.

B.R., A.V., A.M., and D.S.L. contributed equally to this work.

D.B., J.J.L.-M., and J.A.G. are equal co-senior authors of this paper.

Copyright © 2015, American Society for Microbiology. All Rights Reserved.

doi:10.1128/JVI.00337-15

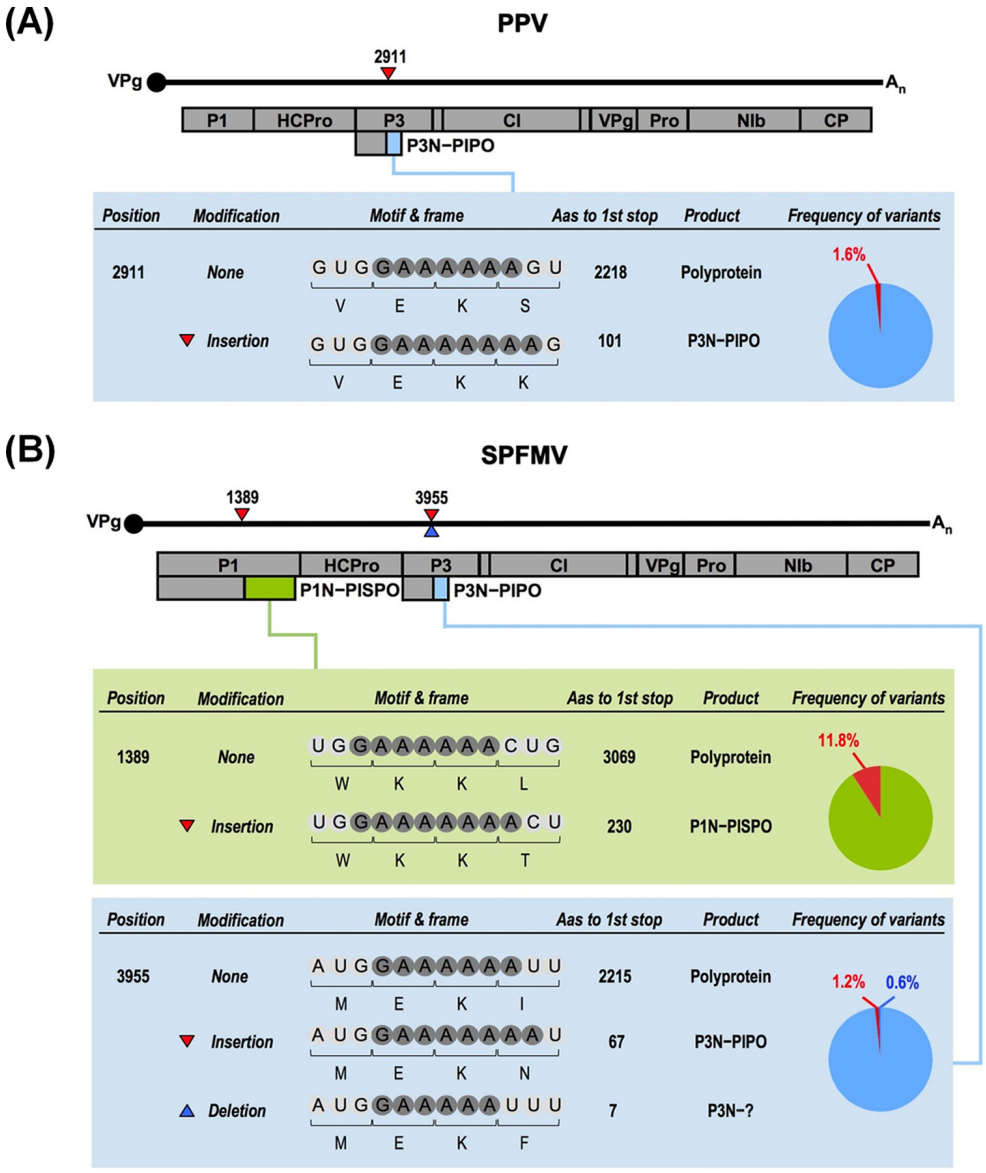

FIG 1 RNA slippage in viruses of the *Potyvirus* genus. The genomes of the potyviruses PPV (A) and SPFMV (B) are depicted schematically. Mature gene products are shown as boxes. Additional ORFs corresponding to out-of-frame PIPO and PISPO regions are also depicted. Sites where indels were detected after RNA-seq analysis are shown with red (insertion) or blue (deletion) triangles. Details of the motif, the resulting frame for the modifications, and the length of the expected products, as well as the RNA slippage percentages, are indicated for each modification. Color codes in the pie charts refer to insertions and deletions compared to the genomic sequence.

motifs, however, are not the rule but the exception, probably because of selective negative pressure supported by nonsense-mediated decay (16) or other mechanisms. Nonetheless, in certain situations, slippage of the polymerase would give rise to the production of new protein variants that are used by the virus, opening the door to new ways of adaptation and evolution.

ACKNOWLEDGMENTS

We are grateful to Beatriz García for technical assistance and to the Computational Systems Biology Group of CNB-CSIC for supplying analytical resources.

D.B. is the Royal Society Edward Penley Abraham Research Professor. This work was supported by Spanish Ministerio de Economía y Competitividad grants AGL2013-42537-R to J.J.L.-M. and BIO2013-49053-R and Plant KBBE PCIN-2013-056 to J.A.G.

REFERENCES

1. **Volchkov VE, Becker S, Volchkova VA, Ternovoj VA, Kotov AN, Netesov SV, Klenk HD.** 1995. GP mRNA of Ebola virus is edited by the Ebola virus polymerase and by T7 and vaccinia virus polymerases. Virology **214:**421–430. http://dx.doi.org/10.1006/viro.1995.0052.
2. **Ratinier M, Boulant S, Combet C, Targett-Adams P, McLauchlan J, Lavergne JP.** 2008. Transcriptional slippage prompts recoding in alternate reading frames in the hepatitis C virus (HCV) core sequence from strain HCV-1. J Gen Virol **89:**1569–1578. http://dx.doi.org/10.1099/vir.0.83614-0.
3. **Hancock JM, Chaleeprom W, Dale J, Gibbs A.** 1995. Replication slippage in the evolution of potyviruses. J Gen Virol **76:**3229–3232. http://dx.doi.org/10.1099/0022-1317-76-12-3229.

Downloaded from http://jvi.asm.org/ on July 17, 2015 by UNIVERSITAT AUTONOMA DE BARCELONA

4. **Simón-Buela L, Osaba L, García JA, López-Moya JJ.** 2000. Preservation of 5′-end integrity of a potyvirus genomic RNA is not dependent on template specificity. Virology **269:**377–382. http://dx.doi.org/10.1006/viro.2000.0229.
5. **Chung BY, Miller WA, Atkins JF, Firth AE.** 2008. An overlapping essential gene in the *Potyviridae*. Proc Natl Acad Sci U S A **105:**5897–5902. http://dx.doi.org/10.1073/pnas.0800468105.
6. **Wei T, Zhang C, Hong J, Xiong R, Kasschau KD, Zhou X, Carrington JC, Wang A.** 2010. Formation of complexes at plasmodesmata for potyvirus intercellular movement is mediated by the viral protein P3N-PIPO. PLoS Pathog **6:**e1000962. http://dx.doi.org/10.1371/journal.ppat.1000962.
7. **Clark CA, Abad JA, Cuellar WJ, Fuentes S, Kreuze JF, Gibson RW, Mukasa SB, Tugume AK, Tairo FD, Valkonen JP.** 2012. Sweetpotato viruses: 15 years of progress on understanding and managing complex diseases. Plant Dis **96:**168–185. http://dx.doi.org/10.1094/PDIS-07-11-0550.
8. **Li F, Xu D, Abad J, Li R.** 2012. Phylogenetic relationships of closely related potyviruses infecting sweet potato determined by genomic characterization of *Sweet potato virus G* and *Sweet potato virus 2*. Virus Genes **45:**118–125. http://dx.doi.org/10.1007/s11262-012-0749-2.
9. **Rodamilans B, San León D, Mühlberger L, Candresse T, Neumüller M, Oliveros JC, García JA.** 2014. Transcriptomic analysis of *Prunus domestica* undergoing hypersensitive response to *Plum pox virus* infection. PLoS One **9:**e100477. http://dx.doi.org/10.1371/journal.pone.0100477.
10. **HannonLab.** 2014. FASTX toolkit. Cold Spring Harbor Laboratory, Cold Spring Harbor, NY. http://hannonlab.cshl.edu/fastx_toolkit/index.html.
11. **Babraham-Bioinformatics.** 2014. FASTQC, a quality tool for high throughput sequence data. Babraham Institute, Babraham, United Kingdom. http://www.bioinformatics.babraham.ac.uk/projects/fastqc/.
12. **Langmead B, Salzberg SL.** 2012. Fast gapped-read alignment with Bowtie 2. Nat Methods **9:**357–359. http://dx.doi.org/10.1038/nmeth.1923.
13. **Dunham JP, Simmons HE, Holmes EC, Stephenson AG.** 2014. Analysis of viral (zucchini yellow mosaic virus) genetic diversity during systemic movement through a *Cucurbita pepo* vine. Virus Res **191:**172–179. http://dx.doi.org/10.1016/j.virusres.2014.07.030.
14. **Koonin EV, Dolja VV.** 1993. Evolution and taxonomy of positive-strand RNA viruses: implications of comparative analysis of amino acid sequences. Crit Rev Biochem Mol Biol **28:**375–430. http://dx.doi.org/10.3109/10409239309078440.
15. **Shabman RS, Jabado OJ, Mire CE, Stockwell TB, Edwards M, Mahajan M, Geisbert TW, Basler CF.** 2014. Deep sequencing identifies noncanonical editing of Ebola and Marburg virus RNAs in infected cells. mBio **5:**e02011. http://dx.doi.org/10.1128/mBio.02011-14.
16. **Garcia D, Garcia S, Voinnet O.** 2014. Nonsense-mediated decay serves as a general viral restriction mechanism in plants. Cell Host Microbe **16:**391–402. http://dx.doi.org/10.1016/j.chom.2014.08.001.

Downloaded from http://jvi.asm.org/ on July 17, 2015 by UNIVERSITAT AUTONOMA DE BARCELONA

AMERICAN SOCIETY FOR MICROBIOLOGY | Journal of Virology

The P1N-PISPO *trans*-Frame Gene of Sweet Potato Feathery Mottle Potyvirus Is Produced during Virus Infection and Functions as an RNA Silencing Suppressor

Ares Mingot,[a] Adrián Valli,[b] Bernardo Rodamilans,[c] David San León,[c] David C. Baulcombe,[b] Juan Antonio García,[c] Juan José López-Moya[a]

Center for Research in Agricultural Genomics, CSIC-IRTA-UAB-UB, Cerdanyola del Vallès, Barcelona, Spain[a]; Department of Plant Sciences, University of Cambridge, Cambridge, United Kingdom[b]; Centro Nacional de Biotecnología CNB, CSIC, Madrid, Spain[c]

ABSTRACT

The positive-sense RNA genome of *Sweet potato feathery mottle virus* (SPFMV) (genus *Potyvirus*, family *Potyviridae*) contains a large open reading frame (ORF) of 3,494 codons translatable as a polyprotein and two embedded shorter ORFs in the −1 frame: PISPO, of 230 codons, and PIPO, of 66 codons, located in the P1 and P3 regions, respectively. PISPO is specific to some sweet potato-infecting potyviruses, while PIPO is present in all potyvirids. In SPFMV these two extra ORFs are preceded by conserved G_2A_6 motifs. We have shown recently that a polymerase slippage mechanism at these sites could produce transcripts bringing these ORFs in frame with the upstream polyprotein, thus leading to P1N-PISPO and P3N-PIPO products (B. Rodamilans, A. Valli, A. Mingot, D. San Leon, D. B. Baulcombe, J. J. Lopez-Moya, and J.A. Garcia, J Virol 89:6965–6967, 2015, doi:10.1128/JVI.00337-15). Here, we demonstrate by liquid chromatography coupled to mass spectrometry that both P1 and P1N-PISPO are produced during viral infection and coexist in SPFMV-infected *Ipomoea batatas* plants. Interestingly, transient expression of SPFMV gene products coagroinfiltrated with a reporter gene in *Nicotiana benthamiana* revealed that P1N-PISPO acts as an RNA silencing suppressor, a role normally associated with HCPro in other potyviruses. Moreover, mutation of WG/GW motifs present in P1N-PISPO abolished its silencing suppression activity, suggesting that the function might require interaction with Argonaute components of the silencing machinery, as was shown for other viral suppressors. Altogether, our results reveal a further layer of complexity of the RNA silencing suppression activity within the *Potyviridae* family.

IMPORTANCE

Gene products of potyviruses include P1, HCPro, P3, 6K1, CI, 6K2, VPg/NIaPro, NIb, and CP, all derived from the proteolytic processing of a large polyprotein, and an additional P3N-PIPO product, with the PIPO segment encoded in a different frame within the P3 cistron. In sweet potato feathery mottle virus (SPFMV), another out-of-frame element (PISPO) was predicted within the P1 region. We have shown recently that a polymerase slippage mechanism can generate the transcript variants with extra nucleotides that could be translated into P1N-PISPO and P3N-PIPO. Now, we demonstrate by mass spectrometry analysis that P1N-PISPO is indeed produced in SPFMV-infected plants, in addition to P1. Interestingly, while in other potyviruses the suppressor of RNA silencing is HCPro, we show here that P1N-PISPO exhibited this activity in SPFMV, revealing how the complexity of the gene content could contribute to supply this essential function in members of the *Potyviridae* family.

Potyviruses (family *Potyviridae*) are important viral pathogens with positive-sense, single-stranded RNA genomes that are able to infect a wide range of plant species. The genomic RNA of potyviruses, around 10 kb in size with a viral protein (VPg) at its 5′ end and polyadenylated at the 3′ end, contains a large open reading frame (ORF) that encodes a polyprotein comprising the following gene products from the N to the C terminus: P1, HCPro, P3, 6K1, CI, 6K2, VPg/NIaPro, NIb, and CP (1, 2). Despite the abundant sequence information available on potyviruses, it was not until 2008 that the presence of a well-conserved second short ORF of around 60 codons, termed PIPO (Pretty Interesting Potyviral ORF) by its discoverers, was predicted as an overlapping product within the P3 region in all members of the family. Thus, this ORF yields a fusion product with the upstream portion of P3 after frameshift (P3N-PIPO), as found in plants infected with turnip mosaic virus (TuMV) (3). More recently, another short ORF termed PISPO (Pretty Interesting Sweet potato Potyviral ORF) was predicted by bioinformatics analysis within the P1-coding sequence of a few members of the *Potyvirus* genus, all related to sweet potato feathery mottle virus (SPFMV), including sweet po-

Received 15 September 2015 Accepted 7 January 2016

Accepted manuscript posted online 20 January 2016

Citation Mingot A, Valli A, Rodamilans B, San León D, Baulcombe DC, García JA, López-Moya JJ. 2016. The P1N-PISPO *trans*-frame gene of sweet potato feathery mottle potyvirus is produced during virus infection and functions as an RNA silencing suppressor. J Virol 90:3543–3557. doi:10.1128/JVI.02360-15.

Editor: A. Simon

Address correspondence to Juan José López-Moya, juanjose.lopez@cragenomica.es.

A.M. and A.V. contributed equally to this article. D.C.B., J.A.G. and J.J.L.-M. are co-senior authors.

Supplemental material for this article may be found at http://dx.doi.org/10.1128/JVI.02360-15.

Copyright © 2016, American Society for Microbiology. All Rights Reserved.

Downloaded from http://jvi.asm.org/ on March 13, 2016 by guest

tato virus G (SPVG) and sweet potato virus 2 (SPV2), with the notable exception of sweet potato latent virus, a potyvirus described as latent (4, 44). In the reference genome of SPFMV (NC_001841.1) (5), the PISPO sequence is nested in the −1 frame (relative to the polyprotein ORF) within the P1-coding region (positions 118 to 2109), which corresponds to the first N-terminal gene product of the large polyprotein (ORF from position 118 to 10599). The PISPO sequence begins at position 1382 and spans 690 nucleotides from the GGAAAAAA (G_2A_6) motif. This motif is identical to the conserved consensus sequence for the PIPO frameshifting, which in SPFMV gives rise to a shorter coding sequence, also in the −1 frame.

Separation of P1 from the other viral products occurs by autoproteolysis (6), and except for the conserved C-terminal protease region, this product is the most variable of the potyvirus proteins (7). SPFMV P1 is the largest among all potyvirus P1 proteins, with 664 to 724 amino acids (aa), resulting in a protein of 74.1 to 80 kDa. Similarity between the N-terminal parts of the P1 proteins of SPFMV and the ipomovirus sweet potato mild mottle virus (SPMMV) has been reported earlier (7). Interestingly, the resemblance between these two proteins ends near the predicted frameshift point of PISPO.

Since the PIPO coding sequence was first described in potyviruses, the new gene product P3N-PIPO has attracted much interest, leading to the identification of several important associated functions (8–12). However, the mechanism by which P3N-PIPO is produced remained unclear until recently, when we and another team independently found evidence that PIPO is expressed by a polymerase slippage mechanism (13, 14). Our previous results also support the idea that PISPO, if it was expressed, would be synthesized by an equivalent polymerase slippage event (14).

One of the key functions of RNA silencing in plants is as a defense barrier against viral infections (15). Viruses, in turn, use diverse strategies to escape from RNA silencing, such as the expression of viral proteins with RNA silencing suppression activity (16). For example, in the *Potyviridae* family, all members of the genus *Potyvirus* described so far express HCPro to counteract RNA silencing. RNA silencing suppression in plant viruses was recently reviewed (17).

By using liquid chromatography coupled to mass spectrometry (LC-MS), we show here that P1N-PISPO is produced in sweet potato plants infected with SPFMV, demonstrating that the product derived from this *trans*-frame viral ORF is indeed expressed during virus infection. Next, we describe that P1N-PISPO exhibits RNA silencing suppression activity, which is associated with the presence of conserved WG/GW motifs, suggesting a mode of action similar to that of other RNA silencing suppressors (RSSs) (18, 19).

MATERIALS AND METHODS

Plant and virus materials. Commercial sweet potato (*Ipomea batatas*) roots were acquired in a local market in Barcelona and were planted on soil to produce fresh aerial tissue (stems and leaves) that was further propagated through cuttings at Center for Research in Agricultural Genomics facilities. The presence of SPFMV in the vegetatively propagated plants was confirmed by reverse transcription-PCR (RT-PCR) of total RNA extracted with TRIzol reagent following the provider's instructions, using primers FMCPFdeg and MFRdeg (see Table S1 in the supplemental material for details on all primer sequences), which were designed to amplify a 389-nucleotide (nt) fragment within the CP-coding region. A robust plant, denoted AM-MB2, with occasional viral symptoms (weak mosaic, leaf spots, and distortions) that tested positive for SPFMV presence was selected for cutting propagation. The complete P1-coding region was also amplified by RT-PCR with FMP1F and 1PMFR specific primers and was sequenced to confirm the presence of the embedded PISPO sequence. The same infected AM-MB2 plant material described here was used for previously published experiments (13).

To boost accumulation of SPFMV in sweet potato AM-MB2 plants, coinfection with isolate Can181-9 of the crinivirus sweet potato chlorotic stunt virus (SPCSV) strain West African (SPCSV-WA), kindly provided by Jesús Navas-Castillo (IHSM-UMA-CSIC La Mayora, Málaga, Spain), was achieved by inoculation with *Bemisia tabaci* whiteflies. Briefly, groups of around 50 viruliferous whiteflies that had acquired SPCSV during 48 h in an infected *Ipomea setosa* plant were caged on fully expanded leaves of AM-MB2 cuttings for a 48-h inoculation period. After insect removal and insecticide treatment, plants were sampled and tested for detection of both SPFMV and SPCSV, in the later case with oligonucleotides SPCSVCP and PCVSCPS, which amplify a 790-nt fragment from the CP-coding sequence of SPCSV.

Isolates of two potyviruses, sweet potato virus C (SPVC) and SPV2, as well as one begomovirus and one badnavirus (both unclassified), were found to be coinfecting the sweet potato AM-MB2 plant after deep-sequencing analysis (see below).

Extraction of total RNA, construction and sequencing of RNA sequencing (RNA-seq) libraries, and preliminary data filtering. Samples of symptomatic tissue of infected plants were collected for RNA extraction with TRIzol reagent. Contaminating DNA was removed from RNA samples with Turbo DNase (Ambion), and RNA was further purified using the RNeasy minikit (Qiagen). RNA libraries were constructed with the ScripSeq complete kit (plant leaf) (Epicenter, Illumina), including barcoding elements to identify the different samples, according to the provider's protocols. Libraries were submitted to BGI (Hong Kong) for Illumina sequencing on a HiSeq 2000 platform, and 100-bp (average) paired-end reads were generated. Sequences with an average quality below 20, as well as sequences with more than 10 nt with quality below 15, were removed using the FASTX toolkit (available from http://hannonlab.cshl.edu/fastx_toolkit/index.html). The quality process was driven with FASTQC (Babraham Bioinformatics) (available at http://www.bioinformatics.babraham.ac.uk/projects/fastqc/).

Alignments and indel analysis. Filtered sequences were mapped versus the references with Bowtie2 (20), allowing a maximum of 3 mismatches, insertions, or deletions (indels) per read. To reduce the number of sequencing errors, only the central part of reads (80 nt) was used, and only paired alignments were considered (21). Alignments were analyzed with SAMtools to create a list of variants in which only indels were included. Reads that presented fewer than 3 nonredundant sequences and reads in which the frameshift caused by the indel was cancelled out by another indel in the same sequence were discarded. To reduce false positives caused by sequencing errors or random errors, the expected indel error was modeled as a Poisson distribution, which was calculated from Illumina indel calling-error rate, PCR error rate, and sample indel frequency. Indels with a false-discovery rate (FDR) higher than 0.05 were removed. Analysis was performed with in-house R scripts.

Phylogenetic and recombination analysis. Initial phylogenetic analysis of the SPFMV, SPVC, and SPV2 isolates found in AM-MB2 was performed with data sets created with the full genome sequences corresponding to 9 SPFMV, 7 SPVC, and 6 SPV2 isolates found in the NCBI nucleotide database, with no filter by identity redundancy. Also, sequences of complete CP regions of all other SPFMV, SPVC, and SPV2 isolates available in the NCBI nucleotide database were considered, after exclusion of partial CP sequences and application of a filter at 97% of identity to reduce redundancy, leading to data sets of 63 SPFMV, 46 SPVC, and 6 SPV2 annotated sequences. Phylogenetic trees were created using the maximum-likelihood algorithm implemented in MEGA6 software (22). The bootstrapping test was driven with 1,000 replicates. CP

Downloaded from http://jvi.asm.org/ on March 13, 2016 by guest

sequence-based trees were used to estimate putative recombination events (see below).

The assembly of SPFMV used the reference genome already described (13), and was driven with Quasirecomb (23). The same procedure was applied to SPVC and SPV2. The reconstruction of sequences used coverage of >10.000 to reduce errors, thereby excluding both extremes, and the option to reduce the false positives was activated. The sequences obtained were used to search for putative recombination events with the software RDP (24) version 3.45, using a threshold of a *P* value equal or less than 0.05 with the methods RDP (25), BootScan (26), Geneconv (26), and MaxChi (27). The recombination points were identified using the SBP and GARD algorithms (28) implemented in the Datamonkey webserver (29).

Constructs of viral gene products for *in vitro* translation and for transient expression of viral proteins by agroinfiltration. Cloning and plasmid production were performed using *Escherichia coli* strain DH5α and standard procedures. Viral products were RT-PCR amplified with appropriate primers, and the products were cloned directionally into pENTR/D-TOPO (Life Technologies). Primers are listed in Table S1 in the supplemental material, which includes information about their use for the modifications required to direct and/or force or avoid the expression of certain gene products in the different frames. Recombinant products with mutations introduced by PCR with appropriate primers were generated and were confirmed by sequencing the pENTR clones. The multiple mutant with the 4 WG/GWs motifs altered was synthesized as follows. A fragment flanked by NcoI and AscI sites engineered upstream and downstream from position 1 to 1964 (Met to Stop) in the P1N-PISPO sequence, with replacement of W with A residues in the WG/GW motifs located at positions 73, 1465, 1795, and 1918 (relative to the initial Met codon), was ordered from GeneScript (USA) and inserted using the unique restriction sites into the pENTR plasmid, linearized with the same enzymes, and ligated with T4 DNA ligase. Clones containing inserts were selected and sequenced to confirm the presence of the mutated motifs. The inserts in pENTR were mobilized using Gateway into the different destination vectors with LR Clonase II enzyme mix (Life Technologies). Reactions were performed, and two clones of the different plasmids were verified. For expression in plants, the pGWB7XX destination plasmid series was used (30, 31), which placed the construct under control of appropriate elements.

***In vitro* translation.** pENTR-P1 was used as the template for PCR amplifications of all constructs used for *in vitro* translation, including unmodified wild-type P1 and variants with P1 interrupted by a stop codon after the slippage site (P1Δ) and P1 with the PISPO sequence interrupted (P1N-PISPOΔ) generated by site-directed mutagenesis with the primers FMP1ΔF and Δ1PMFR for P1Δ and FMPISPOΔF and ΔOPSIPMFR for P1N-PISPOΔ (see Table S1 in the supplemental material). T7 promoter, 5′ untranslated region (5′UTR), and 3′UTR fragments were prepared as described previously (32). mRNAs were produced by *in vitro* transcription using the T7-Scribe Standard RNA IVT kit (Cellscript) and purified by organic extraction and ammonium acetate precipitation, and their quality and amount were assessed by NanoDrop (Thermo Fisher Scientific) and gel electrophoresis. The final concentration was adjusted to 1 g/liter, and *in vitro* translation was carried out using wheat germ extract (Promega) according to the manufacturer's instructions. Labeling of the synthesized proteins was done by including in the reaction mixture L-[^{35}S]methionine and L-[^{35}S]cysteine (PerkinElmer). Samples were resolved by 12% SDS-PAGE and detected with a PhosphorImager.

***Agrobacterium tumefaciens* infiltration of *Nicotiana benthamiana* leaves.** *N. benthamiana* leaves (fully expanded, from 3- to 4-week-old plants grown in a greenhouse) were agroinfiltrated as described previously (33), using *A. tumefaciens* cultures of strain C58C1 or EHA105 transformed with the relevant plasmids. Growth of bacteria was monitored by assessing the optical density at 600 nm (OD_{600}) until it reached 0.5 units. Cultures were induced by acetosyringone and infiltrated with a needleless syringe. For sampling material to be analyzed by LC-tandem MS (LC-MS/MS) (see below), the agroinfiltration was performed with mixed cultures incorporating a construct expressing P1b of CVYV (33) to increase expression of SPFMV proteins. For silencing suppression experiments (see below), negative (empty vector, delta) and positive (CVYV P1b and SPMMV P1) controls were included, following previously described procedures (34, 35).

SDS-PAGE and fractionation of protein products. Plant samples were collected, deep-frozen, and homogenized in extraction buffer. After boiling for 5 min, aliquots were separated by 10% SDS-PAGE. Following staining with Coomassie blue G-250 (SimplyBlue safe stain; Life Technologies), the portion above the RuBisCO was excised and processed.

MS and protein identification by LC-MS/MS analysis. Gel-excised fragments containing protein samples were washed with 25 mM NH_4HCO_3 and acetonitrile (ACN), reduced for 60 min at 60°C with 20 mM dithiothreitol (DTT), and alkylated for 30 min at 30°C with 55 mM iodoacetamide in the dark before being digested for 16 h at 37°C with 0.9 μg trypsin (porcine sequence-grade modified trypsin; Promega). Peptides were extracted from the gel matrix with 10% formic acid and ACN, dyed, and desalted with a C_{18} Top-tip (PolyLC), following the procedure of the provider. Dried-down tryptic peptides mixtures resuspended in 1% formic acid were injected for chromatographic separation in a nanoAcquity liquid chromatograph (Waters) coupled to an LTQ-Orbitrap Velos (Thermo Scientific) mass spectrometer. Peptides were trapped on a Symmetry C_{18} trap column (5 μm by 180 μm by 20 mm; Waters) and separated with a C_{18} reverse-phase capillary column (75 μm, 10 cm nanoAcquity; 1.7-μm BEH column; Waters). The gradient for elution was prepared with 0.1% formic acid in ACN and consisted of 1 to 30% for 60 min, 35 to 45% for 10 min, and 45 to 85% for 5 min, with a flow rate of 250 nl/min. Eluted peptides were subjected to electrospray ionization in an emitter needle (PicoTip; New Objective) with 2,000 V applied. Peptide masses (*m/z* 350 to 1700) were analyzed in full-scan MS data-dependent mode in the Orbitrap with 60,000 full width at half maximum (FWHM) resolution at 400 *m/z*. Up to the 10 most abundant peptides (minimum intensity of 500 counts) were selected for each MS scan and fragmented using collision-induced dissociation in a linear ion trap with helium as the collision gas and 38% normalized collision energy. The targeted mode was used to analyze the presence of predicted peptides in the ORF that contains PISPO (the seven peptides underlined in the sequence LVWEKTG RTIGHKERDQKRSQSKMEVGTLQTSQEDQEGQPKTAPTEAHGE GTAIIDGYATSSSDGHLHCWGSIGESGNDSNSEWEDFLHAFHEEEE NFKISQINTRENSRAHAGSSENCVQEKDEHRIGGQEVHKRAVQEISR SKLFVPSFKTYGRLKRVSGFKNSHNNSKPRTSSCQGWSMEKTCKD NNVVQRFKWHGAESRQTVGPKRSCTTRNARGAWGFTRSAIRRTN ETW) or in the C-terminal part of the P1 (the three peptides underlined in the sequence KLDEQLATRNEIRKGLKVKWRWGLYRLVKKTRKD NQRQRRQRRMEKEQQLLMAMPPQVLTGISIAGGPSASLEMTPTPN GKIFCTPSMKKKKTLKSPKLTQEKIHELTQAVLKIACRKRMSIELV GKKSTKGQYRKFQGANYLFLHLKHMEGLRESVDLRIHTTTQNLV LQAAKVGAWKRPVKTTMLSKGSSGMVLNPDKLLGPRGHAPHGM LVVRGALRGVLYDARMKLGRSVLPYIIQY). Generated raw data were collected with Thermo Xcalibur (v.2.2). For database searching, custom databases were created merging all UniProt entries (as of December 2014) for *I. batatas* plus the predicted list of mature protein sequences from SPFMV plus a list of predicted mature gene products deriving from viruses present in the AM-MB2 sample or for *N. benthamiana* and *A. tumefaciens* plus P1 and P1N-PISPO. Entries from common laboratory contaminants were also added. Sequest search engine searches were performed with Thermo Proteome Discoverer software (v.1.3.0.339), using a target and a decoy database to obtain a false-discovery rate (FDR) (strict, 0.01; relaxed, 0.05) and to estimate the number of incorrect peptide spectrum matches exceeding a given threshold (peptide tolerances of 10 ppm and 0.6 Da, respectively, for MS and MS/MS), with parameters for trypsin allowing up to 2 missed cleavages, considering cysteine carbamidomethylation as fixed and methionine oxidation as variable modifications. Validation was based on FDR, using Percolator (a semisupervised

Downloaded from http://jvi.asm.org/ on March 13, 2016 by guest

learning machine) to discriminate peptide spectrum matches. Only proteins identified with at least 2 high-confidence peptides (FDR of ≤0.01) were considered.

RNA silencing suppression activity assays: GFP imaging, Northern blotting, and RT-qPCR analysis. Leaves of *N. benthamiana* plants were coagroinfiltrated with a green fluorescent protein (GFP)-expressing construct together with constructs of the different viral products or adequate controls. The infiltrated patches were visualized under UV light with a Black Ray B 100 AP lamp, and photographs were taken with a Nikon D7000 digital camera.

Total RNA from *N. benthamiana* tissue was isolated using TRIzol and treated with Turbo DNase (Ambion) to remove contaminating DNA. For Northern blot analysis of mRNAs and small interfering RNAs (siRNAs), approximately 10 and 15 μg of total RNA were resolved on 1.2% agarose (containing 2% formaldehyde) or 15% denaturing polyacrylamide (containing 7 M urea) gels, respectively, and transferred to nylon Hybond-N+ membranes (Amersham) by capillary blotting for the agarose gels or using a transfer apparatus (XCell SureLock; Invitrogen) for the acrylamide gels. Ethidium bromide staining was used to verify equal loading of lanes and monitor the transference processes. After UV cross-linking and prehybridization in UltraHyb buffer (Ambion), blots were hybridized in the same solution with probes specific to the GFP sequence, using a ^{32}P-labeled DNA probe (33) in the case of mRNAs or a ^{32}P-labeled RNA probe (36) in the case of small RNAs. Hybridization signals were detected with a PhosphorImager.

For quantitative real-time reverse transcription-PCR (RT-qPCR) analysis, 1 μg of total RNA was reverse transcribed using the SuperScript III first-strand synthesis system (Invitrogen), and RT-PCRs were performed in a 20-μl volume with gene-specific primers and LightCycler 480 SYBR green I master mix (Roche). A 102-bp GFP fragment was amplified with primers described by Leckie and Stewart (37). Ubiquitin was selected as a reference gene, amplifying a 88-bp fragment using the primers described by Lacomme and coworkers (38) (see Table S1 in the supplemental material). The average cycle threshold (C_T) value for triplicate PCRs was normalized to the average C_T value for the reference gene, yielding the ΔC_T value. An analysis of variance (ANOVA) for at least three independent biological replicates was performed using the Tukey-Kramer test.

Nucleotide sequence accession numbers. Data corresponding to virus sequences are available in GenBank under accession numbers KU511268, KU511269, KU511270, KU511271, and KU511272.

RESULTS

Sequencing the virome of the sweet potato plant AM-MB2. AM-MB2 sweet potato plants, which are naturally infected with several viruses, including SPFMV, were used. With the aim of boosting the load of potyviruses, plants were superinfected with the crinivirus SPCSV, which is known to cause a synergistic effect with potyviruses (39). As shown in Fig. 1A, the superinfection of AM-MB2 plants with SPCSV resulted in a strong enhancement of disease symptoms.

Total RNA isolated from samples of the plants coinfected with SPCSV and SPFMV was analyzed by RNA-seq using Illumina technology (SRA references SRR1693374 and SRR1693416) and compared to equivalent samples deriving from AM-MB2 plants not superinfected with the crinivirus (13). Abundant SPFMV-derived reads were found, together with a smaller number of reads from two additional potyviruses, SPV2 and SPVC. In addition, reads corresponding to a begomovirus and a badnavirus were identified, but in insufficient number to obtain complete coverage of the genomes of these viruses. As expected, the number of reads for potyviruses increased notably after superinfection with SPCSV, as shown in Fig. 1B, whereas no major change in the accumulation of reads was observed for the begomovirus and badnavirus.

Total or partial assemblies of the different viruses were deposited in GenBank, and their preliminary annotations are provided in Tables S2 to S6 in the supplemental material.

Boosting of SPV2 and SPVC accumulation in the crinivirus-superinfected samples allowed us to analyze the presence of insertions/deletions in their genomes. As predicted from our previous findings (13), most of the indels in SPV2 and SPVC genomes were found in the G_2A_6 motifs upstream of *trans*-frame PISPO and PIPO (see Table S7 in the supplemental material).

The assembly of the genomic sequence from SPFMV (see Table S2 in the supplemental material) spanned 10,814 nt, representing almost all of its genome, except for a short region at the 5′ end of ~6 nt. The sequence of SPFMV AM-MB2 encoded the canonical potyvirus gene products in the polyprotein, i.e., P1, HCPro, P3, 6K1, CI, 6K2, VPg/NIaPro, NIb, and CP, as well as the predicted P1N-PISPO and P3N-PIPO, in both cases preceded by G_2A_6 motifs. The genomic organization is summarized in Fig. 1C. Positions in the genome were numbered after alignment with other published SPFMV sequences to facilitate comparison of regions with the reference genome (5) (95.12% identity).

Our data also showed that superinfection with SPCSV resulted in a decrease in the relative proportion of RNA-seq reads with an additional A in the G_2A_6 motifs at the PISPO site (so-called RNA slippage frequency) in SPFMV, while there was no change in slippage at the PIPO site where a less frequent slippage was observed (Fig. 1D).

Phylogenetic analyses were performed with all potyviral sequences in AM-MB2 using whole-genome sequences (Fig. 2A) and selected CP sequences of individual viruses. In the case of the SPFMV isolate, a comparison of trees constructed with whole-genome and CP sequences suggested that it can be placed in the group of recombinant isolates, a frequent occurrence among SPFMV isolates (40, 41). Comparison of our sequence with those of two selected isolates (Piu3 and RC-ARg, accession numbers FJ155666.1 and KF386014.1, respectively) is illustrated in Fig. 2B, where a crosspoint upstream from the CP region is noticeable. Application of adequate analysis tools predicted a recombination site located at position 7227 in the NIa region, further confirming the recombinant nature of the SPFMV AM-MB2 isolate.

Absence of detectable production of P1N-PISPO by frameshifting in *in vitro* translation experiments. To evaluate the putative contribution of translational frameshifting to the production of P1N-PISPO, the SPFMV P1-coding region was cloned after RT-PCR amplification (P1 construct), and appropriate mutations were designed to express truncated proteins in each of the frames. In the P1Δ construct, a stop codon interrupted the main ORF of the polyprotein downstream of the G_2A_6 motif to generate a 54-kDa variant, whereas in the P1N-PISPOΔ construct, the stop was introduced in the PISPO sequence (−1 frame), leading to a putative 47-kDa product without altering the P1-coding sequence. P1, P1Δ, and P1N-PISPOΔ, together with a luciferase control, were used for *in vitro* transcription. The analysis showed a band with a mobility corresponding to ~70 kDa in the P1 sample, compatible with both P1 and P1N-PISPO (expected sizes of 74.1 kDa and 72.7 kDa, respectively) (Fig. 3). However, major protein products derived from translational frameshifting were not detected in the analysis of the two other constructs designed to yield products of different sizes in the P1 and PISPO frames: in P1Δ, the major band was compatible with the expected size of

Downloaded from http://jvi.asm.org/ on March 13, 2016 by guest

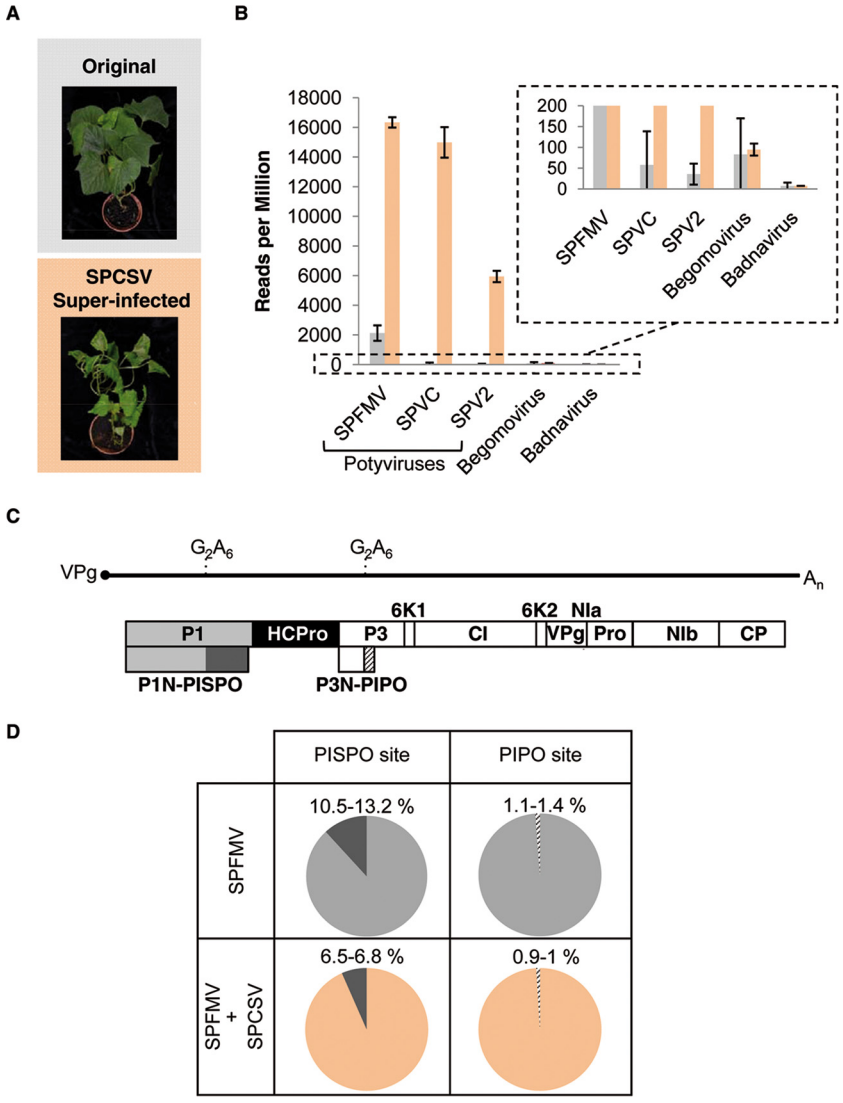

FIG 1 Synergism between SPFMV and SPCSV. (A) Appearance of AM-MB2 plants propagated vegetatively, with a representative original plant (top) and another superinfected with SPCSV (bottom). Pictures were taken 4 months after whitefly-mediated inoculation of the crinivirus. (B) Normalized number of virus-derived RNA-seq reads in AM-MB2 plants (gray bars) compared to those plants superinfected with SPCSV (salmon bars). Individual viruses are indicated, and for each one the average and standard deviation are plotted. The inset with an extended scale was included to accommodate the large differences between the conditions. (C) Genomic organization of the SPFMV genome assembled from the RNA-seq data. The RNA genome of SPFMV is represented as a solid line flanked by a covalently linked VPg (solid circle) and the poly(A) tail, with the three ORFs corresponding to the polyprotein, PISPO, and PIPO depicted as boxes (details of the conserved G_2A_6 motifs are shown). Boxes with names represent the different gene products. (D) Percentages of RNA-seq reads with insertion of 1 nucleotide at the slippage sites in SPFMV. No other alterations were observed at these points, and the numbers show the values for two independent samples used for the RNA-seq analysis (see Table S7 in the supplemental material).

the truncated P1 (54 kDa), while in P1N-PISPOΔ, the pattern was similar to that for the unaltered P1 (compare first and third lanes in Fig. 3, and note the absence of evident products at the expected region for the truncated 47-kDa protein). The results of this experiment support the hypothesis that viral RNA polymerase slippage is the main mechanism that produces the out-of-frame product.

Identification of virus-derived proteins in agroinfiltrated plant tissue by LC-MS/MS analysis. A construct containing the wild-type P1-coding sequence and a construct designed to produce only P1N-PISPO (by insertion of a nucleotide in the G_2A_6 motif) were expressed by agroinfiltration in *N. benthamiana* leaves in the presence of P1b RSS from the unrelated ipomovirus cucumber vein yellowing virus (CVYV) (33). The P1b RSS was included to enhance protein expression levels. Total proteins present in the infiltrated patches were extracted and separated by SDS-PAGE, and the fraction above 50 kDa (to avoid the highly abundant RuBisCO) was excised and analyzed by LC-MS/MS.

The analysis identified more than 180 and 200 proteins in samples expressing the wild-type P1 and the mutant forced to produce P1N-PISPO, respectively. Most of the proteins corresponded to the host plant or to the *A. tumefaciens* bacteria used as the expression vector. In each sample, the overexpressed viral gene products were readily identified with high scores and coverage: for P1, a

Downloaded from http://jvi.asm.org/ on March 13, 2016 by guest

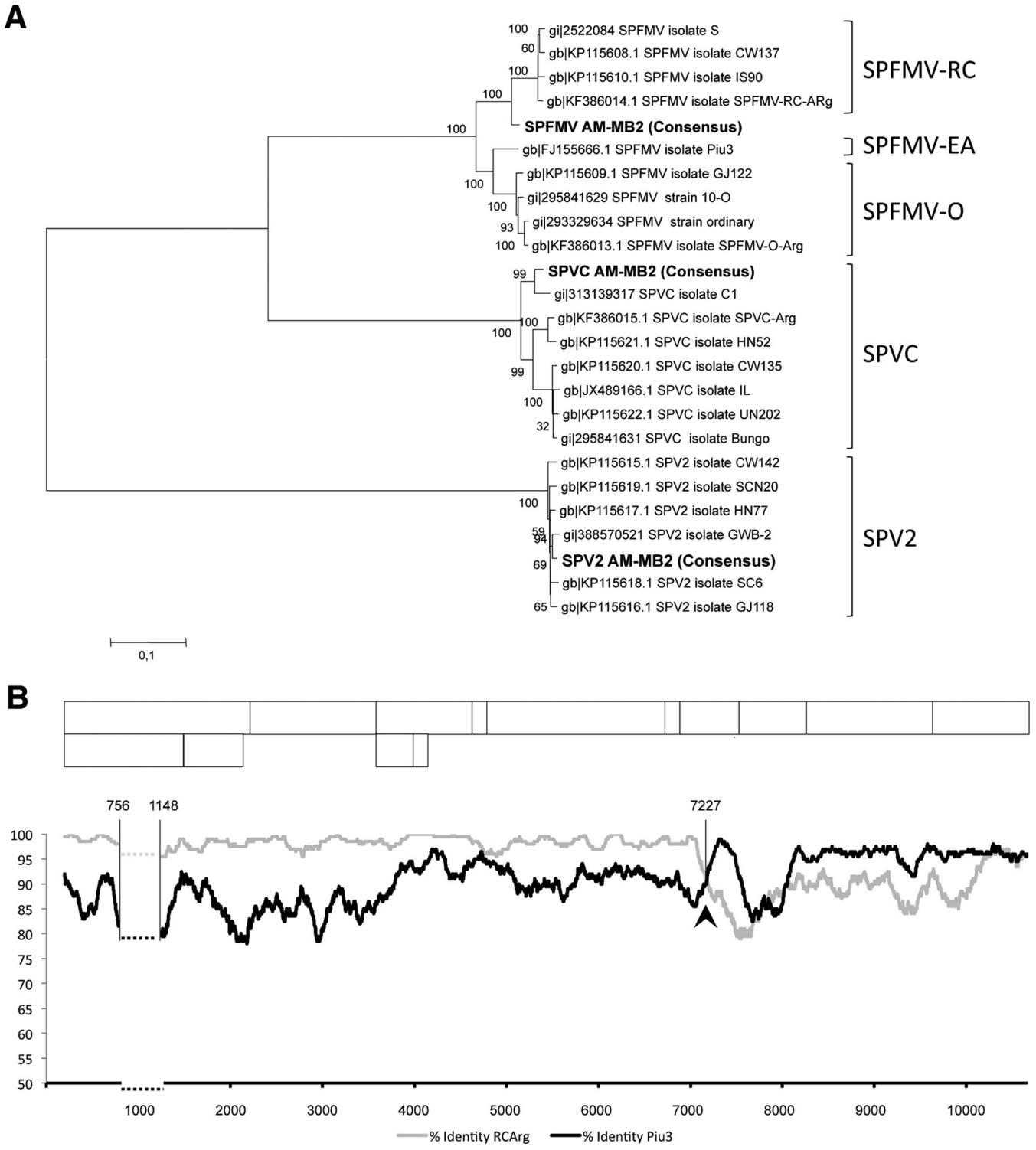

FIG 2 Taxonomic characterization of potyviruses from the AM-MB2 sweet potato plant. (A) Phylogenetic analysis of the complete nucleotide sequences corresponding to the three potyviruses found in AM-MB2 (highlighted in bold), compared to full-length sequences of SPFMV, SPVC, and SPV2 available in GenBank, using alignments and the maximum-likelihood algorithm to generate a tree with 1,000 replications for the bootstrapping test. (B) Plot of nucleotide identities between SPFMV isolate AM-MB2 and isolates Piu3 (EA strain) and RC-ARg (RC strain), after comparison with a sliding window of 100 nt. The recombination site detected by the SBP and GARD analysis is indicated with an arrowhead and the position number in the viral genome. The dashed horizontal lines correspond to a highly divergent region (between the indicated positions in the viral genome) with abundant gaps, which was eliminated to facilitate the global comparison. A schematic drawing of the expected gene products of SPFMV is shown above the plot to facilitate comparison of the recombination site.

Downloaded from http://jvi.asm.org/ on March 13, 2016 by guest

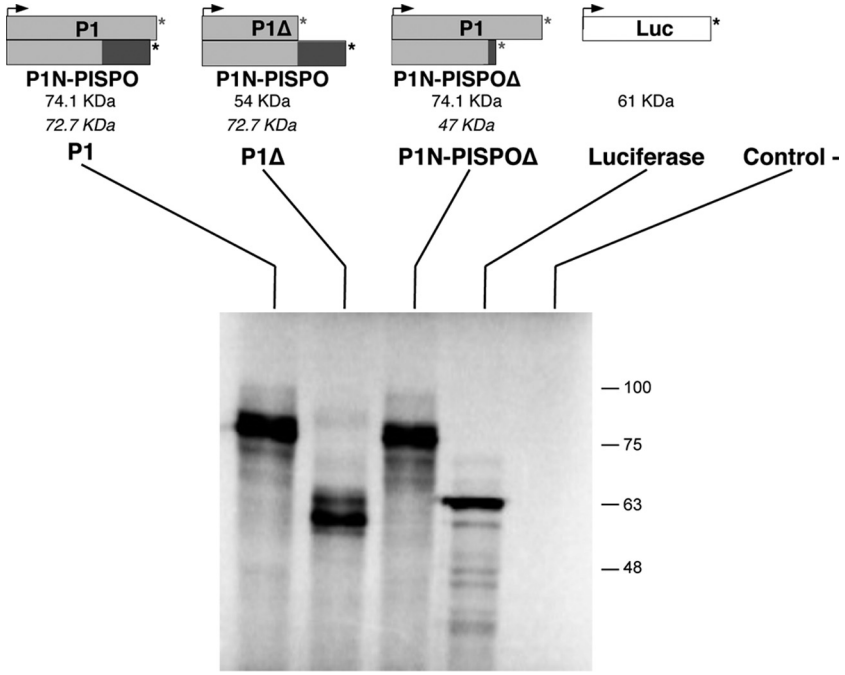

FIG 3 *In vitro* expression of P1-related products. Wild-type and variant constructs were designed to express selected proteins. Arrowheads and asterisks indicate the translation initiation sites (AUG) and stop codons, respectively. Truncated forms with stop codons introduced by mutagenesis are indicated by asterisks in gray. The expected sizes (in kDa) of the anticipated translated protein products are indicated below each construct, with italics used to indicate the *trans*-frame products expected in the case of translational frameshifting. Wheat germ extract was programmed with RNA transcripts, including a luciferase mRNA and water as controls. Each construct is connected to the lanes on the SDS-PAGE analysis of the proteins synthesized after *in vitro* translation and detected by autoradiography. The electrophoretic mobilities of molecular mass markers are shown at the right.

score of 97.38, 13 unique peptides, and 31.33% coverage; for P1N-PISPO, a score of 173.38, 25 unique peptides, and 46.02% coverage. Intriguingly, no peptides corresponding to the PISPO frame were found in the sample that expressed the wild-type P1 gene products.

In order to maximize the chance of detecting P1N-PISPO in further analysis of infected samples, a targeted search mode was adopted by using the information about true peptides derived from overexpression. The detected peptides corresponding to the transiently expressed viral gene products; their distributions along the amino acid sequences are shown in Fig. 4A and B, and complete details are provided in Table 1. The application of this targeted approach confirmed the absence of PISPO-derived peptides in plants transiently expressing wild-type P1. In addition, it also confirmed the identity of the expressed P1N-PISPO protein, as an identified peptide overlapped the frameshifted region and showed the amino acid introduced to force the frameshift (sequence, LVW**E**K [mutation in bold]) (Table 1).

Detection of SPFMV P1N-PISPO in infected sweet potato plants. Total proteins were extracted from plants infected with SPFMV AM-MB2, and the fraction corresponding to protein products of >50 kDa was subjected to LC-MS/MS analysis. The list of peptides corresponding to viral proteins included several gene products expected to accumulate during infection, such as P1, HCPro, CI, and NIb (all of them with sizes above the exclusion limit selected and translated from the long viral ORF). Detection was also positive for 4 peptides corresponding exclusively to the PISPO region of P1N-PISPO and thus derived from a *trans*-frame protein that incorporated PISPO (21.3% coverage). Along with these peptides, peptides corresponding to the P1 protein were detected from upstream of the polymerase slippage signal (11 different peptides, 39% coverage of the P1N region), and therefore common to P1 and P1N-PISPO, and from the C-terminal part (2 peptides, 10% coverage). Scores were 116.56 (13 peptides, 28.46% coverage) for P1 and 196.2 (15 peptides, 32.72% coverage) for P1N-PISPO.

Figure 4C summarizes the coverage and location of the peptides corresponding to the two alternative gene products from the P1 region, P1 and P1N-PISPO, which were present in infected sweet potato samples. Details on all identified virus-derived proteins and the individual peptides found in the analysis are provided in Table 2. Considering the exclusion limit (>50 kDa) used for sampling and that no smaller viral proteins, including the abundant CP (35.1 kDa), were detected by this analysis, our results are compatible with the simultaneous expression and accumulation of both P1 and P1N-PISPO (predicted to be 74.1 and 72.7 kDa, respectively).

P1N-PISPO is an RNA silencing suppressor. Once we determined that P1N-PISPO is produced in plants infected with SPFMV, we investigated putative functions for the novel gene product. Based on our previous experience with proteins encoded at the 5′ ends of potyviral genomes, we tested whether P1N-PISPO exhibits RNA silencing suppression activity. Constructs suitable for the transient expression of selected gene products (Fig. 5A) were coagroinfiltrated with a GFP-expressing construct, and the GFP fluorescence was monitored over time under UV light. Both positive and negative controls were included side-to-side with the tested constructs in the same leaves following the design depicted in

Downloaded from http://jvi.asm.org/ on March 13, 2016 by guest

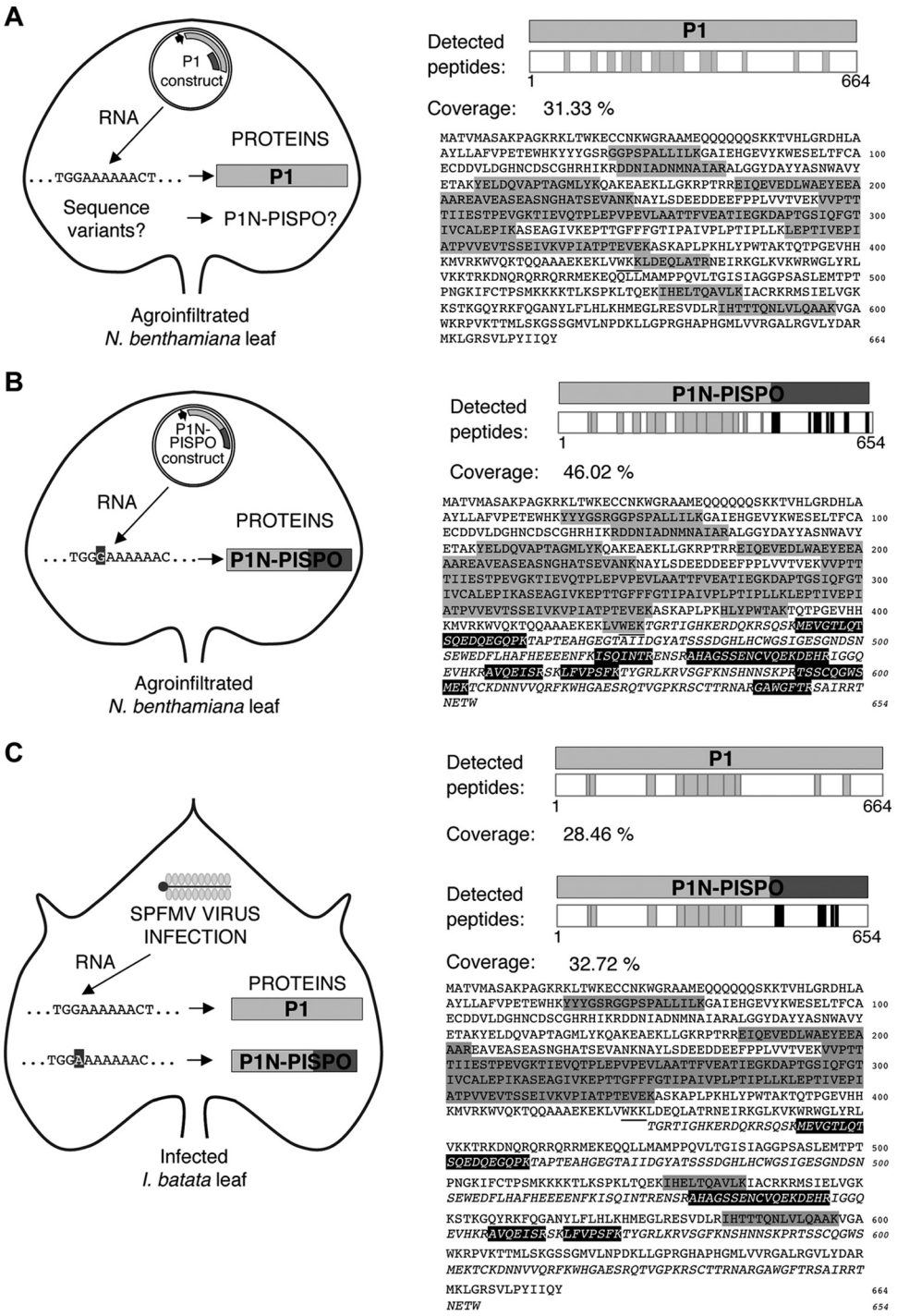

FIG 4 Identification of viral proteins by LC-MS/MS in plant samples. (A) Detection of peptides corresponding to proteins transiently expressed in *N. benthamiana* leaves agroinfiltrated with a construct that contains the wild-type P1 sequence of SPFMV under control of the appropriate promoter for overexpression. The plasmid construct is schematically drawn inside a leaf outline, with a detail of the expected RNA sequence corresponding to the G_2A_6 motif upstream of the PISPO starting point and the detected protein P1. A question mark besides the P1N-PISPO name indicates that no peptides corresponding to the PISPO domain were found in the analysis. The peptides detected are shown (as gray boxes) distributed along the P1 protein sequence in the right panel, and the percentage of coverage is indicated. The sequences of the detected peptides are shaded in gray on the sequence of the P1 gene product, and the frameshift point is underlined. (B) Detection of peptides as in panel A but in the sample agroinfiltrated with the P1N-PISPO construct, which ensures expression of the *trans*-frame product. The PISPO region is highlighted and is depicted in italic lettering in the sequence, starting at the underlined frameshift point. Peptides found in the analysis are shown as boxes (gray for P1N and black for PISPO) in the graphic and shaded in the sequence below, using a gray background in the case of peptides corresponding to the P1N or a black background with white letters for the PISPO region. (C) Detection of viral peptides in the AM-MB2 *I. batatas* plant. The virus SPFMV is represented by a schematic virion inside the outline of the sweet potato leaf, and two variants of viral RNAs with the G_2A_6 or G_2A_7 motifs are indicated (13). Peptides deriving from the common P1N region, from the P1 C-terminal region, and from PISPO are shown in the protein schemes, using gray for the common P1N part and the rest of P1, while the peptides found in the PISPO frame are represented by black boxes. The sequences of peptides are also highlighted in the sequence, with the two variants shown after the frameshift point (underlined), represented in the upper lines for P1 or in the lower (in italic) for PISPO and using as above a gray or black background in the sequence detail, respectively.

Downloaded from http://jvi.asm.org/ on March 13, 2016 by guest

Downloaded from http://jvi.asm.org/ on March 13, 2016 by guest

TABLE 1 SPFMV viral gene products transiently expressed on *N. benthamiana* plant tissue and detected by LC-MS/MS analysis

Sample	Viral protein	Score[a]	Coverage (%)	No. of unique peptides[b]	PSMs (Da)[c]	Size (aa)	Molecular mass (kDa)	Calculated pI	Peptides							
									Sequence[d]	Size (aa)	Position (aa)[e] Initial	Position (aa)[e] Final	Missed cleavages	MH^+ (Da)[f]	PSMs	PEP[g]
Agroinfiltrated P1 construct	P1	97.38	31.33	13 (10 + 3)	26	664	74.1	9.17	GGPSPALLILK	11	71	81	0	1,065.67009	2	0.02370553
									DDNIADNmNAIAR	13	122	134	0	1,448.64372	1	0.002282131
									DDNIADNMNAIAR	13	122	134	0	1,432.65166	1	0.000296073
									YELDQVAPTAGmLYK	15	155	169	0	1,714.84661	2	4.98689E−07
									YELDQVAPTAGMLYK	15	155	169	0	1,698.84929	2	1.07017E−06
									EIQEVEDLWAEYEEAAAR	18	186	203	0	2,150.99516	2	1.30644E−05
									EAVEASEASNGHATSEVANK	20	204	223	0	2,000.91977	1	0.009433393
									VVPTTTIIESTPEVGK	16	246	261	0	1,670.92717	2	5.91988E−05
									TIEVQTPLEPVPEVLAATTFVEATIEGK	28	262	289	0	2,982.59946	1	0.001826707
									DAPTGSIQFGTIVcALEPIK	20	290	309	0	2,117.09990	3	4.50031E−07
									LEPTIVEPIATPVVEVTSSEIVK	23	342	364	0	2,450.36716	4	0.000277995
									VPIATPTEVEK	11	365	375	0	1,183.65911	2	0.002508105
									KLDEQLATR	**9**	**424**	**432**	**1**	**1,073.59978**	**1**	**0.01176776**
									IHELTQAVLK	**10**	**527**	**536**	**0**	**1,151.67961**	**1**	**0.03467921**
									IHTTTQNLVLQAAK	**14**	**584**	**597**	**0**	**1,537.87314**	**1**	**0.000769235**
Agroinfiltrated P1N-PISPO construct	P1N-PISPO	173.38	46.02	25 (17 + 8)	58	654	72.7	6.47	YYYGSR	6	65	70	0	808.36339	2	0.05871485
									GGPSPALLILK	11	71	81	0	1,065.67095	2	0.01128503
									RDDNIADNmNAIAR	14	121	134	1	1,604.74381	1	0.001550777
									DDNIADNmNAIAR	13	122	134	0	1,448.64348	2	8.56681E−05
									YELDQVAPTAGmLYK	15	155	169	0	1,714.83550	2	2.69142E−05
									YELDQVAPTAGMLYK	15	155	169	0	1,698.84050	2	0.00018226
									EIQEVEDLWAEYEEAAAR	18	186	203	0	2,150.98906	5	4.48992E−07
									EAVEASEASNGHATSEVANK	20	204	223	0	2,000.91300	3	0.002131125
									VVPTTTIIESTPEVGK	16	246	261	0	1,670.92192	4	0.0003182
									TIEVQTPLEPVPEVLAATTFVEATIEGK	28	262	289	0	2,982.59671	5	0.02217205
									DAPTGSIQFGTIVcALEPIK	20	290	309	0	2,117.09770	4	6.45506E−06
									ASEAGIVKEPTTGFFFGTIPAIVPLPTIPLLK	32	310	341	1	3,324.89353	2	0.00897333
									ASEAGIVK	8	310	317	0	774.43566	1	0.02094499
									EPTTGFFFGTIPAIVPLPTIPLLK	24	318	341	0	2,569.48111	2	0.000227663
									LEPTIVEPIATPVVEVTSSEIVKVPIATPTEVEK	34	342	375	1	3,615.00620	2	0.008460695
									LEPTIVEPIATPVVEVTSSEIVK	23	342	364	0	2,450.37339	5	3.8468E−06
									VPIATPTEVEK	11	365	375	0	1,183.65825	2	0.008864285
									HLYPWTAK	8	384	391	0	1,015.53710	1	0.1502403
									LVWEK	**5**	***420***	***424***	**0**	**674.38786**	**1**	**0.14696**
									mEVGTLQTSQEDQEGQPK	**18**	***443***	***460***	**0**	**2,020.91570**	**1**	**9.41641E−07**
									ISQINTR	**7**	***519***	***525***	**0**	**831.46898**	**2**	**0.02658513**
									AHAGSSENcVQEKDEHR	**17**	***530***	***546***	**1**	**1,953.85525**	**2**	**2.32708E−07**
									AVQEISR	**7**	***556***	***562***	**0**	**802.44304**	**1**	**0.02908999**
									LFVPSFK	**7**	***565***	***571***	**0**	**837.48924**	**1**	**0.08113639**
									TSScQGWSmEK	**11**	***593***	***603***	**0**	**1,316.52410**	**1**	**0.005354153**
									GAWGFTR	**7**	***598***	***604***	**0**	**794.39562**	**2**	**0.1082382**

[a] Sum of the SEQUEST scores of the individual peptides.

[b] Number of identified peptide sequences (peptide spectrum matches) for the protein, including those redundantly identified. In parentheses are indicated the number of common peptides (corresponding to the N-terminal part of the protein, upstream of the G_2A_6 motif) followed by the differential ones (for the alternative C-terminal part of the P1 or PISPO sequence).

[c] Protonated monoisotopic mass of the peptides.

[d] Modifications are indicated by lowercase letters (m, oxidation; c, carbamidomethyl). The alternative C-terminal parts of P1 or PISPO sequences are in bold.

[e] Positions in the predicted genomic-frame polyprotein. Numbers in italic corresponded to the + 2 frame of PISPO continuing P1N.

[f] Protonated monoisotopic mass of the peptides.

[g] Posterior error probability, i.e., probability that the observed PSM is incorrect.

TABLE 2 SPFMV viral gene products identified by LC-MS/MS analysis of sweet potato tissue samples infected with SPFMV AM-MB2

Viral protein	Score[a]	Coverage (%)	No. of unique peptides[b]	PSMs (Da)[c]	Size (aa)	Molecular mass (kDa)	Calculated pI	Peptides							
								Sequence[d]	Size (aa)	Position (aa)[e] Initial	Position (aa)[e] Final	Missed cleavages	MH$^+$ (Da)[f]	PSMs	PEP[g]
P1N-PISPO	196.22	32.72	15 (11 + 4)	70	654	72.7	6.47	YYYGSR	6	65	70	0	808.36315	1	0.05593261
								GGPSPALLILK	11	71	81	0	1,065.66899	1	0.004198602
								EIQEVEDLWAEYEEAAAR	18	186	203	0	2,150.99101	2	3.99548E−09
								VVPTTTIIESTPEVGK	16	246	261	0	1,670.91252	3	3.90719E−05
								TIEVQTPLEPVPEVLAATTFVEATIEGK	28	262	289	0	2,982.58792	7	3.90915E−06
								DAPTGSIQFGTIVcALEPIK	20	290	309	0	2,117.08965	2	5.44594E−08
								ASEAGIVKEPTTGFFFGTIPAIVPLPTIPLLK	32	310	341	1	3,324.87595	4	0.000152128
								ASEAGIVK	8	310	317	0	774.43645	1	0.03614698
								EPTTGFFFGTIPAIVPLPTIPLLK	24	318	341	0	2,569.46390	6	6.45971E−06
								LEPTIVEPIATPVVEVTSSEIVK	24	342	365	0	2,450.36588	1	2.7674E−05
								VPIATPTEVEK	11	365	375	0	1,183.65666	3	0.01060038
								mEVGTLQTSQEDQEGQPK	**18**	***443***	***460***	**0**	**2,020.91277**	**15**	**4.60753E−10**
								AHAGSSENcVQEKDEHR	**17**	***530***	***546***	**1**	**1,953.84780**	**9**	**5.28656E−08**
								AVQEISR	**7**	***556***	***562***	**0**	**802.44170**	**3**	**0.2101074**
								LFVPSFK	**7**	***565***	***571***	**0**	**837.48723**	**12**	**0.007931116**
P1	116.56	28.46	13 (11 + 2)	35	664	74.1	9.17	YYYGSR	6	65	70	0	808.36315	1	0.05593261
								GGPSPALLILK	11	71	81	0	1,065.66899	1	0.004198602
								EIQEVEDLWAEYEEAAAR	18	186	203	0	2,150.99101	2	3.99548E−09
								VVPTTTIIESTPEVGK	16	246	261	0	1,670.91252	3	3.90719E−05
								TIEVQTPLEPVPEVLAATTFVEATIEGK	28	262	289	0	2,982.58792	7	3.90915E−06
								DAPTGSIQFGTIVcALEPIK	20	290	309	0	2,117.08965	2	5.44594E−08
								ASEAGIVKEPTTGFFFGTIPAIVPLPTIPLLK	32	310	341	1	3,324.87595	4	0.000152128
								ASEAGIVK	8	310	317	0	774.43645	1	0.03614698
								EPTTGFFFGTIPAIVPLPTIPLLK	24	318	341	0	2,569.46390	6	6.45971E−06
								LEPTIVEPIATPVVEVTSSEIVK	24	342	365	0	2,450.36588	1	2.7674E−05
								VPIATPTEVEK	11	365	375	0	1,183.65666	3	0.01060038
								IHELTQAVLK	**10**	**527**	**536**	**0**	**1,151.67827**	**2**	**0.1482055**
								IHTTTQNLVLQAAK	**14**	**584**	**597**	**0**	**1,537.86948**	**2**	**0.2301637**
CI	45.28	19.75	9	21	643	72.2	7.25	STGLPFYLSR	10	1617	1626	0	1,140.60686	3	5.92849E−05
								VLLLEPTRPLAENVHR	16	1630	1645	0	1,857.07461	5	1.30016E−05
								EVEFTTQYPVQIK	13	1735	1747	0	1,581.81047	3	5.24599E−06
								VGNVEIQTcGSPQKK	15	1810	1824	1	1,644.83823	2	0.023518
								GPISYGER	8	1867	1874	0	878.43834	3	0.004448509
								GVTGWLSVGEYAK	13	1991	2003	0	1,366.70268	1	0.000104976
								YKHEAGFGR	9	2038	2046	1	1,064.52701	2	3.29513E−05
								IScINScK	8	2047	2054	0	981.45098	2	0.02123955
								VAYTLQTDLYAIPR	14	2055	2068	0	1,623.87663	1	4.87008E−05
								TVSSSSFTLNSIATLWR	17	2094	2110	0	1,869.97112	3	3.39834E−08

[a] Sum of the SEQUEST scores of the individual peptides. The different viral proteins are listed according to their scores.
[b] Number of identified peptide sequences (peptide spectrum matches) for the protein, including those redundantly identified. In parentheses are indicated the number of common peptides (corresponding to the N-terminal part of the protein, upstream of the G_2A_6 motif) followed by the differential ones (for the alternative PISPO or C-terminal part of P1 sequences).
[c] Protonated monoisotopic mass of the peptides.
[d] Modifications are indicated by lowercase letters (m, oxidation; c, carbamidomethyl). The alternative for PISPO or the alternative C-terminal part of P1 sequences is in bold.
[e] Positions in the predicted genomic-frame polyprotein. Numbers in italic corresponded to the + 2 frame of PISPO continuing P1N.
[f] Protonated monoisotopic mass of the peptides.
[g] Posterior error probability, i.e., probability that the observed PSM is incorrect.

Downloaded from http://jvi.asm.org/ on March 13, 2016 by guest

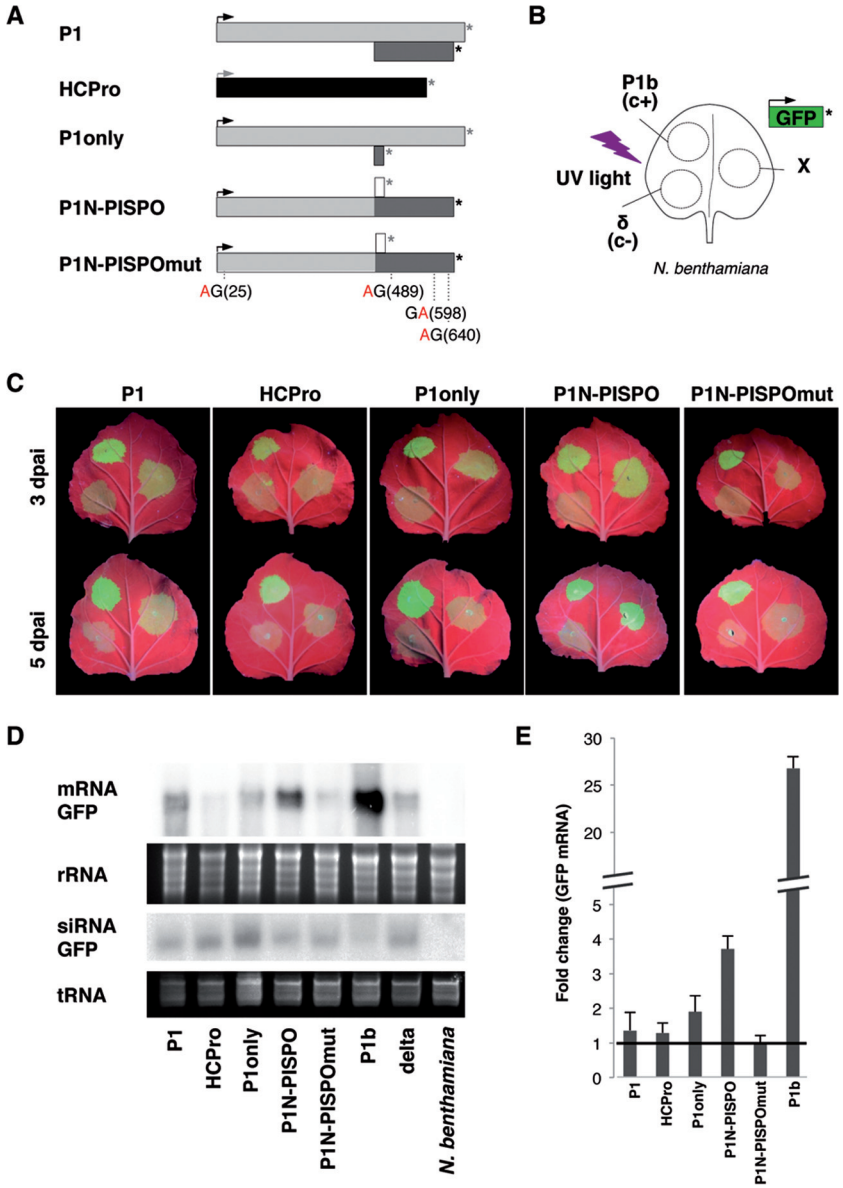

FIG 5 RNA silencing suppression activity of SPFMV P1N-PISPO. (A) The constructs used are represented with the same conventions as in the other figures for AUG and stop codons. The distribution of the four WG/GW motifs present in the sequence (positions in parentheses) in the mutant in which the four W residues were replaced by A residues is indicated. (B) Patch design used for coagroinfiltration in *N. benthamiana* leaves of a GFP-expressing construct together with other constructs expressing SPFMV products (indicated by X), a CVYV P1b positive control (c+), or an empty vector (δ, c−). (C) Pictures of representative agroinfiltrated leaves taken at 3 (top row) or 5 (bottom row) days postagroinfiltration (dpai) under UV light. (D) Northern blot analysis of GFP mRNA and siRNA extracted from agroinfiltrated tissue patches at 3 dpai, comparing the different constructs indicated above each lane. The bottom panels show the ethidium bromide staining of the gels as loading controls. (E) Relative accumulation of GFP mRNAs measured by specific RT-qPCR and normalized against the mean value corresponding to the negative control. The average values ± standard deviations from several experiments, each performed with at least three independent *Agrobacterium* cultures, are plotted. Significant difference in pairwise comparisons and after applying the Tukey-Kramer test were found only for the positive control CVYV P1b (shown with a broken axis to accommodate the large difference) and for the P1N-PISPO samples.

Fig. 5B. The experiment was repeated several times, using at least three independent *Agrobacterium* cultures of each construct.

Compared to other individual SPFMV gene products, only P1N-PISPO showed clear RNA silencing suppression activity at 3 and 5 days postagroinfiltration (dpai) in the visual assay (Fig. 5C), which correlated with higher accumulation of GFP mRNA as observed by Northern blotting (Fig. 5D) and RT-qPCR (Fig. 5E). Differences in GFP fluorescence and accumulation of GFP mRNA between the CVYV P1b positive control and P1N-PISPO suggest that the last is a weaker RSS. This was confirmed by the RT-qPCR analysis, which showed around 5-times-higher levels of GFP mRNA in the presence of P1b (Fig. 5E).

As expected from previous results (18, 36) CVYV P1b prevented to certain extent the generation of GFP-derived siRNAs, while a clear similar effect was not observed for P1N-PISPO (Fig. 5D), suggesting that these two viral proteins might use different mechanisms to suppress the RNA silencing, as we propose below.

Downloaded from http://jvi.asm.org/ on March 13, 2016 by guest

Constructs expressing P1 (wild-type P1 sequence) and P1 only (P1 with an out-of-frame stop codon precluding any expression of PISPO) failed to exhibit enough noticeable RNA silencing suppression activity in our assays. Interestingly, the construct expressing HCPro also failed to exhibit RSS activity, with quantitative values always below those obtained for P1 (Fig. 5C, D, and E). The same P1 and P1N-PISPO constructs tested for RSS activity were used in the LC-MS/MS experiments described above. Although it is not a quantitative assay, the detection of similar numbers of specific peptides in both cases (Table 1) suggests that P1 and P1N-PISPO accumulated at comparable levels in agroinfiltrated leaves in the presence of a heterologous RSS. Hence, these results support the idea that the absence of noticeable silencing suppression activity by the P1 construct is not due to problems in protein expression, accumulation, or stability.

WG/GW motifs play important roles in interactions with Argonaute (Ago) proteins and small RNA binding necessary for activity of some RSSs (18, 19, 42, 43). All four WG/GW motifs present in P1N-PISPO were mutated to AG/GA. The mutated variant (P1N-PISPOmut) was agroinfiltrated in *N. benthamiana* leaves, along with the GFP-expressing construct, to evaluate its activity as an RSS. The mutated product failed to counteract the RNA silencing, as shown by GFP fluorescence under UV light, GFP mRNA Northern blots, and RT-qPCR quantification of GFP mRNA (Fig. 5C to E).

DISCUSSION

Among all the known members of the *Potyvirus* genus (158 species according to the International Committee of Taxonomy of Viruses [ICTV] [2014] release), SPFMV presents several peculiarities. First, its genome is the largest, with an extraordinarily long P1 region (664 to 724 aa), which is surpassed in the *Potyviridae* family only by the equivalent P1 product of the ipomovirus SPMMV (758 aa), which shares some similarity with SPFMV P1 in the N-terminal region (7). The bioinformatic prediction of the additional ORF PISPO within the P1-coding sequence (4, 44) added a further peculiarity, although it was unknown until now whether PISPO was expressed. Our results shed light on these aspects of SPFMV biology, first by demonstrating that the predicted *trans*-framed P1N-PISPO product is expressed during SPFMV infection and then by finding that P1N-PISPO contributes to counteract the RNA silencing-based plant defense to viral infection.

These results might be especially relevant in the context of the devastating and widespread sweet potato viral disease (SPVD) (4, 39). In contrast to many other synergisms involving potyviruses (see reference 45 and references therein), sweet potato viral disease is considered atypical because the potyvirus is the partner with a boost in its accumulation. Although we have confirmed this previous observation with our plant material, many important aspects still remain to be explained. For instance, further research is needed to elucidate whether the rather peculiar RNase 3 RSSs from SPCSV (46–48) and P1N-PISPO are involved in the outcome of this complex interaction. In line with that, another interesting but unexpected observation of our work is related to this unusual synergism: we have noticed a specific reduction in RNA slippage frequency at the PISPO site, but not in PIPO, in plants superinfected with SPCSV (Fig. 1). The different roles of P1N-PISPO and P3N-PIPO during viral infection, named suppression of RNA silencing (this report) or viral movement (9–11), respectively, might provide clues not only to explain this observation but also to understand how changes in the relative amounts of these two gene products could affect the outcome of SPVD in the coinfected plants.

The novel potyviral gene product P1N-PISPO (654 aa, 72.7 kDa) combines a P1N part shared with the canonical P1 (N-terminal portion of 422 aa, equivalent to a 46.5-kDa protein fragment) and the PISPO sequence (232 aa, fragment of 26.1 kDa). The product is similar in size to P1 (664 aa, 74.1 kDa) but with notable differences, including, for instance, the predicted isoelectric points of the two proteins: 9.24 for P1 and 6.17 for P1N-PISPO. Interestingly, an isoelectric point of slightly below 7 is a hallmark of P1s displaying RNA silencing suppression activity in other potyvirids (7).

The expression of P1N-PISPO is likely to result from the translation of RNA variants with a G_2A_7 sequence, generated by polymerase slippage in a G_2A_6 conserved motif (13). This mechanism of expression is supported by examination of sequences corresponding to different potyviruses present in the virome of the AM-MB2 plant, which showed results consistent with polymerase slippage in equivalent G_2A_6 motifs for SPV2 and SPVC (see Table S7 in the supplemental material). Moreover, our experiments designed to identify translational frameshifting in WGE failed to show a noticeable production of truncated frameshifted protein products, and the presence of minor products compatible in size could be also generated by T7 polymerase slippage, as shown by others (14, 49, 50). Consistent with our view that viral RNA polymerase slippage is the most likely mechanism of production of out-of-frame products in potyviruses, the transient expression of wild-type P1 sequence out of the viral infection context resulted in the production only of P1-derived peptides when analyzed with the sensitive mass spectrometry technique (Fig. 4A). Altogether, a strong case can be proposed for viral polymerase transcriptional slippage as the mechanism used to produce the *trans*-frame P1N-PISPO, and likely the same conclusion can be expanded to P3N-PIPO proteins found in all other potyvirids. The combination of our analysis with SPFMV, SPVC, and SPV2 suggests that polymerase slippage might occur in all sweet potato potyviruses where the PISPO sequence was predicted (4).

When facing the challenge of detecting a previously unknown gene product that was predicted bioinformatically, we decided to adopt a straightforward approach using mass spectrometry. Similar techniques have been used previously to identify viral infections in plants, including those produced for potyviruses (51), but to our knowledge, this is the first time that it serves to demonstrate that an out-of-frame gene product is being expressed in infected plant tissues. We believe that this new method is a convenient approach that gives fast and unequivocal proof of protein translation without the need of obtaining specific antibodies, which is a time-consuming procedure that may fail depending on the antigenicity of the target protein. Mass spectrometry allowed unambiguous detection of both P1 and P1N-PISPO together in the same sample, showing that the two gene products coexist in infected plants. Although the methodology is not quantitative, the abundance and number of peptides might provide some indication of the expression levels and the stability of the mature proteins. For example, compared to another large viral product, CI, the high coverage obtained for P1 and P1N-PISPO suggests that these two proteins are quite stable. While we have shown mass spectrometry to be a useful method for identifying novel gene products, further research is required to determine the turnover

Downloaded from http://jvi.asm.org/ on March 13, 2016 by guest

and subcellular localization of P1N-PISPO during the infection cycle and to evaluate its impact in pathogenicity.

The functions of potyviral P1s have remained elusive for many years, but recent results are revealing the importance of P1 during potyvirus infection (32, 52). In the case of SPFMV and other potyviruses infecting sweet potato, the presence of P1N-PISPO adds a further layer of complexity to efforts to unravel the role(s) of these gene products in the infection context (53). To start addressing this, our experiments show a clear role for P1N-PISPO as an RSS. Interestingly, for all the members of the *Potyvirus* genus tested so far, the essential RNA silencing suppression activity was found associated with HCPro, which was the first characterized RSS (54, 55). In other members of the *Potyviridae* family, however, the RNA silencing suppression function is often shifted to P1 products, as has been observed in ipomoviruses (18, 33, 56), tritimoviruses (57), and poaceviruses (58). These RSSs belong to a distinct group of P1 proteins that appears to be evolutionarily separated from typical P1 proteins of members of the genus *Potyvirus* (7, 59). Our finding that the P1N-PISPO product acts as an RSS would serve to expand this list of known P1-related sources of RNA silencing suppression activity in the family *Potyviridae* and might help in our understanding of the evolutionary acquisition of this important viral function.

Whereas the P1b protein of the ipomovirus CVYV displays a strong RSS activity that depends on its ability to bind small RNAs (36), the P1 protein of SPMMV suppresses RNA silencing by interfering with RISC activity, specifically through blocking Ago binding via WG/GW hooks (18). Interestingly, a recent study showed that the native SPFMV P1, which shares noticeable sequence similarity with SPMMV P1 (7), does not work as an RSS but gains this functionality when mutations are introduced to create additional WG/GW motifs in positions near the ones present in SPMMV P1 (60). In our experiments, P1 also failed to show a clear RSS activity, confirming the observations of Szabó and coworkers (60).

Our result that an SPFMV P1N-PISPO variant in which all the WG/GW motifs have been mutated loses RNA silencing suppression activity suggests that P1N-PISPO disrupts RNA silencing by a mechanism involving Ago hooks, similar to that of SPMMV P1 (18). The fact that the silencing activities of SPFMV P1N-PISPO and SPMMV P1 are both quite weak further supports the hypothesis that these suppressors share a similar mechanism of action. However, we cannot rule out that the correlation between functionality and presence of WG/GW in SPFMV P1N-PISPO could correspond to Ago-independent disturbances caused, for instance, by conformational alterations derived from mutations of W residues, as might be the case in other RSSs (42).

Giner and coworkers suggested that the expression of a weak RSS in SPMMV could be a viral strategy to cause only mild damage in the host, allowing sweet potato potyvirids to survive in infected perennial plants for an extended period (18). This idea is in agreement with the weak RSS activity of SPFMV P1N-PISPO. We can also speculate that sweet potato potyvirids might not depend exclusively on the weak RNA silencing suppression activities of their P1N-PISPOs found here and that other viral products could help to counteract RNA silencing during infection. In this regard, for instance, the VPg of the potyvirus PVA has been found to counteract RNA silencing (46, 61). Additionally, the levels of expression of HCPro in other potyviruses were reported to be regulated by P1 (62). In the case of SPFMV, although our transient agroinfiltration experiments with individual gene products showed no clear antisilencing activity for P1 or HCPro, preliminary results suggest that P1-HCPro might display some activity. Taking into account that the expression of the P1 construct by agroinfiltration does not produce P1N-PISPO (Fig. 4), contributions of P1 and/or HCPro to silencing suppression during SPFMV infection cannot be ruled out. Indeed, the context of the viral infection is quite different from that in the transient agroinfiltration assays, and therefore further work will be needed to fully understand the modes of action and the relationships of all viral factors that might be participating in counteracting the RNA silencing-based host defenses.

The switch of the antisilencing role from established suppressors such as HC-Pro or P1 (the strength of which could be adjusted through regular mutation/selection processes) to P1N-PISPO with its rather peculiar expression mechanism deserves some attention from an evolutionary point of view. As mentioned above, whereas the main RNA silencing suppression activity lies with HCPro in members of the genus *Potyvirus*, it is supplied by a P1-type protein in ipomoviruses, tritimoviruses, and poaceviruses, likely highlighting two evolutionary lineages in the family *Potyviridae*. Thus, we can speculate that the existence of a P1-related RNA silencing suppressor in the potyvirus SPFMV could be the result of a recombination event between a potyvirus and an ipomovirus in sweet potato, which is supported by the notable similarity between the N termini of the P1 proteins from SPFMV and the ipomovirus SPMMV (7).

Importantly, the fact that all members of the potyvirids produce P3N-PIPO suggests that this gene product appeared very early in the evolutionary history of these viruses. Potential strategies developed to deal with risks associated with RNA polymerase slippage, such as genomic modifications in the viral progeny (14, 63) or those derived from mRNA decay (64), could have favored the more recent emergence of P1N-PISPO in a subset of potyviruses. Thus, understanding how potyvirids counteract problems derived from this peculiar gene expression mechanism will certainly deserve further experimental work.

To summarize, our results highlight the enormous genomic flexibility of viruses, which allows them to profit from particular biochemical features of their gene products, such as the slippage capacity of the RNA polymerase, to expand their gene dotation and explore alternative pathways to improve adaptation to a variety of host and environmental conditions.

ACKNOWLEDGMENTS

This work was funded by Mineco grants AGL2013-42537-R to J.J.L.-M. and BIO2013-49053-R to J.A.G. and by Plant KBBE PCIN-2013-056 to J.A.G. A.M. is a recipient of FPI fellowship BES-2011-045699. D.C.B. is the Royal Society Edward Penley Abraham Research Professor.

We thank Jesús Navas (IHSM-UMA-CSIC La Mayora, Málaga, Spain) for providing us with SPCSV-infected material and the anonymous reviewers for their insightful contributions. We acknowledge the assistance of Eliandre de Oliveira and María Antonia Odena (Proteomics Platform of Barcelona Science Park, UB, a member of the ProteoRed-ISCIII network). We also thank Claire Agius for valuable help.

Downloaded from http://jvi.asm.org/ on March 13, 2016 by guest

FUNDING INFORMATION

Ministerio de Economía y Competitividad (MINECO) provided funding to Juan José López-Moya under grant number AGL2013-42537-R. Ministerio de Economía y Competitividad (MINECO) provided funding to Juan Antonio Garcia under grant number BIO2013-49053-R. EC | Directorate-General for Research and Innovation provided funding to Juan Antonio Garcia under grant number Plant KBBE PCIN-2013-056.

The funders had no role in study design, data collection and interpretation, or the decision to submit the work for publication.

ADDENDUM IN PROOF

During the preparation of this work, we became aware that another paper on the same subject arrived at equivalent conclusions (Untiveros M, Olspert A, Artola K, Firth AE, Kreuze JF, Valkonen JP, Mol Plant Pathol, http://dx.doi.org/10.1111/mpp.12366, in press).

REFERENCES

1. **Valli A, García JA, López-Moya JJ.** 2015. Potyviridae, p 1–10. *In* Encyclopedia of life sciences. John Wiley & Sons, Ltd., Chichester, United Kingdom.
2. **Revers F, García JA.** 2015. Molecular biology of potyviruses. Adv Virus Res **92:**101–199. http://dx.doi.org/10.1016/bs.aivir.2014.11.006.
3. **Chung BY-W, Miller WA, Atkins JF, Firth AE.** 2008. An overlapping essential gene in the Potyviridae. Proc Natl Acad Sci U S A **105:**5897–5902. http://dx.doi.org/10.1073/pnas.0800468105.
4. **Clark CA, Davis JA, Abad JA, Cuellar WJ, Fuentes S, Kreuze JF, Gibson RW, Mukasa SB, Tugume AK, Tairo FD, Valkonen JPT.** 2012. Sweetpotato viruses: 15 years of progress on understanding and managing complex diseases. Plant Dis **96:**168–185. http://dx.doi.org/10.1094/PDIS-07-11-0550.
5. **Sakai J, Mori M, Morishita T, Tanaka M, Hanada K, Usugi T, Nishiguchi M.** 1997. Complete nucleotide sequence and genome organization of sweet potato feathery mottle virus (S strain) genomic RNA: the large coding region of the P1 gene. Arch Virol **142:**1553–1562. http://dx.doi.org/10.1007/s007050050179.
6. **Verchot J, Koonin EV, Carrington JC.** 1991. The 35-kDa protein from the N-terminus of the potyviral polyprotein functions as a third virus-encoded proteinase. Virology **185:**527–535. http://dx.doi.org/10.1016/0042-6822(91)90522-D.
7. **Valli A, López-Moya JJ, García JA.** 2007. Recombination and gene duplication in the evolutionary diversification of P1 proteins in the family *Potyviridae*. J Gen Virol **88:**1016–1028. http://dx.doi.org/10.1099/vir.0.82402-0.
8. **Choi SH, Hagiwara-Komoda Y, Nakahara KS, Atsumi G, Shimada R, Hisa Y, Naito S, Uyeda I.** 2013. Quantitative and qualitative involvement of P3N-PIPO in overcoming recessive resistance against *Clover yellow vein virus* in pea carrying the cyv1 gene. J Virol **87:**7326–7337. http://dx.doi.org/10.1128/JVI.00065-13.
9. **Wen RH, Hajimorad MR.** 2010. Mutational analysis of the putative pipo of soybean mosaic virus suggests disruption of PIPO protein impedes movement. Virology **400:**1–7. http://dx.doi.org/10.1016/j.virol.2010.01.022.
10. **Vijayapalani P, Maeshima M, Nagasaki-Takekuchi N, Miller WA.** 2012. Interaction of the trans-frame potyvirus protein P3N-PIPO with host protein PCaP1 facilitates potyvirus movement. PLoS Pathog **8:**e1002639. http://dx.doi.org/10.1371/journal.ppat.1002639.
11. **Wei T, Zhang C, Hong J, Xiong R, Kasschau KD, Zhou X, Carrington JC, Wang A.** 2010. Formation of complexes at plasmodesmata for potyvirus intercellular movement is mediated by the viral protein P3N-PIPO. PLoS Pathog **6:**e1000962. http://dx.doi.org/10.1371/journal.ppat.1000962.
12. **Hisa Y, Suzuki H, Atsumi G, Choi SH, Nakahara KS, Uyeda I.** 2014. P3N-PIPO of *Clover yellow vein virus* exacerbates symptoms in pea infected with *White clover mosaic virus* and is implicated in viral synergism. Virology **449:**200–206. http://dx.doi.org/10.1016/j.virol.2013.11.016.
13. **Rodamilans B, Valli A, Mingot A, San León D, Baulcombe D, López-Moya JJ, García JA.** 2015. RNA polymerase slippage as a mechanism for the production of frameshift gene products in plant viruses of the *Potyviridae* family. J Virol **89:**6965–6967. http://dx.doi.org/10.1128/JVI.00337-15.
14. **Olspert A, Chung BY-W, Atkins JF, Carr JP, Firth AE.** 2015. Transcriptional slippage in the positive-sense RNA virus family *Potyviridae*. EMBO Rep **16:**995–1004. http://dx.doi.org/10.15252/embr.201540509.
15. **Baulcombe D.** 2004. RNA silencing in plants. Nature **431:**356–363. http://dx.doi.org/10.1038/nature02874.
16. **Valli A, López-Moya JJ, García JA.** 2009. RNA silencing and its suppressors in the plant-virus interplay, p 1–29. *In* Encyclopedia of life sciences. John Wiley & Sons, Ltd., Chichester, United Kingdom.
17. **Csorba T, Kontra L, Burgyán J.** 2015. Viral silencing suppressors: Tools forged to fine-tune host-pathogen coexistence. Virology **479–480:**85–103. http://dx.doi.org/10.1016/j.virol.2015.02.028.
18. **Giner A, Lakatos L, García-Chapa M, López-Moya JJ, Burgyán J.** 2010. Viral protein inhibits RISC activity by argonaute binding through conserved WG/GW motifs. PLoS Pathog **6:**e1000996. http://dx.doi.org/10.1371/journal.ppat.1000996.
19. **Azevedo J, Garcia D, Pontier D, Ohnesorge S, Yu A, Garcia S, Braun L, Bergdoll M, Hakimi MA, Lagrange T, Voinnet O.** 2010. Argonaute quenching and global changes in Dicer homeostasis caused by a pathogen-encoded GW repeat protein. Genes Dev **24:**904–915. http://dx.doi.org/10.1101/gad.1908710.
20. **Langmead B, Salzberg SL.** 2012. Fast gapped-read alignment with Bowtie 2. Nat Methods **9:**357–359. http://dx.doi.org/10.1038/nmeth.1923.
21. **Wright CF, Morelli MJ, Thébaud G, Knowles NJ, Herzyk P, Paton DJ, Haydon DT, King DP.** 2011. Beyond the consensus: dissecting within-host viral population diversity of foot-and-mouth disease virus by using next-generation genome sequencing. J Virol **85:**2266–2275. http://dx.doi.org/10.1128/JVI.01396-10.
22. **Tamura K, Stecher G, Peterson D, Filipski A, Kumar S.** 2013. MEGA6: Molecular Evolutionary Genetics Analysis version 6.0. Mol Biol Evol **30:**2725–2729. http://dx.doi.org/10.1093/molbev/mst197.
23. **Töpfer A, Zagordi O, Prabhakaran S, Roth V, Halperin E, Beerenwinkel N.** 2013. Probabilistic inference of viral quasispecies subject to recombination. J Comput Biol **20:**113–123. http://dx.doi.org/10.1089/cmb.2012.0232.
24. **Martin DP, Lemey P, Lott M, Moulton V, Posada D, Lefeuvre P.** 2010. RDP3: a flexible and fast computer program for analyzing recombination. Bioinformatics **26:**2462–2463. http://dx.doi.org/10.1093/bioinformatics/btq467.
25. **Martin D, Rybicki E.** 2000. RDP: detection of recombination amongst aligned sequences. Bioinformatics **16:**562–563. http://dx.doi.org/10.1093/bioinformatics/16.6.562.
26. **Martin DP, Posada D, Crandall KA, Williamson C.** 2005. A modified bootscan algorithm for automated identification of recombinant sequences and recombination breakpoints. AIDS Res Hum Retroviruses **21:**98–102. http://dx.doi.org/10.1089/aid.2005.21.98.
27. **Smith JM.** 1992. Analyzing the mosaic structure of genes. J Mol Evol **34:**126–129.
28. **Kosakovsky Pond SL, Posada D, Gravenor MB, Woelk CH, Frost SDW.** 2006. GARD: a genetic algorithm for recombination detection. Bioinformatics **22:**3096–3098. http://dx.doi.org/10.1093/bioinformatics/btl474.
29. **Delport W, Poon AFY, Frost SDW, Kosakovsky Pond SL.** 2010. Datamonkey 2010: a suite of phylogenetic analysis tools for evolutionary biology. Bioinformatics **26:**2455–2457. http://dx.doi.org/10.1093/bioinformatics/btq429.
30. **Tanaka Y, Nakamura S, Kawamukai M, Koizumi N, Nakagawa T.** 2011. Development of a series of gateway binary vectors possessing a tunicamycin resistance gene as a marker for the transformation of Arabidopsis thaliana. Biosci Biotechnol Biochem **75:**804–807. http://dx.doi.org/10.1271/bbb.110063.
31. **Nakagawa T, Suzuki T, Murata S, Nakamura S, Hino T, Maeo K, Tabata R, Kawai T, Tanaka K, Niwa Y, Watanabe Y, Nakamura K, Kimura T, Ishiguro S.** 2007. Improved Gateway binary vectors: high-performance vectors for creation of fusion constructs in transgenic analysis of plants. Biosci Biotechnol Biochem **71:**2095–2100. http://dx.doi.org/10.1271/bbb.70216.
32. **Pasin F, Simón-Mateo C, García JA.** 2014. The hypervariable amino-terminus of P1 protease modulates potyviral replication and host defense responses. PLoS Pathog **10:**e1003985. http://dx.doi.org/10.1371/journal.ppat.1003985.
33. **Valli A, Martín-Hernández AM, López-Moya JJ, García JA.** 2006. RNA silencing suppression by a second copy of the P1 serine protease of *Cu-*

Downloaded from http://jvi.asm.org/ on March 13, 2016 by guest

cumber vein yellowing ipomovirus, a member of the family *Potyviridae* that lacks the cysteine protease HCPro. J Virol **80:**10055–10063. http://dx.doi.org/10.1128/JVI.00985-06.
34. **Carbonell A, Dujovny G, García JA, Valli A.** 2012. The *Cucumber vein yellowing virus* silencing suppressor P1b can functionally replace HCPro in *Plum pox virus* infection in a host-specific manner. Mol Plant Microbe Interact **25:**151–164. http://dx.doi.org/10.1094/MPMI-08-11-0216.
35. **Valli A, Dujovny G, García JA.** 2008. Protease activity, self interaction, and small interfering RNA binding of the silencing suppressor P1b from *Cucumber vein yellowing ipomovirus*. J Virol **82:**974–986. http://dx.doi.org/10.1128/JVI.01664-07.
36. **Valli A, Oliveros JC, Molnar A, Baulcombe D, García JA.** 2011. The specific binding to 21-nt double-stranded RNAs is crucial for the anti-silencing activity of *Cucumber vein yellowing virus* P1b and perturbs endogenous small RNA populations. RNA **17:**1148–1158. http://dx.doi.org/10.1261/rna.2510611.
37. **Leckie BM, Stewart CN, Jr.** 2011. Agroinfiltration as a technique for rapid assays for evaluating candidate insect resistance transgenes in plants. Plant Cell Rep **30:**325–334. http://dx.doi.org/10.1007/s00299-010-0961-2.
38. **Lacomme C, Hrubikova K, Hein I.** 2003. Enhancement of virus-induced gene silencing through viral-based production of inverted-repeats. Plant J **34:**543–553. http://dx.doi.org/10.1046/j.1365-313X.2003.01733.x.
39. **Karyeija RF, Kreuze JF, Gibson RW, Valkonen JP.** 2000. Synergistic interactions of a potyvirus and a phloem-limited crinivirus in sweet potato plants. Virology **269:**26–36. http://dx.doi.org/10.1006/viro.1999.0169.
40. **Untiveros M, Fuentes S, Kreuze J.** 2008. Molecular variability of *Sweet potato feathery mottle virus* and other potyviruses infecting sweet potato in Peru. Arch Virol **153:**473–483. http://dx.doi.org/10.1007/s00705-007-0019-0.
41. **Tugume AK, Cuellar WJ, Mukasa SB, Valkonen JP.** 2010. Molecular genetic analysis of virus isolates from wild and cultivated plants demonstrates that East Africa is a hotspot for the evolution and diversification of sweet potato feathery mottle virus. Mol Ecol **19:**3139–3156. http://dx.doi.org/10.1111/j.1365-294X.2010.04682.x.
42. **Pérez-Cañamás M, Hernández C.** 2015. Key importance of small RNA binding for the activity of a glycine-tryptophan (GW) motif-containing viral suppressor of RNA silencing. J Biol Chem **290:**3106–3120. http://dx.doi.org/10.1074/jbc.M114.593707.
43. **Chattopadhyay M, Stupina VA, Gao F, Szarko CR, Kuhlmann MM, Yuan X, Shi K, Simon AE.** 2015. Requirement for host RNA silencing components and the virus silencing suppressor when second-site mutations compensate for structural defects in the 3′ UTR. J Virol **89:**11603–11618. http://dx.doi.org/10.1128/JVI.01566-15.
44. **Li F, Xu D, Abad J, Li R.** 2012. Phylogenetic relationships of closely related potyviruses infecting sweet potato determined by genomic characterization of *Sweet potato virus G* and *Sweet potato virus 2*. Virus Genes **45:**118–125. http://dx.doi.org/10.1007/s11262-012-0749-2.
45. **Syller J.** 2012. Facilitative and antagonistic interactions between plant viruses in mixed infections. Mol Plant Pathol **13:**204–216. http://dx.doi.org/10.1111/j.1364-3703.2011.00734.x.
46. **Cuellar WJ, Kreuze JF, Rajamäki M-L, Cruzado KR, Untiveros M, Valkonen JPT.** 2009. Elimination of antiviral defense by viral RNase III. Proc Natl Acad Sci U S A **106:**10354–10358. http://dx.doi.org/10.1073/pnas.0806042106.
47. **Tugume AK, Amayo R, Weinheimer I, Mukasa SB, Rubaihayo PR, Valkonen JP.** 2013. Genetic variability and evolutionary implications of RNA silencing suppressor genes in RNA1 of sweet potato chlorotic stunt virus isolates infecting sweetpotato and related wild species. PLoS One **8:**e81479. http://dx.doi.org/10.1371/journal.pone.0081479.
48. **Weinheimer I, Jiu Y, Rajamäki M-L, Matilainen O, Kallijärvi J, Cuellar WJ, Lu R, Saarma M, Holmberg CI, Jäntti J, Valkonen JPT.** 2015. Suppression of RNAi by dsRNA-degrading RNaseIII enzymes of viruses in animals and plants. PLoS Pathog **11:**e1004711. http://dx.doi.org/10.1371/journal.ppat.1004711.
49. **Molodtsov V, Anikin M, McAllister WT.** 2014. The presence of an RNA:DNA hybrid that is prone to slippage promotes termination by T7 RNA polymerase. J Mol Biol **426:**3095–3107. http://dx.doi.org/10.1016/j.jmb.2014.06.012.
50. **Wons E, Furmanek-Blaszk B, Sektas M.** 2015. RNA editing by T7 RNA polymerase bypasses InDel mutations causing unexpected phenotypic changes. Nucleic Acids Res **43:**3950–3963. http://dx.doi.org/10.1093/nar/gkv269.
51. **Luo H, Wylie SJ, Jones MGK.** 2010. Identification of plant viruses using one-dimensional gel electrophoresis and peptide mass fingerprints. J Virol Methods **165:**297–301. http://dx.doi.org/10.1016/j.jviromet.2010.01.022.
52. **Martinez F, Daros JA.** 2014. Tobacco etch virus protein P1 traffics to the nucleolus and associates with the host 60S ribosomal subunits during infection. J Virol **88:**10725–10737. http://dx.doi.org/10.1128/JVI.00928-14.
53. **Ivanov KI, Eskelin K, Lohmus A, Makinen K.** 2014. Molecular and cellular mechanisms underlying potyvirus infection. J Gen Virol **95:**1415–1429. http://dx.doi.org/10.1099/vir.0.064220-0.
54. **Anandalakshmi R, Pruss GJ, Ge X, Marathe R, Mallory AC, Smith TH, Vance VB.** 1998. A viral suppressor of gene silencing in plants. Proc Natl Acad Sci U S A **95:**13079–13084. http://dx.doi.org/10.1073/pnas.95.22.13079.
55. **Kasschau KD, Carrington JC.** 1998. A counterdefensive strategy of plant viruses: suppression of posttranscriptional gene silencing. Cell **95:**461–470. http://dx.doi.org/10.1016/S0092-8674(00)81614-1.
56. **Mbanzibwa DR, Tian Y, Mukasa SB, Valkonen JP.** 2009. *Cassava brown streak virus* (*Potyviridae*) encodes a putative Maf/HAM1 pyrophosphatase implicated in reduction of mutations and a P1 proteinase that suppresses RNA silencing but contains no HC-Pro. J Virol **83:**6934–6940. http://dx.doi.org/10.1128/JVI.00537-09.
57. **Young BA, Stenger DC, Qu F, Morris TJ, Tatineni S, French R.** 2012. Tritimovirus P1 functions as a suppressor of RNA silencing and an enhancer of disease symptoms. Virus Res **163:**672–677. http://dx.doi.org/10.1016/j.virusres.2011.12.019.
58. **Tatineni S, Qu F, Li R, Morris TJ, French R.** 2012. Triticum mosaic poacevirus enlists P1 rather than HC-Pro to suppress RNA silencing-mediated host defense. Virology **433:**104–115. http://dx.doi.org/10.1016/j.virol.2012.07.016.
59. **Rodamilans B, Valli A, García JA.** 2013. Mechanistic divergence between P1 proteases of the family *Potyviridae*. J Gen Virol **94:**1407–1414. http://dx.doi.org/10.1099/vir.0.050781-0.
60. **Szabó EZ, Manczinger M, Göblös A, Kemény L, Lakatos L.** 2012. Switching on RNA silencing suppressor activity by restoring argonaute binding to a viral protein. J Virol **86:**8324–8327. http://dx.doi.org/10.1128/JVI.00627-12.
61. **Rajamäki ML, Streng J, Valkonen JP.** 2014. Silencing suppressor protein VPg of a potyvirus interacts with the plant silencing-related protein SGS3. Mol Plant Microbe Interact **27:**1199–1210. http://dx.doi.org/10.1094/MPMI-04-14-0109-R.
62. **Tena Fernández F, González I, Doblas P, Rodríguez C, Sahana N, Kaur H, Tenllado F, Praveen S, Canto T.** 2013. The influence of cis-acting P1 protein and translational elements on the expression of potato virus Y helper-component proteinase (HCPro) in heterologous systems and its suppression of silencing activity. Mol Plant Pathol **14:**530–541. http://dx.doi.org/10.1111/mpp.12025.
63. **Shabman RS, Jabado OJ, Mire CE, Stockwell TB, Edwards M, Mahajan M, Geisbert TW, Basler CF.** 2014. Deep sequencing identifies noncanonical editing of Ebola and Marburg virus RNAs in infected cells. mBio **5:**e02011. http://dx.doi.org/10.1128/mBio.02011-14.
64. **Garcia D, Garcia S, Voinnet O.** 2014. Nonsense-mediated decay serves as a general viral restriction mechanism in plants. Cell Host Microbe **16:**391–402. http://dx.doi.org/10.1016/j.chom.2014.08.001.

Downloaded from http://jvi.asm.org/ on March 13, 2016 by guest